

ศิลาเคมีของหินอัคนีทางใต้ของเหมืองทองคำชาติรี จังหวัดพิจิตร



นายเกื้อกูล มะโหด

สถาบันวิทยบริการ จุฬาลงกรณ์มหาวิทยาลัย

วิทยานิพนธ์นี้เป็นส่วนหนึ่งของการศึกษาตามหลักสูตรปริญญาวิทยาศาสตรมหาบัณฑิต

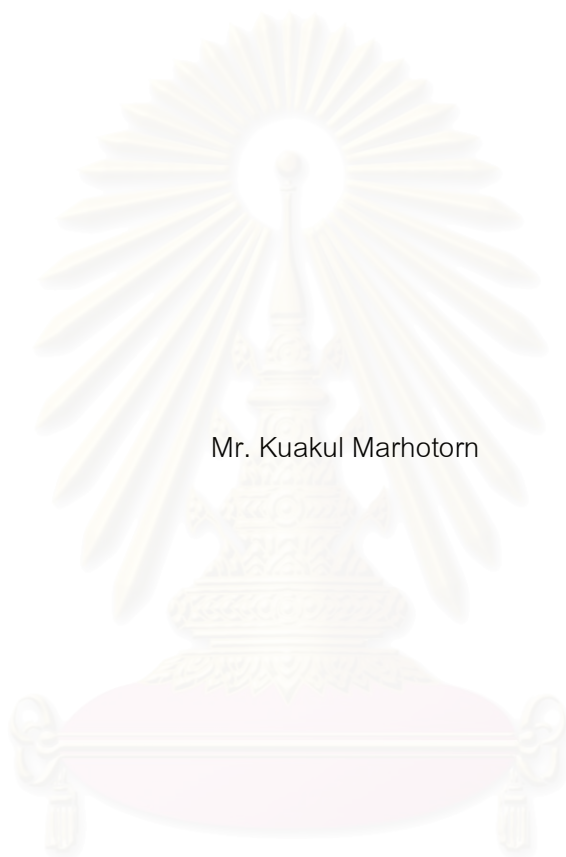
สาขาวิชาธรณีวิทยา ภาควิชาธรณีวิทยา

คณะวิทยาศาสตร์ จุฬาลงกรณ์มหาวิทยาลัย

ปีการศึกษา 2551

ลิขสิทธิ์ของจุฬาลงกรณ์มหาวิทยาลัย

PETROCHEMISTRY OF IGNEOUS ROCKS IN THE SOUTHERN PARTS OF
THE CHATREE, CHANGWAT PICHIT



Mr. Kuakul Marhotorn

สถาบันวิทยบริการ

A Thesis Submitted in Partial Fulfillment of the Requirements
for the Degree of Master of Science Program in Geology

Department of Geology

Faculty of Science

Chulalongkorn University

Academic Year 2008

Copyright of Chulalongkorn University

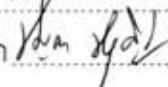
เกื้อกูล มะโหธร : ศิลาเคมีของหินอัคนีทางใต้ของเหมืองทองคำชาติรี จังหวัดพิจิตร.

(PETROCHEMISTRY OF IGNEOUS ROCKS IN THE SOUTHERN PARTS OF THE CHATREE GOLD MINE, CHANGWAT PICHIT) อ.ที่ปรึกษาวิทยานิพนธ์หลัก: รศ. ดร. ปัญญา จารุศิริ, 162 หน้า.

พื้นที่ศึกษา N และ V ทางใต้ของเหมืองทองคำชาติรี จังหวัดพิจิตร ตั้งอยู่ในแนวหินภูเขาไฟเลย-เพชรบูรณ์-นครนายกยุคเพอร์เมียนถึงไตรแอสสิก โดยปรากฏหินสองชนิดทางศิลปะรรณา ได้แก่ หินแกรโนไดออไรต์เนื้อดอกและหินแอนดีไซต์ ซึ่งหินชนิดแรกมีหลักฐานการแทรกซอนเข้าไปในหินชนิดหลัง หินแกรโนไดออไรต์เนื้อดอกประกอบด้วยผลึกดอกแพลจิโอเคลส ควอร์ต อัลคาไลน์-เฟลด์สปาร์ ฮอร์นเบลนด์และไบโอไทต์ในเนื้อพื้นที่มีควอร์ตเม็ดละเอียด การเปลี่ยนแปลงโดยส่วนใหญ่เป็นแบบโพแทสสิกโดยทางการเปลี่ยนแปลงสภาพแบบฟิลลิกอยู่บ้าง แร่ไพไรต์เป็นแร่พื้นฐานพบในสายแร่และสายแร่ขนาดเล็ก ซาลโคไพไรต์และโมลิปดีไนต์พบน้อย หินเย้าแอนดีไซต์มีเนื้อดอกขนาดไม่ใหญ่มากนักและประกอบด้วยผลึกดอกแพลจิโอเคลสและฮอร์นเบลนด์ในเนื้อพื้นจำพวกเนื้อแก้วและผลึกขลุ่ย การเปลี่ยนแปลงสภาพของหินภูเขาไฟเกิดเป็นบริเวณกว้างโดยที่รอบๆเป็นแบบโปรไฟรลิติก

ตัวอย่างหิน 22 ตัวอย่าง ที่เปลี่ยนแปลงและผุพังน้อยที่สุดทั้งที่เป็นหินอัคนีแทรกซอนและหินภูเขาไฟได้ถูกคัดเลือกเพื่อหาธาตุเคลื่อนตัวเร็วและธาตุเคลื่อนตัวช้าโดยใช้วิธี XRF, ICP-OES และ ICP-MS ทั้งการศึกษาด้านศิลปะรรณาและเคมีสามารถจำแนกหินได้เป็นหินแกรโนไดออไรต์ถึงโทนาไลต์ และหินจำพวกบะซอลติกแอนดีไซต์ ในทางธรณีเคมีพบว่าหินที่ศึกษาเป็นจำพวกแคล-อัลคาไลน์ ที่เป็นหินแกรนิตในแนวโค้งภูเขาไฟและหินบะซอลต์โทลีโอต์เกาะโค้งและภูเขาไฟแนวโค้ง จากไดอะแกรมของธาตุพบน้อยและธาตุหายากพบว่าหินแกรโนไดออไรต์สอดคล้องกับหินอัคนีแทรกซอนยุคเทอร์เชียรีของอาเซอร์ไบจานของประเทศอิหร่าน เป็นที่เชื่อว่ากระบวนการเกิดแหล่งแร่ของพื้นที่ N และ V เป็นแบบทองแดงโพรไฟร์ซึ่งเกิดในระดับต้นโดยการมุดตัวของแผ่นมหาสมุทรในช่วงอายุเพอร์เมียนถึงไตรแอสสิกระหว่างแผ่นลำปาง-เชียงรายและแผ่นนครไทย

ภาควิชา.....ธรณีวิทยา.....
สาขาวิชา.....ธรณีวิทยา.....
ปีการศึกษา.....2551.....

ลายมือชื่อนิสิต.....เกื้อกูล มะโหธร.....
ลายมือชื่ออ.ที่ปรึกษาวิทยานิพนธ์หลัก.....

487 22256 23 : MAJOR GEOLOGY

KEYWORDS : PETROGRAPHY / CHEMISTRY / ALTERATION / SUBDUCTION /
TRACE AND REE

KUAKUL MARHOTORN : PETROCHEMISTRY OF IGNEOUS ROCKS IN THE
SOUTHERN PARTS OF THE CHATREE GOLD MINE, CHANGWAT PICHIT
ADVISOR: ASSOC. PROF. PUNYA CHARUSIRI, Ph. D., 162 pp.

The studied N and V Prospects in the southern parts of Chatree Gold Mine, Changwat Pichit is located in the central part of the north-trending Permo-Triassic Loei-Petchabun-Nakhon Nayok Volcanic Belts. Two main types of igneous rocks are recognized petrographically, namely porphyritic granodiorite and andesite. The former show lines of evidence of intrusion into the latter. The porphyritic granodiorite is characterized by phenocrysts of plagioclase (An_{30}), k-feldspar, quartz, hornblende and biotite set in fine-grained quartz-rich groundmass. Associated alterations are predominant potassic alteration with minority of phyllic alteration. Pyrite is principal ore in veins and veinlets whereas chalcopyrite and molybdenite are present in small amount. The andesite host is unvariably porphyritic and largely composed of altered plagioclase and hornblende phenocrysts set in glassy-microlite groundmass. The alteration of volcanic rocks are widespread and is peripheral with propylitic alteration.

Twenty-two least-altered and least-weathered samples of both plutonic and volcanic rocks were selected for mobile-and immobile-elemental analyses using XRF, ICP-OES and ICP-MS methods. Both petrographically and chemically, these studied igneous rocks can be classified as granodiorite to tonalite and basaltic andesite. Geochemically, the studied rocks belong to the calc-alkaline affinity occurring as volcanic arc granite and island arc tholeiite to volcanic arc basalt. Spider diagrams of trace and rare-earth elements reveal that granodiorite shows a pattern consistent with those of the Tertiary intrusive igneous rocks of Azerbaijan, Iran. Principal mineralization at the studies N and V prospects is believed to belong to porphyry-copper type occurring in the shallow intrusive environment and was formed as a result of oceanic subduction during Permo-Triassic Period between Lumpang-Chiang Rai and Nakhon Thai plates.

Department : Geology
Field of Study : Geology
Academic Year : 2008

Student's Signature

Advisor's Signature



ACKNOWLEDGEMENTS

Foremost, I would like to thank my advisors Associated Professor Dr. Punya Charusiri to their advice and encouragement throughout the course of this study and for his advice and criticism for the manuscript.

Sincerely, appreciations also provide to Department of Geology, Akita University, Japan for allow the author to use laboratory facilities for the part of Microscopy, XRF, ICP-OES and ICP-MS. I would like to thank Professor Dr. Isao Takashima for his advice and help about XRF and ICP-OES analysis. I sincerely thank to Professor Dr. Daizo Ishiyama for ICP-MS analysis.

Sincerely, appreciations also provide to Department of Geology, Chulalongkorn University for allow the author to use laboratory facilities for the microscopic, Mr. Veerasak Lunwongsa, Miss. Saranya Nuanlaong, Miss. Sasikan Janplook and Miss. Ladda Tangwattananukul who offered an accommodation during field observation.

Financial support for the research was provided by Akara Mining CO., LTD. and Akita University research grant to Professor Dr. Isao Takashima and Professor Dr. Toshio Mizuta. I would like to thank Dr. Krit Wonin (Kasetsart University) for their very helpful suggestions and constructive criticisms.

Last, special thanks are given to my parent, brothers, sister and friends for their encouragement and helps.

สถาบันวิทยบริการ
จุฬาลงกรณ์มหาวิทยาลัย

CONTENTS

	PAGE
ABSTRACT IN THAI.....	iv
ABSTRACT IN ENGLISH.....	v
ACKNOWLEDGEMENTS.....	vi
CONTENTS.....	vii
LIST OF TABLES.....	ix
LIST OF FIGURES	x
CHAPTER I INTRODUCTION.....	1
1.1 General statement.....	1
1.2 Location and accessibility.....	3
1.3 Objectives.....	4
1.4 Methodology	5
1.5 Geography and physiography.....	9
1.6 Previous work in the study area	9
CHAPTER II REGIONAL SETTING.....	14
2.1 Tectonic framework of Thailand.....	14
2.2 Igneous rocks of Thailand.....	18
2.2.1 Intrusive rocks.....	18
2.2.2 Extrusive rocks.....	25
CHAPTER III GEOLOGY.....	29
3.1 Regional geology.....	29
3.2 Detailed geology.....	36
3.3 Geology of the Prospect area.....	43
CHAPTER IV PETROGRAPHY.....	45
4.1 Evidence of contact zone	45
4.2 Petrographic characteristics of intrusive rocks	51
4.3 Petrographic characteristics of extrusive rocks	67

	PAGE
4.4 Ore petrographic study	79
CHAPTER V GEOCHEMISTRY.....	87
5.1 Classification of Igneous rocks	87
5.2 Chemical Affinity	97
5.3 Signatures of trace and rare earth elements	101
CHAPTER VI DISCUSSION	107
6.1 Petrochemical characteristics of the studied igneous rocks.....	107
6.2 Relationships of mineralization/alteration to the studied rocks.....	115
6.3 Age Constraints.....	119
6.4 Tectonic setting.....	122
CHAPTER VII CONCLUSION.....	126
REFERENCES.....	127
APPENDICES	142
APPENDIX A Description petrographic study	143
APPENDIX B Chemical data analysis of XRF, ICP-OES and ICP-MS.....	146
APPENDIX C Calibration curve of Major and Minor element by XRF.....	152
APPENDIX D Calibration curve of Trace element by ICP-OES.....	154
APPENDIX E Calibration curve of Rare earth element by ICP-MS.....	161
BIOGRAPHY.....	162

LIST OF TABLES

TABLE	PAGE
Table 1.1. Previous data of Chatree gold deposit, Pichit-Petchabun, Thailand.....	12
Table 2.1. Summary of granitoid belts in Thailand (modified from Charusiri et al., 1993).....	23
Table 4.1. Mineral symbols for rock-forming mineral (Kretz, 1983).....	48
Table 4.2. Description ore petrography of drill-hole no. 2580 DD at N Prospect, Chatree gold mine, Thailand.....	80
Table 5.1. Major-oxide and trace element contents of the Chatree igneous rocks determined using XRF and ICP-OES method.....	89
Table 5.2. Trace and REE concentrations of the Chatree granodiorite rock determining using ICP-MS method.....	92
Table 5.3. Chemical analyses of major elements and their CIPW Norms.....	93
Table 6.3. Previous data of porphyry type.....	124

LIST OF FIGURES

FIGURE	PAGE
Figure 1.1. Rout map of the study area (topographic map scale 1:50,000, series L7017, sheet 5238 III).....	4
Figure 1.2. Flow chart show the method of study.....	6
Figure 1.3. Quick-bird remote sensing image of the Chatree gold mine.....	11
Figure 2.1. Tectonic model of Thailand during Permo-Trassic Period after Charusiri (2002).....	17
Figure 2.2. Igneous distribution patterns of granites with three granites province in Thailand (modified after Charusiri et al., 1993, Nantasin et al. 2005 and Salam et al., 2008).....	24
Figure 2.3. Volcanic belts of Thailand (modified from Intasopa, 1993, Charusiri et al., 2002 and Phajuy et al., 2004).....	28
Figure 3.1. Simplified geological maps of the study area (modified from Jungyusuk and Khositantont (1992)).....	35
Figure 3.2. Surface and subsurface geologic map and cross section of the study area (modified after Coming et at., 2006).....	42
Figure 3.3. Subsurface geology of the N Prospect, southern part of Chatree gold mine.....	44
Figure 3.4. Subsurface geology of the V Prospect, southern part of Chatree gold mine.....	44
Figure 4.1. Samples of altered and least altered rocks were selected for petrographic and geochemical study from drill-hole no. 2580DD.	46
Figure 4.2. Samples of altered and least altered rocks were selected for petrographic and geochemical study from drill-hole no. 3131DD..	47
Figure 4.3. A slab specimen of evidence of contact is occurred between granodiorite and andesite (N Prospect) shown that in figure a. Photomicrograph (b.) of granodiorite intruded into andesite	49

FIGURE	PAGE
Figure 4.4. Slab specimens of andesite (a) (N Prospect) host which is crosscut by intrusive vein and formed highly fractured, stock works, veinlets and micro-faults. (b) Sequence of veins-first: quartz-opaque mineral vein crosscut andesite and second: quartz-chlorite vein with opaque ore in the central zone.....	50
Figure 4.5. A slab specimen of porphyritic granodiorite of N Prospect showing fine-grained groundmass and porphyritic texture. The dark color is mica (a). (b) Photomicrograph (b) of (a) showing euhedral plagioclase (Pl) and K-feldspar (Kfs) phenocryst set in fine-grained quartz (Qtz) groundmass and sericite (Src) replaced at the fracture of plagioclase.....	54
Figure 4.6. Photomicrographs of porphyritic granodiorite, N Prospect. (a) Plagioclase (Pl) phenocryst altered to sericite (Src) in fracture set in fine-grained quartz (Qtz) groundmass.....	55
Figure 4.7. Photomicrographs of porphyritic granodiorite at N Prospect, Chatree gold deposits. (a) Altered biotite (Bt) phenocryst set in fine-grained quartz (Qtz) groundmass which is surrounded by fine-grained quartz groundmass and some subrounded-quartz. (b) Relic euhedral hornblende (Hbl) phenocryst altered to chlorite-biotite-opaque and surrounded of chlorite (Chl) and biotite phenocryst set in fine-grained quartz groundmass.....	56
Figure 4.8. A slab specimen (a) of porphyritic granodiorite of N Prospect showing fine-grained groundmass and porphyritic texture which is coss-cut by quartz-sulfide veinlets. (b) Photomicrograph zoning plagioclase (Pl) phenocrysts and k-feldspar (Kfs) set in fine-grained quartz (Qtz) groundmass.....	57

FIGURE	PAGE
Figure 4.9. Photomicrographs of porphyritic granodiorite at N Prospect, Chatree gold deposits. (a) Euhedral plagioclase (Pl) phenocryst set in fine-grained somewhat recrystallized quartz (Qtz) groundmass and fractured long rectangular minor secondary chlorite (Chl). (b) Relic plagioclase phenocryst strongly altered to sericite (Src) associated and show cored texture set in fine-grained quartz groundmass.....	58
Figure 4.10. Photomicrographs of porphyritic granodiorite at N Prospect, Chatree gold deposits. (a) Vermicular quartz (Qtz) phenocryst is replaced by fine-grained silicified quartz groundmass and formed embayment. Rectangular opaque (Op) mineral associated with sericite (Src). Inclusion of biotite (Bt) formed in vermicular quartz phenocryst. Relic hornblende (b) phenocryst altered to chlorite-biotite associated with opaque mineral.....	59
Figure 4.11. Photomicrographs of porphyritic granodiorite (N Prospect) showing plagioclase (Pl) phenocryst is replaced by sericite in fracture and formed in fine-grained quartz (Qtz) groundmass (a). Relic hornblende (Hbl) altered to biotite-chlorite-opaque mineral. Plagioclase formed by fine-grained quartz reolaced into fracture plagioclase phenocryst (b). Rim of plagioclase is replaced and altered to k-feldspar (Kfs). Secondary biotite (Bt) formed at bottom of (b).....	60
Figure 4.12. Photomicrographs of porphyritic granodiorite at N Prospect. (a) Relic diamond-shaped hornblende (Hbl) phenocryst altered to chlorite (Chl)-bitote (Bt)-cubic to subangular opaque (Op) mineral set in fine-grained quartz (Qtz)-enriched groundmass. (b) Relic hornblende altered to chorite set in fine-grained quartz groundmass with rare anhedral apatite (Ap).....	61

FIGURE	PAGE
Figure 4.13. Photomicrographs of porphyritic granodiorite, N Prospect. (a) Fine-grained mica or sericite (Src) vein crosscut the plagioclase phenocryst and fine-grained quartz (Qtz) groundmass. (b) Plagioclase (Pl) phenocryst crosscut by quartz-opaque mineral which chlorite (Chl) and sericite are formed at rim of vein. In addition, sericite formed in the fracture of plagioclase phenocryst.....	62
Figure 4.14. Photomicrographs of porphyritic granodiorite, N Prospect. (a) Zoned-plagioclase (Pl) phenocryst is altered to sericite (Src) set in fine-grained quartz (Qtz) groundmass. Alteration assemblages are chlorite (Chl)-biotite (Bt)-sericite (Src)-opaque (Op) mineral. (b) (Sample no. DDN7) Fine-grained granodiorite is cross cut by quartz vein and chlorite associated with opaque mineral set in fine-grained quartz groundmass.....	63
Figure 4.15. A slab specimen of andesite dyke rock (a) (N prospect) showing micro to porphyritic texture. (b) Photomicrograph of andesite dyke showing feldspar (Fs) phenocryst replaced by secondary biotite (Bt). The characteristic of groundmass is glassy and microlite of plagioclase (Pl).....	65
Figure 4.16. Photomicrographs of andesite dyke (N Prospect) (Sample no. DDN11). (a) Relic hornblende phenocryst with the oblique two cleavages (120° and 60°) by angle set in plagioclase (Pl) glassy groundmass with rare epidote (Ep) formed around phenocryst. (b) Secondary biotite replacing relic feldspar set in glassy-flowed groundmass of hydrothermal quartz, plagioclase and rare epidote.....	66
Figure 4.17. (a) A slab specimen of altered andesite with aphanitic texture and crosscut by various veinlets. (b) Photomicrograph from part of (a) showing altered plagioclase (Pl) phenocryst.....	68

FIGURE	PAGE
Figure 4.18. Photomicrographs of altered andesite, at N Prospect, altered plagioclase (Pl) phenocrysts in dotted red boxes set in fine-grained glassy groundmass enriched in devitrified glassy material. Opaque (Op) mineral is disseminated in glassy groundmass.....	69
Figure 4.19. A slab specimen of weathered andesite showing abundant green phenocrysts in fine-grained groundmass. (b) Photomicrograph from the same sample of above (a) showing altered twining plagioclase (Pl) phenocryst which is replaced by epidote (Ep).....	71
Figure 4.20. Photomicrographs of weathered andesite of V Prospect. (a) Very altered plagioclase (Pl) phenocryst set in groundmass and surrounded by chlorite (Chl), opaque, microlite and accessory unidentified mineral (apatite?) (Ap). (b) The same sample of above showing relic plagioclase phenocryst set in flow-plagioclase.....	72
Figure 4.21. A slab specimen (a) of altered green andesite (V prospect) showing abundant green phenocryst and fine-grained groundmass. Photomicrograph (b) showing altered twining plagioclase (Pl) phenocryst which is replaced by epidote (Ep) set in glassy and flow texture. Cubic opaque (Op) mineral formed in groundmass.....	73
Figure 4.22. Photomicrographs of altered andesite showing relic plagioclase (Pl) replaced by subhedral epidote (Ep) and set in devitrified/chloritized glassy groundmass. Chlorite (Chl) formed as irregular shape in the rock.....	74

FIGURE	PAGE
Figure 4.23. Photomicrographs of altered andesite showing relic hornblende with 120° and 60° cleavage altered to epidote (Ep) set in devitrified/chloritized glassy groundmass with some microlite. Opaque (Op) mineral is disseminated in groundmass.....	75
Figure 4.24 Photomicrographs of altered andesite at V prospect, Chatree gold deposits. (a) (b) Relic plagioclase (Pl) phenocryst altered to chlorite (Chl) and minor sericite (Src) at rim and fractured, set in the groundmass enriched in microlite, devitrified glassy materials, and some opaques. Note that flow texture is also present.....	76
Figure 4.25. Photomicrographs of altered andesite at V prospect. (a) (b) Relic plagioclase (Pl) phenocryst is mainly replaced by epidote (Ep) mainly in the cores and formed in glassy groundmass.....	77
Figure 4.26. Photomicrographs of altered andesite at V prospect. (a) (b) Relic plagioclase (Pl) phenocrysts altered to epidote (Ep), particularly in the core in glassy and devitrified (chloritized) groundmass and microlite.....	78
Figure 4.27. A slab specimen (a) of porphyritic granodiorite crosscut by quartz (Qtz)-chalcopyrite (Ccp)-pyrite (Py)-molybdenite (Mo) veinlet. Black circle is prepared for polished section. Photomicrograph (b) (in reflected light) from the same sample of (a) showing anhedral pyrite and chalcopyrite disseminated in fine-grained groundmass.....	81
Figure 4.28. Photomicrographs from the same vein) in porphyritic granodiorite showing chalcopyrite (Ccp)-pyrite (Py)-molybdenite (Mo) assemblage. (a) Euhedral pyrite and rounded quartz formed as inclusion in anhedral chalcopyrite. (b) Molybdenite formed characteristics of sheet, sandwiched sheet and undulated texture.....	82

FIGURE	PAGE
Figure 4.29. A slab specimen of porphyritic granodiorite ((a) crosscut by quartz sulfide veins. Photomicrograph from the same sample of above showing disseminated pyrite formed in quartz groundmass with plagioclase and chlorite.....	83
Figure 4.30. Photomicrographs from the same vein of the porphyritic granodiorite showing (a) anhedral chalcopyrite (Ccp)-pyrite (Py) assemblage and (b) larger cubic pyrite (Py) formed associated with smaller sphalerite (Sp) and chalcopyrite (Ccp) in quartz-bearing vein.....	84
Figure 4.31. (a) A slab specimen of andesite rock showing various veins cross cutting quartz (Qtz)-opaque (Op) mineral vein.(b) Photomicrograph (in reflected light) showing disseminated pyrite (Py) and chalcopyrite (Ccp) blebs in groundmass and cross cut by chlorite (Chl)-opaque (Op) mineral vein.....	85
Figure 4.32 Photomicrographs from the quartz-sulfide vein of andesite (see in figure 4.31a) showing (a) anhedral chalcopyrite (Ccp)- and larger euhedral cubic pyrite (Py) assemblage and (b) anhedral sphalerite ore formed at the rim of irregular resorbed pyrite grain.....	86
Figure 5.1. Plots Q-A-P for the rocks from the N prospect. Chatree gold deposit is mainly set in tonalite and granodiorite field (streckeisen, 1976).....	95
Figure 5.2. TAS diagram for intrusive rock of N prospect based on the diagram of Cox et al., (1979) alkaline-subalkaline (Irvine and Baragar, 1971) is mainly fall in granodiorite.....	95
Figure 5.3. Plots of alkaline and subalkaline basalts in terms of wt% Na ₂ O+K ₂ O versus % SiO ₂ (Le Maitre, 2002) and alkaline-subalkaline (Irvine and Baragar, 1971) for volcanic rocks of N&V prospects is mainly fall in the basaltic andesite.....	96

FIGURE	PAGE
Figure 5.4. Plots of Zr/TiO_2 versus Nb/Y for volcanic rocks of N&V prospects based on the diagram of Winchester and Floyd (1977). The rock plots fall in the field of subalkalic- basalt.....	96
Figure 5.5. Na_2O vs. K_2O diagram represents the affinity of granodiorite in stusy area (after Chappell and White, 1974).....	98
Figure 5.6. Plots of Si_2O vs. K_2O , Low-K series, calc-alkaline and high-K calc-alkaline boundaries are from Peccerillo & Taylor (1976).....	98
Figure 5.7. Plots of $FeO+FeO_3$ versus SiO_2 nomenclature of Miyashiro (1974), the volcanic rocks at N and V prospect of Chatree gold deposits are classified as calc-alkaline rocks.....	99
Figure 5.8 Plots of K_2O versus SiO_2 nomenclature of Peccerillo & Taylor (1976), the volcanic rocks at N and V prospect of Chatree gold deposits are classified as calc-alkaline rocks.....	99
Figure 5.9. AFM diagrams with the Irvine and Baragar (1974) dividing line for tholeiitic and calc-alkaline trends. The volcanic rock is mainly filled into the calc-alkaline field.....	100
Figure 5.10 Plots of Y versus Cr for volcanic rocks of N&V prospects based on diagram of modified after Pearce et al. (1984).....	102
Figure 5.11. Plots Zr/Y vs. Zr plots for volcanic rocks of N&V prospects which fall within the field of volcanic arc basalts. Diagram from Pearce and Norry (1979).....	102
Figure 5.12. Plots of Zr versus Ti for volcanic rocks of N&V prospects based on based on the diagram of Pearce & Cann (1973).....	103
Figure 5.13. Plots $Zr-Ti/100-Sr/2$ diagram of Pearce and Cann (1973), wherein N and V prospect volcanic rock exhibits Island-Arc Tholeiites.....	103
Figure 5.14. Log Nb vs. log Y which show the rocks in the N zone fall in the volcanic arc felsic field. Diagram from Gill (1978).....	104

FIGURE	PAGE
Figure 5.15. Log Rb vs. (Nb-Y) discrimination plot of granitic rocks from the N-zone of Chatree gold mine. Diagram from Pearce et al. (1984).....	104
Figure 5.16. Log Rb vs. (Nb-Y) discrimination plot of granitic rocks from the N prospect of Chatree gold mine is fall in Volcanic-arc Granite field (VAG). Diagram from Pearce et al. (1984).....	105
Figure 5.17. Log Rb vs. (Y-Ta) discrimination plot of granitic rocks from the N prospect of Chatree gold mine is fall in Volcanic-arc Granite field. Diagram from Pearce et al. (1984).....	105
Figure 5.18. Chondrite-normalized REE plots of selected samples from the same suit in the Chatree granodiorite. The rock displays lack a Eu anomaly. Also shown on the diagram is the pattern of Azerbaijan granodiorite, Iran (Hezarkhani, 2005).....	106
Figure 6.1. Photomicrographs of characteristic of Porphyritic granodiorite (a,b in plane-polarized light). (a) Porphyritic granodiorite form Borehole at Kam Chang Kok, Hong Kong, and photo by Wan (1994). (b) Porphyritic granodiorite form the study area, N Prospect, Chatree mine.....	111
Figure 6.2. Photomicrographs (a, b in plane-polarized light) of (a) very fine-grained groundmass and oscillatory zoning in a plagioclase phenocryst in a diorite porphyry, western North America (Sibley et al., 1976). (b) Zoning plagioclase set in fine grained groundmass of porphyritic granodiorite, Chatree gold mine.....	112
Figure 6.3. Model for the development of vermicular textures in quartz phenocrysts (Fig a, b, c and d. Empire Mine, Idaho, USA) base on the work proposed by Chang et al. (2004) (Fig.e). Photomicrograph of embayed quartz phenocryst set in a groundmass of fine-grained silicate minerals, Chatree gold deposit (Fig. d).....	113

FIGURE	PAGE
Figure 6.4. Features seen in outcrop (a) and photomicrograph under microscope (b) that help determine the relative ages of plutonic rocks (Huber, 1987).	114
Figure 6.5. Features seen in hand specimen of the drill-core sample (a) and photomicrograph under microscope from the core (b) showing intrusion of granodiorite and andesite inclusion in granodiorite, N prospect, Chatree gold deposit.....	114
Figure 6.6. Cross section through a subduction zone and continental arc (modified from Winter, 2001 and Richards, 2003). Note that this scenario can be applied to the N-and V-Prospepects of the chatree Au mine for subduction related to alteration and mineralization.	120
Figure 6.7. Schematic cross section through a porphyry Cu-forming volcanic-plutonic system (modified after Lowell and Guilbert, 1970, Silotoe, 1973, Irianto and Clark, 1995), Richards, 2003).....	120
Figure 6.8. Model for the alteration&porphyry show styles of the N and V Prospect, Chatree gold mine(modified after Lowell and Guilbert, 1970, Silotoe, 1973, Irianto and Clark, 1995), Richards, 2003). N Prospect shows characteristic of potassic alteration with minor phyllic alteration whereas the V Prospect is propylitic alteration style.....	121
Figure 6.9. Model of tectonic setting of Loei-Perchabun volcanic belt. (modified from Charusiri et.al, 2002 and Salam et al., 2008).....	123

CHAPTER I

INTRODUCTON

1.1 General statement

Gold has a widespread occurrence in several countries around the world (Boyle, 1979). It also has influenced on the exploration and the settlement of mankind. Ancient gold mines have been known in Egypt (Botros, 2004), in Spain, France, Great Britain (Arias, 2000), in Yugoslavia (Spiering et al., 2000), Romania (Neacsu et al., 2009), Greece (Michael, 2004), Turkey (Yigit, 2007), India (Mishra et al., 2005), China (Zaw, 2007), Japan, and the U.S.S.R (Belogub, 2008). Boyle (1979) concluded that ancient placers have yielded gold from several essential rivers such as Tagus (Portugal), Guadalquivir (Spain), Tiber (Italy), Po (Italy), Rhone (France), Rhine (Germany), Hebrus and Maritsa, (Bulgaria, Greece, Turkey), Gra (U.S.A), Nile (Egypt), Zambezi (Zambia), Niger (Guinea, Mali, Niger, and Nigeria), Senegal (Senegal), Pactolus (in ancient Lydia, Turkey)), Oxus (Amu Darya that flows through the golden land of Samarkand) (Uzbekistan), Indus (Pakista), Ganges (India and Bangladesh), Lena (Russia), Aldan (Russia), Amur, (Russia), Yangtze (China), and a multitude of others. The artisans of the earliest civilizations of Anatolia (Catal Hijyilk), Mesopotamia (Sumer), and the Indus Valley (Harappa and Mohenjo-Daro) worked in gold obtained from many sites in the Caucasus and Middle Asia, the Middle East, and the Indian Peninsula. Boyle (1979) reported that the Egyptians mined gold extensively in eastern Egypt and Sudan (Nubia) as far back as 4,000 years ago. It was from them that the Persians, Greeks, and Romans in turn learned the techniques of gold prospecting, mining, and metallurgy. Boyle (1979) noted that the Greeks and Romans mined gold ores from the extensive metalliferous regions of their empires. Pliny the Elder (A.D. 23-79) in his *historia naturalist* written in the early years of our era, repeatedly mentioned the mining and metallurgy of gold and during the Renaissance Agricola referred to it, as had many others before him during the middle Ages.

In Thailand gold occurrences have been reported in several localities. Most of them are placer or secondary deposits, derived from primary vein deposits. Gold-

bearing quartz veins are commonly observed in granite, diorite, volcanic, and some metamorphic rocks (Muenlek et al., 1988). Native gold was also found as very small inclusions in chalcopyrite veins and veinlets of Phu Lon deposit in Nong Khai Province, NE Thailand (Muenlek et al., 1988). Copper ores at Phu Hin Lek Fai and Phu Thong Daeng porphyry copper deposits in Loei Province, NE Thailand (Jacobson et al., 1969) to contain some native gold as inclusions. The well-known Toh Moh gold deposit, near the Malaysia border in Narathiwat Province is an only gold mine producing gold from quartz vein at present. The other known potential areas for gold are in the provincial areas of Loei, Udon Thani, Petchabun and Nong Khai in the northeast, Prachinburi and Chachoengsao in the east, Phrae, Lampang and Chiang Rai in the North, and Prachab Khire Khan and Nakhon Srithammarat in the south (DMR, 2000).

Charusiri et al. (2003) reported the epithermal gold deposits which can be subdivided into 2 types, i. e. those of the low-sulfidation (quartz-andularia) and high-sulfidation (acid-sulfate) affinities. Both types are inferred to take place in convergent plates of the compressional tectonic environments. Deposits of low-sulfidation affinities possess neutral pH in reducing environments with the interaction of deeply circulating groundwater and interacted magnetic/country rocks, then giving rise to alkaline-chlorite fluids. Deposits of high-sulfidation affinities are directly the main products of magma and with the minimum reaction with the enclosing rocks. Field and petrographic observations indicate that low-sulfidation Au deposits are principally disseminated or cavity-filling quartz vein/veinlets. On the other hand, high sulfidation deposits are copper and arsenic sulfosalts. Important gangues of low-sulfidation are adularia and calcite whereas those of high sulfidation are kaolinite, alunite, pyrophyrite and diaspores. Additionally, based upon the studies of fluid inclusions and alteration mineralogy, it implies that the temperatures of formation range from 180° C to 200° C and the depths of formation vary from 1,000 to 1,500 m. Gold of low sulfidation deposits may form at lower temperature (160°-200° C) than those of high sulfidation (200°-260° C).

Akara mining company, a wholly-owned subsidiary of Australia's Kingsgate Consolidated NL, was established in 1993 to develop the gold mine that has been discovered along the Loei-Petchabun volcanic belt. The mine is named as Chatree Gold Mine after a famous Thai geologist (Mr. Chatree Chaichanapumhol) who joined the

exploration team at the time. Unfortunately, he passed away after this deposit has been found.

The Chatree gold deposits are located at the boundary between Thap Klo District, Petchabun Province and Wang Pong District, Phichit Province, (see Fig. 1.1) central Thailand. Diemar et al. (2000) reported that gold-silver mineralization has occurred as a low sulfidation quartz-carbonate-andularia style epithermal. The ore reserves and resource of C-H Zone were reported about 8,200 of gold tones with grade of 2.3 g/t of Au and 10 g/t of Ag. Total production at Chatree in 2004 was about 150,000 ounces of gold and 396,000 ounces of silver from a total resource of 33 million tones at 1.7 g/t Au and 11g/t Ag (Kingsgate Company, 2007). Ore reserves are estimated to maintain the mining activity for more than 10 years (Kromkhun et al., 2005).

1.2 Location and accessibility

The Chatree mine is situated closely to Khao Pong and Khao Mo mountain range (Fig. 1.1) which have an elevation of about 100 meters above mean sea level. Geologically, this gold deposit is located on the edge of Tertiary Chao Phaya basin that is on the boulder of Petchabun and Pichit Provinces about 280 kilometers north (or 4.5 hours drive) of Bangkok, and about 45 kilometers southeast of Pichit city.

The study area of N and V Prospects is far from C-H Zone 2.5 approximately km to the southern parts. The N Prospect was investigated by core-log sampling of the hole-no. 2580 DD. N prospect with Grid reference in UTM system is 676911E and 1799311N. The V prospect is investigate by core-log sampling of the Hole no. 3131 DD with Grid reference in UTM system is 676275E and 1799601N. The route map is modified from the Royal Thai Survey topographic map scale 1:50,000, sheet number 5141 IV, edition 1-RST and series L7071 of Ban Wang Sai Phun Nai.

The study area can be accessed annually and comfortably by three ways. The first is done by using the Highway No.1 from Bangkok passing Pathum Thani, Saraburi, Lopburi and turning right to Highway No. 11 from Amphoe Tak Fa to Amphoe Thap Klo. The other ways by train to Taphan Hin station of Pichit province, or by an airplane to Pitsanok, then following Highway no. 11.

The study is lying in the north part of Amphoe Thap Klo which is between Pichit and Petchabun province and, can be accessed easily by road No.1301 (Ban Nong Khanak), about 6 km from Khaosai Junction and turn right into Chatree gold mine.

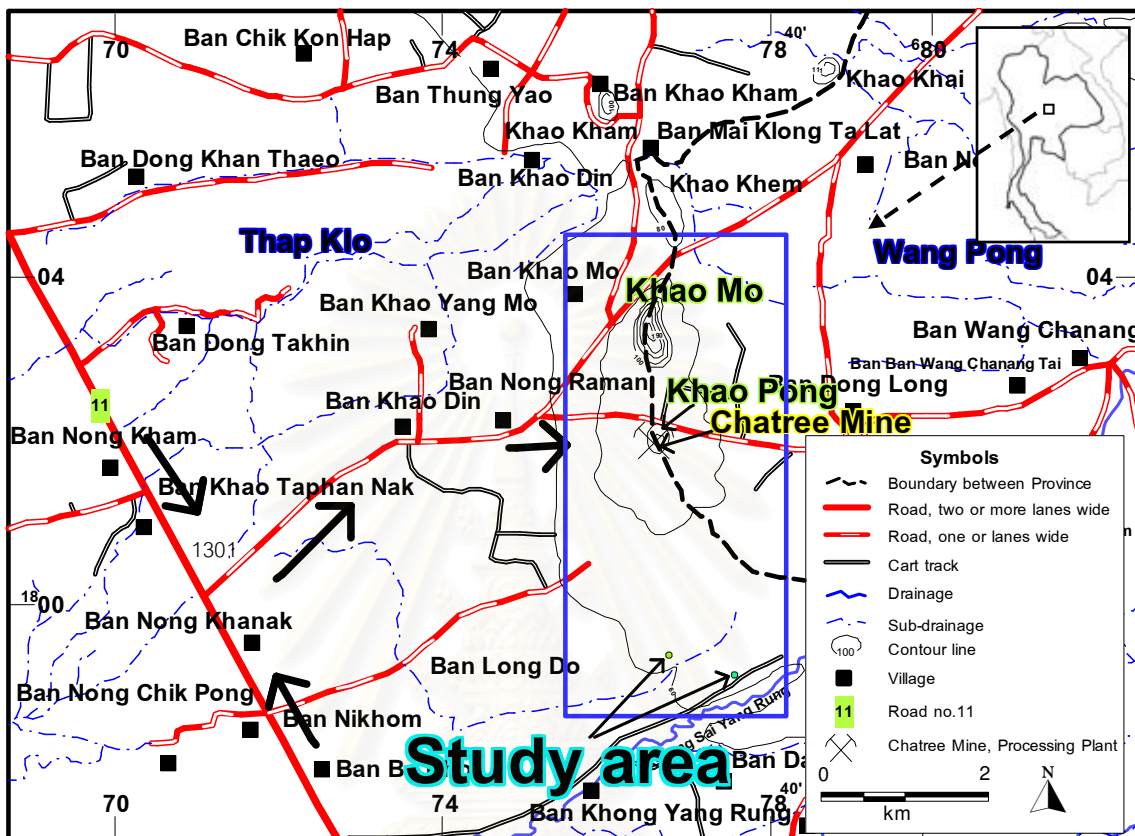


Figure 1.1 Route map to Wang Pong District of Petchabun province and Thap Klo District of Pichit province, north-central Thailand showing the location of the study area (blue box).

1.3 Objectives

No previous work has done so far for the petrographic and geochemical studies of the N and V Prospects. Only the ore assays, such as those of Cu, Au, Pb and Zn ores, were only reported for every 1-m core of 2580DD (171 m-long) and 3131DD (90 m-long)

This study is based on two drill holes of N and V prospect. In thesis, special emphasis is placed on the detailed investigations on petrography and geochemistry of core rocks to explain alteration of rocks. So the regolith (20 m-long) in the drill holes overlying the hard rocks will not be studied. Interpretation on tectonic setting is based

mainly on the results of petrography and geochemistry of the least altered and least weathered igneous rocks along with the published data on age dating

The important objective of the present investigation is the study of petrography and geochemistry of what? The principle aims of this thesis are:

1. study petrography and geochemistry
2. present mineralization assemblages and alteration styles, and
3. interpret tectonic setting.

1.4 Methodology

A detailed method of study is shown as the flow chart in Fig 1.2. It consists of two three topics as explained below.

The first stage is pre-field investigation comprising preparation of all technical data such as aerial photograph interpretation on the apparent geology features with regional trends, structures, geomorphology, rock units and field accessibility. In this stage, the author also studied the previous works on the regional geology and stratigraphy of the study area. The second stage is the field investigation such as field data and rock sampling for laboratories. The final stage is the post-field investigation. This stage is studying in laboratories including the petrography and geochemistry. In addition, chemical analyzes of selected specimens were carried out by using XRF, ICP-OES and ICP-MS. Finally, discussion and conclusion will be performed and resulted in the final thesis.

1.4.1 Field study

1.4.1.1 Field investigation

The first step was carried out specifically for mapping the intrusive rocks distribution in the study area and compared with the work done by Corbett (2004) in order to find out field relationship and collecting samples for further laboratory studies. The field investigation has done during January-July, 2007. The detailed geologic map was prepared from the result of the field investigation and laboratory evidences modified after Coming et al. (2006). The igneous rocks were categorized based on mesoscopic investigation into three groups, namely fine-grained granodiorite, andesite and andesite dykes.

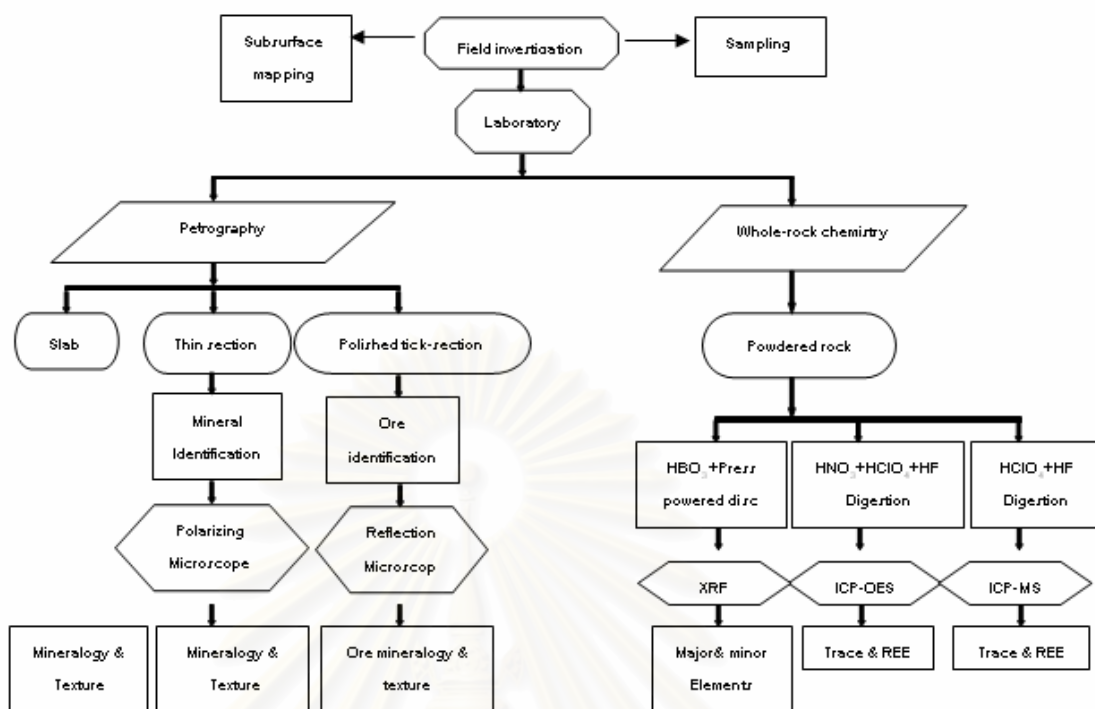


Fig. 1.2 Flow chart showing sequences of work used in this study.

1.4.1.2 Core sampling

Core logging well sampling was done after field survey. Two prospects (N and V zones) were selected for this study, 68 samples of rock slabs was selected for mesoscopic analysis, and 37 samples of altered and least altered rocks were selected for microscopic study from drill-hole no. 2580DD. Correlation with rock-chip samples were made from drill-hole no. 2407RC, 2408RC, 2409RC, 2410RC, 2411RC and 2412RC.

V prospect, altered and least altered rocks were selected for microscopic study from drill-hole no. 3131DD. Correlation with rock-chip samples were made from drill-hole no. 2071RC, 3082RC, 3083RC, 3084RC, 3085RC, 3086RC, 3087RC, 3088RC, 3130RC and 3636 RC.

1.4.2 Laboratory study

1.4.2.1 Petrography

1.4.2.1.1 Slabs and thin sections

The rock samples were slab-cut and prepared as thin sections. The thin sections

were usually set at 30 microns thickness and covered glass. These thin sections were used for mineral identification, texture, alteration and paragenesis by polarizing microscope. An Introduction to the Rock-forming Minerals (Deer et al., 1966), Petrography of Igneous and Metamorphic Rocks (Philpotts, 1989) and Rock-forming Mineral in Thin sections (Pichler, 1997) were used for mineral and texture identifications. Consequently, those textures were interpreted after Hibbard (1995). The symbols of rock forming minerals were used following American Mineralogist (Kretz, 1983).

1.4.2.1.2 Polished section

For ore mineral classification, six samples of each rock type (N Prospect) were prepared as polished section. The un-covered slightly thick sections were polished by 12, 6, 3, 1 and 3 μm of diamond pastes. The polished sections were later classified under reflected light of microscope.

1.4.2.2 whole-rock analysis

1.4.2.2.1 X-Ray Fluorescence Spectrometer

In this study, major and minor elements were carried out by X-Ray Fluorescence Spectrometer (XRF). All the major and minor element contents were reported as oxide. The least altered samples were selected and all opaques were taken out from the samples

The powdered rock samples were prepared as pressed pellets by using HBO_3 (boric acid) as the blindmaterial at the ratio of sample: binder of 8:2 and mixed in tungsten carbide mill and pressed at the pressure of 400 kg/cm^2 for 1 minute. The analyses were done for major and minor elements by XRF model PW2400 following the method described by Takashima et al. (2005). The XRF method was done at the Department of Applied Earth Science and Technology, Faculty of Engineering and Resource Sciences, Akita University, Japan.

1.4.2.2.2 Inductively Coupled Plasma-Optical Emission Spectroscopy (ICP-OES)

The other trace elements namely Niobium (Nb) and Yttrium (Y) and rare earth elements; Lanthanum (La), Cerium (Ce), Praseodymium (Pr), Neodymium (Nd) , Samarium (Sm), Europium (Eu), Gadolinium (Gd), Dysprosium (Dy), and Ytterbium (Yb)

were analyzed by Inductively Coupled Plasma Optical Emission Spectrometer (ICP-OES), following the method reported by Boss et al. (2004).

The powdered rock samples were prepared by dissolving 0.2 g of the powdered rock samples in the acid mixture of conc. HNO_3 , HF and HClO_4 and diluted to 100 ml and was used for analyses by ICP-OES method for trace and rare earth elements, respectively. The calibration curve of each element was prepared from the standard solution for ICP-OES and evaluated the reliability of the analyses by analyzing the reference rock material; i.e., GSJ standard which prepared by Japanese Rock Standard. The ICP-OES method was done at the Department of Earth Science and Technology, Faculty of Engineering and Resource Science, Akita University.

1.4.2.2.3 Inductively Coupled Plasma-Mass Spectrometry (ICP-MS)

In this study, rare earth element were carried out by Inductively Coupled Plasma Mass Spectrometry (ICP-MS) which is one of the powerful tools for multi-element analysis for various kinds of materials with very low concentration less than ppb level (Sato et al., 1999). The 17 rare earth elements are Scandium (Sc), Yttrium (Y), Lanthanum (La), Cerium (Ce), Praseodymium (Pr), Neodymium (Nd), Promethium (Pm), Samarium (Sm), Europium (Eu), gadolinium (Gd), Terbium (Tb), Dysprosium (Dy), Holmium (Ho), Erbium (Er), Thulium (Tm), Ytterbium (Yb), and Lutetium (Lu).

The powdered rock samples were decomposed by a mixture of perchloric (HClO_4) and hydrogen fluoride (HF) in small Teflon reaction vessels covered by a duralumin container at 150°C on a hot plate. The ICP-MS method was also found to be suitable for granitic rocks for which digestion have been difficulty because of some refractory minerals such as zircon and spinel (Sato et al., 1999). The calibration curve of each element was prepared from the standard solution for ICP-MS and evaluated the reliability of the analyses by analyzing the reference rock material; JB-1 and JB-1HINA which prepared by Japanese Rock Standard. The ICP-MS method was done at the Department of Earth Science and Technology, Faculty of Engineering and Resource Science, Akita University.

1.5 Geography and Physiography

The study area is covered by regolith, a layer of loose, heterogeneous material covering solid rock and surrounded by flat area. It is divided by water drainage between Pichit province in the east and Phetchabun province in the west. Land in study area has an elevation of 5-10 meters higher than the surrounding low lying. Land uses in the study area are characterized by a layer of laterite averaging some 5 meters in thickness. The term regolith was first defined by George (1897) (American geologist) who stated, "In places this covering is made up of material originating through rock-weathering or plant growth in situ". In other instances it is of fragmental and more or less decomposed matter drifted by wind, water or ice from other sources. This entire mantle of unconsolidated material, whatever its nature or origin, it is proposed to call the regolith (George, 1897). However, the regolith (20 m-long) in the study area overlying the granodiorite rocks will not be studied in more detail.

The study area is in the tropical zone and climate can be divided into three seasons, i.e. summer, rainy and winter. The summer season commonly ranges from March to April and the highest temperature. The rainy season usually starts in May and will last till range from November to February and the lowest temperature (Aswasereelert, 2001). Most of the lands in this area are used for cultivation. The cultivation crops are mainly maize, graphs, sugar cane, peanut, season fruits etc. Most of crops have been cultivated in the undulating terrain surrounding the mining site.

1.6 Previous works in the study area

It is widely accepted that in the Loei-Petchabun volcanic belt, there are more intrusive than volcanic rocks exposed in Loei subprovince, i.e., diorite at Amphoe Ban Na, Nakhon Nayok (Sitthihaworn and Tiyaipairach, 1982), porphyritic quartz-monzonite, monzonite, diorite and granodiorite in Phu Lon area, Amphoe Sankho, Changwat Nongkhai (Sitthithaworn, 1989), diorite and granodiorite at Amphoe Khok Samrong and Tambon Khok Krathiem, Chagwat Lopburi, diorite and granodiorite at Amohoe Pak Chong, Changwat Nakhorn Ratchasima, and granodiorite of Changwat Phetchabun. These intrusive rocks are commonly associated with andesite, rhyolite and andesitic tuff, and generally produce skarn deposits of iron and copper (usually malachite and

chalcopyrite). In some relatively well studied areas, such as the Phu Lon, significance amounts of native gold, electrum, silver and molybdenite in affiliation with magmatite and chalcopyrite have been reported to relative intrusion which show indication of skarn and porphyry copper deposit (Sithithaworn et al., 1992).

In the Chatree region, there are 4 stratigraphic units, viz. Unit 1: Fiamme breccia (and Andesitic volcanoclastic facies, Unit 2: Epiclastic and fine volcanoclastic sedimentary facies and Rhyolite Breccia Facies, Unit 3: Polymict and Monomict Andesite Breccia Facies and Unit 4: Polymict and Monomictic Andesitic Breccia facies and Coherent (Cumming et al., 2004).

The geology, mineralization, alteration and geochronology in Chatree gold deposit has been studied intensively by several geoscientists (Diemar, 2000; Marhotorn, 2002; Deesawat, 2002; Kromkhun et al., 2005; Crossing, 2004; Corbett, 2004; Cumming et al., 2004; Sangsiri and Pisutha-Arnond, 2008, Nakchaiya et al., 2008; Marhotorn et al., 2008; Tangwattananukul et al., 2008; Salam et al., 2008) . The Quick-bird image of prospect area is shown in Figure 1.3 all existing previous data appears Table 1.1.

Very recently, Salam et al. (2008) reported geochronology of mineralization and timing of plutonic and volcanic activities. These will be explained in more detail in the discussion part.

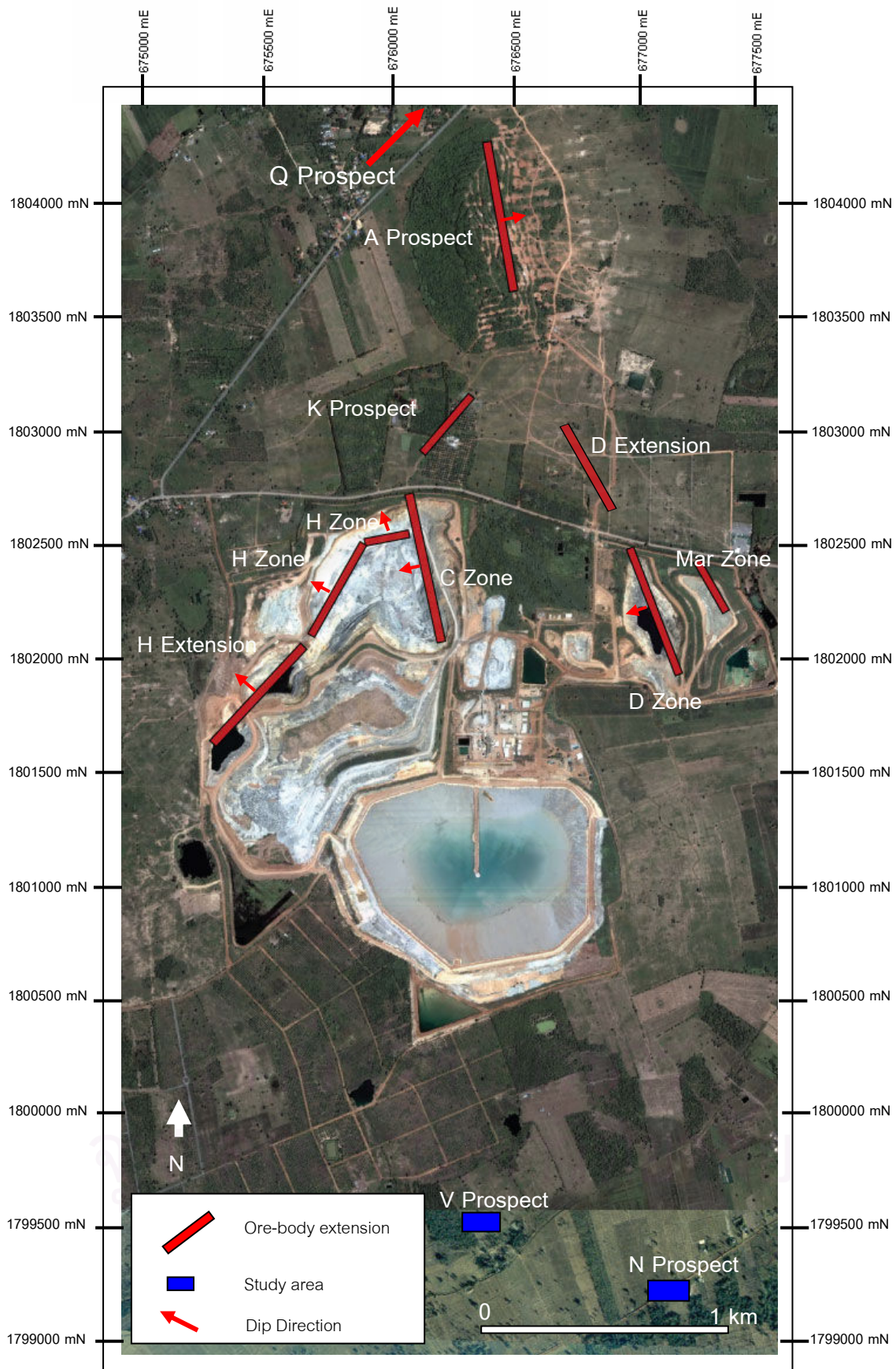


Fig. 1.3 Quick-bird remote sensing image in the year of 2002, Chatree gold mine showing locations of A Prospect, C Zone, D Zone, H Zone, K Prospect, Mar Zone, Q Prospect and the study area (N and V Prospects - box areas) in the southern part.

Table 1.1 Reviews of the existing previous data of Chatree gold deposit, Pichit-Petchabun, Thailand.

No.	Prospect	Rock Type	Mineralization	Epithermal/Alteration	References
1	Regional Chatree Deposit	4 stratigraphic units (coherent, non-coherent, sedimentary rock)	The major ore assemblages are banded quartz-carbonate-sulphide ores (chalcopyrite, sphalerite etc.) and banded quartz-carbonate-pyrite veins (occurring along the C prospect, D prospect, H north prospect and H central prospect).	Low sulfidation, quartz-carbonate and yellow sulfides	Cumming et al. (2006)
		Sedimentary rock, Volcanic rock, Intrusive rock	As both veins and veinlets	-	Crossing (2005)
		Sedimentary rock, Volcanic rock, Intrusive rock	Observed in the area of A, K, N and Q	A, K, N and Q which are silicification, locally in association with siliceous fluidised breccias and overprinting the K-feldspar alteration, potassic alteration, may be related to a plumbing system for the early grey silicification, respectively	Corbett (2004)
2	N	Multiphasal intrusions (granodiorite)	Porphyry Mo-Cu mineralization related to overprinting diorite intrusions. Low grade Au and Ag with Cu consistently in the order of 0.16%	Potassic alteration occurs as pervasive and vein magnetite with minor secondary biotite and grades to marginal propylitic alteration characterised by pyrite-chlorite-epidote dominant assemblages.	Corbett (2004)
		granodiorite, andesite	Quartz-sulfide vein, sulfide disseminated throughout the rock and also formed veinlet which associated with quartz veinlet and unmineralized calcite (secondary?) veinlet in the late stage)	Pervasive potassic alteration (biotite-chlorite-K-feldspar), Phyllic selective alteration (quartz-chlorite-sericite-opaque veins)	Marhotom et al. (2008)
3	C-H	Coherent and non-coherent	coherent and non coherent (monolithic breccia) units show strong alteration with associated Au-Ag mineralization	Propylitic alteration (chlorite, epidote)	Nakchaiya et al. (2008)
		Coherent	Depositional environment of host volcanic sequences mainly subaerial to shallow submarine. There are five vein stages of mineralization.	Low sulfidation, hydrothermal alteration indication gray quartz, quartz-calcite-chlorite-illite-ikkite/smectite-sericite-ankerite-domite-epidote-andularia-pyrite-hematite-rhodochrosite-chacedony-sphalerite-galena-chalcopyrite-electrum, quartz-k feldspar-carbonate-epidote-pyrite, calcite veinlet and joint surface coating	Kromkhum and Zaw, (2005)

Table 1.1 (Cont.)

No.	Prospect	Rock Type	Mineralization	Epithermal/Alteration	References
3	C-H	Veins in volcanic	Gold, chalcopyrite, pyrite, sphalerite, electrum, fluid inclusion (178° and 268°), salinities less than 5.3 wt.% NaCl equiv.	Low sulfidation, quartz-carbonate	Marhotorn (2002)
		Basaltic dyke	Not associated with mineralization	Propylitic alteration (chloride, epidote sericite)	Tangwattana nukul et al. (2008)
		Veins, stockworks and breccias	Gold, silver, galena and sphalerite. Gold values occur over a wide range of grade, with the average being 2.5 ppm.	Low sulfidation	Diemar et al. (2000)
		Volcanic and vein	Quartz-calcite vein/veinlet associated with quartz, calcite, andularai, pyrite (Low sulfidation). Gold, chalcopyrite, pyrite and sphalerite are significant in quartz-calcite vein/veinlet style.	K-silicate plus porphyritic, cherty quartz, milky quartz, quartz-calcite vein/veinlet, clay, supergene oxidation	Deesawat (2002)
4	H	Coherent and non-coherent	Five vein stages, gold and mineralization associated with stage 2, the mineral of stage 2 consisting of quartz, calcite, chlorite, illite, illite-smectite, sericite, ankerite, dolomite, epidote, andularia, pyrite, hematite, rhodochrosite, chalcedony, sphalerite, galena, chalcopyrite and electrum	Hydrothermal alteration	Krumkhun (2005)
5	Q	Silica-sericite-pyrite-milled matrix	Gold mineralization is controlled by later pyrite on fractures	related to a plumbing system for the early grey silicification	Corbett (2004)
6	K	grey silica breccia	High Au-Ag mineralisation occurs in association with pyrite-yellow sphalerite-carbonate and silver minerals, and so displays an association with carbonate-	locally in association with siliceous fluidised breccias and overprinting the K-feldspar alteration.	Corbett (2004)
7	A East	silicification of the host sediments	Association with the quartz-ginguro veins, likened to low sulphidation adularia-sericite epithermal Au-Ag quartz vein deposit.	Low sulfidation, silicification	Corbett (2004)
		non-coherent	The host rocks distal from the mineralized zones are dominated by propylitic alteration assemblage such as chlorite/serpentine and/or Fe-Ti oxides	silicification, quartz-adularia alteration and propylitic	Sangsiri and Pisutha-Amorn (2008)
8	V	Andesite	Altered porphyritic andesite characterized by sericitized andesine, relict hornblende and strongly porphyritic texture. Groundmass with plagioclase, sericite and opaque minerals exhibits prominent flow and glassy textures.	Prophyritic (more epidote, chlorite), mineralogy is characterized by epidote replacing plagioclase, chlorite replacing amphibole, and sericite replacing plagioclase and devitrified glass.	Marhotorn et al. (2008)

CHAPTER II

REGIONAL SETTING

2.1 Tectonic Framework of Thailand

The tectonic evolution of Thailand has been systematically re-constructed by Bunopas and Vella (1983), then by Bunopas and Vella (1992) and subsequently revised by Charusiri et al. (2002). Based on the tectonic evolution syntheses of Bunopas and Vella (1992), Thailand was composed of two main tectonic terranes, the Shan-Thai in the west, and the Indochina in the east. Their amalgamation line is situated along the Nan Suture. The Shan-Thai block occupied eastern Myanmar, western Thailand, Laos, Cambodia and some parts of Vietnam. In Thailand, the Shan-Thai terrane comprised basement of granitoids and high-grade metamorphic rocks which were believed to be of Precambrian age (DMR, 1999). The basement was overlain by sedimentary and metamorphic sequences of Palaeozoic, Mesozoic and Cenozoic ages. While the Indochina terrane comprised Permian platform-carbonate and deep-water clastic rocks is covered by the Mesozoic sequence of the Khorat Group, without any exposed Precambrian rocks. Bunopas and Vella (1992) stated that Shan-Thai and Indochina blocks were amalgamated along a moderately high angle, westward-dipping Benioff zone, to form the so-called Nan Suture, before the end of the Triassic. There were two fold-belts, originating from mid-Paleozoic to Triassic sedimentary basins, located between the Shan-Thai and Indochina. They were the Sukhothai Fold-Belt and the Loei Fold-Belt, along the eastern side of the Shan-Thai block and the western side of the Indochina block, respectively. Bunopas and Vella (1992) divided the tectonic evolution in Thailand into four episodes: Archaeotectonic, Palaeotectonic, Mesotectonic and Neotectonic

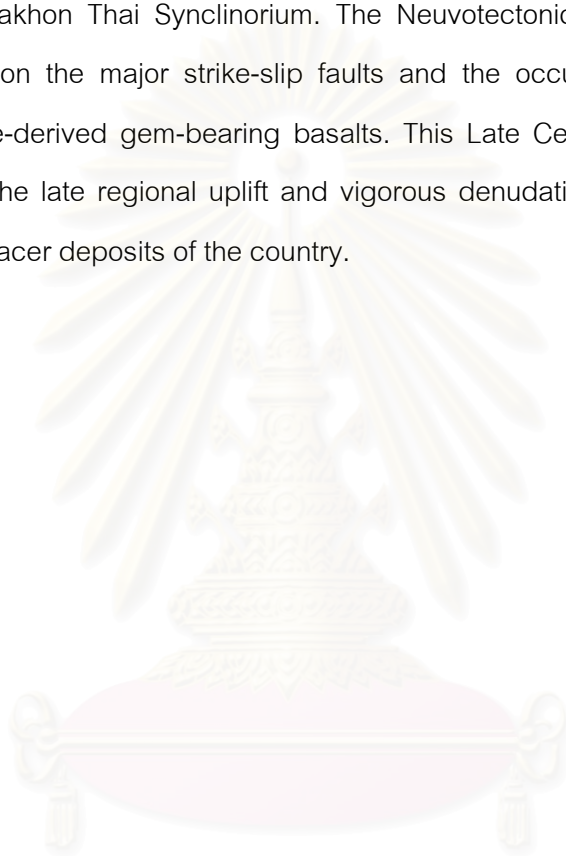
Charusiri et al. (2002) collected and gave the more recent information, particularly geochronology and petrology, and presented the latest synthesis of Thai tectonic evolution. They proposed two new small geological terranes, named as the Lampang – Ching Rai block and the Nakhon Thai block in the former Sukhothai fold-belt and Loei fold-belt, respectively. These new geological blocks were related to major

terranes, Shan-Thai and Indochina, which were initially associated with the Gondwana supercontinent.

Thailand comprises two major tectonic terranes, the Shan-Thai and Indochina, which were amalgamated in the Late Triassic. Four main tectonic stages are recognized herein on tectonostratigraphic and geochronological grounds, viz. Archaeotectonic, Paleotectonic, Mesotectonic and Neotectonic.

In the archaeotectonic stage, the Shan-Thai and Indochina microcontinents constituted detached, probably Precambrian, high-grade metamorphic, cratonic fragments of the Gondwana and Pan-Cathaysia supercontinents, respectively. The paleotectonic stage commenced with a major marine transgression (Paleotethys) over both Shan-Thai and Indochina extending from the Cambrian to the Permian. Following oceanic subduction during the Middle Paleozoic, two newly proposed, smaller tectonic blocks intervened between Shan-Thai and Indochina, namely the paleotethyan "Nakhon Thai" ocean floor to the east and the "Lampang-Chiang Rai" (Fig. 2.1) volcanic arc to the west. Rapid drifting of Shan-Thai to lower latitudes from its parent landmass is recorded by Permo-Carboniferous, glacio-marine diamictes. A transition to warmer environment recorded for Shan-Thai, and all terranes were close to the paleo-equator, as shown by carbonate platform facies along the continental margin during the Late Permian. Flysch- and arc-type sedimentation took place during Triassic over almost all terranes. The advent of the mesotectonic stage is marked by the collision of all terranes, termination of Paleotethys, development of the major NE- and NW-trending strike-slip faults, and the emplacement of the voluminous Eastern (I-type granitoids with Cu-Fe-Pb-Zn-Au deposits) and Central (S-type dominated, Sn-W-Nb-Ta-REE deposits) Granite Belts. Paleomagnetic relationships demonstrate that Shan-Thai was very close to Indochina at low latitudes in the northern hemisphere during the very Late Paleozoic. All terranes attained the mid-latitudes of the northern hemisphere and came to a halt during very Late Triassic to Early Jurassic times. Thrusting of Shan-Thai over Lampang-Chiang Rai, eastern Lampang-Chiang Rai over Nakhon Thai, eastern Nakhon Thai block over western Indochina in eastern Thailand, and partly Shan-Thai over Indochina, triggering the Mesotethyan incursion to the west, may have generated Jurassic-Cretaceous, continental sedimentation over much of Lampang-Chiang Rai, Nakhon Thai, western

and southwestern Indochina, respectively. The end of the Mesotectonic stage (Early Tertiary) is marked by the termination of Mesotethyan transgression in the Shan-Thai/Western Burma collision, causing the generation of the Western (richly-mineralized S-and I-type) Granite Belt. The collision of India with Asia during the Early Eocene marked the beginning of the neotectonic stage, which in turn caused the regional uplift of the Mesozoic Khorat and affiliated basins and the generation of the Phu Phan Anticline and Nakhon Thai Synclinorium. The Neotectonic stage is marked by the reverse motion on the major strike-slip faults and the occurrence of Middle to Late Miocene, mantle-derived gem-bearing basalts. This Late Cenozoic eruption may have been linked to the late regional uplift and vigorous denudation, generating major, Sn-, Au-, and gem-placer deposits of the country.



สถาบันวิทยบริการ
จุฬาลงกรณ์มหาวิทยาลัย

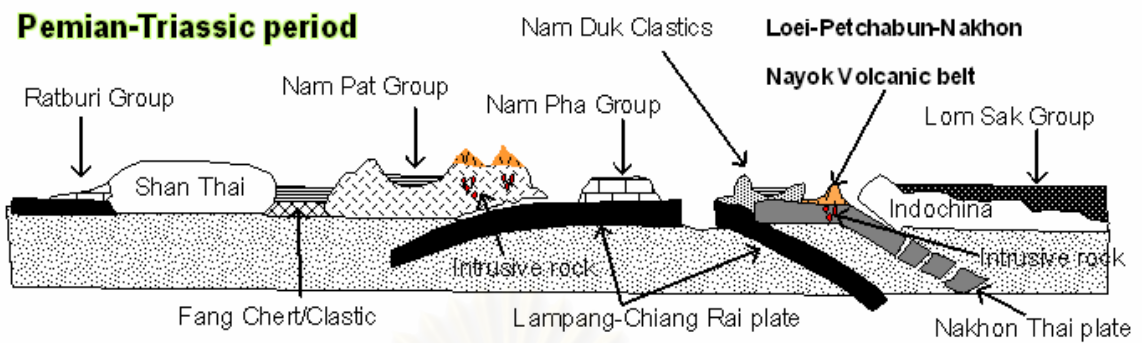


Fig. 2.1 Tectonic model of Thailand during Permo-Trassic Period showing distribution and interaction of tectonic plates (modified from Charusiri et al., 2002).

สถาบันวิทยบริการ
จุฬาลงกรณ์มหาวิทยาลัย

2.2 Igneous Rocks of Thailand

Intrusive and extrusive igneous rocks are widespread in Thailand, except for the northeastern part of the country (Khorat Plateau). It is evident that metallic and non metallic ores, especially those of hydrothermal origin, including tin, tungsten, copper, iron, gold, columbite-tantalite, feldspar, fluorite, lithium-bearing minerals, and rare earth-bearing minerals (monazite and xenotime) are closely related to some types of granitoid in space and time (Charusiri et al., 1993). A better understanding of the evolution and distribution of granites would be of benefit to mineral exploration in Thailand.

2.2.1 Intrusive Rocks

The granites of the Thailand crop out as the north-south trending elongated zone more than 2500 km long and 600 km wide extending throughout the Southeast Asian region (Charusiri et al., 1993) (Fig. 2.2). The regional extension of these belts is to Malaysia, Singapore and Indonesia in the south and the southern Yunan in the north. It is well documented that granite belt is one of the world (Charusiri, 1989). The exploited tin minerals from this region comprise three-quarters of the total world tin production (Nakapadungrat, 1982). From 1983 till the present, 40% of primary tin ores has been recovered in this region. These granites can be grouped into three sub-parallel magmatic belts or provinces based on their field occurrence, petrography and chemical characteristics

Eastern Granitoid Belt

This belt of mainland SE Asia extends from Billiton Island in the south, Indonesia, eastern Peninsular Malaysia, eastern Thailand through the edge of Khorat plateau in the central and ends at Laos and southern Yunan in the north. Generally this granitic belt is emplaced in Upper Paleozoic sedimentary and volcanic clastic sequences. Granitic activity was accompanied by volcanism which persisted from Carboniferous to the Late Triassic. The largest body of granitoid rocks is the Tak Batholith in Tak province, north Thailand which has been systematically studied by Teggin (1975). Smaller plutons are located in the areas of Phrae-Nan, Lumpang, Loei, Chantaburi and Narathiwat province.

This terrain is characterized by high level epizonal, felsic to mafic plutonic rock with diorite, granodiorite and granite predominant rock types. Subvolcanic and volcanic

suites of expanded composition range similar to those of the plutonic rocks are a common association within this terrain. Characteristic petrographies of the granites are coarse to medium-grained, equigranular, phaneritic texture with subordinate porphyritic and foliated textures. Dark colored xenoliths of mafic composition are relatively abundant. Essential minerals in the granites are 2 feldspar (alkaline and plagioclase), quartz, and hornblende, and biotite. Alkali feldspar is dominantly pink orthoclase. Plagioclase is mainly composed of rich calcium but oligoclase to andesine is insignificant. Plagioclase formed complex zoning being very common. Greenish brown to green hornblende and biotite are major mafic minerals and muscovite is rare. Geochemical studies of Eastern Granitoid Belts (Mahawat, 1982 and Charusiri, 1989) indicated that the granitoids originate from differential crystallization of partial melting from true magma, "sensu stricto". According to the classification of Chappel and White (1974), this granite is of I-type affinity. The Eastern Granitoid Belt possesses a widest range of SiO₂ content (57.16 to 76.33%). A large quantity of magnetite is also present in the rocks. The granitoids are called magnetite series granitoid, following the classification of Ishihara et al. (1981). Magnetite, zircon, sphene and apatite are common accessory minerals.

Charusiri et al. (1993) sub-divided granitoid of Eastern belt, using petrological and ⁴⁰Ar/ ³⁹Ar geochronological characteristics, into 4 episodes. It has been found that ages of the granitoids range from 210 to 245 Ma and can be grouped into 4 intervals; viz. 210 Ma, 220-225 Ma, 227-235 Ma, and 240-245 Ma. With integration of geological study in Loei province, it has been interpreted the granitoids of older interval (>240 Ma or earlier Triassic to Permo-Triassic) is likely to be associated with and related temporally and spatially to gold mineralization whereas granitoids of younger interval (220-225 Ma) are responsible for iron, copper, lead and zinc mineralization. The average age of granitoids at Doi Ngom, Phare province is 235 Ma. A granitic trend from Chantaburi province to the Thai-Cambodia border was dated at approximately 210 Ma (Late Triassic), which is younger than that of Tak province.

Central Granitoid Belt

Central Granitoid Belt occupies mainly the north-western part of the country extending from the Thai-Myanmar border in the north to Gulf of Thailand and covers also

the eastern part of the Peninsular area. The Central Granitoid Belt covers most of Thailand (Charusiri et al., 1993). In most cases, the granites intruded Lower Paleozoic sedimentary sequences and show close association with migmatite and the high grade metamorphic rocks of the region. Lithologically, these granites are coarse to very coarse grained porphyritic with large (up to 6-7 cm long) K-feldspar, phenocryst and often show preferred orientation in the matrix comprising quartz, K-feldspar, plagioclase and biotite. Hornblende, sphene, zircon, apatite and ilmenite are common accessory mineral. Primary muscovite and tourmaline were observed in the Ternary plots, these granites are syenogranite, monzogranite, quartz syenite and quartz monzonite. Within Thailand, this granitoid belt encloses the areas of Chaingrai, Chiangmai, Lampang, Lumphun in the north; Chonburi, Rayong in the east; and Suratthani, Nakorn Srithammarat, Songla, Yala in the south. In comparison, the granitoids of the Central Granitic belt is quite different from those of the Eastern Belt in both origin and geological environment. The country rocks intruded by Central Belt granitoids are mainly Late Paleozoic to Early Mesozoic clastic sedimentary rocks without any associated voluminous volcanic or volcano-sedimentary rocks.

More than 90% of granitoid rocks in this belt are largely confined to granite *sensu stricto*, following the classification of Streckeisen (1976). The belt is considered to be characterized by mesozonal, porphyritic, coarse-grained, biotite-rich plutons (Hutchison, 1983; Cobbing et al., 1986; Charusiri, 1989). Mafic minerals such as green hornblende are not common. Muscovite is normally found and increasingly present in the areas adjacent to tin-tungsten deposits. Quartz is found in equal amounts to feldspar. Long laths of megacrystic feldspar are frequently microcline and microcline-perthite. Geochemistry of granitoids in this belt verifies that they originated from the partial melting of pre-existing upper crustal rocks or pelitic sediments. According to the classification of Chappel and White (1974), the granitoids are of S-type affinity, narrow range of SiO₂ content (65.20-77.21%) but contains high to very high alkali elements. In other category, when ilmenites in these granitoids are taken into consideration, the granitoids are classified as ilmenite-series granitoids (Ishihara, 1977). However, geological and petrochemical analyses indicate that I-type granitoids and magnetite-

series granitoids are sporadically present as well, however in a much smaller amount in this belt (Charusiri et al., 1993).

$^{40}\text{Ar}/^{39}\text{Ar}$ dating (Charusiri, 1989) estimates the age of the Central Granitoid Belt as 180-220 Ma. This period is further subdivided into 2 intervals; 200-220 Ma for northern Thailand, and 180-200 Ma for southern Thailand. The ages of mineralization of Major tin-tungsten deposits such as Doi Mok, Chiangrai province, Tung Luang, Lampang province; Tung Po-Tung Kamin, Songkla province; and Pinyok, Yala province, etc., are mainly in the same of granites in the Central Belt. However, some known tin-tungsten deposits which carry rare earth elements (Khantaprab et al., 1990) such as Samoeng in Chiangmai province, and Khao Kamoi in Supanburi province have been proven to be 56 Ma (Tertiary) whereas the main phase granitoids in those areas were previously stated to be of 220-240 Ma (Teggin, 1975; Nakapadungrat et al., 1984). Charusiri et al., 1991) concluded from their recalculation of Rb-Sr whole-rock data that most of the granitoids of the Central belts are of S-type affinity on the basis of high initial Sr isotopic constraints.

Western Granitoid Belt

Western Granitoid Belt lies to the west of the Central Granitoid Belt along the Thai-Myanmar border from Mae Lama Stock, adjunct to northern end of the Moei-Uthai Thani fault zone to Phuket Island in the southwest of the Thai Peninsula. In general, the Western Granitoid Belt contains small to moderate batholiths and plutons of mainly restricted compositional range with a minor amount of the expanded type. Most of these granite plutons intruded into Permo-Carboniferous pebbly rocks of Kangkrachan group with a few exceptions, such as the Mae Lama Stock in Mae Hong Son which intruded into Cambrian and Ordovician and Ordovician sedimentary rock units. Intrusion of the Western Granitoid Belt into the border zone of the Central Granitoid Belt is not uncommon and the earlier often show less deformed features. Clarke and Beddoe-Stephens (1987) assigned Cretaceous Sn-W associated granite in northern Sumatra to the Western Granitoid Belt.

Geological, petrochemical and mineralogical studies on granitoids of the belt reflect true granite (Streckeisen, 1976) which, again, is similar to those of Central Granitoid Belt. Hornblende is relatively rare whereas brown biotite and muscovite are

very common, as well as quartz and microcline. Geochemically, about 98% of the granitoid rocks in this belt are of S-type and ilmenite-series granitoids are present locally, e.g. those in Phuket and Phang Nga areas (Charusiri, 1989) and in Amphoe Muang Prachaub Khirikhan. The Western Granitoid Belt also has a wide range of SiO₂ content (56.01-75.83%) similar to those of the Eastern Granitoid Belt. However, the majority of the granites of Western Granitoid Belt are highly alkali and possess S-type of Ilmenite Series characteristics. The calc-alkaline variety of the I-type of Magnetite Series granite plutons is present in very small numbers.

Age determination using the ⁴⁰Ar/ ³⁹Ar method the granitoids from this belt reveals that both I-type and S-type granitoids in the Western Belt is 50-88 Ma (Late Cretaceous to Early Tertiary). These ages of granitoid emplacement can be further subdivided into 2 periods, 65-88 Ma and 50-60 Ma. Associated tin and tungsten deposits together with rare earth elements are inferred to have been related temporally and spatially with S-type granitoid also occur, but in smaller amounts, and are related to tin and tungsten-mineralization in northern and southern Thailand. These granites were reported by Nakapadungrat et al. (1984) to have 130 Ma age using the Rb-Sr whole-rock method.

Earlier works, such as those of Mitchell (1977), Hutchison (1978), Pongsapich et al. (1983), indicated that granites of SE Asia can be divided into 3 major belts on the basis of lithological, geological, and geochronological characteristics. These have been named the Western, Central, and Eastern Belts, Their details have been re-synthesized by many authors later based on new data, i.e. Charusiri et al. (1993). The characteristics of these granitic belts are summarized and illustrated (Table 2.1).

Charusiri et al. (1993) subdivided granitoids of these 3 belts into 3 periods by using ⁴⁰Ar/ ³⁹Ar dating data and those previously reported by other methods. They concluded Eastern Granitoid Belt formed in Early to Late Triassic (245-210 Ma), the Central granitoid belt in Late Triassic (220-180 Ma) to Middle Jurassic, and the Western Granitoid belt in Late Cretaceous to Middle Tertiary (80-50 Ma). I-type granitoid rocks are inferred to be related to Cu-Fe-Au-Sb mineralization and are largely limited to Eastern Granitoid belt.

Table 2.1 Summary of granitoid belts in Thailand (modified from Charusiri et al., 1993).

Topic	Western belt	Central belt	Eastern belt
Compositoin	True granite (Streckeisen, 1976), syeonogranite, monzogranite, quartz monzodiorite, quratz monzonite	<u>Sensu stricto</u> (Streckeisen, 1976), syenogranite, monzogranite, quartz syenite and quartz monzonite.	Gabbro, though quartz diorite and granodiorite, to granite.
Age	130-90 and 45 Ma; Rb-Sr W.R. 50-88 Ma ; $^{40}\text{Ar} / \text{Ar}^{39}$ 130-78 Ma ; $^{40}\text{Ar} / \text{Ar}^{39}$	180-220 Ma ; $^{40}\text{Ar} / \text{Ar}^{39}$ 220-240 Ma; Rb-Sr W.R. 73 Ma ; K-Ar biotite age	243 – 200 Ma 210 – 245 Ma ; $^{40}\text{Ar} / \text{Ar}^{39}$
Country rocks	Permian to Carboniferous clastic sedimentary rocks without volcanic associate.	Late Paleozoic to Early Mesozoic clastic sedimentary rocks without associated volcanic or tuff.	Upper Paleozoic clastic and volcanic tuff, sediments and shelf carbonates.
Pluton characteristics	Small to moderate batholith and pluton of restrict compositional range, commonly contain pegmatite and aplite.	Mesozonal, biotite-rich plutons	Display varying zone from "true granite" in the central part of the batholith graded to more mafic rich granitoid (quartz diorite, granodiorite) at the edge of the batholith.
Mineral assemblage	Quartz, microcline, biotite, muscovite and rarely hornblende	Quartz, muscovite, biotite feldspar (microcline and microcline-perthite) with rarely green hornblende.	Quartz, alkali-feldspar (orthoclase), plagioclase (oligoclase to andesine), greenish brown to green hornblende and biotite with subordinate muscovite.
Grain size and textures.	Coarse grained porphyritic with large K-feldspar phenocryst.	Megacrystic to equigranular and porphyritic, medium to coarse-grained, well-defined clastic texture, well-defined subhorizontal foliation	Mostly medium-to-coarse- grained and equigranular, but are locally porphyritic
Accessory mineral	Illmenite, apatite, sphene and zircon.	Allanite, apatite, garnet, monazite, sphene, tourmaline, zircon.	Apatite, sphene. zircon, magnetite and allnite.
Associated deposits	Tin, tungsten, REE-barring minerals	Tin, tungsten, REE-barring minerals	Base-metal, gold and iron mineralization tin-tungsten deposit
Origin of magma	-	Partial melting of pre-existing upper crustal rocks origin.	Originate from differential crystallization or partial melting from "true" magma
Affinity (A.)(Chappel and White (1974) (B.) Ishihara (1977)	S-type and I-type affinity ilmenite-series and magnetite-series	S-type affinity ilmenite and magnetite-series	I-type affinity magnetite series
Intial Sr isotopic ratio	0.719 – 0.744	0.725- 0.730 and 0.710 -0.727	0.705 – 0.715
Distribution	Dominant in Myanmar, Tak, Kanchanaburi, Prachaub Khirikhan, Ranong, Phang Nga and Phuket	Chiangrai, Chiangmai, Lampang, Lamphun, Chonburi, Rayong, Suratthani, Nakom Srithammarat, Songkla and Yala	Billiton Island, Indonesia, through eastern-Peninsular Malaysia, along western Khorat plateau edga of Thailand

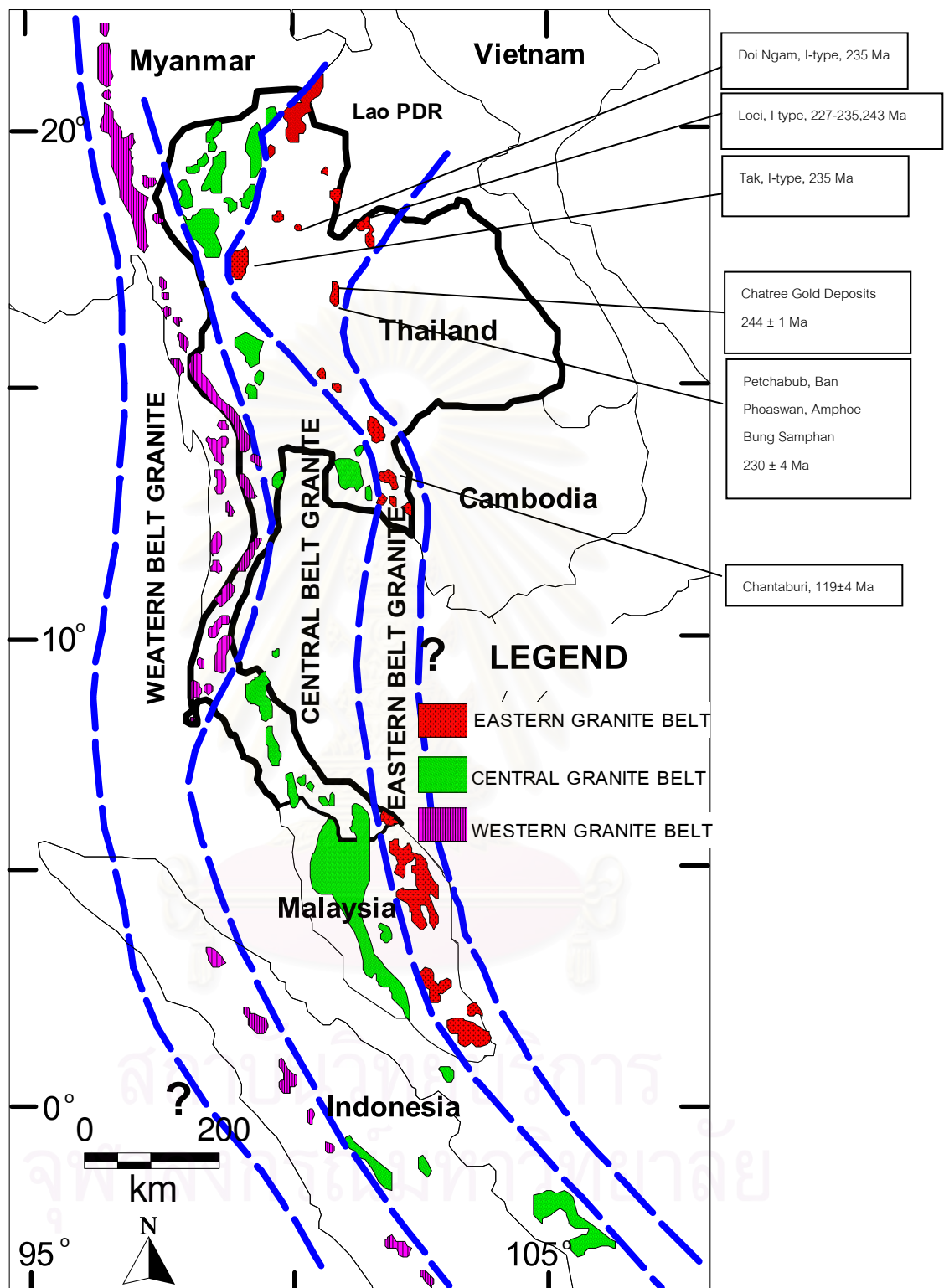


Fig. 2.2 Index map of mainland SE Asia showing distribution of granitoids and their ages of Eastern Belt during 220-245 Ma. Numbers in boxes are in million years (modified after Charusiri et al., (1993), Nantasiri et al. (2005) and Salam et al. (2008)).

2.2.2 Extrusive Rocks

Volcanic rocks are distributed in most part of Thailand, however, records of volcanic rocks exposed in Southern Thai Peninsular are very few. Based on their tectonic setting, distribution and ages of eruption, these volcanic rocks can be broadly grouped into Ching Mai Volcanic Belt, Ko Chang-Tak-Ching Khong Volcanic Belt, Loei-Prachanbun Volcanic Belts and Late Cenozoic Basalts (Jungyusuk and Khositanon, 1992, Phajuy et al., 2004. Charusiri (1989) divided into 4 volcanic belts; Chiang Mai-Chiang Rai (CC), Chiang Khong- Tak (CT), Loei-Petchabun-Nakhon Nayok (LPN) and Volcanic Rock along Nan-Chanthaburi Suture Zone (NCZ) (Fig 2.3).

Chiang Mai-Chiang Rai (CC) volcanic belt are basic lavas, hyaloclastic and pillow breccias (Panjasawatwong, 1993). Chemical characteristics of the San Kamphang basic volcanic rocks indicate that they are tholeiitic and transitional alkaline in composition. The basic volcanic rock Chiang Rai area may have formed in a subduction environment, but, the rest has erupted in an intraplate environment (Macdonald and Barr, 1978; Barr et al., 1990). Interpretation of the origin of the intraplate basalt is in controversy, whether it be continent affinities (Barr et al., 1990) or oceanic affinities (Panjasawatwong, 1993 and Panjasawatwong et al., 1995). The correlation ages of these volcanic rocks have been reported to be Late Carboniferous to Late Permian (Garman Geological Mission or GGM, 1972) and Mid Permian to Permo-Triassic (Chuaviroj et al., 1980; Bunopas, 1981; Bunopas and Vella, 1983; Panjasawatwong, 1993).

Chiang Khong- Tak (CT) volcanic belt is the most abundant volcanic rocks exposed in northern Thailand. The rocks vary in composition from intermediate to acid represented by andesite, rhyolite and pyroclastic rocks. Stratigraphic correlation indicates that the eruption of these volcanic rocks occurred in Permo-Triassic period. (Piyasin, 1972, 1975; Bruan and Hahn, 1976 and Charoenpravat, et al., 1987). However, subordinate volcanic eruptions possibly occurred in Upper Triassic to Lower Jurassic periods.

Loei-Phetchabun-Nakhon Nayok (LPN) Volcanic Belt is the main calc-alkaline rocks in the country which formed as the accurate belt with N-S trending along the western margin of the Khorat Plateau to Sra Kaeo in Eastern Thailand near Cambodia

border. Andesite and rhyolite are the predominant rock types with subordinate basaltic variety. Several episodes of volcanic activities occurred in this area which likely started as early as Middle Devonian (Intasopa, 1993). Other volcanic activities occurred during the Permo-Triassic period and ended at Late Tertiary. Rhyolite from the eastern Pakchom district yield a Rb/Sr isochem age of 374 ± 33 Ma with an initial $^{87}\text{Sr}/^{86}\text{Sr}$ ratio of 0.706 and the spilitic basalt (located 16 km south of Pakchom) gave a Rb/Sr isochem age of 361 ± 11 Ma with an initial ratio of 0.70455 (Intasopa, 1993). Both ages confirm the ages obtained from the stratigraphic correlation, Upper Middle Devonian in the early phase and Late Devonian in the later phase (Chairangsee et al., 1990; Jungyusuk and Khositanon, 1992).

Nan Suture (or Nan-Chanthaburi Suture Zone (NCZ)) and the Sukhothai Fold Belt reported by Singharajwarapan et al. (2000) that reflect the processes associated with the collision between the Shan-Thai and Indochina Terranes in Southeast Asia. The Shan-Thai Terrane rifted from Gondwana in the Early Permian. Preliminary geochemical data from volcanic rocks in the Loei Fold Belt, to the east of the Nan Suture, support subduction-related arc volcanism in that area, but Intasopa and Dunn (1994) showed that these volcanic rocks have diverse tectonic settings of eruption and range in age from Late Devonian to Triassic. The present evidence suggests that most of the volcanic rocks in the Loei volcanic province are older than the Sukhothai Fold Belt and are probably related to an older arc.

Late Cenozoic volcanic rocks are mainly basalts which distribute sporadically in the northern, eastern and central part of Thailand. These basalts can be subdivided into two major groups, the corundum-bearing basalt and the corundum-barren basalts. However, based on geochemistry the basalt can be subdivided categorized into basanitoids and hawaiiite basalts (Barr and Macdonald, 1981). The basanitoids comprise nephelinite, basanite, nepheline hawaiiite, and mugearite. In contrast, the hawaiiite basalts comprise alkaline olivine basalts, hawaiiite and mugearite. It is clearly noted that corundum is commonly associated with basanitoid basalts and not restricted to certain age. Major gemstone variety is sapphire, ruby, topaz, zircon and black spinel. Charusiri et al. (2004) observed at the area of Khao Kradong, Buri Ram Province, NE Thailand, Cenozoic basalt is middle to subalkaline basalt. The rocks are transitional from

hawaiite to alkali olivine basalt. In terms of tectonic setting, Khao Kradong volcano is regarded as representative of Cenozoic basalts of continental-rift origin. Sutthirat et al. (2001) reported that an inclusion of corundum (ruby) was found in a clinopyroxene xenocryst in alkali basalt from the late-Cenozoic Chanthaburi-Trat volcanics of eastern Thailand.

Jungysusuk and Khositantont (1992) interpreted the significance of gold occurrence in both Tak-Chiangkhong and Loei-Petchabun belts and typically associated with intrusive and shallow intrusive bodies. In Tak-Chiangkhong belt, gold can be found in the volcanic hosted quartz veins within the Phrae-Lampang volcanic province. Genesis of the gold-bearing quartz vein has not clear. However, they appear to be associated with gold-carrying hydrothermal fluids which were initiated by the late stage granite intrusion. Gold is typically disseminated within the veins which are typically formed in the N-S trend within the metavolcanic host rocks. This gold deposit may be classified as vein or stock-works depositing type.

The Chatree gold mine is located in the Loei-Petchabun volcanic belt extending approximately N-S through central Thailand. Volcanic rocks along the Loei-Petchabun Volcanic Belt formed in several stages from Late Devonian and extending to the Late Tertiary, with features indicating a diverse range of tectonic settings (Intasopa, 1993). The geochronological data of Charusiri (1989) and Intasopa (1993) show that the volcanism of the Loei-Petchabun-Nakhon Nayok Volcanic Belt occurred from Middle Paleozoic to to Late Cenozoic.

สถาบันวิทยบริการ
จุฬาลงกรณ์มหาวิทยาลัย

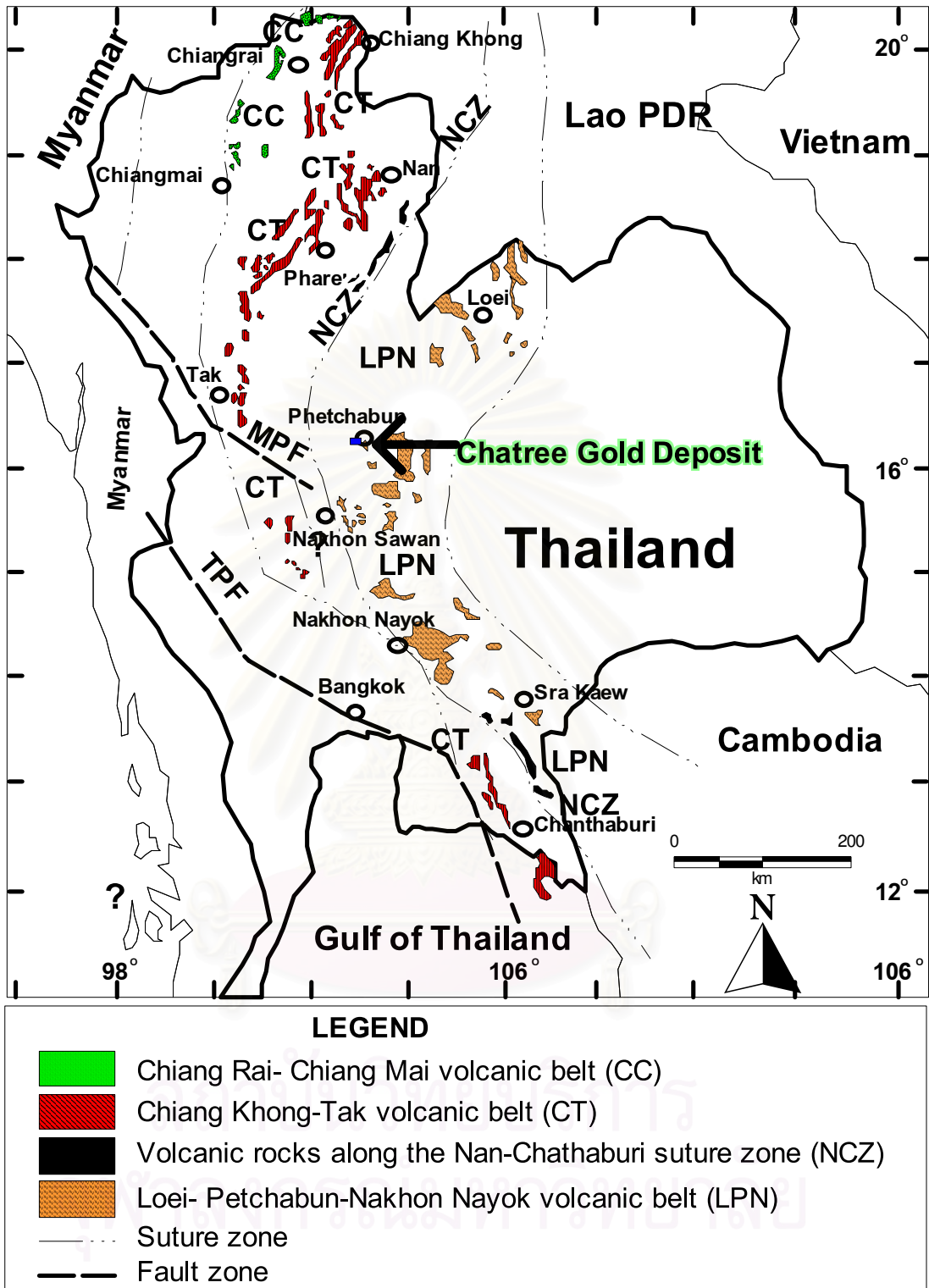


Fig. 2.3 Index map of northern half of Thailand showing location of the Chatree gold mine deposit within the Loei - Phetchabun -Nakhon Nayok Volcanic Belt (LPN) as well as the major faults and sutures in Thailand (modified from Intasopa, 1993, Charusiri et al., 2002 and Phajuy et al., 2004).

CHAPTER III

GEOLOGY

3.1 Regional Geology

The Chatree deposit lies within the Loei-Phetchabun-Nakhon Nayok (LPN) Volcanic Belt which extends from northern Laos through central Thailand and occupies east of Raub Bentong structure in Peninsular Malaysia (Intasopa, 1992). In Thailand, this volcanic belt is dominated by Upper Permian and Triassic parallel zones of island arc felsic to intermediate volcanic and Triassic marine sedimentary rocks which were formed above a subduction zone prior to and during the collision in the Triassic of the Shan-Thai and Southeast Asian continental plates (Bunopas and Vella, 1992). The volcanism is characterized by 3 volcanic successions, specifically Carboniferous basaltic andesite flows; Permo-Triassic andesitic-rhyolitic tuffs, flows and sub-intrusives, which mark the western margin of the Belt; and Neogene basaltic and rhyolitic flows, which are recorded in the southern portion of the Belt possibly representing the reactivation of a zone of crustal weakness (Intasopa, 1992). Permo-Triassic intrusives perceived as calc-alkaline, I-type granites including diorite, quartz diorite, granodiorite and quartz monzonite bodies are distributed throughout the Belt (Barr and Macdonald, 1991 and Garwin, 1993). Major structures in the Belt, from north to south comprise the southerly plunging Loei anticlinorium, the north-northwest oriented Chum Phae synclinorium and the west-northwest trending Saraburi anticlinorium (Garwin, 1993). Metal mineralization occurs in the Belt, characterized by base metals (Cu, Pb, Zn), iron ore, barite, manganese, pyrite, silver and gold. The majority of metallogenesis in the Belt is likely related to the Permo-Triassic intrusive magmatic-arc-related rocks and structural preparation provided by anticlinal folds formed during the late Triassic Indosinian Orogeny (Garwin, 1993, Charusiri et al., 1993).

The Chatree region is situated within the Loei-Phetchabun volcanic Nakhon Nayok belt, an arcuate belt of calc-alkaline volcanics that extends north-south along the western margin of the Khorat Plateau from Loei Province in the north to Ko Chang in the Gulf of Thailand. This large belt contains volcanic rocks of felsic to mafic compositions,

which deposited during several episodes of volcanic activities extending from Mid-Devonian to Late Tertiary (Jungyusuk and Khositant, 1992). They sub-divided the belt into six provinces and Chatree is within the Phetchabun Province, which is dominated by andesite and basaltic andesite. These volcanics are commonly associated with intrusive bodies of microgabbro, diorite, and granodiorite. Field relationships observed by Jungyusuk (1989) near Chon Daen in Phetchabun Province suggest that andesitic lavas flow over and locally crosscut mid Permian Limestones and are overlain by Tertiary sediment.

Crossing (2004) considered the Loei-Phetchabun-Ko Chang volcanic belt is considered to be a fossil continental arc developed on the Indo-China Plate during easterly directed subduction. It is situated within the Loei Fold Belt, a Palaeozoic-Mesozoic feature that consists of a series of north-south trending granitoid belts and associated volcanics. The Loei Fold Belt was formed as a result of collision between the Shan-Thai and Indo-China Plates, which resulted in the amalgamation or interaction of fossil arcs and microcontinents.

3.1.1 Sediments and sedimentary rocks

The Chon Daen-Thap Klo area is underlain by both sedimentary and igneous rocks ranging in age from Carboniferous to Quaternary. The Carboniferous unit consists mainly of limestone containing crinoids and coral fossils that are Lower to Mid-Carboniferous in age (DMR, 1999). Upper Carboniferous-Permian unit consists of sandstone (in part volcanic derived), shale, conglomerate and chert. Generally, this formation strikes NE-SW and dips SE. The rocks are locally metamorphosed along the contact with granodiorite.

The region of the Chatree deposit can be described following description of the geology of the Chon Daen-Thap Klo District (DMR, 1999). The Chon Daen-Thap Klo area is underlain by both sedimentary and igneous rocks ranging in age from Carboniferous to Quaternary. The Carboniferous unit consists mainly of limestone containing crinoids and coral fossils that are Lower to Mid-Carboniferous in age (DMR, 1999). Upper Carboniferous-Permian unit consists of sandstone (in part volcanic

derived), shale, conglomerate and chert. Generally, this formation strikes NE-SW and dips SE. The rocks are locally metamorphosed along the contact with granodiorite.

Fossiliferous limestone is often present at various stratigraphic levels, and vary from thin beds interbedded within the andesite lavas and pyroclastic (eg east of Khao Khieo) to very thick and persistent beds of massive limestone dominated by crinoids fossils more distal to the volcanic centres. These limestones are best exposed near Noen Maprang (Crossing, 2004).

Based on regional geologic map modified from Chongrakmani and Sattayarak (2004) regional geologic map shown in Figure 3.1. The sedimentary rocks can be divided into six formations as below; is

Phra Wihan Formation (PWF)

The rock is compose of sandstone, white pink, orthoquartzitic, cross-bedded, massive, with pebbly layers on the upper bed; some intercalations of reddish brown. The age of the rock is Lower-middle Jurassic period. The rock found in the NE of the regional geologic map.

Phu Kradung Formation (PKF)

The rock of this formation is found mostly in the NE of the regional area. The rocks are shale, brown, reddish-brown, purplish-red, micaceous; siltstone and sandstone, brown, gray, micaceous, small scale cross-bedding with some lime-nodule conglomerate. The age of the rock is lower Jurassic period.

Nam Phong Formation (NPF)

This formation exposes in the SE of the regional area. The rocks are sandstone, reddish brown, brown, cross-bedded, conglomerate, pebbles consisting of quartz, chert, red siltstone and sandstone, up to 10 cm in diameter; shale and siltstone, brown, reddish-reddish-brown. This Upper Triassic formation was found in the NE part of the regional area.

Huai Hin Lat Formation (HHLF)

Rocks in this Formation are dominated by yellowish brown conglomerate, yellowish brown to reddish brown sandstone, reddish brown siltstone, green conglomeratic sandstone showing cross-bedding. Part of these rocks is thermal by

metamorphosed. This Upper Triassic formation was found in the western part of the regional area.

Pha Nok Khao Formation (PNKF)

This formation consists of well bedded to massive limestones with black chert lenses, sandstone and shale. The age is also Lower-Middle Permian.

Unconsolidated diposits (Q)

The Quaternary sediments are the terrace deposit, talus pile and colluvial deposit, composing of gravel, sand, silt and clay. They were found in the western and eastern parts of the regional area. The western part of regional area is the study area.

3.1.2 Igneous rocks

The igneous rocks in this regional area are composing chiefly of felsic to intermediate volcanic rocks, pyroclastic rocks and plutonic rocks.

Volcanic and pyroclastic rocks

The rock are tuff, lapillistone, agglomerate, volcanic breccia, andesite and basaltic andesite. The unit indicates Permo-Triassic age as they were observed to lie between the Middle-Upper Permian and Upper Triassic unit.

Volcanic rocks with mafic to felsic compositions occur as lava flows, pyroclastic deposits, and dyke and sills. The volcanic rocks predominantly andesite, andesite tuff, basaltic andesite, andesitic breccia, rhyolite and rhyolitic tuffaceous rocks. Their ages rang from Middle-Upper Permian to Lower Jurassic (Jungyusuk and Khosithanont, 1992). Plutonic rocks are covered by unconsolidated sediments, however, airborne magnetic indicate that dykes and stocks of granodiorite intruded in the area, particularly in the southern part of the Chatree deposit. Stratigraphic relations constrain the age of these plutonic rocks to a minimum Triassic age (DMR,1999). Diemar et al. (1992) have been observed volcanic rocks in this belt which are basaltic andesite and andesite cross cut and flowed over middle Permian limestone and locally overlain by Triassic sedimentary rocks. Crossing (2004) has been interpreted in the Chatree region there are several andesitic volcanic centers and a couple of rhyolitic centres. Proximal to the andesictic volcanic edifices are intercalated lavas,

pyroclastics and volcanoclastic sediments displaying significant lateral facies variation and complex interfingering with adjacent volcanic centers. Thick andesite lava flows interdigitate with andesitic auto breccias, and these are interbedded with lithic (lapilli) tuffs of andesitic and mixed province, and less volumetrically important crystal and ash fall tuffs. The lithic tuffs are often very large and consistent and extend well beyond the andesite lavas, suggesting they may be large valley filling or submarine mass flows rather than air-fall tuffs. The volcano-sedimentary sequence is mostly gently folded, with dips mostly less than 30 and rarely exceeding 45 except near faults. In general the bedding becomes shallower dipping in the eastern half toward the edge of the Khorat plateau. Steeper dips occur in two NE-SW trending structural zones discussed below, especially in the immediate vicinity of large faults.

The Chatree gold mine is located in the Loei-Petchabun Volcanic Belt extending approximately N-S through central Thailand. Volcanic rocks along the Loei-Petchabun Volcanic Belt formed in several stages from Late Devonian and extending to the Late Tertiary, with features indicating a diverse range of tectonic settings (Intasopa, 1993). The geochronological data of Charusiri (1989) and Intasopa (1993) show the rocks of the Loei-Petchabun Volcanic Belt are Permo-Triassic to Miocene.

Loei-Petchabun-Ko Chang volcanic belt, an arcuate belt of calc-alkaline volcanics that extends north-south along the western of the Khorat Plateau from Loei Province in the north to Ko Chang in Gulf of Thailand. It is situated within the Loei-Fold Belt, a Paleozoic-Mesozoic feature that consists of a series of north-south trending granitoid belts and associated volcanics. The Loei Fold Belt formed as a result of collision between the Burmalayan and Indo-Sinain Plates, which resulted in the amalgamation of a collection of fossil arcs and micro-continents (Crossing, 2004).

Plutonic rocks

The intrusive rocks can be divided into 3 phases, including diorite, granodiorite and granite. The diorite is the dark grey with porphyritic texture. The phenocrysts are plagioclase and hornblende with the size of 1 x 1.5 cm. The granodiorite is the dark grey, mainly fine grained with porphyritic texture with 1x 0.5 cm. Phenocryst is hornblende. The granite is white in color. It has a porphyritic texture with phenocryst of plagioclase.

Muscovite was observed to be common in this granite. The plutonic rocks are of Triassic age but some may be younger. Become some of them were observed to intrude the Upper Triassic sediment units. The study area is located on boundary between Pichit and Phetchabun provinces, north-central Thailand. The study area lies within Loei-Phetchabun volcanic fold belt (Diemar et al., 2000) which extends from northern Laos through central Thailand and occupies east of Raub Bentong structure in Peninsular Malaysia. In Thailand, the belt is significantly bound by Upper Permian and Triassic parallel zones of ancient island arc that contains felsic to intermediate volcanic and marine sedimentary rocks.

Plutonic rocks are covered by unconsolidated sediments, however, airborne magnetic data indicate that dykes and stocks of granodiorite intruded in the area, particularly in the southern part of the Chatree deposit. Stratigraphic relations constrain the age of these plutonic rocks to a minimum Triassic age (DMR, 1999). Crossing (2004) mapped various intrusive rocks ranging in composition from felsic to mafic inplated into the sequence as small to medium sized stocks and dykes. Most common are mafic intrusive dominated by diorite but ranging in composition from granodiorite to dolerite, and texturally from fine, even grained to porphyritic. Granitic intrusions occur as several clusters of stocks and dikes, often associated with regional structural trends. Two such clusters occur in the vicinity of Chatree mine where they appear to be spatially associated with intersecting the southeast structural trends. However the largest cluster is arranged along a NE-SW structural trend extending through Ban Khlong Takhian, and most of these are porphyritic texture. Large intrusions of granodioritic and diorite composition also occur to the south and southeast of this area, and some of these are also porphyritic (Crossing, 2004).

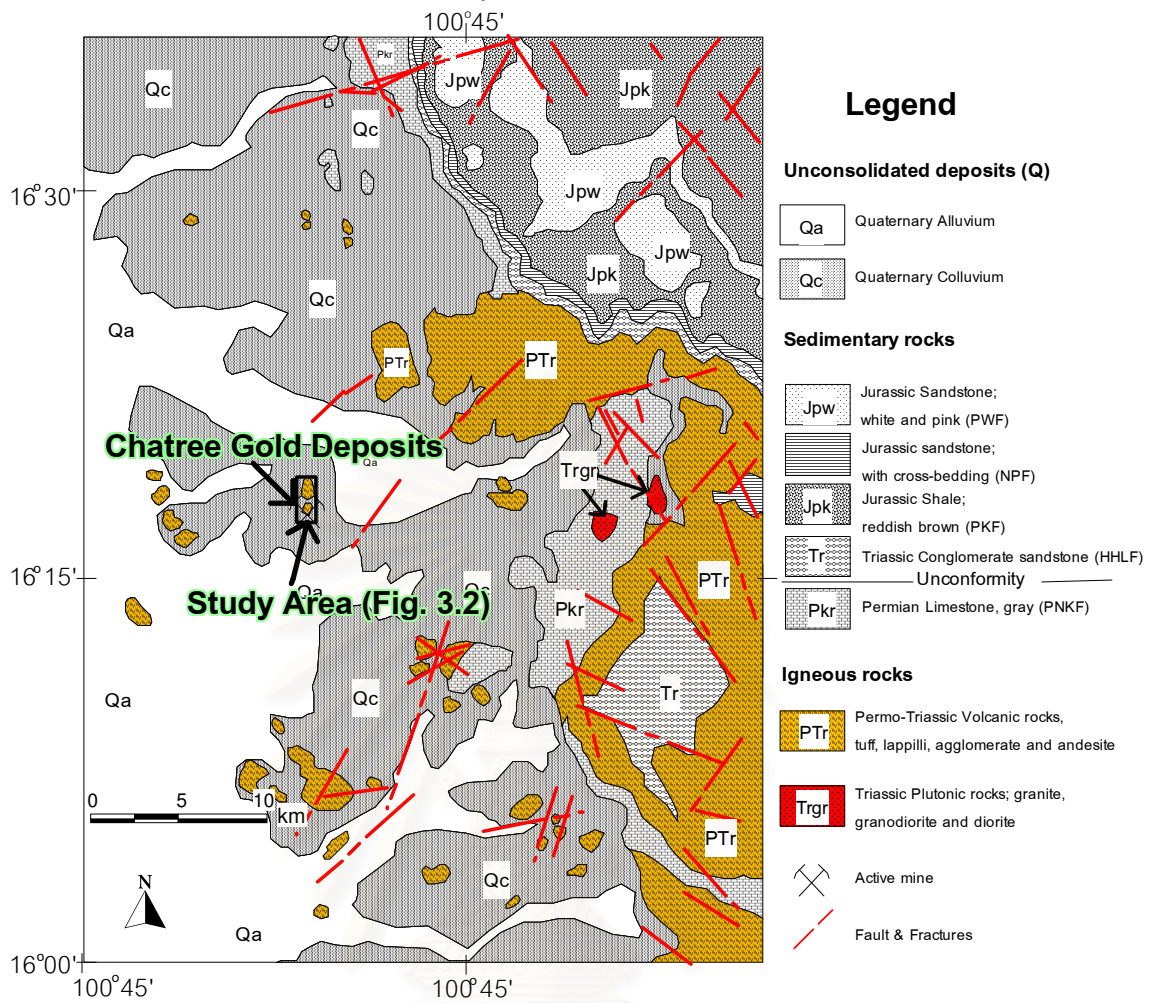


Fig. 3.1 Regional geologic map of the study area (modified from Chonglakmani et al., 2004). Abbreviation, PWF; Phra Wihan Formation, PKF; Phu Kradung Formation, NPF; Nam Phong Formation, HHLF; Huai Hin Lat Formation, PNKF; Pha Nok Khao Formation and Q; Quaternary Unit.

สถาบันวิทยบริการ
จุฬาลงกรณ์มหาวิทยาลัย

3.2 Detailed geology

In this section, geology of A Prospect, C-H zone, K Prospect and Q prospect of the Chatree gold deposit is described. N and V Prospects will be described herein and are described in the next chapter in much more detail.

A Prospect

At A East prospect, oblique normal movement on east dipping bedding parallel faults has created dilational fracture systems at the intersection of steep-dipping feeder structures; to form carrot shaped mineralisation zones. Sigmoidal veins parallel to the core axis dominate in west to east bored drill holes, and so it is recommended future east to west drilling might provide vein intersections at higher angles to the core axis (Corbett, 2004).

A Prospect, the results reveal of the A Prospect, the host rocks proximal to the mineralized zones are dominated by silicification, quartz-adularia alteration, followed by carbonates and finally Fe-sulfide – Fe-Ti-oxide – sphene/leucoxene assemblages. The host rocks distal from the mineralized zones are dominated by propylitic alteration assemblage such as chlorite/serpentine and/or Fe-Ti oxides (Sangsiri and Pisutha-Arnond, 2008).

C-H e and H zone

Gold-silver mineralization occurs as a low sulfidation quartz-carbonate-adularia style epithermal, occurring in shallow to steeply dipping structures carrying gold-silver bearing veins, breccias and stockworks, within a 7.5 by 2.5 kilometer zone silicified latitic and trachytic volcanic fragmentals and flows. The system is aligned in a north-northwest direction and enclosed by two large overlapping interpreted caldera structures. In the deposit, gold occurs as native gold and electrum in silica, calcite and on the boundaries of, in fractures within and as electrum, AgS and AgSe. Average silver/gold ratio in the deposit is 5:1. The associated 1-2% sulfides are represented 98% by pyrite with subordinate chalcopyrite, sphalerite and galena in decreasing amounts (Diemar et al., 2000).

Marhotorn (2002) mapped the C-H Zone and studied fluid inclusions. He interpreted the C-H Zone that emplacement of felsic to intermediate intrusive occurred in the Permo-Triassic Period. The country rock formed silicification and initiation of

brecciation by hydraulic fracturing. Hydrothermal fluid enriched in gas phase of magmatic sources ascended along normal faults for many times. The hydraulic fracturing increased permeability within and around the breccia bodies. The gas phased mixed with meteoric fluid, leading to more rapid cooling and dilution of the acidic fluid with temperatures between 178 and 268 °C and salinities less than 5.3 wt.% NaCl equiv. These fluids flowed laterally along the highly permeable rocks of Permo-Triassic Volcanic Formation where initial acid leaching enhanced the secondary of the host rock formation by the development of vuggy quartz. Late stage meteoric water dominated hydrothermal fluid activity at a lower temperature of around 163 °C. With decreasing temperature, silica-rich fluids deposited and sealed most of the pore spaces within the hosting rocks. The result of overprinting is comp structure presented in Milky quartz alteration zone. The latest stage, supergene alteration resulted from Post-breccia wallrock alteration fracturing/jointing and accompanying Cenozoic weathering and oxidation. Deesawat (2002) studied the drill hole No. 261 RCD, 471 RCD, 260 DDH, 470 DDH and 259 DDH and mapping in the C-H during this study have delineated zone of K-silicate plus porphyritic alteration, cherty quartz alteration, Milky quartz alteration, quartz-calcite vein/veinlet alteration, clay alteration and Supergene oxidation. Gold associated with quartz-calcite vein/veinlet alteration.

Kromkhun and Zaw (2005) reported the H zone of the Chatree deposit is classified as a low-sulfidation epithermal deposits and consists of plagioclase-pyroxene-phyrosene-phyric andesite, andesite lithic breccias, crystal-rich andesitic pumice breccias, crystal-rich quartz-rich volcanic sandstone/mudstone and limestone. The depositional environment of host volcanic sequence is mainly subaerial to shallow submarine. There are five vein stages: gray quartz, quartz-calcite-chlorite-illite-ikkite/smectite-sericite-ankerite-domite-epidote-andularia-pyrite-hematite-rhodochrosite-chacedony-sphalerite-galena-electrum - chalcopyrite, quartz-k-feldspar-carbonate-epidote-pyrite, calcite veinlet and joint surface coating.

C-H Zone was petrographically classified, and geochemically analyzed. The volcanic rocks belong to both coherent and non-coherent suites, the former being older in stratigraphy. Petrographic investigation reveals that the coherent rocks are mainly andesite to basaltic andesite. Compositionally, the non-coherent suite also bears similar

characteristics. Polymictic and monomictic breccias are classified in the non-coherent suite. Only the coherent and monolithic breccia units show strong alteration with associated Au-Ag mineralization (Nakchaiya et al., 2008).

In the late stage, dyke rocks at C-H Zone of Chatree gold mine form part of the Permo-Triassic Loei-Phetchabun-Nakhon Nayok volcanic belt. Dikes are recognized – one in the northeast-southwest direction and the other in the north-south direction. Petrographically, the dike rocks bear similar porphyritic texture and can be mainly classified as andesite, trachytic andesite and basaltic andesite. Andesite is characterized by plagioclase (oligoclase) and hornblende and shows strongly porphyritic textures (Tangwattananukul et al., 2008).

K Prospect

At K Prospect, early grey silicification displays wall rock halos of K-feldspar supporting the relationship to an intrusion source, localized by bedding plane faults. High Au-Ag mineralization occurs in association with pyrite-yellow sphalerite-carboate and silver minerals, and so displays an association with carbonate-base metal Au style (Corbett, 2004).

N Prospect

Chatree Gold deposits Prospect N drill hole 2580 DD displays many features typical of porphyry Mo-Cu-Au deposits such as multiphase intrusions, alteration and vein deposition, low grade Cu mineralization and no significant Au has been identified. Drill hole DDH 2580 provides the first diamond core test of the Prospect N porphyry target (Corbett, 2004). A coarse diorite with feldspar to 3 mm continues from surface to an interpreted quartz-bearing fault at 137 m where a chilled margin suggests the finer grained dioritic intrusion down hole is younger (Corbett, 2004). Alteration of drill hole DD 2580 formed early K-feldspar halos, indicative of emplacement during early potassic alteration, and later halos of silica-sericite-pyrite (phyllic) alteration. Although two potassic altered diorite intrusions, as well as post-mineral dykes, are recognized at N Prospect, there appears to be only one event of Cu mineralization, associated with quartz veins. Two weak events of molybdenite may be present, Au grades are very low, and Cu consistently in the order of 0.16% in the RC and diamond drilling (Corbett, 2004).

Marhotorn et al. (2008) studied igneous rocks (38 samples for rock slabs and 26 samples for thin sections) from drill-hole no. 2580DD and correlation with rock chip of hole no. 2407RC, 2408RC, 2409RC, 2410RC, 2411RC and 2412RC. Mesoscopic and microscopic determinations of core-log samples from the 171-m long N zone reveals that felsic porphyry and aphanitic mafic rocks were cross cut by subsequent alteration and mineralization. Two types of alteration were recognized-namely pervasive and selective patterns. The pervasive style was dominated by replacement of biotite, chlorite, sericite and k-feldspar. The selective style of alteration was observed as veins and veinlets. Petrographically, felsic rocks in the N zone bear similar microporphyritic to porphyritic and phaneritic textures and collectively classified as porphyritic fine-grained granodiorite. The aphanitic intermediate-mafic rocks bear similar porphyritic andesite. The granodiorite is characterized by plagioclase (An_{30}) frequently zoned, quartz (anhedral and vermicular) and relict hornblende. The groundmass is mainly fine-grained quartz, apatite and incipient sphene. Quartz and K-feldspar replaced rims of plagioclase phenocrysts. Porphyritic andesite is characterized by altered plagioclase and glassy groundmass. Alterations are mainly of biotite, chlorite, sericite and rare epidote. Chemically, these igneous rocks belong to the calc-alkaline affinity. Binary plots of trace element data for the studied rocks point to tectonic setting of volcanic arc granite system. Spider diagram of trace and rare-earth elements reveal that calc-alkaline intermediate igneous rocks are consistent with those of the Tertiary intrusive rocks of Azerbaijan, Iran which occurred in the subduction zone related to the magmatic arc environment.

Q Prospect

Prospect Q contains silica-sericite-pyrite-milled matrix breccias which may be related to a plumbing system for the early grey silicification, and may be controlled by the flat west dipping faults. Gold mineralisation is controlled by later pyrite on fractures, best developed in the presence of carbonate (Corbett, 2004).

V Prospect

Marhotorn et al. (2008) studied rocks of the V zone petrographically, the rock for petrography of rock-slab for 30 sample, thin section amount 17 sample for classification from drill-hole no. 3131DD and correlation with rock chip of hole no. 2071RC, 3082RC,

3083RC, 3084RC, 3085RC, 3086RC, 3087RC, 3088RC, 3130RC and 3636 RC. The rock of V zone is mainly porphyritic aphanitic intermediate to mafic rocks with abundant green minerals and minor vein systems. The rock in the V zone is dominated by altered porphyritic andesite, relic plagioclase and hornblende, strongly porphyritic texture. The altered porphyritic andesite characterized by epidote and chlorite replaced feldspar, sericitized andesine. Groundmass with plagioclase, sericite and opaque minerals exhibits prominent flow and glassy textures. Alteration mineralogy is characterized by epidote replacing plagioclase, chlorite replacing plagioclase, and sericite replacing plagioclase and devitrified glass. Binary plots of trace element data for the studied rocks point to tectonic setting of island-arc tholeiites and volcanic arc basalt.

Commimg et al. (2006) divided stratigraphic units and grouped the facies volcanic in the Chatree mine that occur at specific levels in the stratigraphy. The facies at Chatree have been grouped into certain stratigraphic units based from composition, texture and position in the stratigraphy. There are 4 stratigraphic units that are constrained within levels in the stratigraphy which are composed of different facies. These units are mention below.

Unit 1: Fiamme breccia (and Andesitic volcanoclastic facies); Lithic rich Fiamme Breccia, Quartz rich fiamme breccia, Polymictic hematitic breccia and Polymictic mud matrix breccia

Unit 2: Epiclastic and fine volcanoclastic sedimentary facies and Rhyolite Breccia facies; includes inter - bedded Volcanoclastic sandstones, Laminated carbonaceous mudstones and minor Limestone and Calcareous siltstone and Rhyolitic breccia facies. In the Northern part contains Monomictic andesitic breccia, Plagioclase phyric andesite and Polymictic andesitic breccia

Unit 3: Polymict and Monomict Andesite Breccia Facies; This group includes massive Polymictic Andesitic Breccia, Andesitic Basaltic Breccia which is inter - bedded and overlain by Volcanoclastic Sandstones, Laminated Carbonaceous Mudstones and minor Limestone. This group also includes some isolated zones of the Monomictic Andesitic Breccia, Plagioclase phyric andesite and Hornblende phyric andesite.

Unit 4: Polymict and Monomictic Andesitic Breccia facies and Coherent andesite; this group includes the Monomictic Andesitic Breccia, Plagioclase phyrlic andesite and Hornblende phyrlic andesite and some Polymictic andesitic breccia.

Surface and subsurface map (Figure 3.2) has been modified from Coming et al., 2006. The geological maps show large zones of Lithic rich fiamme breccia on the western and eastern zones of the Chatree mine, large zones of Polymictic andesitic breccias, coherent andesite and monomictic andesitic breccias towards the south and western zones and more abundant fine grained epiclastic and volcanoclastic sediments towards the north. A small zone is monomictic rhyolite breccias. The large zone to the south is the N – Prospect granodiorite. Generally the bedding is dipping towards the east on the eastern flank and towards the west on the western flank conforming to a broad anticline. Fault structures have been interpreted from geophysical data and from drill core and mine exposures.



สถาบันวิทยบริการ
จุฬาลงกรณ์มหาวิทยาลัย

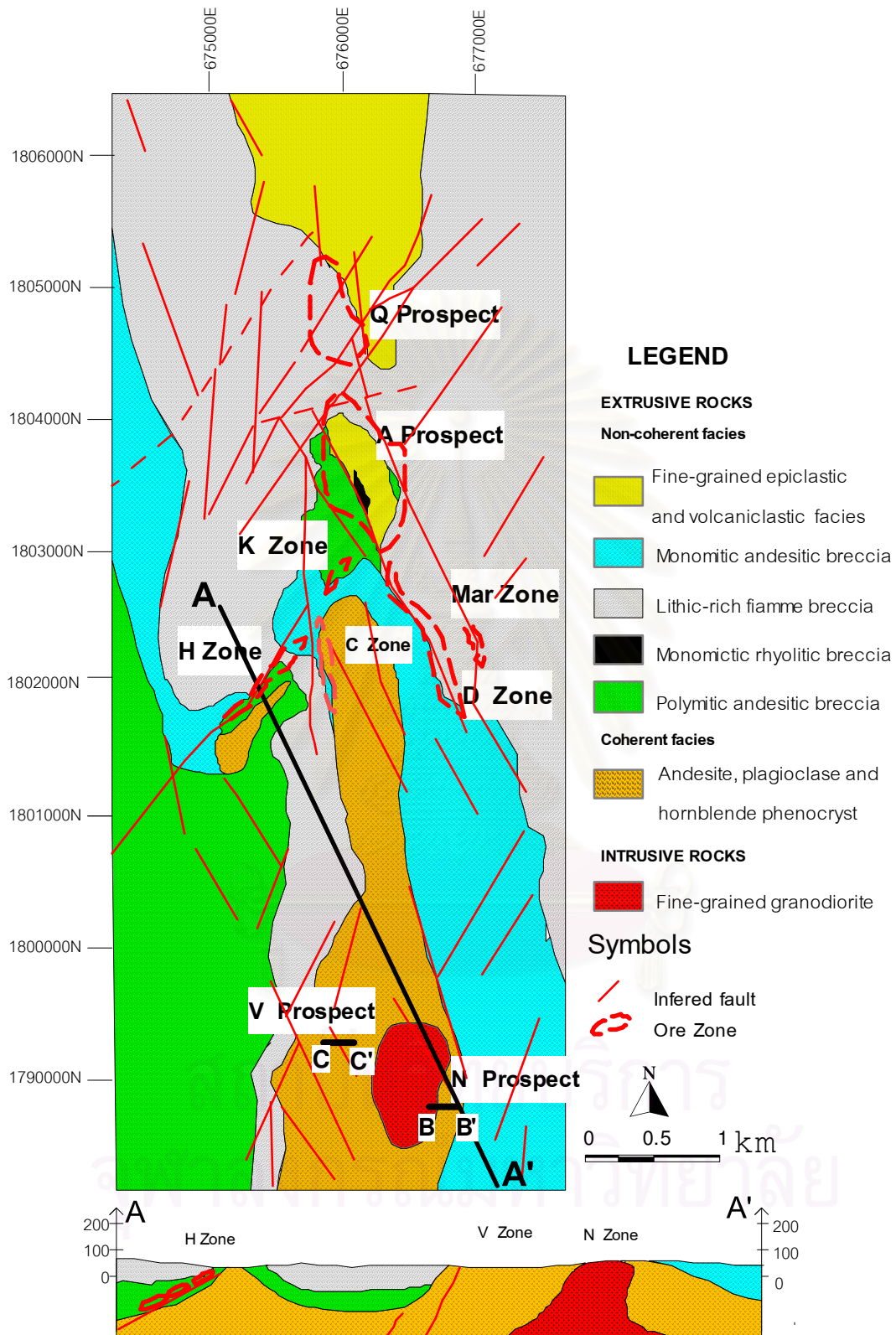


Fig. 3.2 Surface and subsurface geologic map and cross section (A-A') of the study and surrounding areas, Chatree gold deposit, Pichit, central Thailand (modified after Coming et al., 2006).

3.3 Geology of the Prospect area

In the study area there are two prospects, N Prospect and V Prospect. The N Prospect has distance far from C-H Prospects 2.5 km the south. The V Prospect is 2 km far from C-H Zone and. The distance between N and V Prospect is approximately 500 m approximately. The rock units are separated by petrography and chemistry as follows; N Prospect, the rocks are altered porphyritic granodiorite, andesite dyke and altered andesite. The study area is covered by regolith, a layer of loose, heterogeneous material covering granodiorite. This zone is covered by regolith at the depth of 0 to 20 m from surface. The granodiorite found at the depth of 20 to 137 m. Andesite contain altered plagioclase phenocryst and high altered set in glassy groundmass and found at the depth 137 to 171 of drill-hole no. 2580 DD, decline -55° E. The porphyritic graodiorite intruded into andesite host and show evidence of contact. Next, andesite dyke, thickness is 2 m and 0.5 m cross cutting the fine grained graodiorite at the depth of 39 to 41 m. and 43.8 to 44.3 m, respectively. The graodiorite is porphyritic and minor equigranular, the phenocryst size is $<1-3$ mm and fine-grained groundmass size is less than 1 mm, porphyritic texture shows characteristic of microphenocryst to phenocryst. The grain size classification of igneous rock is based on Hughes (1982). Cross section of subsurface geology at the N prospect is shown in Fig. 3.3.

V Prospect, the author separated into two types with regolith and andesite. The upper most, the regolith is reddish brown color the thickness size is 0 to 18 m from surface. The lower is andesite formed at the depth of 18-90 m which separate into two zones. The upper, the weathered of andesite which is abundant of altered mineral. The lowest, altered andesite, flow texture, devitrified, altered plagioclase, microporphyritic replaced by epidote. Rare mineralization is formed vein and dissemination in the andesite host. The quartz, epidote, tremolite-actinolite and calcite vein size 1.5 m cross cut the andesite rock at the depth of 77 to 79.5 m. Cross section of subsurface geology at the N Prospect is shown in Fig. 3.4.

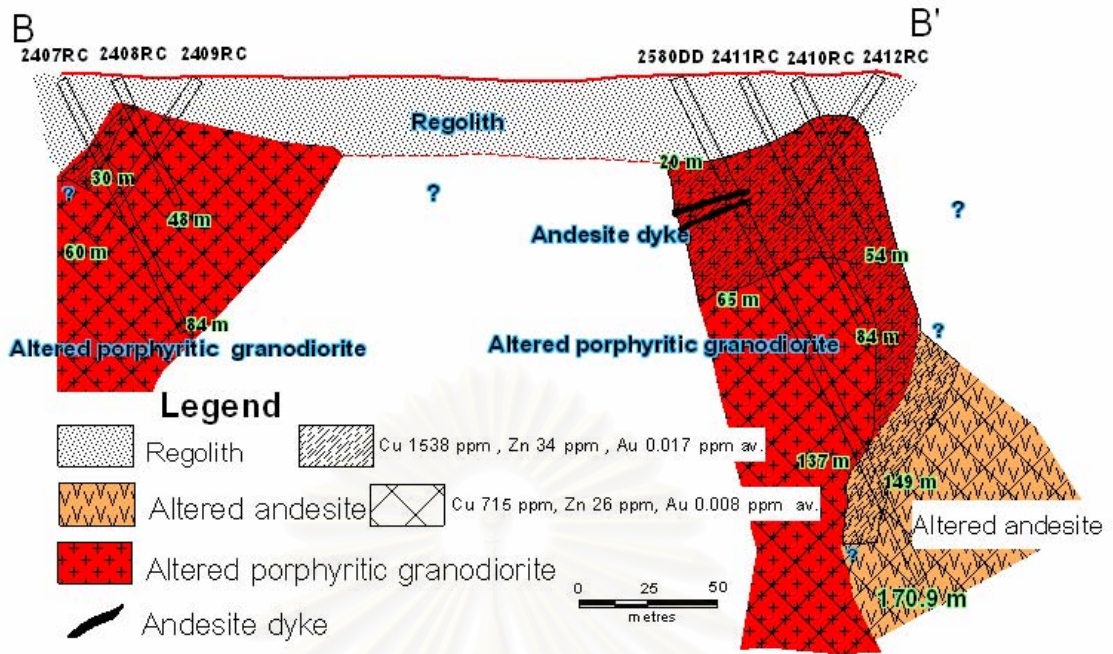


Fig. 3.3 Cross section along line B-B' (in Fig. 3.2) showing subsurface geology of the N-Prospect, southern part of the Chatree mine.

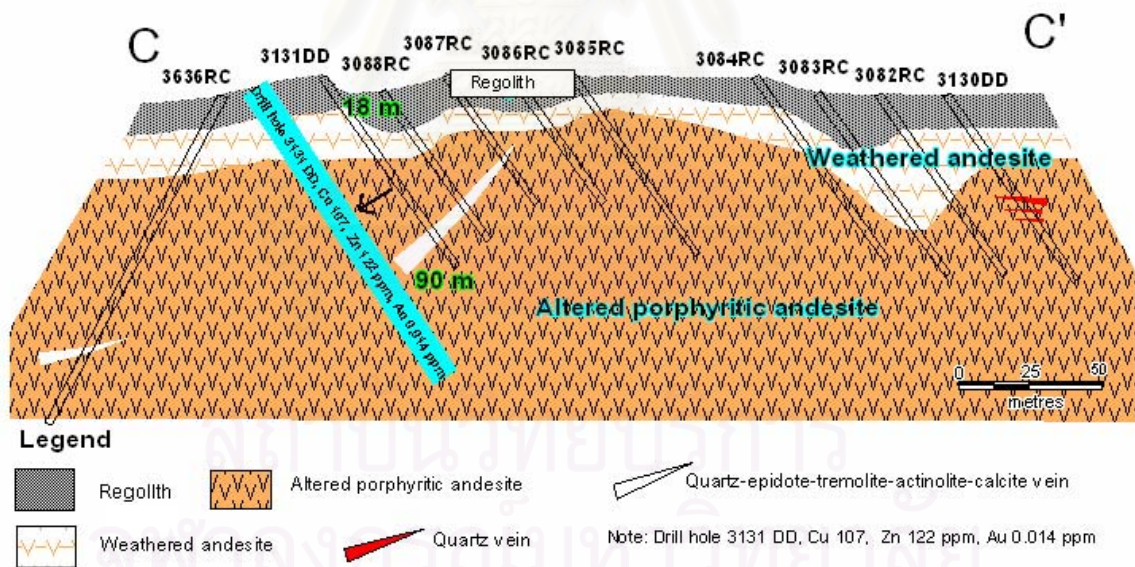


Fig. 3.4 Cross section along line C-C' (in Fig. 3.2) showing subsurface geology of the V-Prospect, south of the Chatree mine.

CHAPTER IV

PETROGRAPHY

The thin section was usually set at 30 microns thickness and covered glass. These thin sections were used for mineral identification, texture and paragenesis by polarizing microscope. The textbooks include Igneous Rocks (Barker, 1983), An introduction to the rock-forming minerals (Deer et al., 1966), Igneous Petrology (Hughes, 1982), Atlas of igneous rocks their textures (Mackenzie et al., 1982), Petrography of Igneous and Metamorphic Rocks (Philpotts, 1989) and Rock-forming Mineral in Thin section (Pichler, 1997) were used for mineral and texture identifications. Consequently, those textures were interpreted after Hibbard (1995) and Bard (1987). The symbols are used in this thesis as shown in Table 4.1 following that of Kretz (1983) and Siivola et al. (2007).

4.1 Geology of igneous rocks

4.1.1 Evidence of contact zone

The N Prospect, founded evidence of contact zone, the rock for petrography of rock-slap for 38 sample ,thin section amount 28 sample for classification from drill-hole no. 2580DDH (thickness 171 m) (Fig. 4.1) and correlation with rock chip of hole no. 2407RC, 2408RC, 2409RC,2410RC,2411RC and 2412RC. The rock samples were slab-cut and prepared as thin section. N Prospect is founded by evidence of contact which is contact between porphyritic granodiorite and andesite. The evidences of contact zone are intruded by porphyritic granodiorite toward andesite. The evidences are highly fractured, brecciated, intruded, micro-fault and stock work and veinlets (Fig. 4.3a 4.4a, 4.4b). The xenolite of andesite host founded in edge of porphyritic granodiorite which represented of contact by intrude of porphyritic granodiorite (Fig. 4.3b).

The V Prospect, the rock for petrography of rock-slap for 30 sample ,thin section amount 17 sample for classification from drill-hole no. 3131DD (thickness 90 m) (Fig. 4.2) and correlation with rock chip of hole no. 2071RC, 3082RC, 3083RC, 3084RC, 3085RC, 3086RC, 3087RC, 3088RC, 3130RC and 3636 RC. The drill-hole no. 3131D DH is decline -55° E.

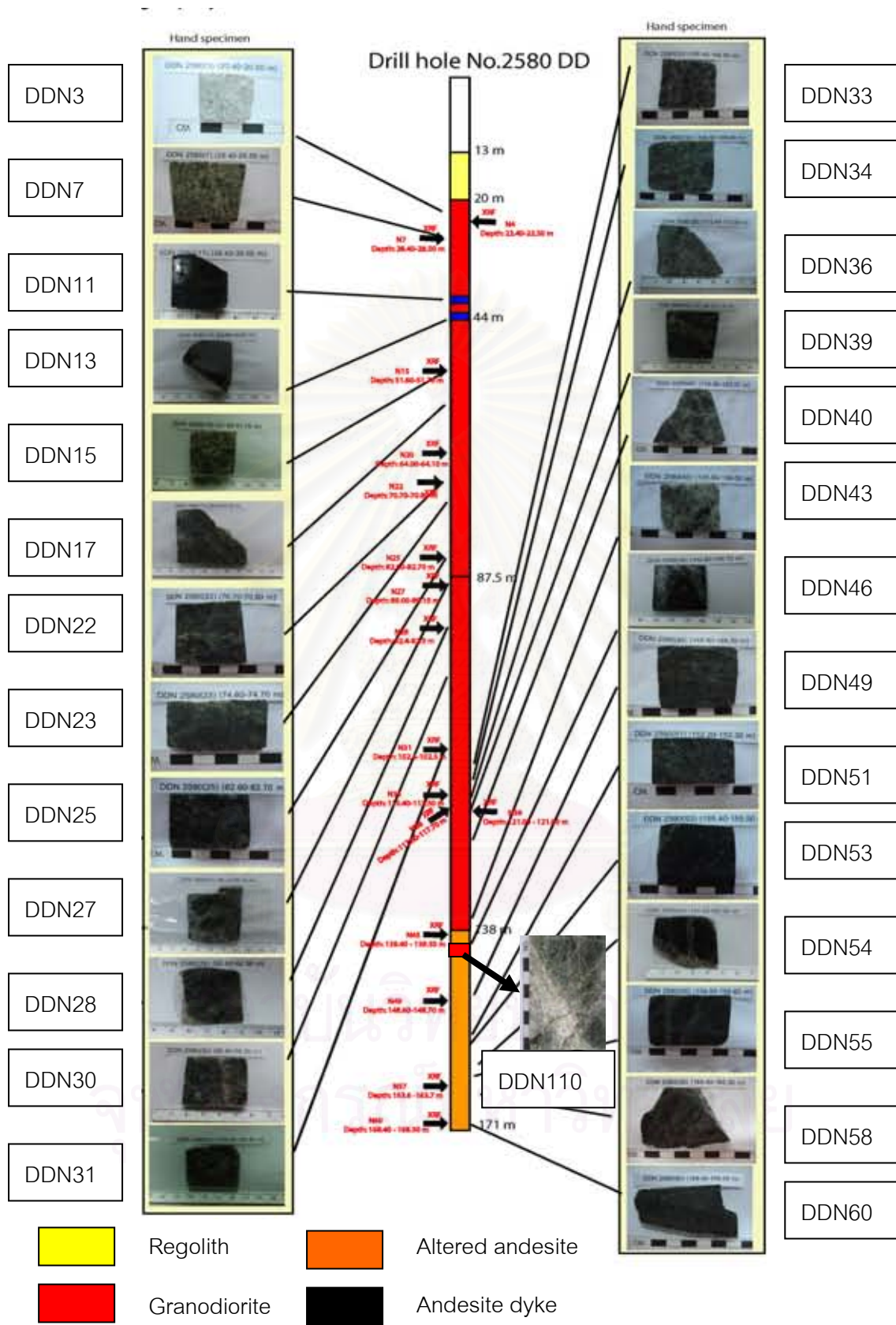


Fig. 4.1 Samples of altered and least altered rocks were selected for petrographic and geochemical study from drill-hole no. 2580DD.

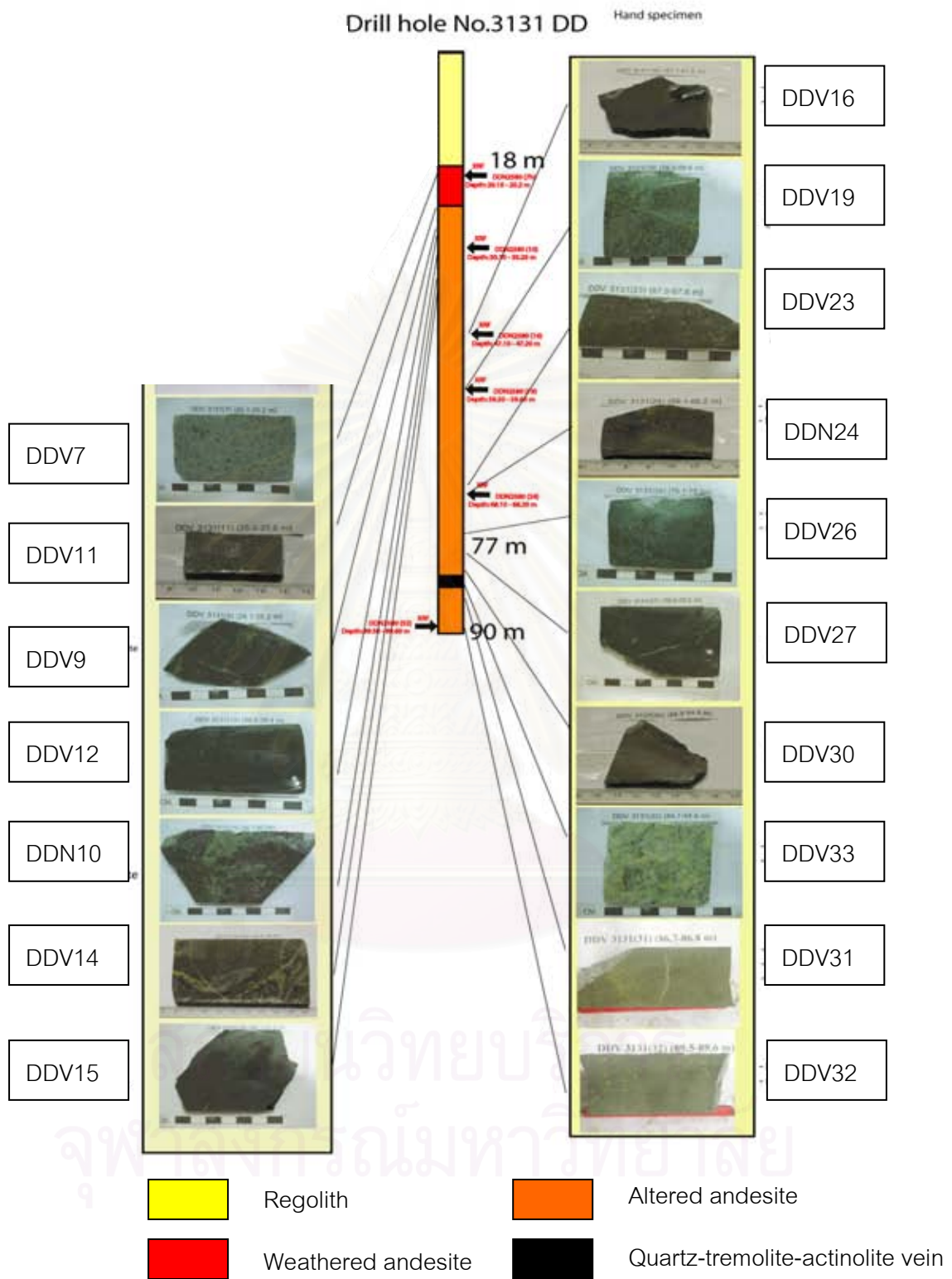


Fig. 4.2 Samples of altered and least altered rocks were selected for petrographic and geochemical I from drill-hole no. 3131DD.

Table 4.1 Mineral symbols for rock-forming mineral (modified after Kretz, 1983 and Siivola et al., 2007)

Acm acmite	Chu clinochumite	Ilm ilmenite	Pgt pigeonite
Act actinolite	Czo clinozoisite	Jd jadeite	Pl plagioclase
Agt aegirine-augite	Crd cordierite	Jh johannsenite	Prh prehnite
Ak akermanite	Crn corundum	Krs kaersutite	Pen protoenstatite
Ab albite	Cv covellite	Kls kalsilite	Pnp punpellyite
Aln allanite	Crs cristoballite	Kln kaolinite	Py pyrite
Alm almandine	Cum cummingtonite	Ktp kataphorite	Prp pyrope
Anl anal-clte	Dsp diaspore	Kfs K-feldspar	Prl pyrophyllite
Ant. Anatase	Dg diginite	Krn kornerupine	Po pyrrotite
And andalusite	Di diopside	Ky kyanite	Qtz quartz
Adr andradite	Dol dolomite	Lmt laumontite	Rbk riebeckite
Anh anhydrite	Drv dravite	Lws lawsonite	Rds rhodochrosite
Ank ankerite	Eck eckermannite	Lpd lepidolite	Rdn rhodonnite
Ann annite	Ed edenite	Lct leucite	Rt rutile
An anorthite	Elb elbaite	Lm linonite	Sa sanidine
Atg antigorite	En enstatite (ortho)	Lz lizardite	Scp scapolite
Ath anthophyllite	Ep epidote	Lo loellingite	Src sericite
Ap apatite	Fst fassite	Mgh muaghemite	Srp serpentine
Apo apophyllite	Fa fayalite	Mkt magnesiokatoptrite	Sd siderite
Arg aragonite	Fac ferroactinolite	Mrb magnesioriebeckite	Sil sillimanite
Arf arfvedsonite	Fed ferroederite	Mgs magnesite	Sdl sodalite
Apy arsenopyrite	Fs ferrosilite (ortho)	Mag nurgnetite	Sps spessartine
Aug augite	Fts ferrotschermakite	Mrg margarite	Sp sphalerite
Ax axinite	Fl fluorite	Mel melilite	Spn sphene
Brt barite	Fo forsterite	Mc microcline	Spl spinel
Brl beryl	Gn galena	Mo molybdenite	Spd spodumene
Bt biotite	Grt garnet	Wrz monazite	St staurolite
Btm boehmite	Ged gedrite	Mtc monticellite	Stb stilbite
Bn bornite	Gh gehlenite	Mnt montmorillonite	Str strontianite
Brk brookite	Gbs gibbsite	Mul nullite	Tlc talc
Brc brucite	Glit glauconite	Ms muscovite	Tmp stronpsonite
Cal calcite	Gln glaucophane	Ntr natrolite	Ttn titanite
Ccn cancrinite	Gt geothite	Ne nepheline	Toz topaz
Crn carnegieite	Gr graphite	Nrb norbergite	Tur tourmaline
Cst cassiterite	Grs grossularite	Nsn nosean	Tr tremolite
Cls celestite	Gru grunerite	OI olivine	Trd tridymite
Cbz chabazite	Gp gypsum	Omp omphacite	Tro trolite
Cc chalcocite	HI halite	Oam orthoamphibole	Ts tschermakite
Ccp chalcopyrite	Hs hastingsite	Op Opaque mineral	Usp ulvospinel
Chl chlorite	Hyn hauyne	Or orthoclase	Vrm vermiculite
Ctd chloritoid	Hd hedenbergite	Opx orthopyroxene	Ves vesuvianite
Chn chondrodite	Hem hematite	Pg paragonite	Wth Witherite
Chr chromite	Hc hercynite	Prg pargasite	Wo wollastonite
Ccl chrysocolla	Hul heulandite	Pct pectolite	Zn zircon
Ctl chrysotile	Hbl hornblende	Pn pentlandite	Zo zoisite
Cen clinoenstatite	Hu humite	Prv perovskite	
Cfs clinoferrosilite	Ill illite	Phl phlogopite	

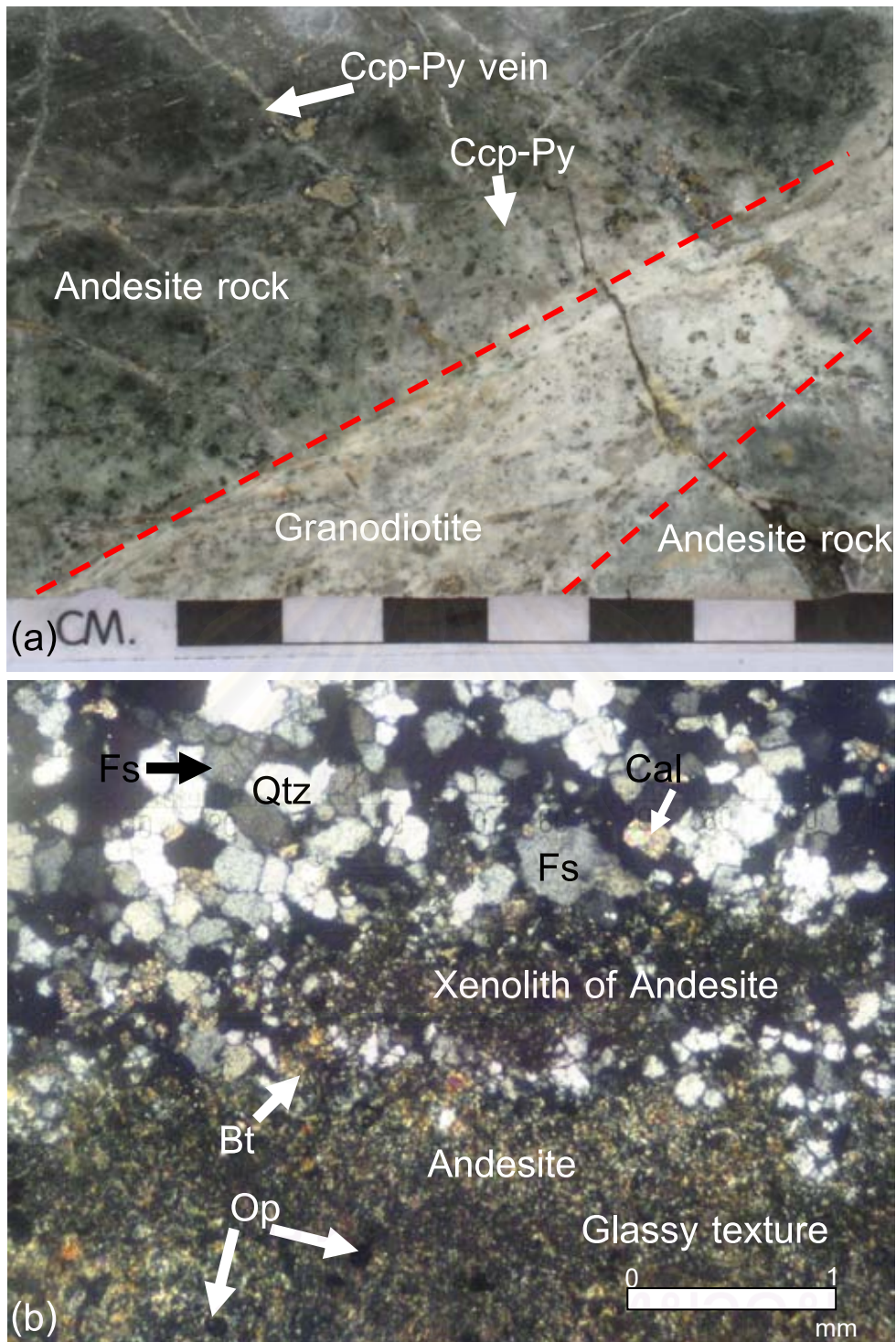


Fig. 4.3 A slab specimen (Sample no. DDN110) (at depth 146-146.1 m) of evidence of contact is occurred between granodiorite and andesite (N Prospect) shown that in figure a. Photomicrograph (b.) (cross-polarized light) of granodiorite intruded into andesite which is founded xenolith of andesite set in granodiorite. The granodiorite is mainly composed with quartz (Qtz), feldspar (Fs) and secondary calcite (cal). The andesite is glassy texture and dominant of secondary biotite (Bt) with opaque (Op) mineral.

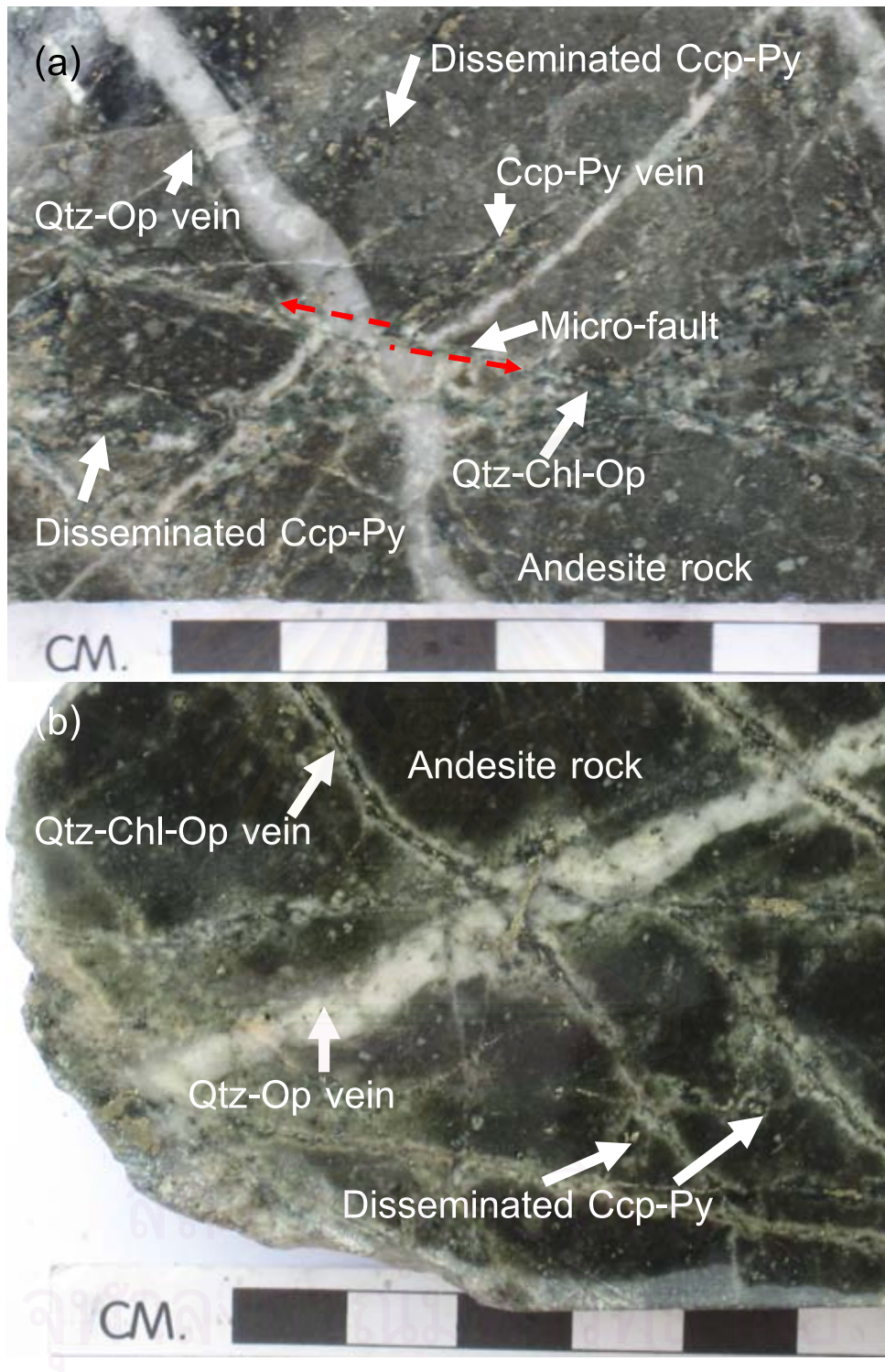


Fig 4.4 (a) (N Prospect) Slab specimens of andesite host which is crosscut by intrusive vein and formed highly fractured, stock works, veinlets and micro-faults. (b) Sequence of veins-first: quartz-opaque mineral vein crosscut andesite and second: quartz-chlorite vein with opaque ore in the central zone.

4.2 Petrographic characteristics of intrusive rocks

Porphyritic granodiorite (N Prospect)

In hand specimen (Fig. 4.5a), it is white to gray, fine-grained, porphyritic shows phenocrysts (up to 3 mm) of feldspars, quartz and biotite and chlorite-replaced mafic mineral. The rock contains mostly feldspar phenocrysts. The fine-grained groundmass is composed of quartz as the main minerals. The granodiorite is cross cut by quartz-sulfide veins and veinlets (Fig. 4.8a).

Microscopically, the rock is characterized by euhedral phenocrysts (~70%) set in fine-grained groundmass (~30%).

Plagioclase (~50%) phenocryst (Figs. 4.5b and 4.9a) is generally subhedral to euhedral, oligoclase to andesine (An_{30}). Albite and caldsbad-albite twins are common in the rock. Idiomorphic plagioclase phenocrysts are size up to 3 mm. Plagioclase is replaced by sericite along the cleavages of plagioclase (Figs. 4.6a and 4.6b). The plagioclase is replaced by silicified quartz groundmass (Fig. 4.11b). Intergrowth zoning plagioclase showing in Figures 4.8b, 4.11b and 4.14a set in fine-grained quartz groundmass. Plagioclase phenocryst is replaced by sericite and show cored texture in the middle part. Phenocryst of plagioclase altered to sericite in the fracture show sericitization and some grain strongly altered. Distinct zoning plagioclase set in silicified quartz groundmass. The zoning of plagioclase is especially typically of plagioclase in intermediate silica rock and shallow intrusion. Oscillatory zoning indicate magma mixing. Rim of plagioclase is replaced by silicified quartz groundmass and altered to k-feldspar.

Quartz phenocryst (~5%) size is 0.2 to 1 mm and formed anhedral to subhedral shaped. Quartz phenocryst showing corroded texture by replacement of fine-grained silicified quartz groundmass. In addition, quartz phenocryst forms vermicular (embayment) texture (Fig. 4.10a). The quartz phenocrysts are mostly irregular with rounded outlines although some small quartz phenocrysts may have one or a few short, straight edges. The phenocrysts typically have many wormy embayments. Some of the embayments are short and close to the margin, whereas others are long and go into the core of the grain. The embayments are usually very narrow, with widths ranging from 0.01 to 0.4 mm, but mostly 0.03–0.4 mm. All the embayments have smooth and rounded edges. The grain size of the quartz phenocryst varies greatly; from 0.5 to 2 mm. Quartz

phenocrysts in this suite are commonly rounded, suggesting that pressures fluctuated during crystallization (Whitney, 1988).

K-feldspar (~5%) K-feldspar is rarely widespread in the rock. In the rock K-feldspar is similar to quartz, but quartz lacks cleavage, lacks twinning, does not alter, exhibits undulatory extinction, and is uniaxial. Subhedral K-feldspar phenocrysts are size less than 3 mm.

Hornblende (~5%) (Fig 4.7b, 4.10b, 4.11a, 4.12a and 4.12b) commonly present relic diamond and prism shaped. Euhedral hornblende phenocryst is 0.5 mm Av of size. Some grain present relic two directions along the crystal with an angle of 60 or 120 degrees of cleavages. Hornblende has been completely replaced by biotite and chlorite. The hornblende can form cored texture which is inner of chlorite and outer of biotite. The altered hornblende associated with biotite- chlorite±opaque mineral.

Biotite phenocryst (Fig 4.7a) and secondary bitotite (~<2%), biotite phenocryst shows euhedral texture and set in silicified fine-grained quartz groundmass. In addition, biotite altered from hornblende phenocryst and associated with chlorite. Biotite and quartz phenocrysts formed during the last stage of the crystallization of the magma. Biotite phenocrysts are brown, up to 3 mm in diameter, Fe-enriched and subhedral. biotite forms small ragged crystals interpreted as of hydrothermal origin. Biotite form branching is typical of hydrothermal.

Chlorite (~<2%) altered from amphibole phenocryst which is less than 0.5 to 1 mm of size. Chlorite is green color under non-polarized light, and dark grey to isotopic under plane-polarized. Chorite associated with biotite and opaque mineral. Chlorite formed veinlet associated with quartz, serite, calcite, opaque mineral.

Sericite (~<1%) formed fine grained mica which is altered from k-feldspar or plagioclase phenocryst. In the area that have been subjected to hydrothermal alteration. Sericite replaced in fracture of k-feldspar, plagioclase and formed cored-texture (Fig. 4.9b). In addition, it's formed both single sericite veinlet (Fig. 4.13a) and associated with quartz-opaque mineral veinlet. Sericite vein is size 0.5 to 1 mm cross-cut the rock.

The quartz (~30%) groundmass are 0.1 mm in size and consists of subhedral crystals of fine-grained quartz, chlorite, sericite, apatite, sphene, zircon and opaque mineral.

Accessory mineral (~<1%) compose of apatite, sphene and zircon. Rare euhedral apatite is size average 0.15 mm which occurred in quartz groundmass and plagioclase phenocryst. Apatite is found as elongate crystals, commonly associated with plagioclase. Incipient sphene form both irregular and anhedral shaped size is less than 0.1 mm associated with groundmass. Zircon is rarely founded in the rock. These minerals occur both as inclusions in the silicate phases (i.e. plagioclase and K-feldspar) and interstitial to them (in the groundmass).

Mineralization, the mineralization is composing rectangular and irregular opaque mineral set in groundmass and quartz vein size 0.1 mm -1.5 cm associated with opaque, chlorite, sericite. Irregular shaped of opaque mineral is 0.5 replaced plagioclase phenocryst. Sericite formed in area of quartz vein size is 0.4 mm and founded sericite vein and chlorite vein cross cut feldspar phenocryst. Sulphide minerals are pyrite, chalcopyrite, sphalerite and molybdenite occurring as associated with quartz veinlet. In additional, pyrite, chalcopyrite and sphalerite disseminated in groundmass of the rock. Opaque mineral formed cubic and rectangular sizes less than 0.1 to 0.5 mm disseminated in quartz groundmass and associated with chlorite and sericite grain.

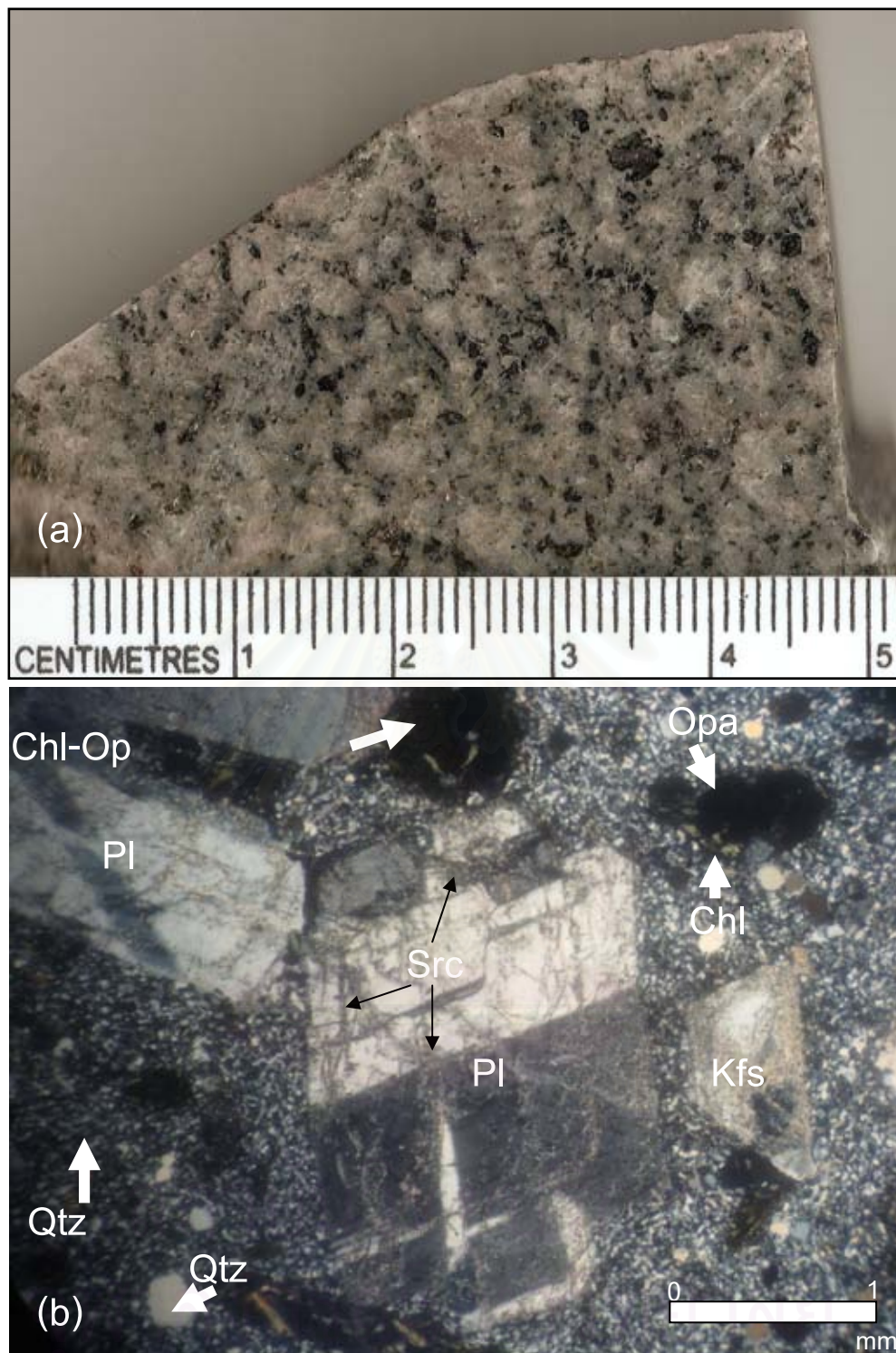


Fig. 4.5 (a) A slab specimen (Sample no. DDN30) of porphyritic granodiorite of N Prospect showing fine-grained groundmass and porphyritic texture. The dark color is mica. (b) Photomicrograph (b) (cross-polarized light) of (a) showing euhedral plagioclase (Pl) and K-feldspar (Kfs) phenocryst set in fine-grained quartz (Qtz) groundmass and sericite (Src) replaced at the fracture of plagioclase. Chlorite (Chl) associated with opaque (Opa) mineral.

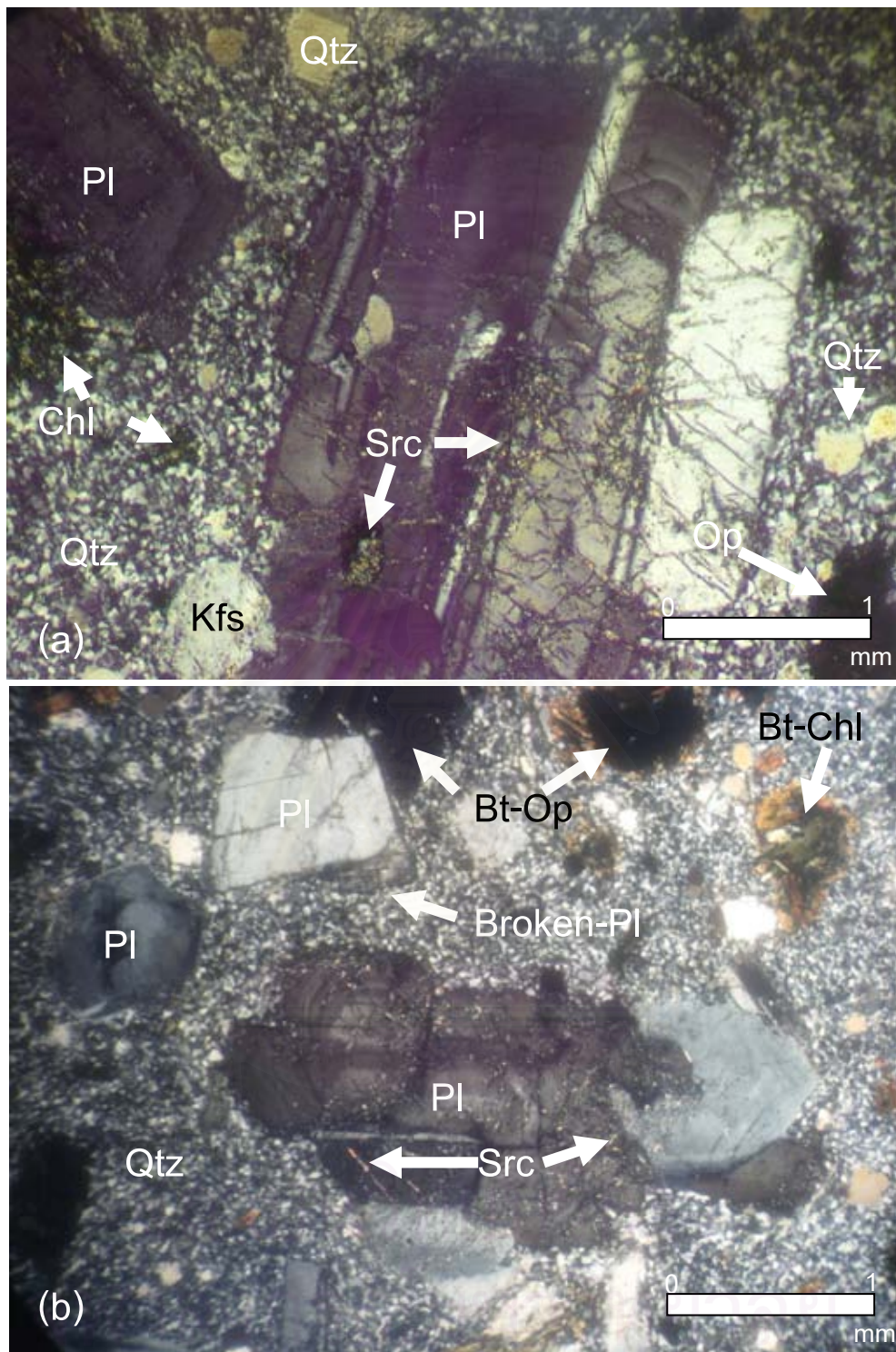


Fig. 4.6 Photomicrographs ((a) and (b) in cross-polarized light) of porphyritic granodiorite, N Prospect. (a) (Sample no. DDN34) Plagioclase (PI) phenocryst altered to sericite (Src) in fracture set in fine-grained quartz (Qtz) groundmass. Note that the rock is composed of plagioclase, quartz, chlorite, sericite and opaque (Op) mineral. (b) (Sample no. DDN30) Plagioclase phenocrysts partly replaced along the rim by quartz-sericite and biotite-chlorite present at top right. Biotite-chlorite-opaque mineral with rare sericite is alteration assemblage.

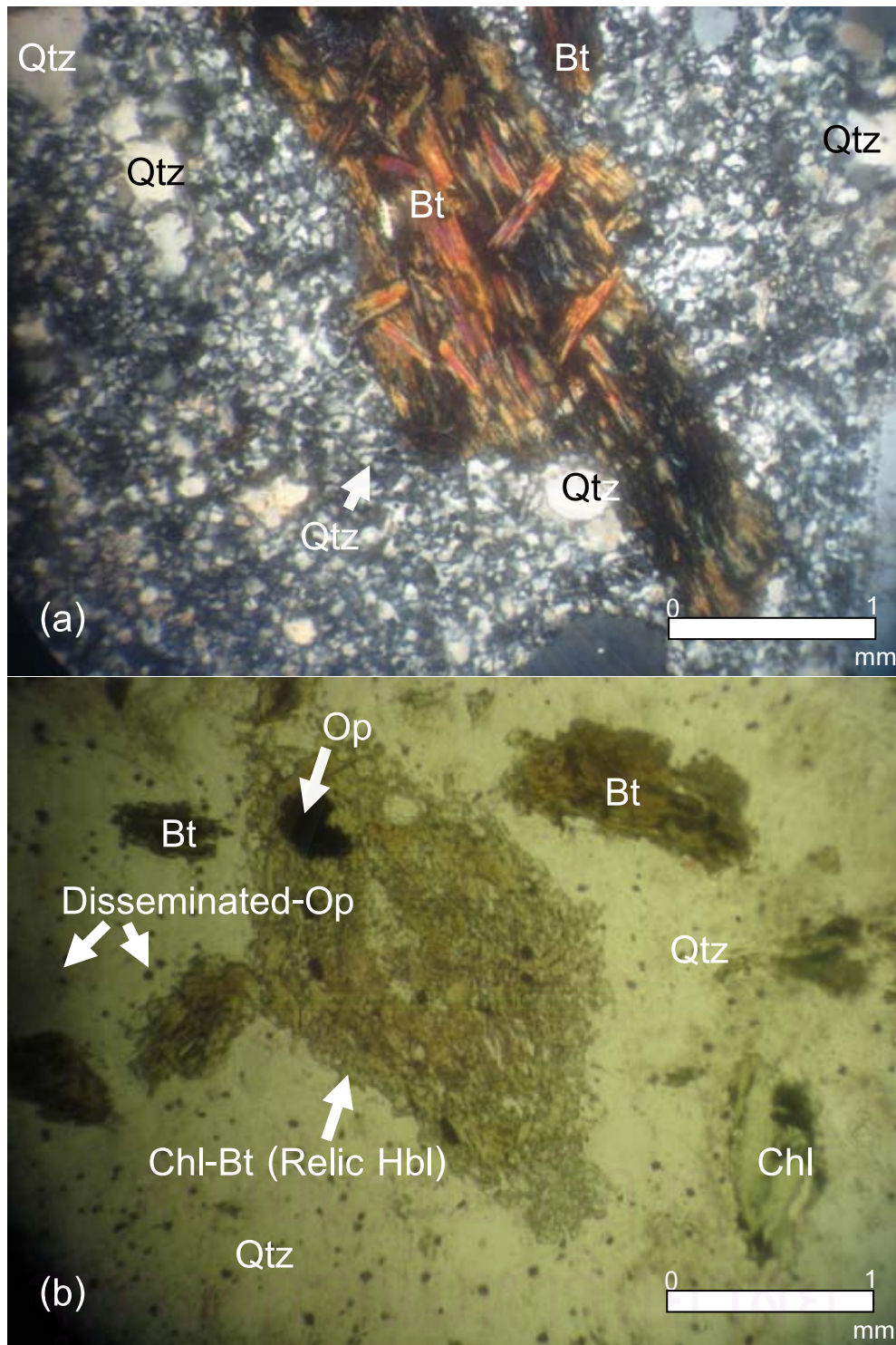


Fig. 4.7 Photomicrographs ((a) in cross-polarized light and (b) in plane-polarized light) of porphyritic granodiorite at N Prospect, Chatree gold deposits. (a) (sample no. DDN30) Altered biotite (Bt) phenocryst set in fine-grained quartz (Qtz) groundmass which is surrounded by fine-grained quartz groundmass and some subrounded-quartz. (b) (Sample no. DDN30) Relict euhedral hornblende (Hbl) phenocryst altered to chlorite-biotite-opaque and surrounded of chlorite (Chl) and biotite phenocryst set in fine-grained quartz groundmass. Opaque (Op) mineral disseminated in groundmass and associated with chlorite-biotite.

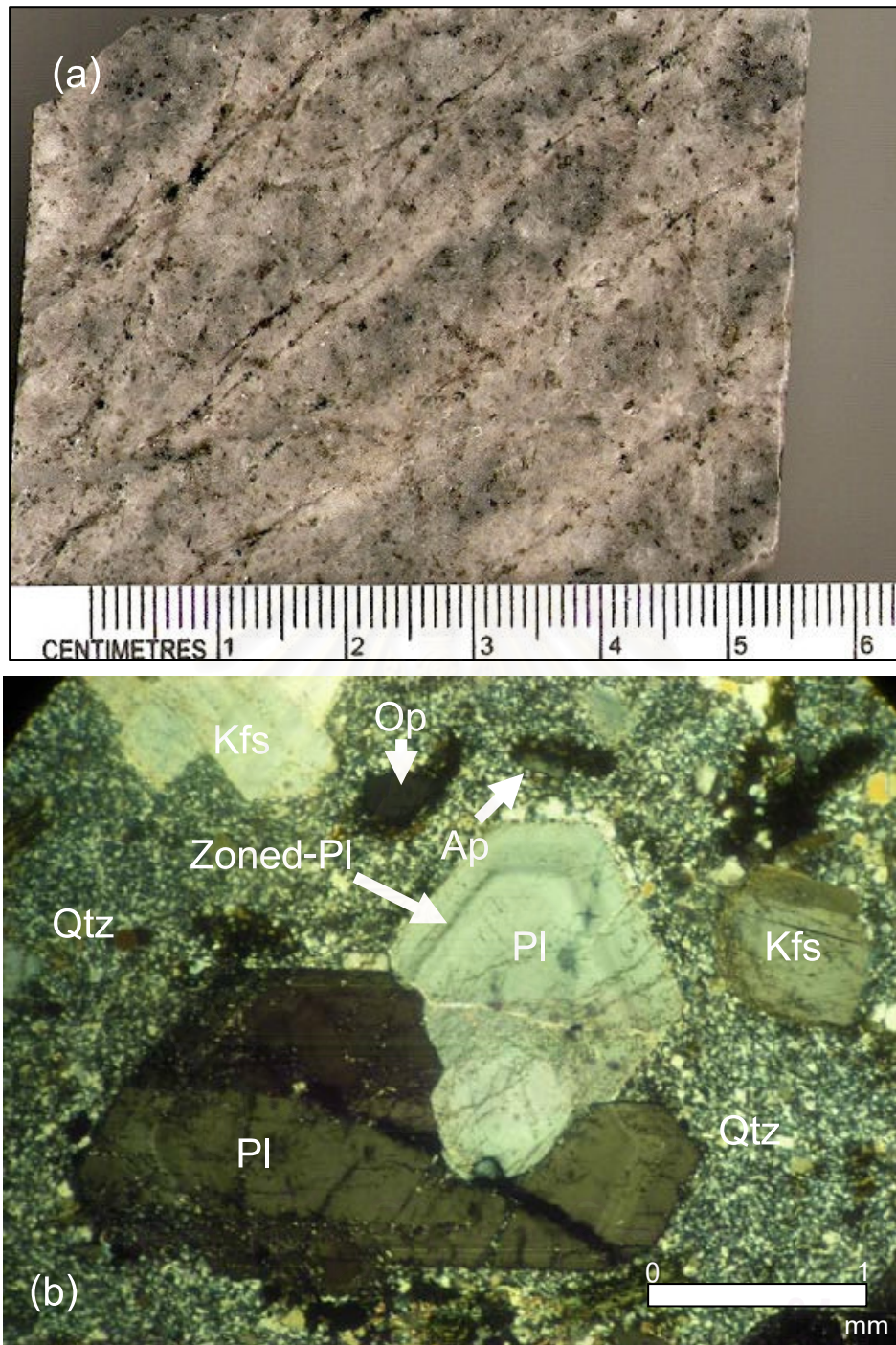


Fig. 4.8 A slab specimen (a) (sample no. DDN36) of porphyritic granodiorite of N Prospect showing fine-grained groundmass and porphyritic texture which is cross-cut by quartz-sulfide veinlets. (b) Photomicrograph (in cross-polarized light) from the same sample of (a), showing intergrowth zoning plagioclase (Pl) phenocrysts and k-feldspar (Kfs) set in fine-grained quartz (Qtz) groundmass and rare sericite (Src) replaced at the fracture of plagioclase. Opaque (Op) mineral formed anhedral shaped.

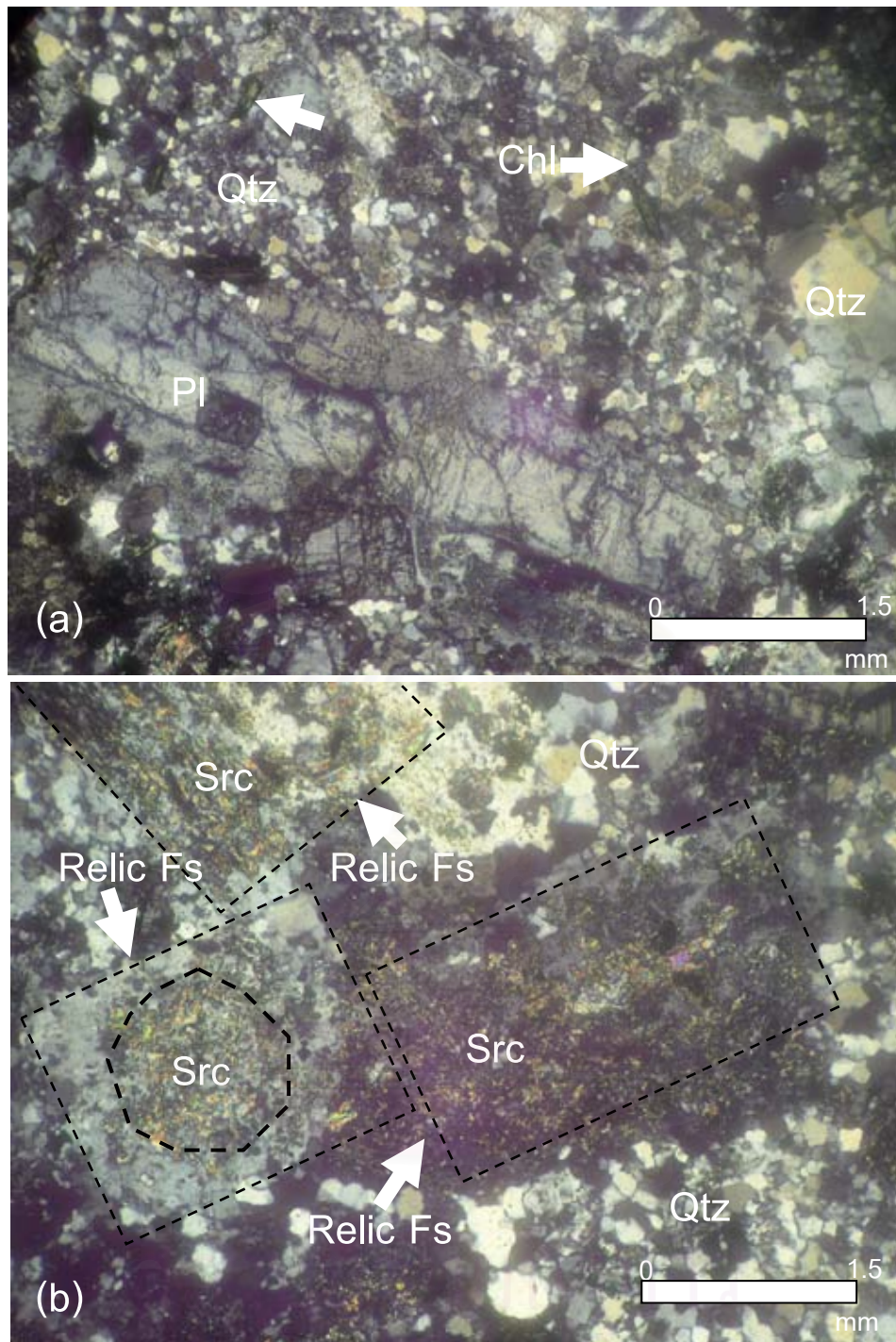


Fig. 4.9 Photomicrographs ((a) and (b) in cross-polarized light) of porphyritic granodiorite at N Prospect, Chatree gold deposits. (a) (Sample no. DDN7) Euhedral plagioclase (Pl) phenocryst set in fine-grained somewhat recrystallized quartz (Qtz) groundmass and fractured long rectangular minor secondary chlorite (Chl). (b) (Sample no. DDN15) Relic plagioclase phenocryst strongly altered to sericite (Src) associated and show cored texture set in fined-grained quartz groundmass.

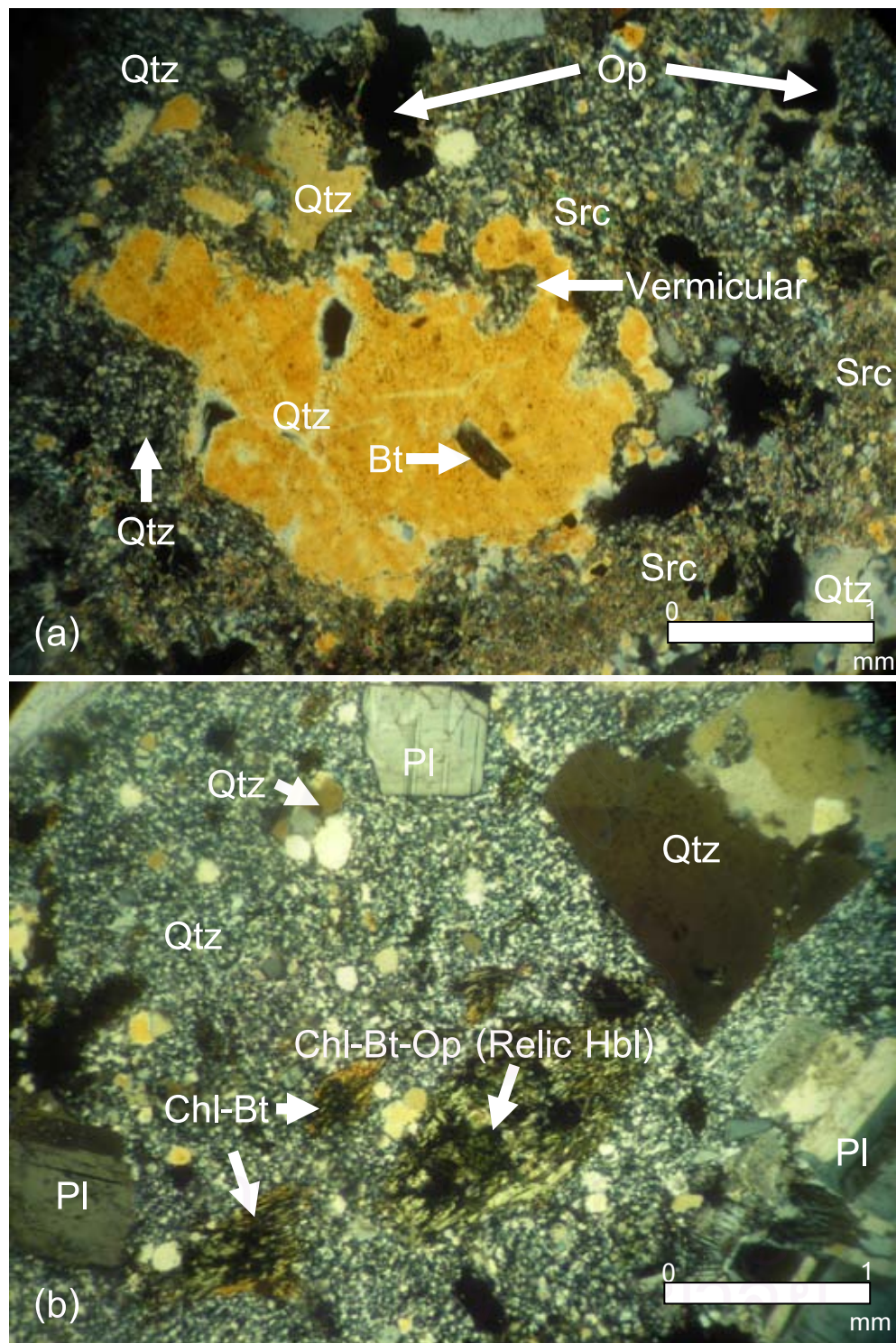


Fig. 4.10 Photomicrographs ((a) and (b) in cross-polarized light) of porphyritic granodiorite at N Prospect, Chatree gold deposits. (a) (Sample no. DDN34) Vermicular quartz (Qtz) phenocryst is replaced by fine-grained silicified quartz groundmass and formed embayment. Rectangular opaque (Op) mineral associated with sericite (Src). Inclusion of biotite (Bt) formed in vermicular quartz phenocryst. Relic hornblende (b) (Sample no. DDN36) phenocryst altered to chlorite-biotite associated with opaque mineral. Subhedral quartz and twin plagioclase phenocrysts set in fine-grained groundmass enriched in quartz and chlorite (devitrified glass).

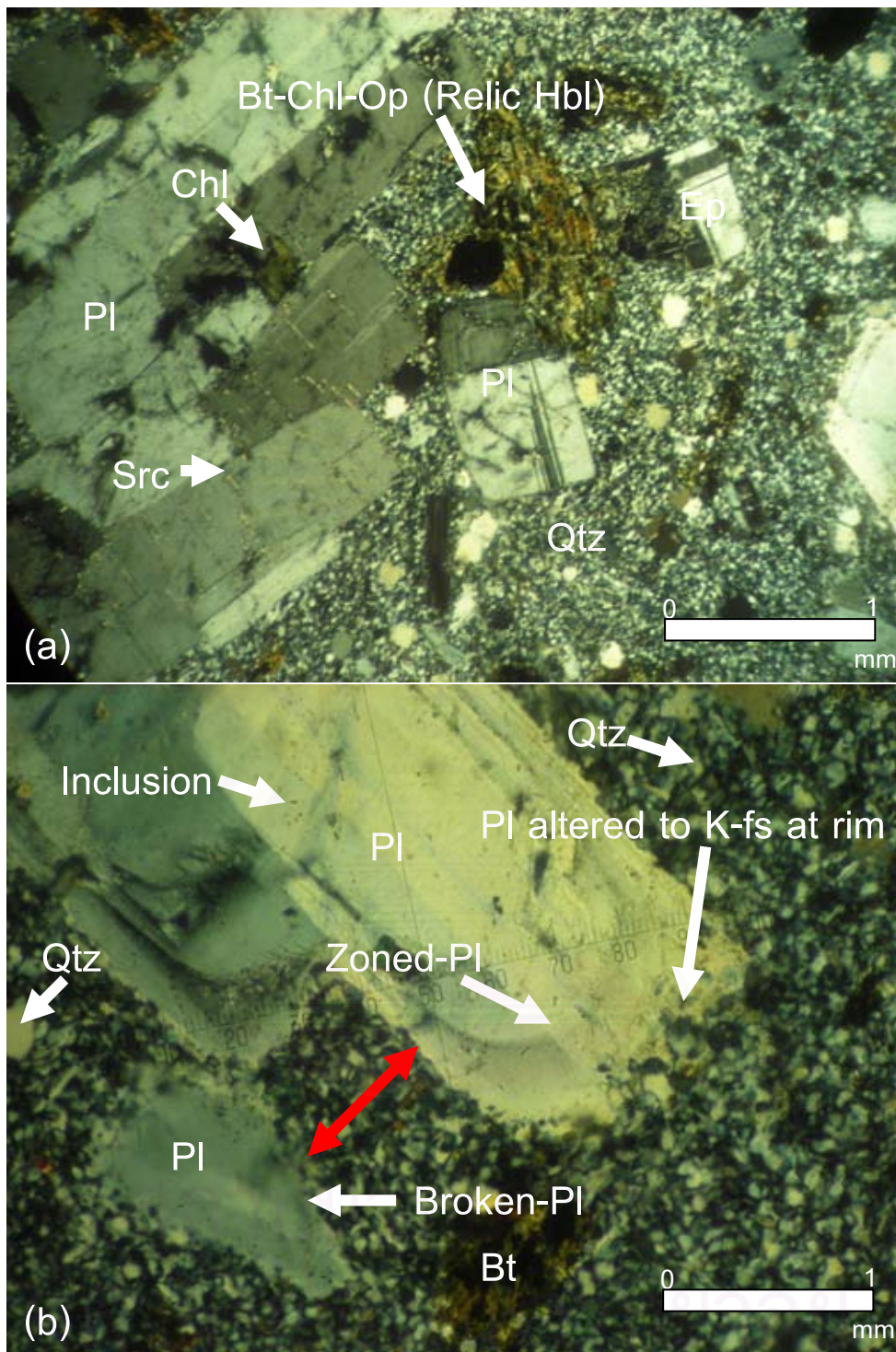


Fig 4.11 Photomicrographs ((a) and (b) in cross-polarized light) of porphyritic granodiorite (N Prospect) showing plagioclase (Pl) phenocryst is replaced by sericite in fracture and formed in fine-grained quartz (Qtz) groundmass (a) (Sample no. DDN22). Relic hornblende (Hbl) altered to biotite-chlorite-opaque mineral. Plagioclase formed by fine-grained quartz reloaded into fracture plagioclase phenocryst (b). Rim of plagioclase is replaced and altered to k-feldspar (Kfs). Secondary biotite (Bt) formed at bottom of (b) (Sample no. DDN28).

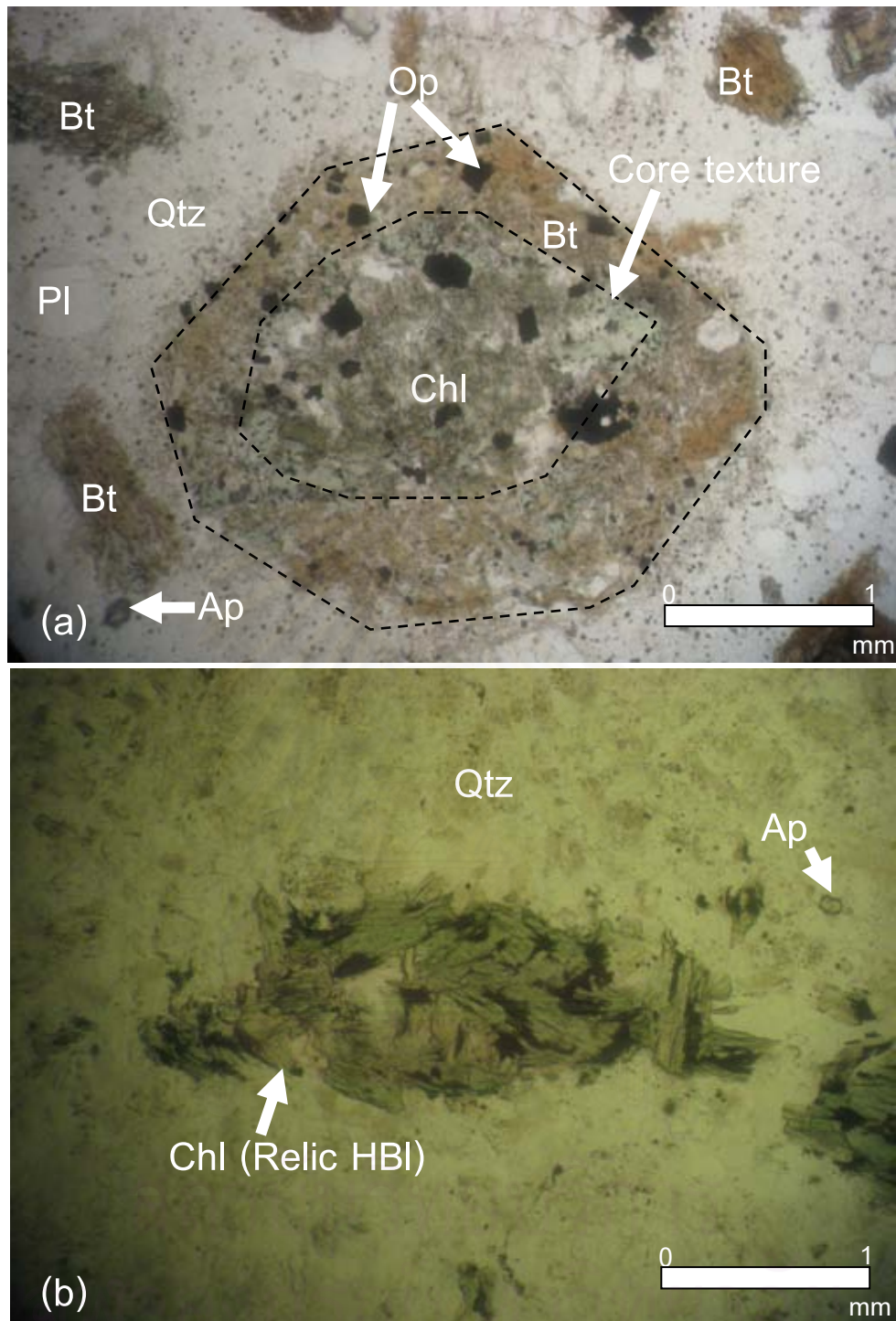


Fig 4.12 Photomicrographs ((a) and (b) in plane-polarized light) of porphyritic granodiorite at N Prospect. (a) (sample no. DDN30) Relic diamond-shaped hornblende (Hbl) phenocryst altered to chlorite (Chl)-bitotite (Bt)-cubic to subangular opaque (Op) mineral set in fine-grained quartz (Qtz)-enriched groundmass. Secondary biotite was also formed around phenocryst. (b) (Sample no. DDN7) Relic hornblende altered to chlorite set in fine-grained quartz groundmass with rare anhedra apatite (Ap).

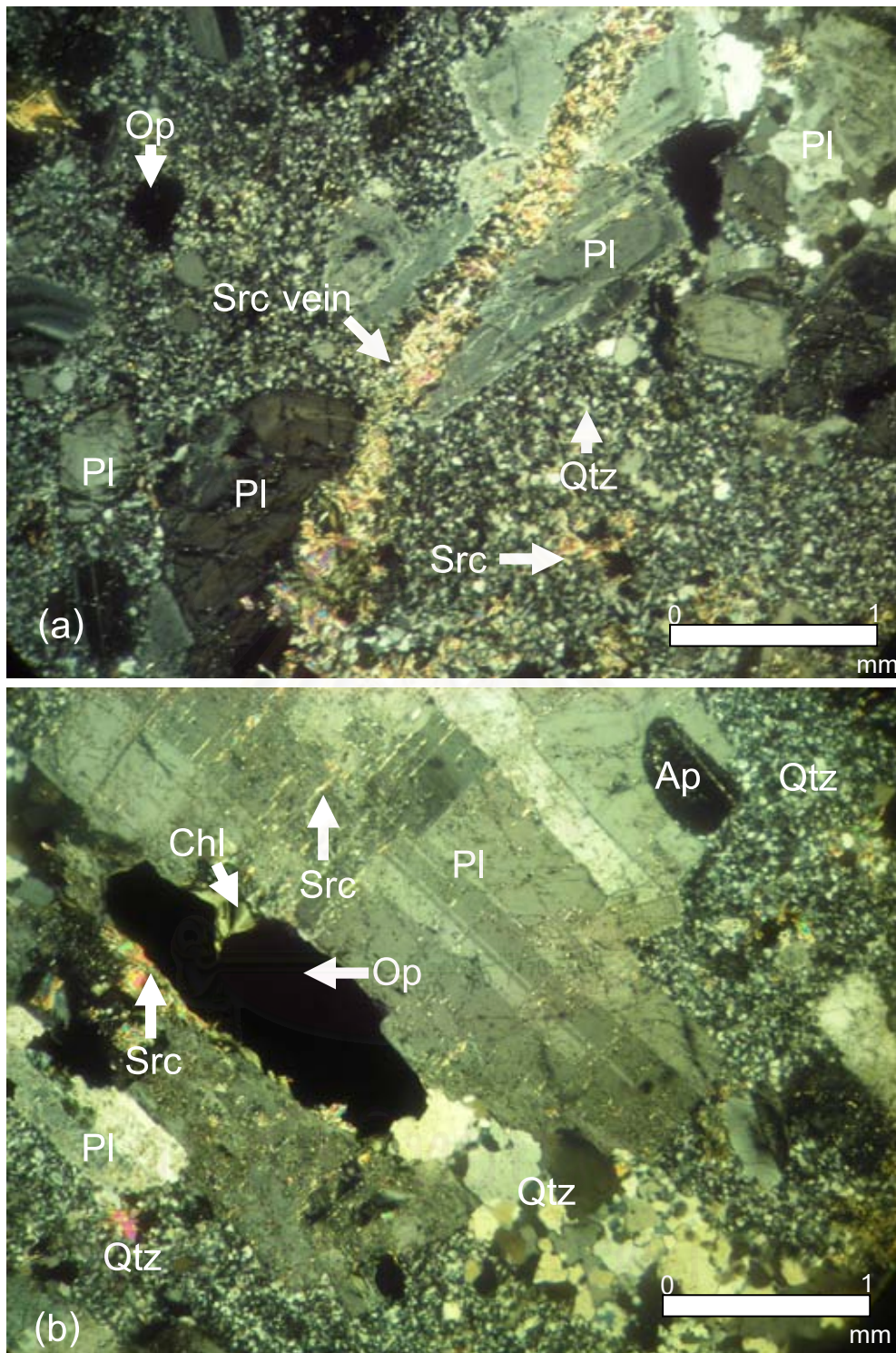


Fig. 4.13 Photomicrographs ((a) and (b) in cross-polarized light) of porphyritic granodiorite, N Prospect. (a) (Sample no. DDN36) Fine-grained mica or sericite (Src) vein crosscut the plagioclase phenocryst and fine-grained quartz (Qtz) groundmass. (b) (Sample no. DDN36) Plagioclase (Pl) phenocryst crosscut by quartz-opaque mineral which chlorite (Chl) and sericite are formed at rim of vein. In addition, sericite formed in the fracture of plagioclase phenocryst. At top right, subeuhedral apatite (Ap) formed at plagioclase phenocryst.

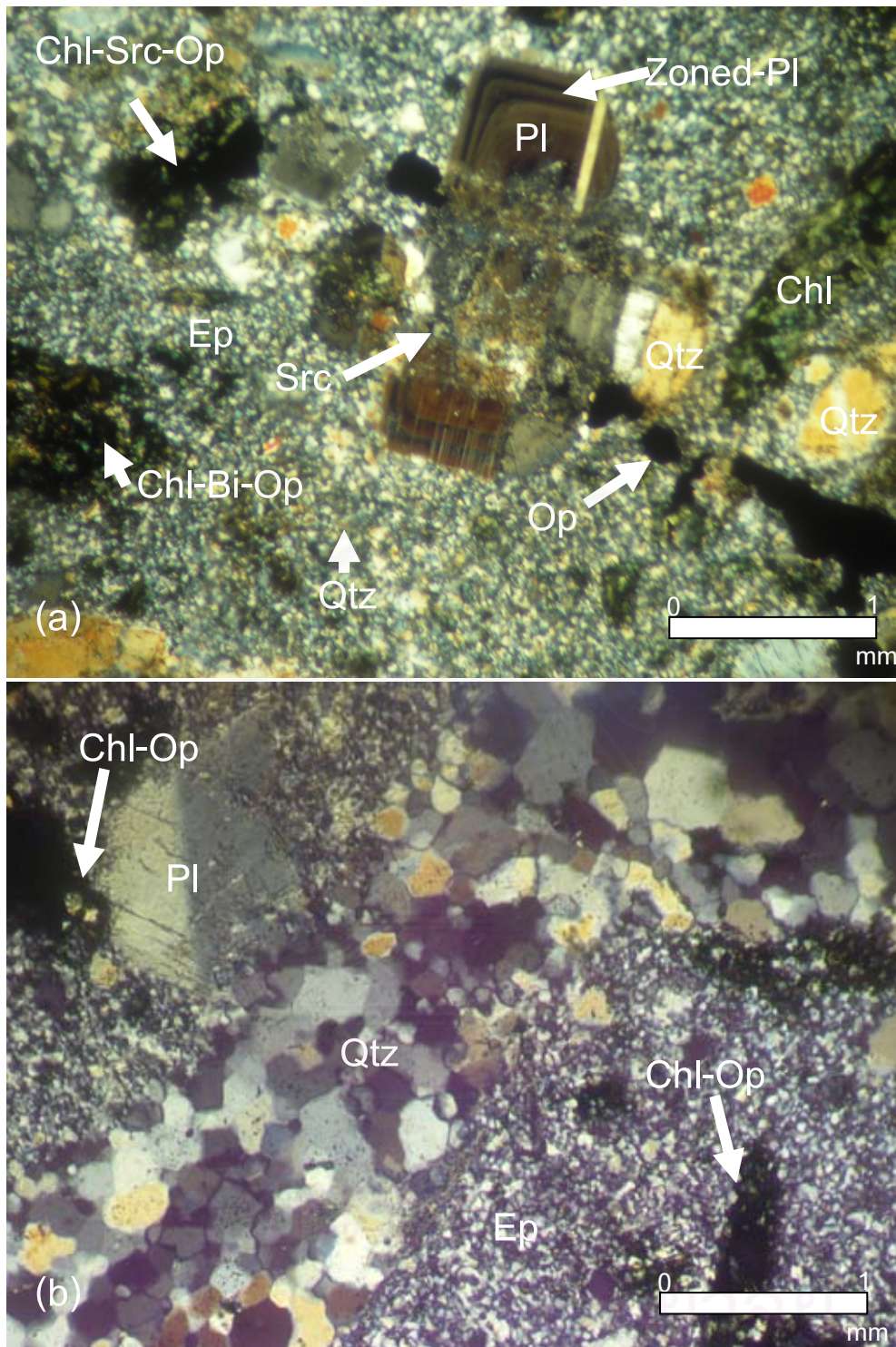


Fig. 4.14 Photomicrographs ((a) and (b) in cross-polarized light) of porphyritic granodiorite, N Prospect. (a) (Sample no. DDN35) Zoned-plagioclase (PI) phenocryst is altered to sericite (Src) set in fine-grained quartz (Qtz) groundmass. Alteration assemblages are chlorite (Chl)-biotite (Bt)-sericite (Src)-opaque (Op) mineral. (b) (Sample no. DDN7) Fine-grained granodiorite is cross cut by quartz vein and chlorite associated with opaque mineral set in fine-grained quartz groundmass.

Andesite dyke

Andesite dyke in the hole of 2580 DDH of N zone form thickness is 2 m and 0.5 m cross cut the fine grained gabbro at the depth of 39 to 41 and 43.8-44.3 m, respectively. In hand specimen, the studied slab is dark gray, very fine-grained with micro-porphyritic texture (Fig. 4.15a).

Microscopically, (Figs. 4.15b, 4.16a and 4.16b) the rock is characterized by phenocrysts (~15%) of anhedral to subhedral plagioclase, altered biotite, and relic hornblende set in groundmass (~85%) of fine-grained, glassy and flowed as characterized by the alignment and orientation of microlite of plagioclase.

Phenocrysts of plagioclase and hornblende are generally range in size from 0.1 up to 1 mm. The altered subhedral phenocryst plagioclase (~10%) size about 1 mm, biotite (~2%) size is 0.5 mm, quartz (~<2%) size is 0.5 mm, Relict hornblende (~1%) size about 2 mm less than 1 mm and show two cleavage of 120 and 60 by angle. Rare opaque mineral set in phenocryst of feldspar altered

The groundmass with the average size of minerals less than 0.1 formed microlite of plagioclase (~60%) and glassy (~25%). Rare anhedral epidote set in groundmass.

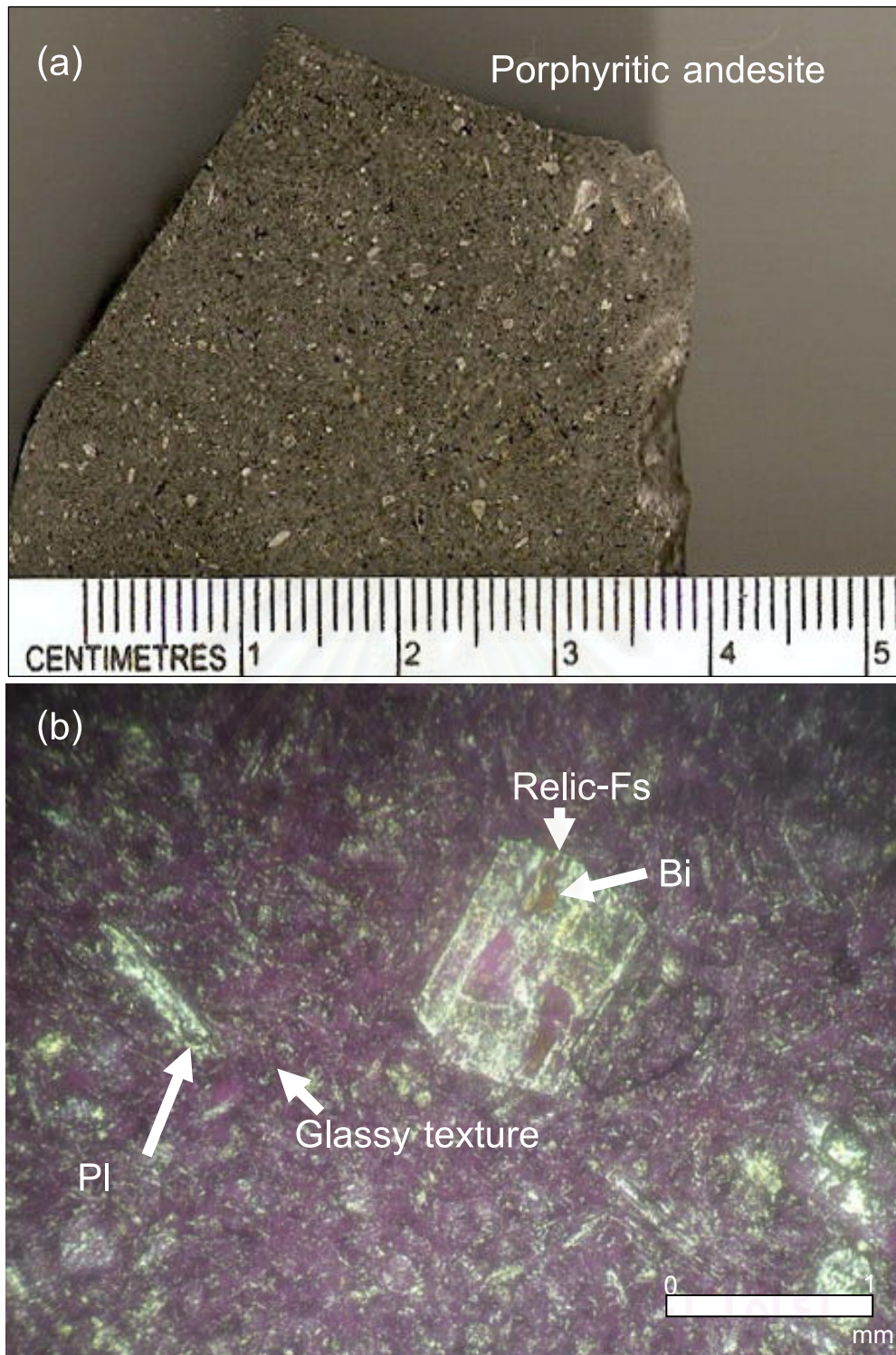


Fig. 4.15 A slab specimen of andesite dyke rock (a) (Sample no. DDN11) (N prospect) showing micro to porphyritic texture. (b) (Sample no. DDN11) Photomicrograph (cross-polarized light) of andesite dyke showing feldspar (Fs) phenocryst replaced by secondary biotite (Bi). The characteristic of groundmass is glassy and microlite of plagioclase (Pl).

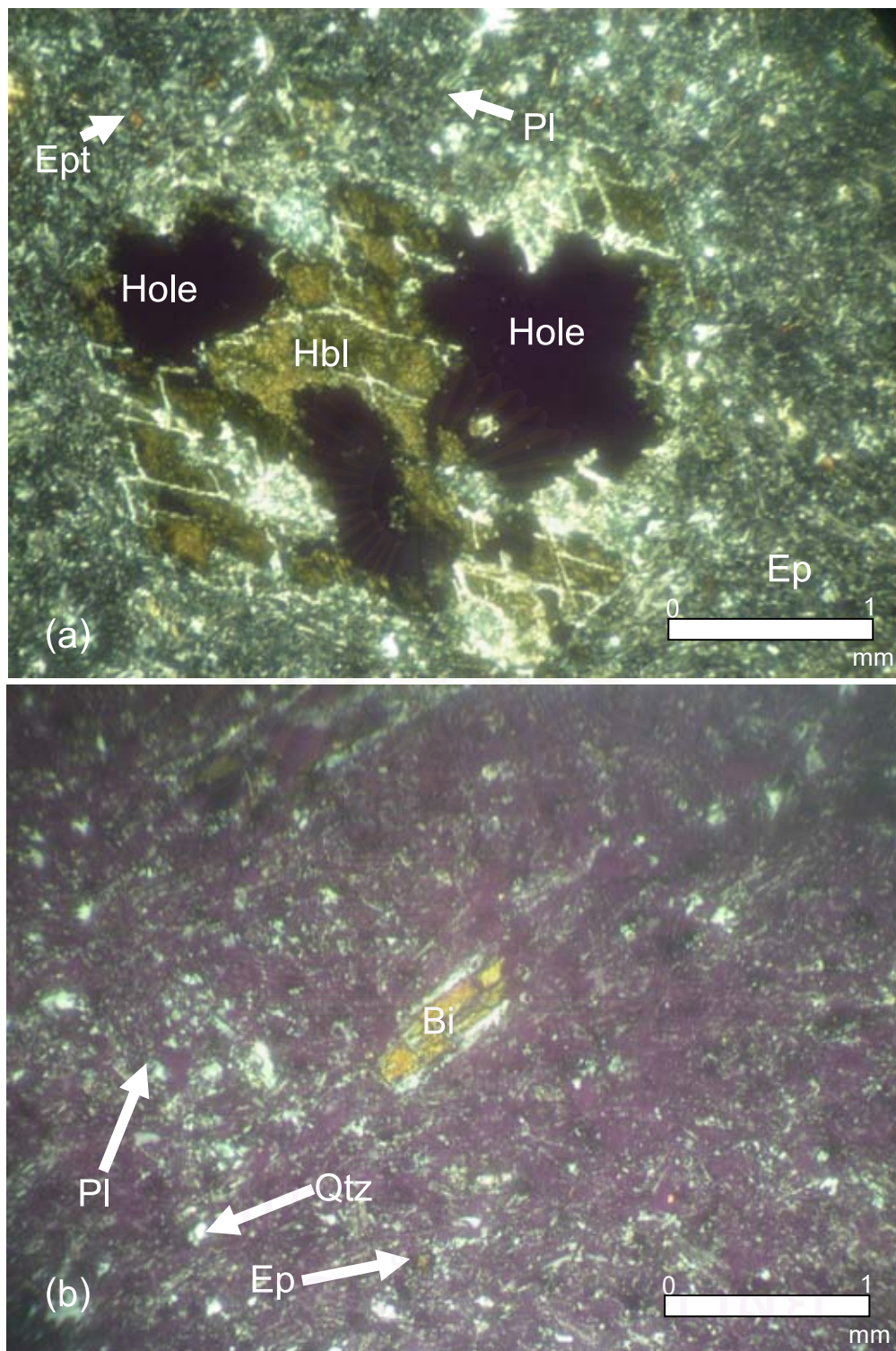


Fig. 4.16 Photomicrographs ((a) and (b) in cross-polarized light) of andesite dyke (N Prospect). (a) (Sample no. DDN11) Relic hornblende phenocryst with the oblique two cleavages (120° and 60°) by angle set in plagioclase (Pl) glassy groundmass with rare epidote (Ep) formed around phenocryst. (b) (Sample no. DDN13) Secondary biotite replacing relic feldspar set in glassy-flowed groundmass of hydrothermal quartz, plagioclase and rare epidote.

4.3 Petrographic characteristics of extrusive rocks

Altered andesite (N zone)

Altered andesite formed at the depth of (137-171 m) of drill-hole no. 2580 DDH, decline of -55° E. The andesite is intruded by fine-grained diorite at the depth of 137 m.

In hand specimen (Fig. 4.17a), the rock is gray to black color in fresh, brown color in weathered, aphanitic texture. The rock is cross cut by quartz-sulfide mineral veins, quartz-chlorite-epidote-sulfide mineral veins, epidote veins and calcite veins.

Microscopically, the rock is characterized by groundmass (~70%) of glassy materials and rare fine-grained quartz. Subhedral to euhedral phenocryst (~30%) set in groundmass.

Abundance of highly altered plagioclase phenocrysts (~30%) (Fig. 4.17b) size is 1 mm average. Secondary biotite present through the rock which is especially altered from plagioclase.

The glassy (~60%) materials and rare recrystalline quartz is groundmass. Irregular to rectangular opaque (3%) mineral varies in size less than 0.1 to 0.4 mm associated with chlorite and rare epidote (~2%). Opaque mineral veinlet size 0.3 mm disseminated in groundmass (Fig. 4.18a and 4.18b) and associated with chlorite vein. Epidote veinlet is size 2 mm cross cut through the rock. Calcite (~1%) veinlet size less than 0.1 mm cross cut the rock and chlorite (~4%) occur at the rim of quartz grain.

Paragenesis of mineralization, the first stage the rock is cross cut by quartz sulfide vein. The second, quartz-chlorite-epidote-sulfide is formed veinlet and cross cut the rock. The third, formed epidote vein cross cut again (Fig. 4.17a). Finally, unmineralized calcite veinlet is cross-cut the rock.

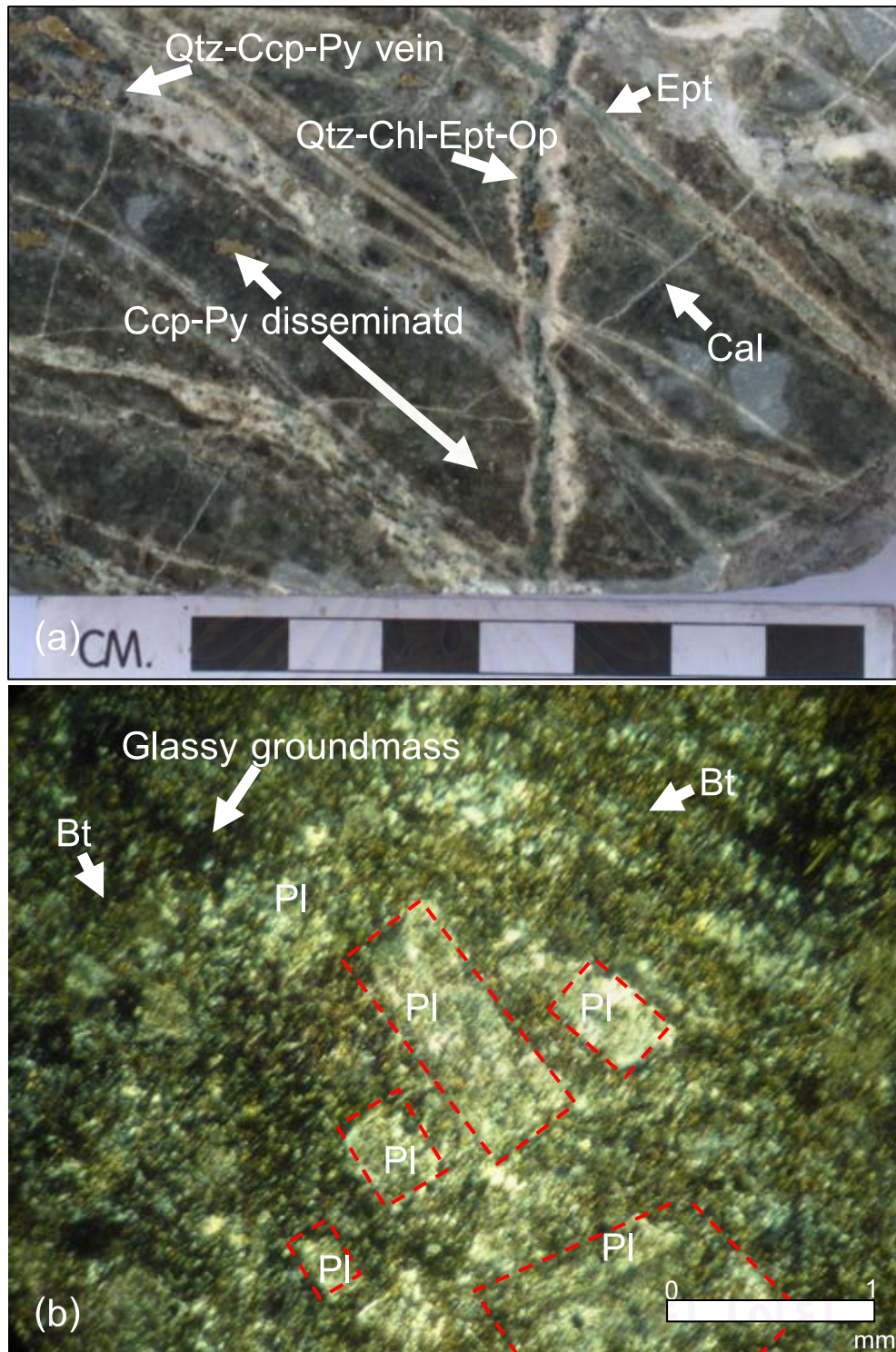


Fig. 4.17 (a) A slab specimen (Sample no. DDN116) of altered andesite with aphanitic texture and crosscut by various veinlets. The first stage—the rock is cross cut by quartz (Qtz)-Chalcopyrite (Ccp)-pyrite (Py) vein. The second—quartz (Qtz)-chlorite (Chl)-epidote (Ep)-opaque (Op) is formed as veinlet and cross cut the rock. The third—epidote vein formed. The last—unmineralized calcite (Cal) is formed with thickness size less than other veins. (b) Photomicrograph from part of (a) (in cross-polarized light) showing altered plagioclase (Pl) phenocryst in glassy groundmass and surrounded by secondary biotite (Bt) formed during hydrothermal alteration.

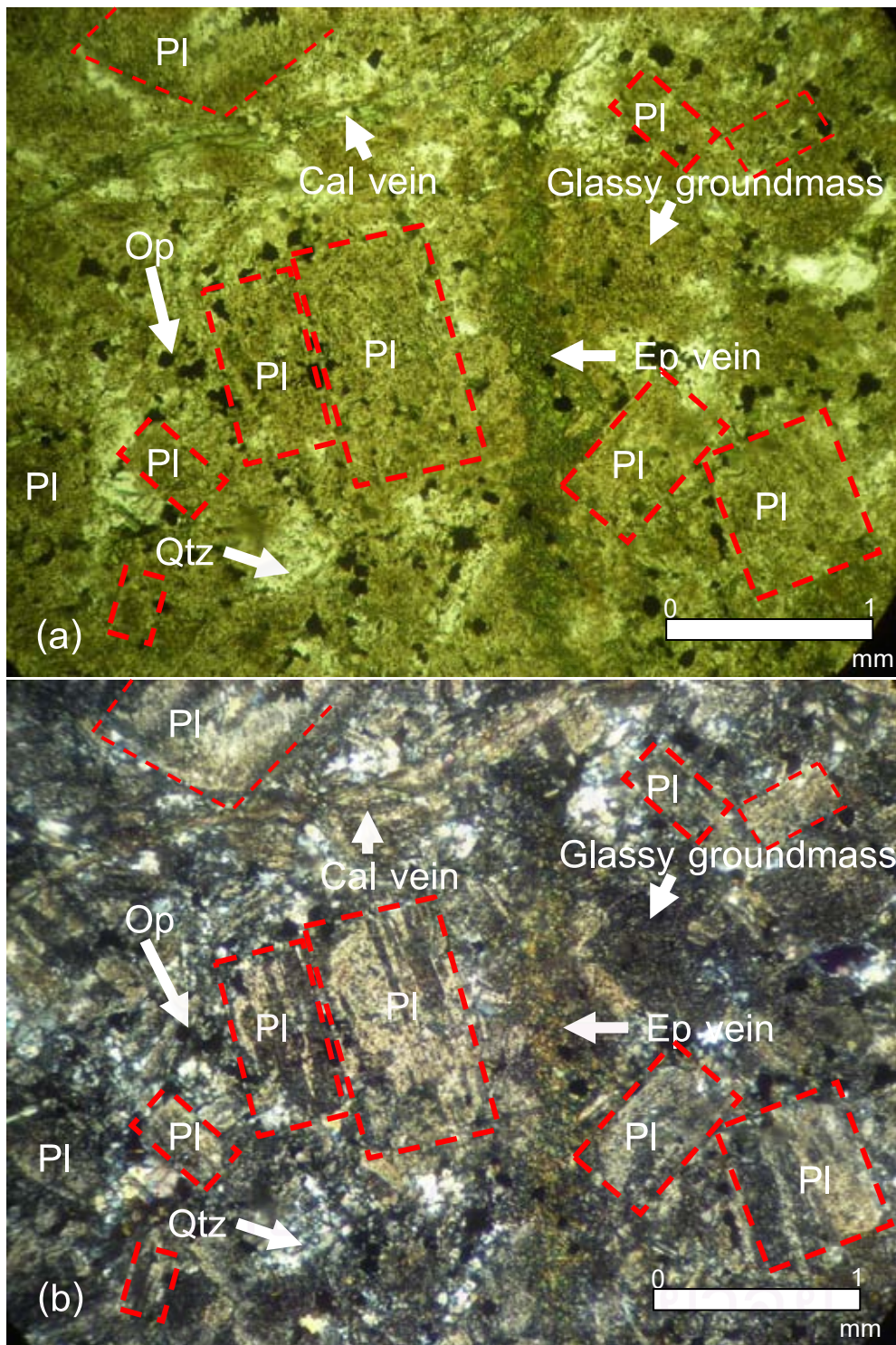


Fig. 4.18 Photomicrographs (Sample no. DDN58) of altered andesite ((a) in plane-polarized light and (b) in cross-polarized light), at N Prospect, altered plagioclase (Pl) phenocrysts in dotted red boxes set in fine-grained glassy groundmass enriched in devitrified glassy material. Opaque (Op) mineral is disseminated in glassy groundmass. Epidote (Ep) vein crosscut the rock in the first stage and the calcite (Cal) vein formed in the later stage. Rare recrystalline quartz (Qtz) formed as anhedral shape associated in glassy groundmass and opaque mineral.

Weathered, altered andesite (V Prospect)

In hand specimen (Fig 4.19a 4.21a), the rock is dominant green color of phenocryst and fine-grained groundmass, porphyritic textures and veinlets size less than 1 mm to 1 mm.

Microscopically, the rock is characterized by very fine-grained groundmass (~70%). Subhedral to euhedral phenocrysts (~30%) set in groundmass. Secondary minerals include epidote, chlorite, sericite and pyrite.

Groundmass (70%), the groundmass is composed of plagioclase (Fig. 4.19a), glass. The texture is characteristic of porphyritic, glassy, flow and microlite texture. Cubic and rectangular opaque mineral is size 0.2 mm set in groundmass.

Phenocryst (~30%) is composed of plagioclase (~25%) (Fig. 4.20a, 4.20b, 4.19b) and hornblende (~5%) (Fig. 4.23a and 4.23b). Relic of plagioclase phenocryst is replaced by epidote (Fig. 4.19a and 4.21b, 4.22a, 4.22b, 4.25a, 4.25b, 4.26a, 4.26b). The plagioclase is mainly altered to chlorite and epidote. The hornblende phenocryst is altered become to epidote. Plagioclase is size less than 1 to 2 mm approximately. Hornblende phenocryst is size less than 1 mm av. which is present of relic diamond shape and relic two directions along the crystal with an angle of 60 or 120 degrees of cleavages. Epidote is altered partly the plagioclase and hornblende (Fig. 4.23a, 4.23b). Chlorite is mainly altered from relic feldspar (Fig. 4.24a, 4.24b)

At the depth of 77 to 79.5 m the rock is composed of tremolite-actinolite-quartz-calcite-opaque vein cross cut the rock. Tremolite-actionote showing prismatic shaped.

Mineralization, veinlet of rectangular opaque mineral size 0.5 approximately and single grain of opaque show cubic shaped. In this Prospect (V Prospect) is less veinlet than N Prospecr and interpreted to low significant of mineralization.

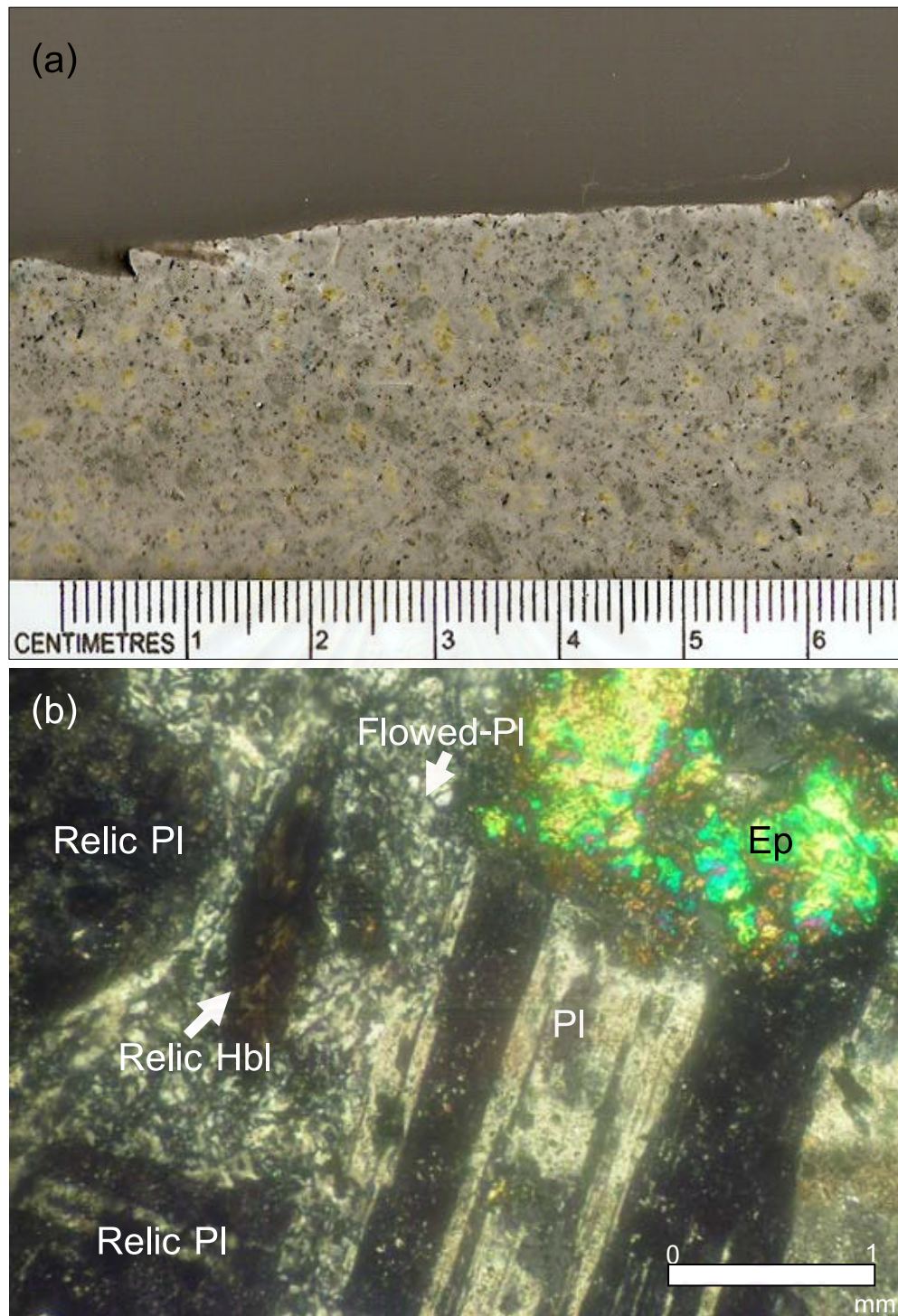


Fig. 4.19 A slab specimen of weathered andesite (a) (V project) (Sample no. DDV11) showing abundant green phenocrysts in fine-grained groundmass. (b) Photomicrograph (in cross-polarized light) from the same sample of above (a) showing altered twinning plagioclase (PI) phenocryst which is replaced by epidote (Ep). Note that relic hornblende is also observed.

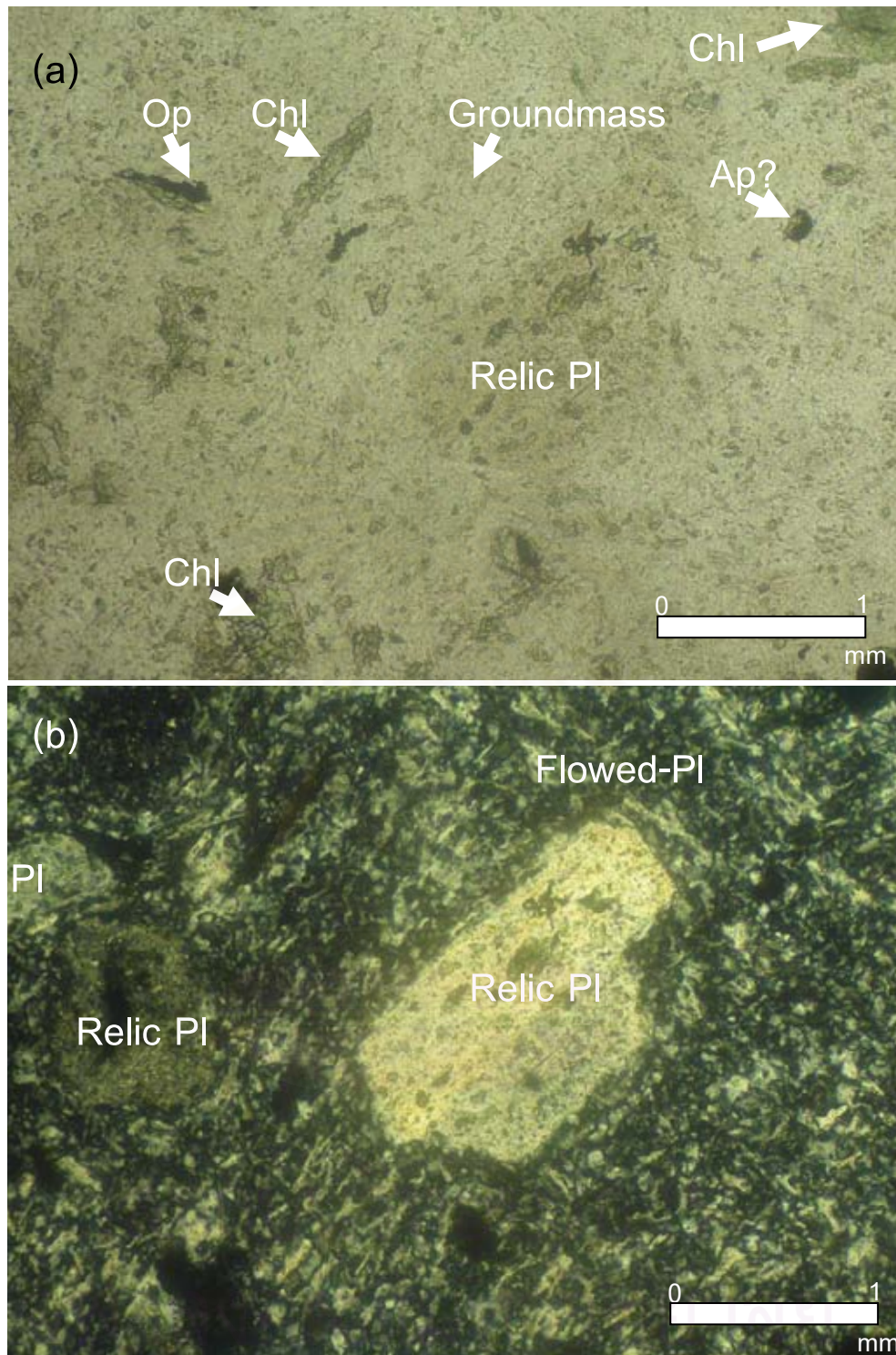


Fig. 4.20 Photomicrographs of weathered andesite of V Prospect (Sample no. DDV17) ((a) in plane polarized light and (b) in cross-polarized light). (a) Very altered plagioclase (PI) phenocryst set in groundmass and surrounded by chlorite (Chl), opaque, microlite and accessory unidentified mineral (apatite?) (Ap). (b) The same sample of above showing relic plagioclase phenocryst set in flowed-plagioclase.

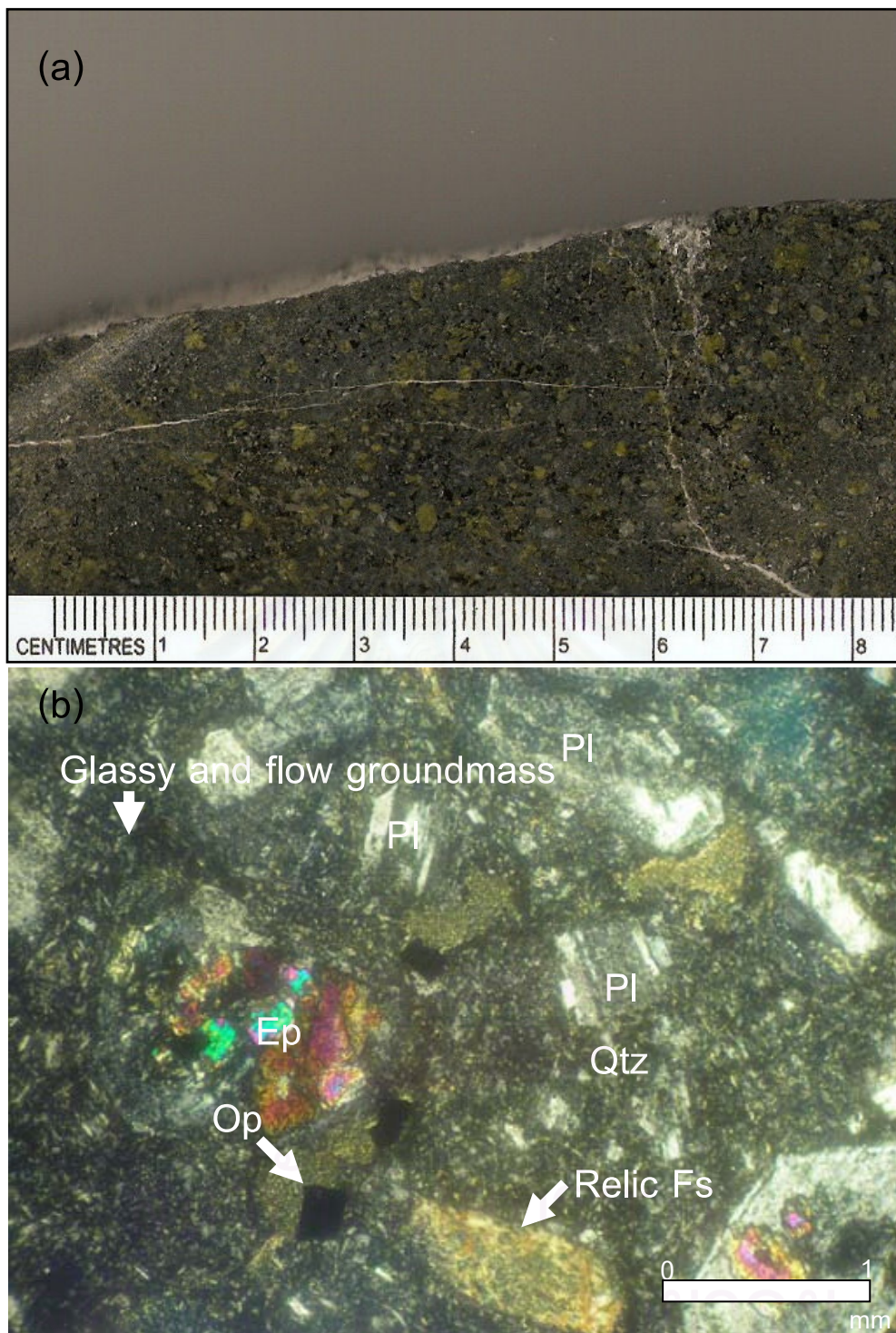


Fig. 4.21 (a) (Sample no. DDV26) A slab specimen of altered green andesite (V prospect) showing abundant green phenocryst and fine-grained groundmass. Photomicrograph (b) (in cross-polarized light) (Sample no. DDV15) showing altered twinning plagioclase (Pl) phenocryst which is replaced by epidote (Ep) set in glassy and flow texture. Cubic opaque (Op) mineral formed in groundmass.

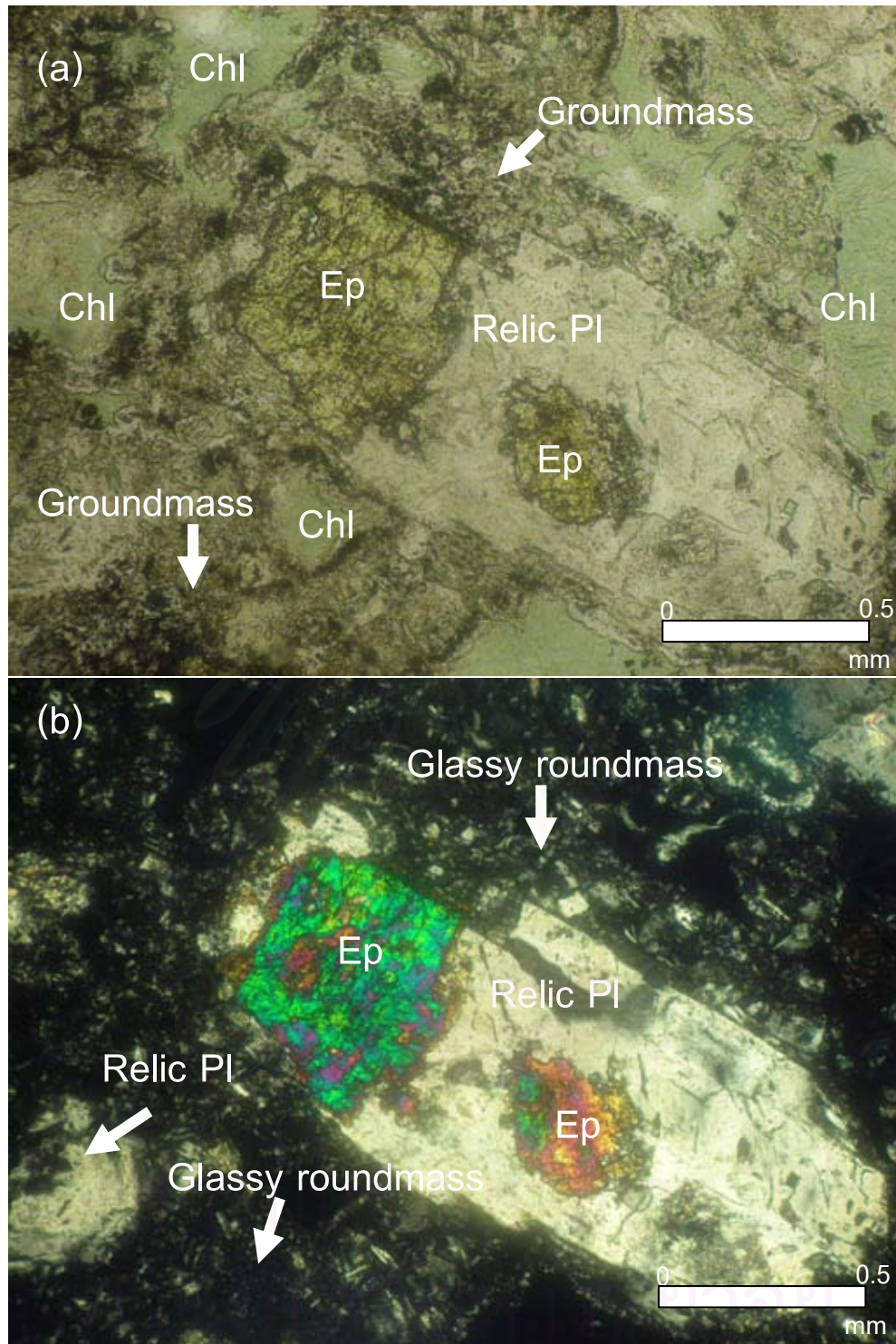


Fig. 4.22 Photomicrographs of altered andesite (Sample no. DDV26) (V prospect) ((a) in plane-polarized light and b in cross-polarized light) showing relic plagioclase (PI) replaced by subhedral epidote (Ep) and set in devitrified/chloritized glassy groundmass. Chlorite (Chl) formed as irregular shape in the rock.

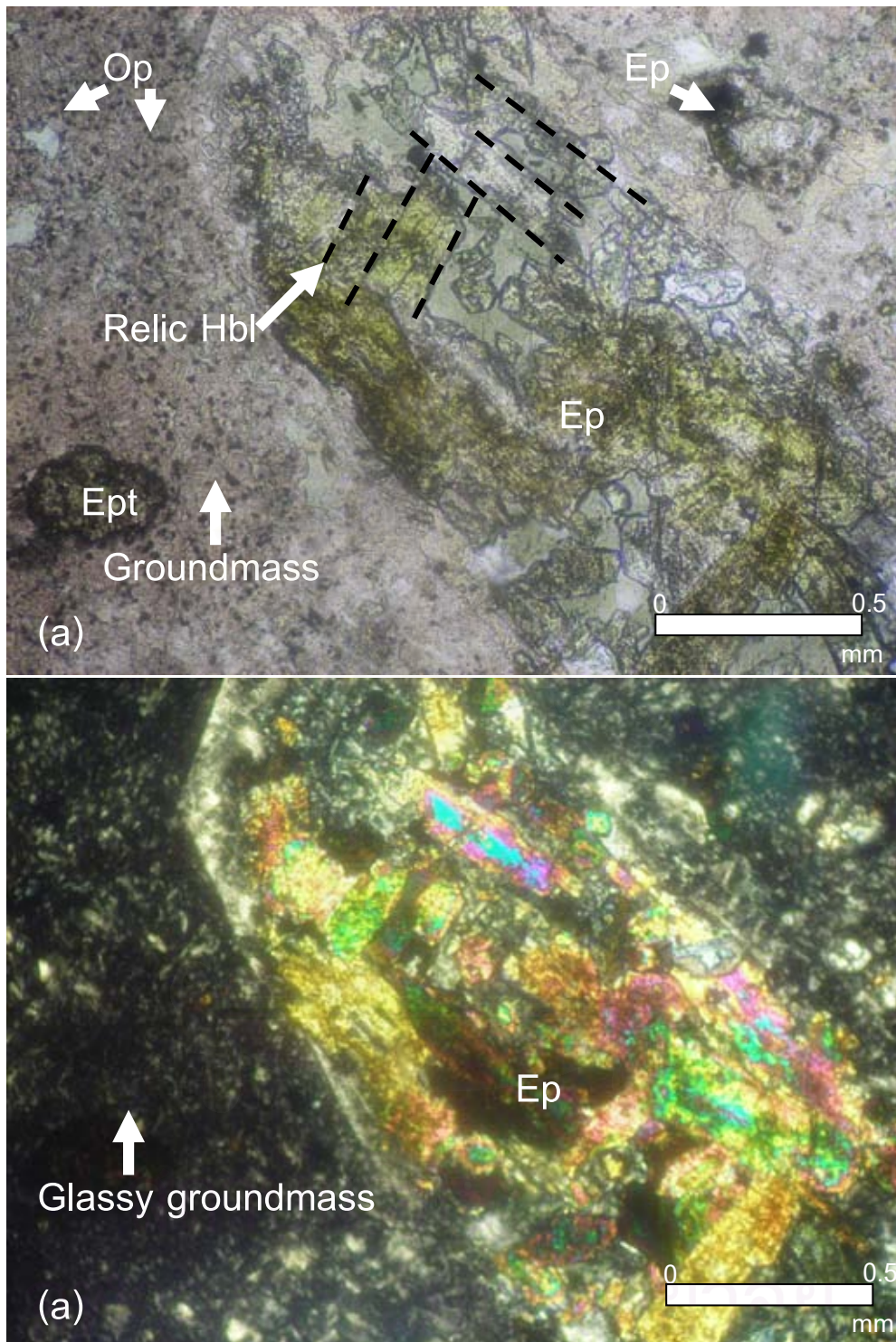


Fig 4.23 Photomicrographs of altered andesite (Sample no. DDV31) (V Prospect) ((a) in plane-polarized light and (b) plane-polarized light) showing relic hornblende with 120° and 60° cleavage altered to epidote (Ep) set in devitrified/chloritized glassy groundmass with some microlite. Opaque (Op) mineral is disseminated in groundmass.

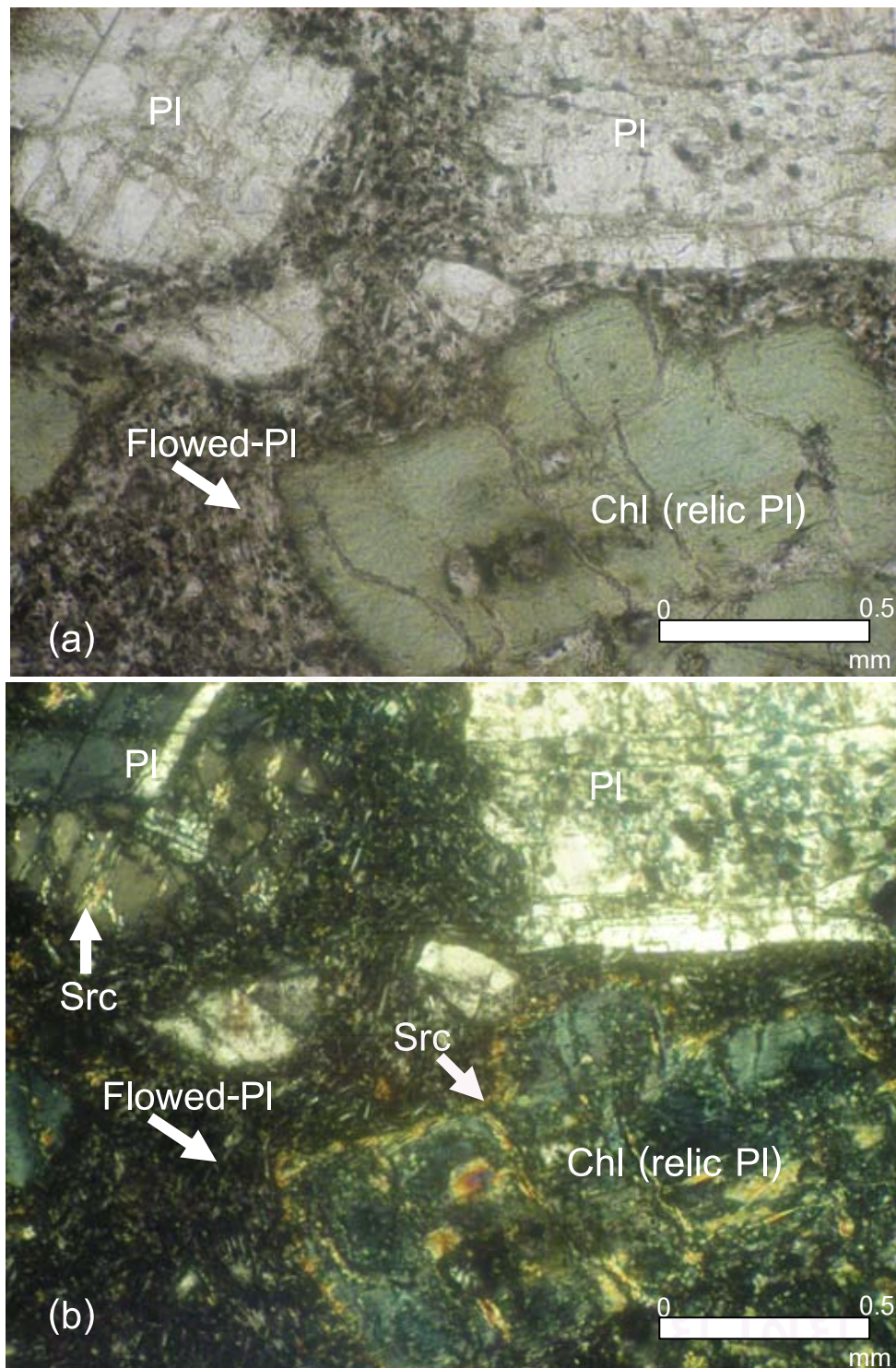


Fig. 4.24 Photomicrographs of altered andesite at V prospect (Sample no. DDV10) ((a) in plane-polarized light and (b) in cross-polarized light), Chatree gold deposits. (a) (b) Relic plagioclase (PI) phenocryst altered to chlorite (Chl) and minor sericite (Src) at rim and fractured, set in the groundmass enriched in microlite, devitrified glassy materials, and some opaques. Note that flow texture is also present.

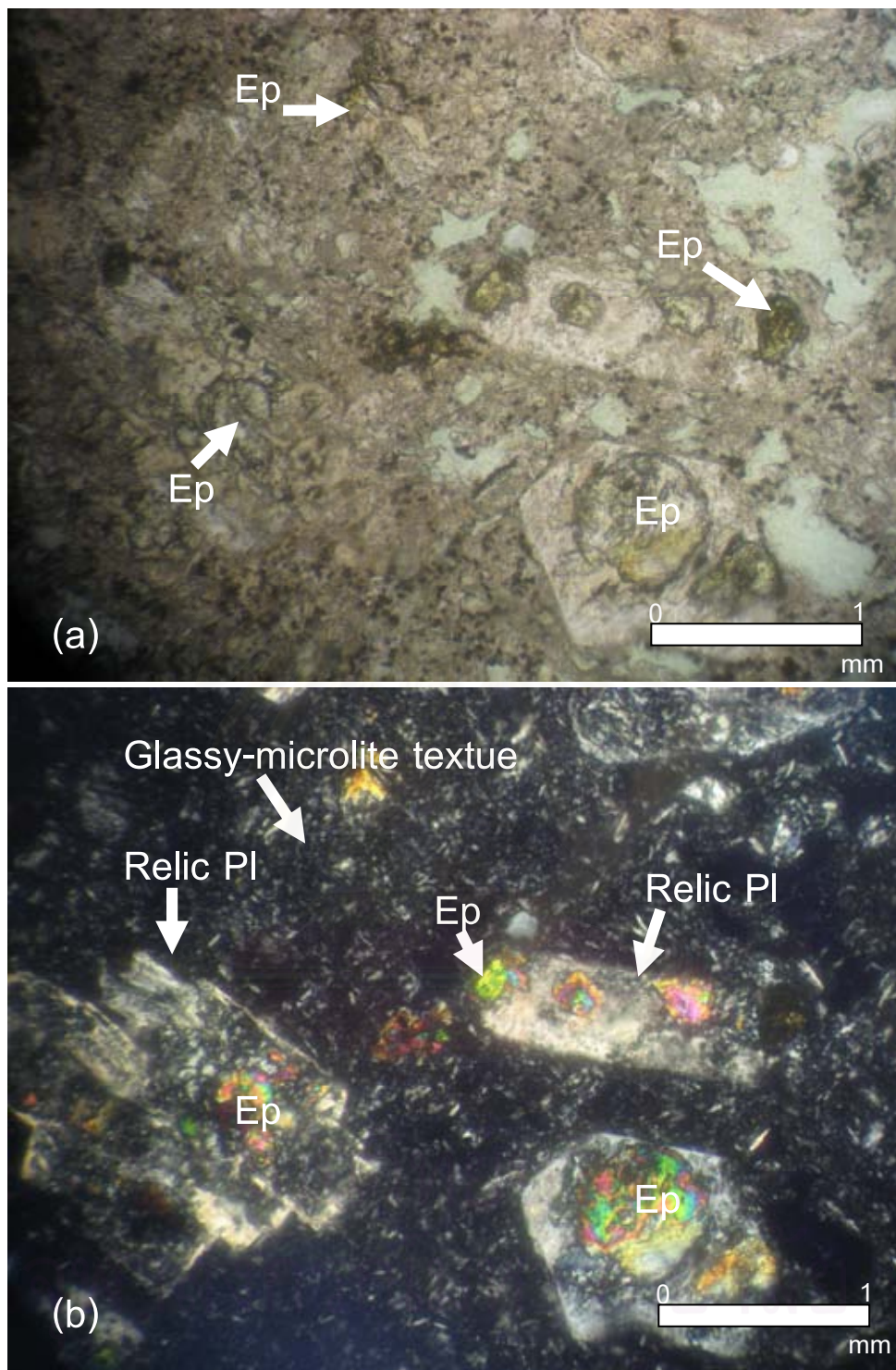


Fig. 4.25 Photomicrographs (Sample no. DDV31) ((a) in plane polarized-light of the same sample of figure (b) in cross-polarized light) of altered andesite at V prospect (sample no. DDV31). (a) (b) Relic plagioclase (PI) phenocryst is mainly replaced by epidote (Ep) mainly in the cores and formed in glassy groundmass.

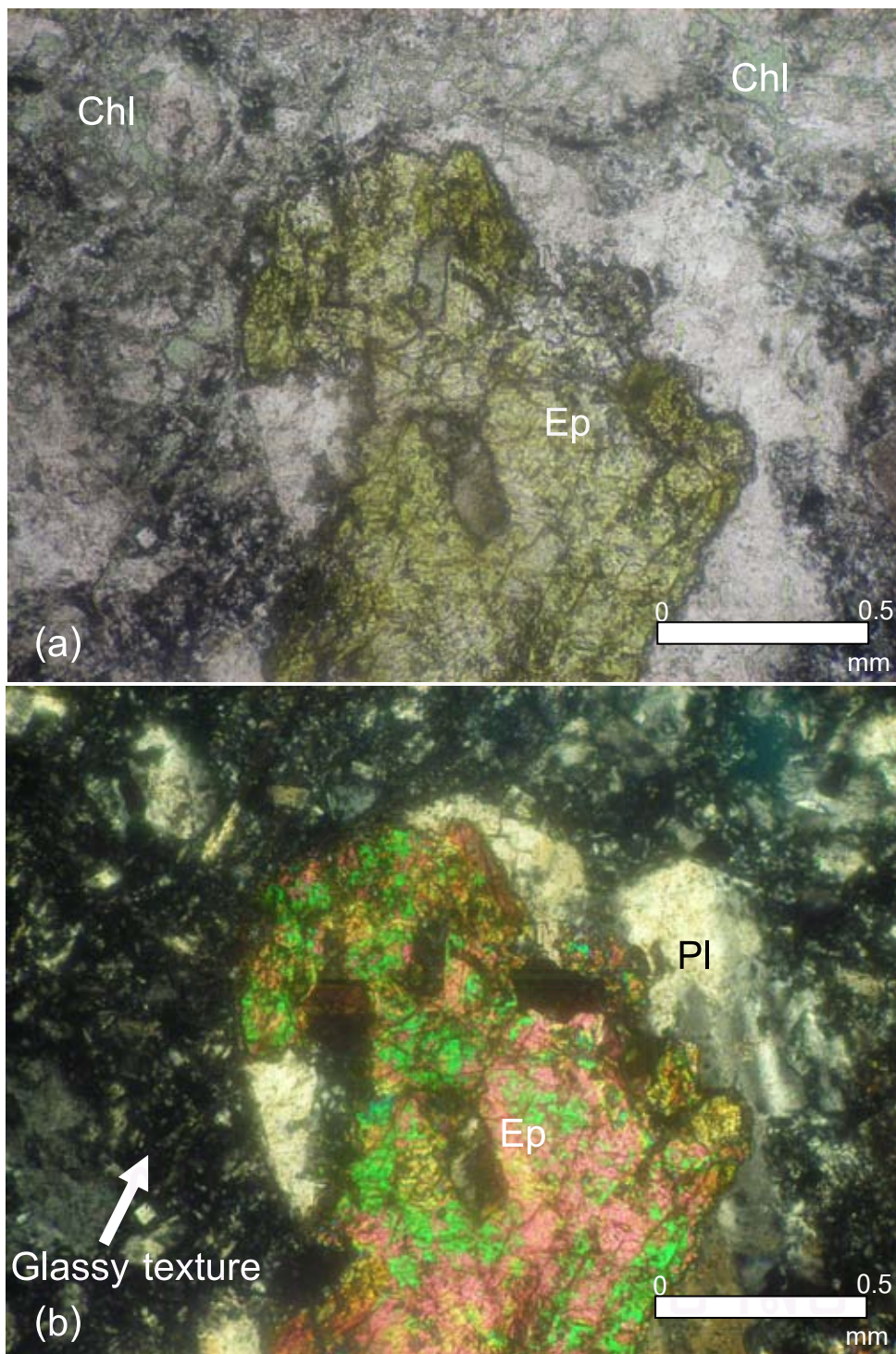


Fig. 4.26 Photomicrographs (Sample no. DDV36) ((a) in plane-polarized light and (b) in cross-polarized light) of altered andesite at V prospect. (a) (b) Relic plagioclase (PI) phenocrysts altered to epidote (Ep), particularly in the core in glassy and devitrified (chloritized) groundmass and microlite.

4.4 Ore petrographic study

Porphyritic granodiorite and andesite (N prospect)

Six samples of polished section were prepared for determining ore minerals. Ore minerals of N prospect occur principally in quartz vein (Fig 4.27a) and disseminated in groundmass (Fig 4.27b). It is defined by presence of chalcopyrite, pyrite, molybdenite and sphalerite. Ore minerals formed various characteristic, disseminated in groundmass, associated with quartz vein, single grain, and inclusion in ore, visible to invisible. The ore assemblage vein is subdivided into 4 stage of time as following;

1. First stage, quartz-chalcopyrite-pyrite-molybdenite vein (in fine-grained granodiorite) (Figs. 4.27a, 4.27b, 4.28a, 4.28b)
2. Next, quartz-chalcopyrite-pyrite-splalartite-chlorite vein (in fine-grained granodiorite and andesite) (Figs. 4.29a, 4.29b, 4.30a, 4.31b)
3. Then, Quartz- chalcopyrite-pyrite-splalartite-chlorite-epidote vein (in Andesite)
4. Later, Epidote vein with rare ore (in Andesite) (Figs. 4.31a, 4.31b, 4.32a, 4.32b)
5. Finally, unmineralization of calcite vein (in Andesite) (Figs. 4.31a)

Chalcopyrite occurs mostly with quartz vein and rare in groundmass of fine-grained granodiorite with size ranging from 0.1-0.5 mm and has angular to Irregular shape. However, chalcopyrite founded both in fine-grained granodiorite and andesite. The time of forming mineral later than pyrite because cubic pyrite changed to anhedral at egde of grain which is repaced by chalcopyrite.

Pyrite is usually formed as subhedral to euhedral crystal (avg. 0.3 mm). It is invariably associated with vein of quatz, sphalerite, chalcopyrite and molybdeniite vein. In addition, pyrite appears also as aggregate with chalcopyrite, inclusion in chalcopyrite, single anhedral grains disseminated in groundmass of granodiorite and andesite.

Sphalerite commonly occurs as aggregate, subhedral to anhedral shape and associated with chalcopyrite and pyrite. The size of sphalerite is range between < 0.05 mm and 0.2 mm. It is filled and replaced at rim both of pyrite and chalcopyrite grains

indicating the time of forming mineral later than pyrite and chalcopyrite. Sphalerite associated quartz-chalcopyrite-pyrite assemblage and rarely in groundmass of fine-grained granodiorite and andesite.

Molybdenite is usually formed sheet, sandwiched and undulated set in quartz vein by single crystal. The mineral assemblage is quartz-chalcopyrite-pyrite-molybdenite. The size is ranging from 0.1-0.5 mm. Molybdenite is mainly found in quartz vein in fine-grained granodiorite. Not found in andesite.

Table 5.1 Description ore petrography of drill-hole no. 2580 DD at N prospect, Chatree gold mine, Thailand.

Running no.	Sample. No.	Depth (m)	Rock name	Hydrothermal ore assemblages
1	DDN101	19.10-19.20	prophyritic granodiorite	Quartz-chalcopyrite-pyrite-sphalerite-chlorite
2	DDN103	50.5-50.6	prophyritic granodiorite	Quartz-chalcopyrite-pyrite-sphalerite-chlorite
3	DDN106	63.7-63.8	prophyritic granodiorite	Quartz-chalcopyrite-pyrite-sphalerite-chlorite
4	DDN108	120.5-120.6	prophyritic granodiorite	Quartz-chalcopyrite-pyrite-molybdenite
5	DDN109	139.4-139.5	Andesite	Quartz-chalcopyrite-pyrite-sphalerite-chlorite-calcite
6	DDN116	161.20-161.30	Andesite	Quartz-chalcopyrite-pyrite-sphalerite-chlorite-epidite vein and unmineralization of calcite vein

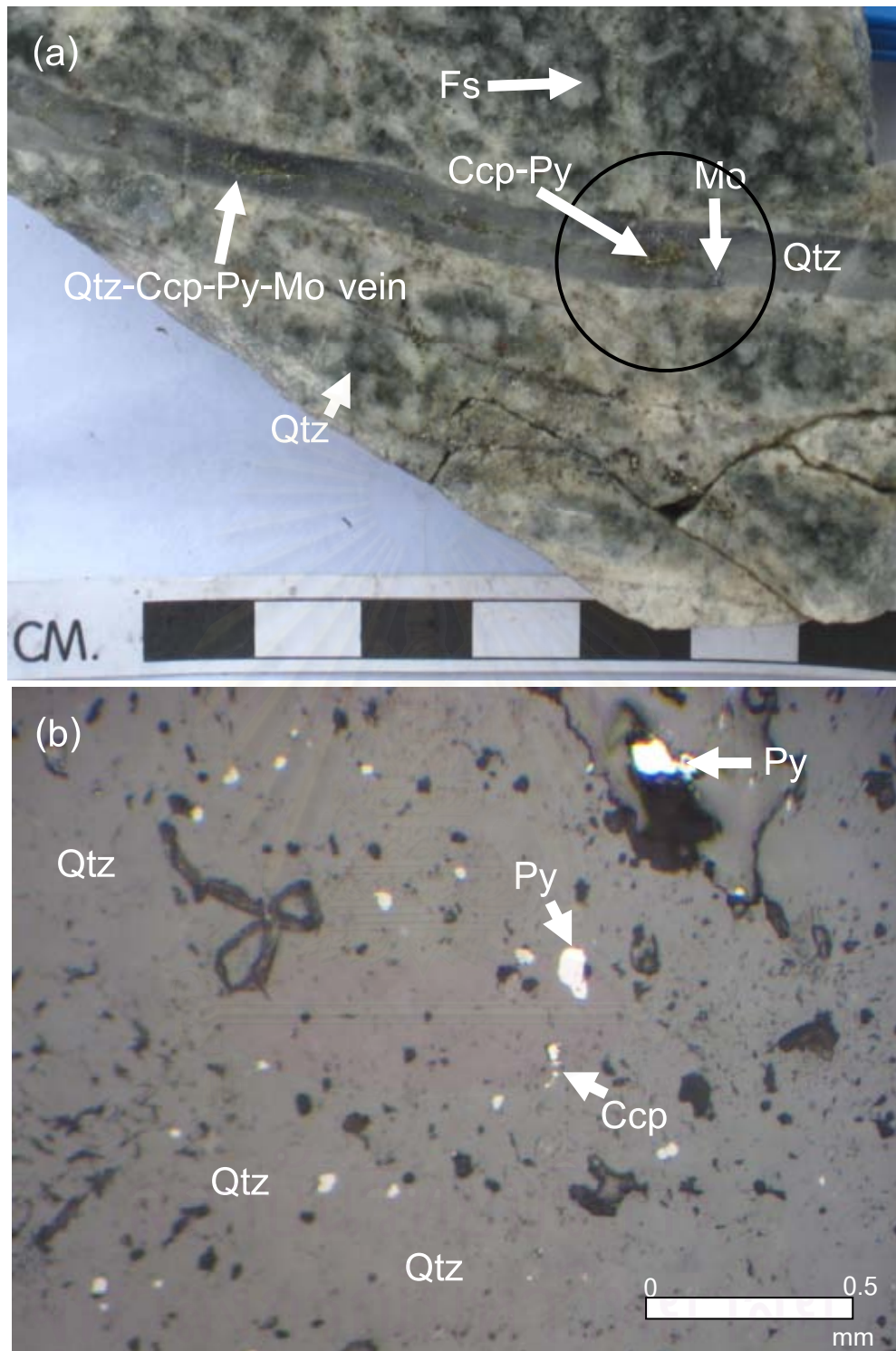


Fig. 4.27 A slab specimen (Sample no. DDN108) (a) of porphyritic granodiorite crosscut by quartz (Qtz)-chalcopyrite (Ccp)-pyrite (Py)-molybdenite (Mo) veinlet. Black circle is prepared for polished section. Photomicrograph (b) (in reflected light) from the same sample of (a) showing anhedral pyrite and chalcopyrite disseminated in fine-grained groundmass.

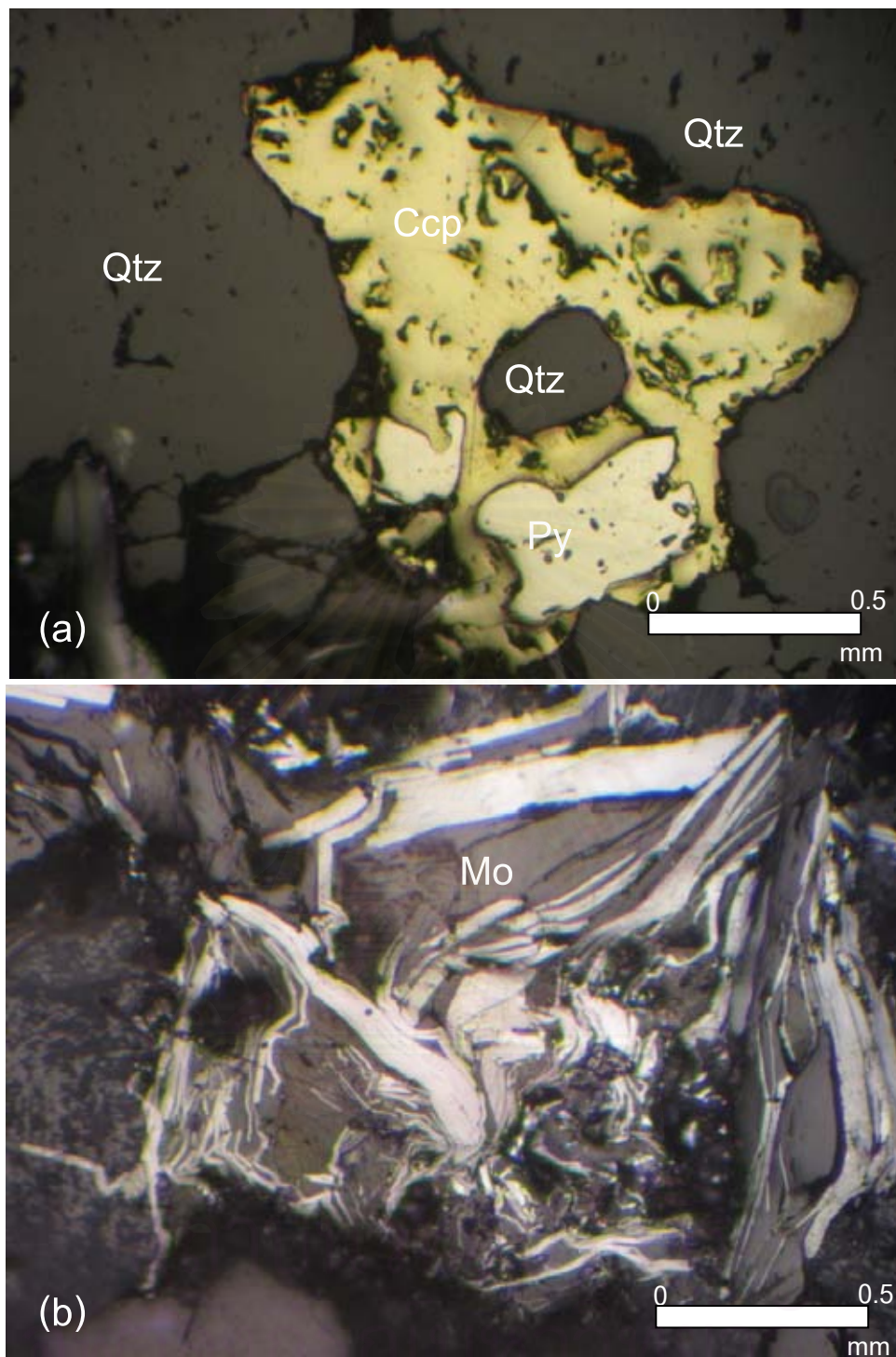


Fig. 4.28 Photomicrographs ((a) and (b) in reflected light) from the same vein (see in Figure 4.27a) in granodiorite showing chalcopyrite (Ccp)-pyrite (Py)-molybdenite (Mo) assemblage. (a) Euhedral pyrite and rounded quartz formed as inclusion in anhedral chalcopyrite. (b) Molybdenite formed characteristics of sheet, sandwiched sheet and undulated texture.

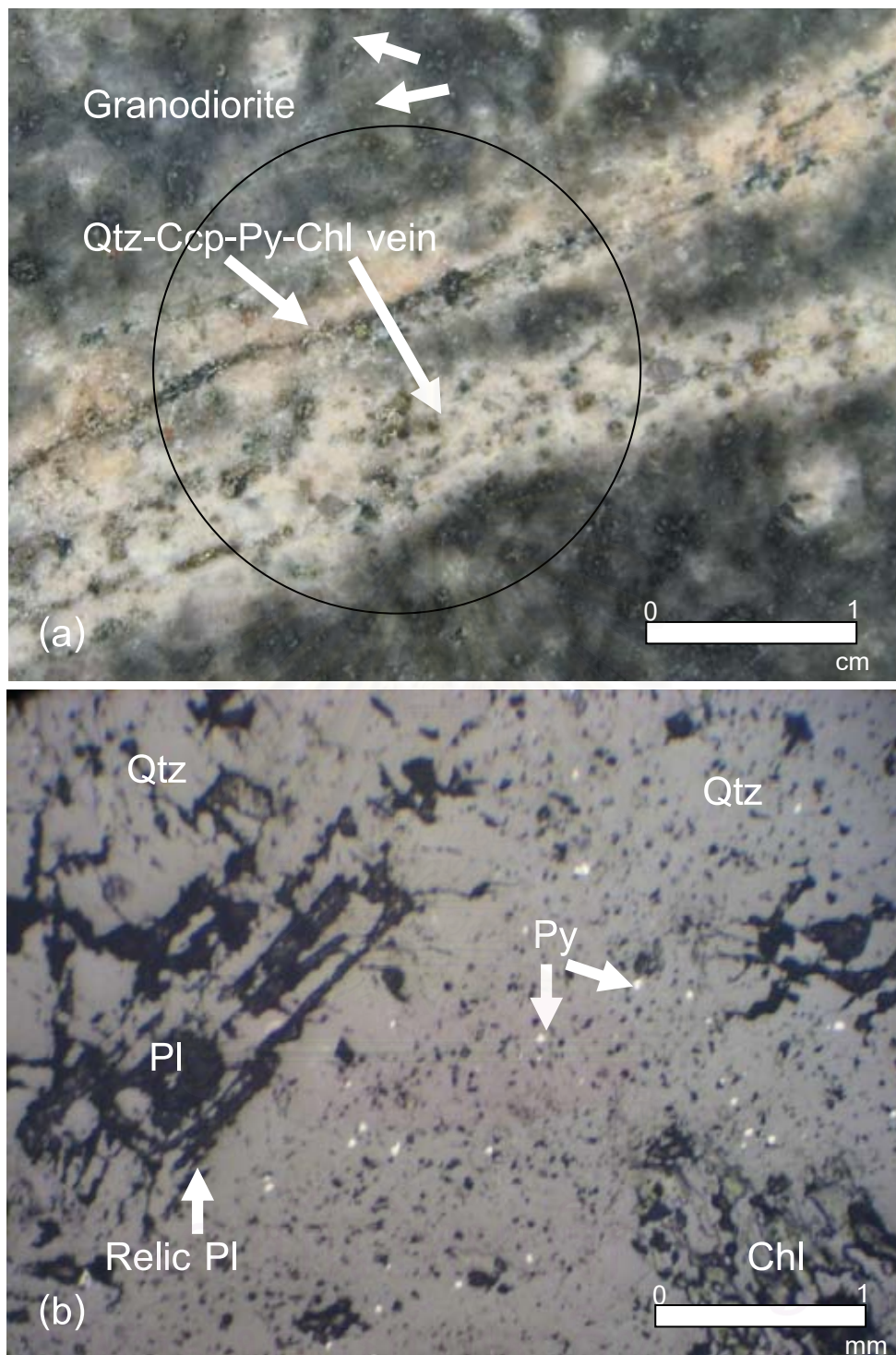


Fig. 4.29 A slab specimen of porphyritic granodiorite (Sample no. DDN106) (a) crosscut by quartz (Qtz)-chalcopyrite (Ccp)-pyrite (Py)-chlorite (Chl). Black circle is prepared for polished section. (b) Photomicrograph (in reflected light) from the same sample of above showing disseminated pyrite formed in quartz groundmass with plagioclase and chlorite.

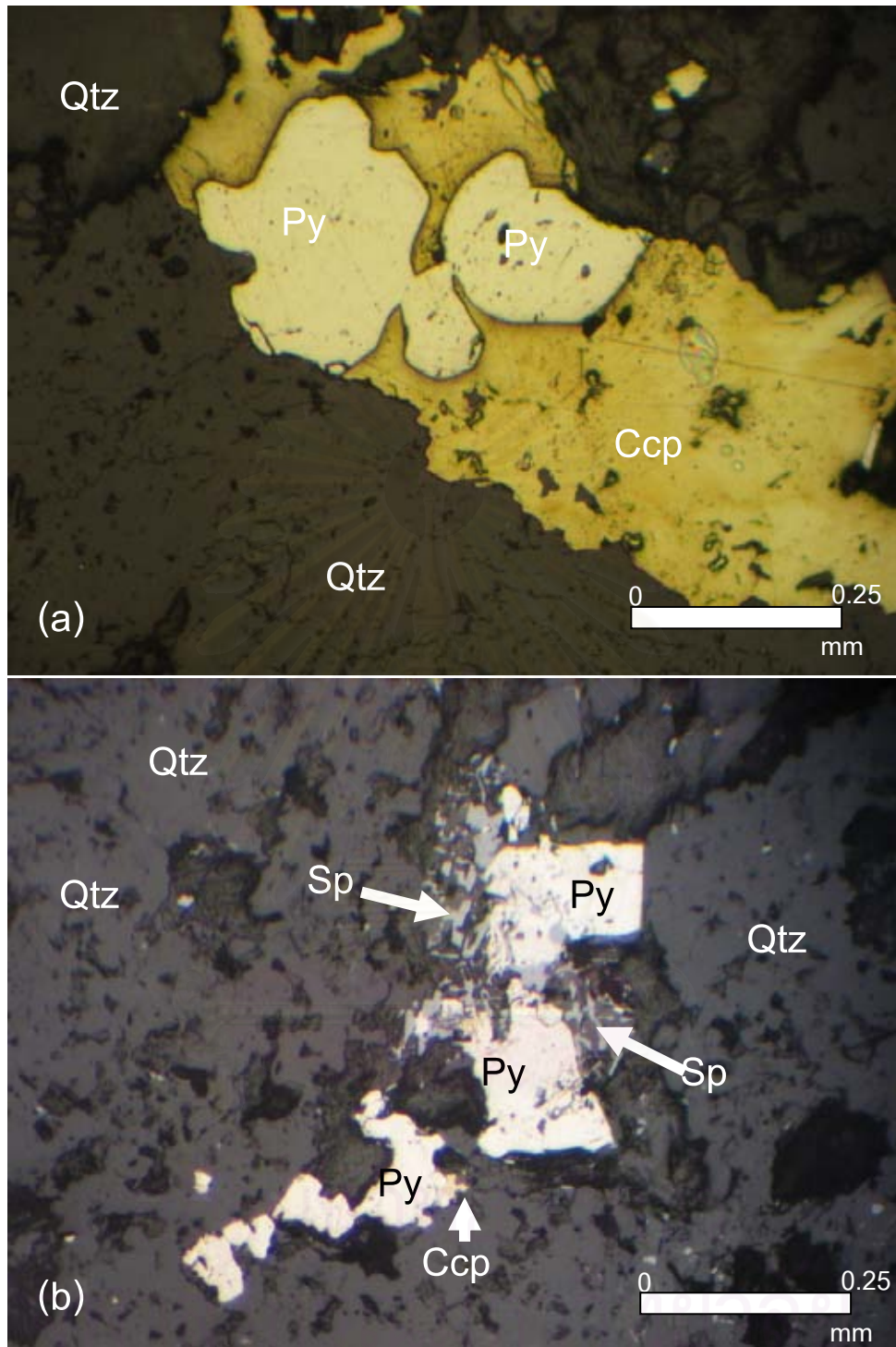


Fig. 4.30 Photomicrographs ((a) and (b) in reflected light) from the same vein (see in figure 4.29a) of the granodiorite showing (a) anhedral chalcopyrite (Ccp)-pyrite (Py) assemblage and (b) larger cubic pyrite (Py) formed associated with smaller sphalerite (Sp) and chalcopyrite (Ccp) in quartz-bearing vein..

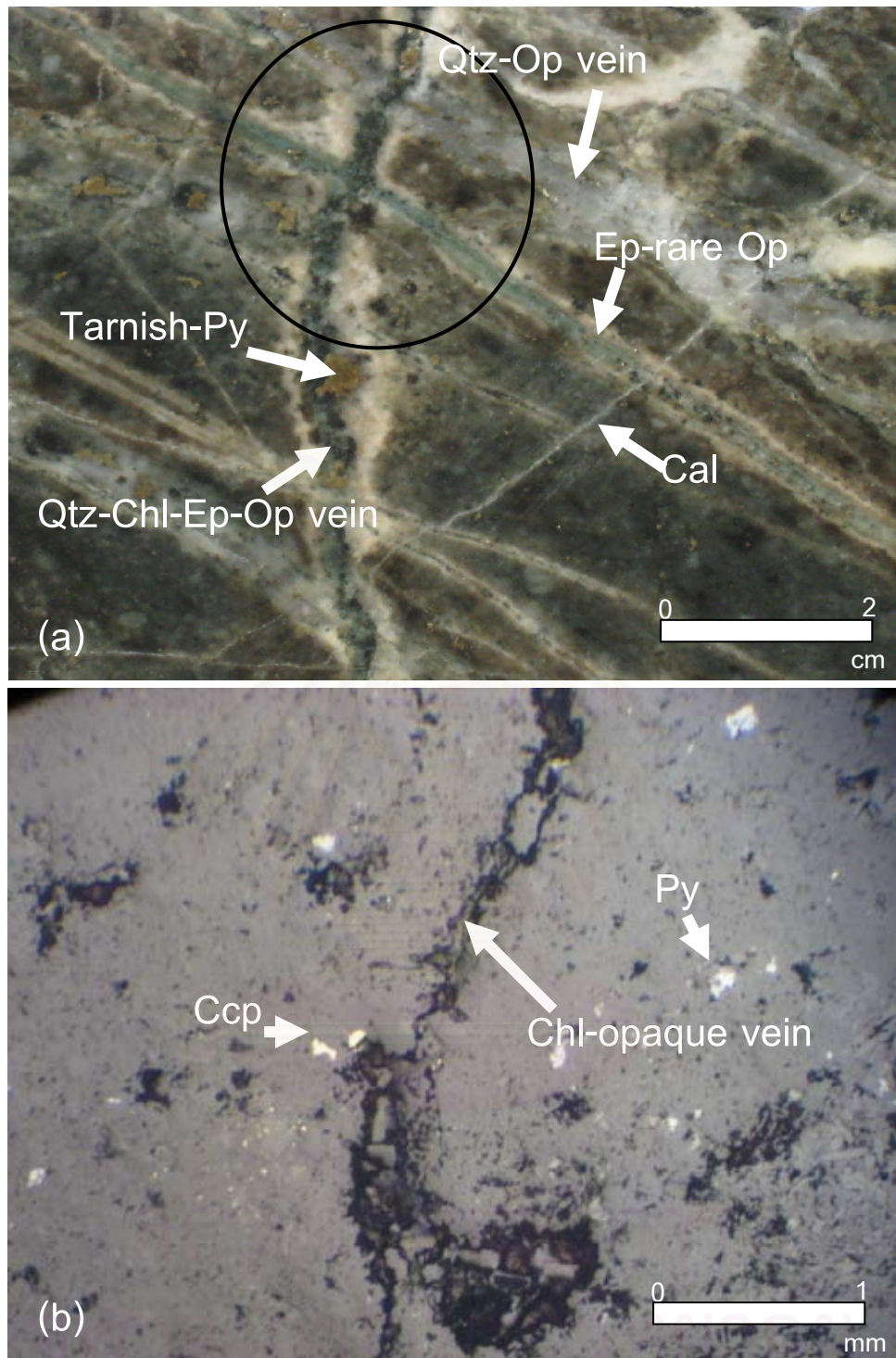


Fig. 4.31 (a) (Sample no. DDN116) A slab specimen of andesite rock showing various veins cross cutting quartz (Qtz)-opaque (Op) mineral vein. The second stage is quartz (Qtz)-chlorite (Chl)-epidote (Ep) - opaque (Op) mineral vein cross cut. The third stage is the epidote (Ep)-opaque (Op) mineral vein crosscut the quartz-chlorite-epidote- opaque mineral vein. The calcite (Cal) crosscut the rock in the latest stage. In the black circle is sample for polished section. Black circle of figure (a) is prepared for polished section.(b) Photomicrograph (in reflected light) showing disseminated pyrite (Py) and chalcopyrite (Ccp) blebs in groundmass and cross cut by chlorite (Chl)-opaque (Op) mineral vein.

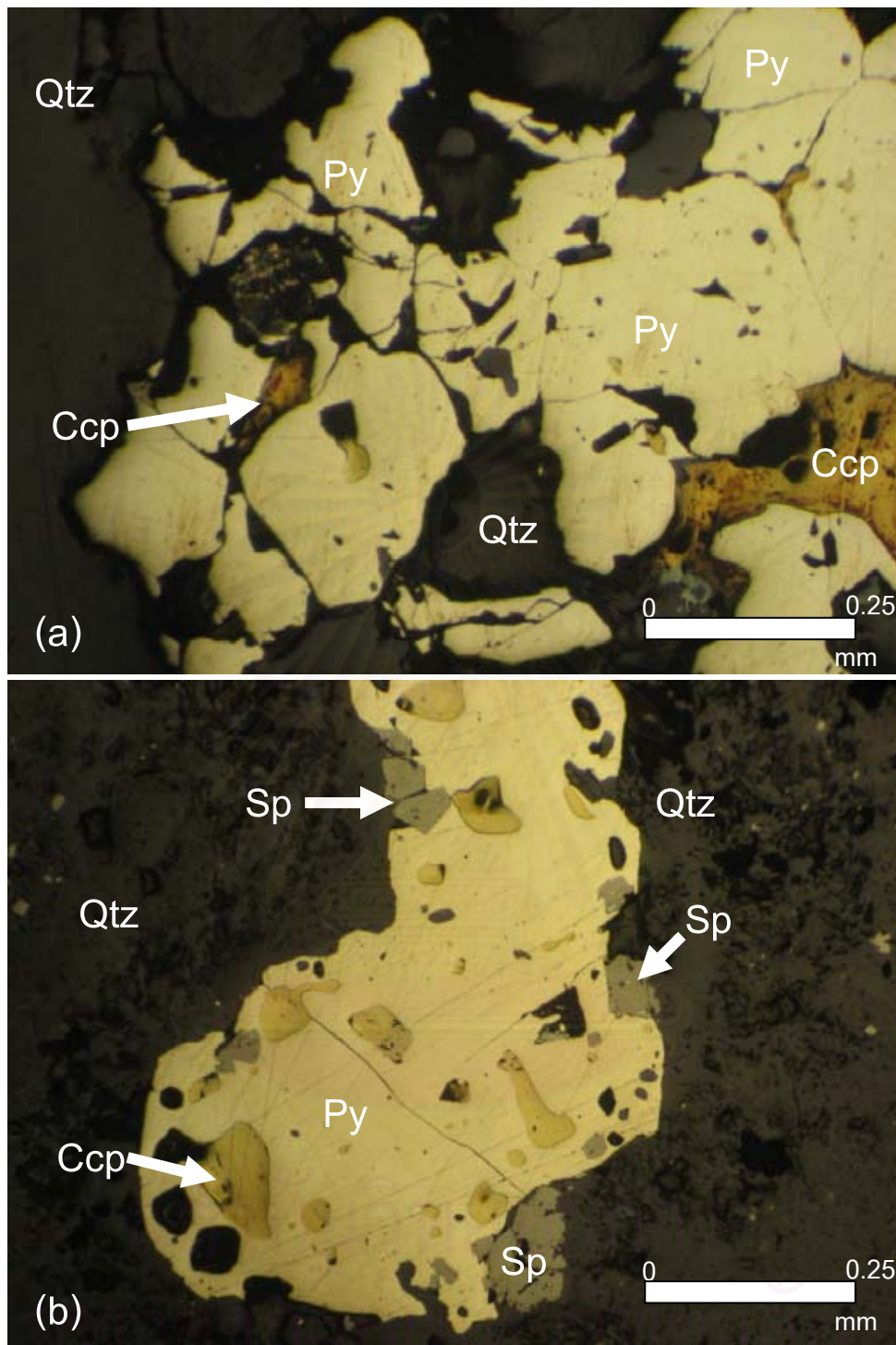


Fig. 4.32 Photomicrographs ((a) and (b) in reflected light) from the quartz-sulfide vein of andesite (see in figure 4.31a) showing (a) anhedral chalcopyrite (Ccp)- and larger euhedral cubic pyrite (Py) assemblage and (b) anhedral sphalerite ore formed at the rim of irregular resorbed pyrite grain containing and chalcopyrite (Ccp) inclusion.

CHAPTER V

GEOCHEMISTRY

After macroscopic and microscopic studies of the igneous rock, 22 less altered samples were selected and analyzed for major oxides, trace elements and rare earth element by XRF (22 samples), ICP-OES (7 samples) and ICP-MS (3 samples) at Akita University. Samples which contained less altered or very few secondary minerals were considered to be fresh. Major-oxide and trace element contents of the Chatree igneous rocks were determined using XRF and ICP-OES method and shown in Table 5.1. Trace and REE concentrations of the Chatree granodiorite rock determined using ICP-MS method and show in Table 5.2.

5.1 Classification of Igneous rocks

5.1.1 Rock nomenclature based on major oxides and trace element

Fine-grained granodiorite

The intrusive rocks contain approximately 64.79– 67.52% SiO₂, 17.01- 19.11% Al₂O₃, 1.93- 3.1% FeO, 0.24- 0.38% Fe₂O₃, 0.01- 0.04% MnO, 2.91- 4.01% MgO, 2.41 - 3.78% CaO, 2.92- 4.95% Na₂O, 0.39- 1.66% K₂O, 0.38- 0.50% TiO₂, and 0.16- 0.23% P₂O₅ and 0.51-1.89% SO₃.

CIPW norm of intrusive rocks consist of 29.12-41.35% quartz, 16.30-36.99% albite, 11.00-17.09% anorthite, 2.56-10.85% orthoclase, 1.58-3.52% thenardite, 8.76- 11.33% hyperstene, 0.19-0.29% magnetite, 0.43- 0.56% illmenite, 0.33-0.47% apatite and 2.47-7.44% corundum (Table 5.3).

Normative compositions of the granodiorite range from tonalite to granodiorite (Fig. 5.1). As shown in the plots of plutonic rock, most studied rocks are fallen in intermediate composition in the fields of tonalite to granodiorite based on QAP plot diagram of Streckeisen (1976). The name 'granodiorite' is the correct nomenclature for this rock type and it is consistent with the TAS diagram of Cox et al. (1979) and alkaline-subalkaline of Irvine and Baragar (1971) (Fig. 5.2).

The total alkalis and silica of these rock types as well as those of the fine-grained granodiorite plotted in the TAS diagram of Wilson Cox et al., (1979) in order to find out or

re-confirm the correct nomenclature of those rocks. The rock name 'granodiorite' is the correct nomenclature of this rock type. Hence all the rock nomenclatures used in this study are named based on the QAP diagram of Streckeisen (1976) as well as the TAS diagram of Cox et al. (1979) and diving alkaline-subalkaline of Irvine and Baragar (1971). Therefore, the rocks are granodiorite to tonalite.

Andesitic rock

The extrusive rocks contain approximately 49.6– 57.05 % SiO_2 , 16.05- 20.23% Al_2O_3 , 4.4- 8.78% FeO , 0.54-1.08 % Fe_2O_3 , 0.06- 0.24% MnO , 5.27- 9.16% MgO , 3.3 – 10.82% CaO , 1.04- 3.45% Na_2O , 0.79- 5.64% K_2O , 0.51- 0.74% TiO_2 , 0.19- 0.27% P_2O_5 and 1.19-2.41 % SO_3 .

Classification of alkaline and subalkaline basalts in terms of wt% $\text{Na}_2\text{O}+\text{K}_2\text{O}$ versus % SiO_2 of Le Maitre (2002) and alkaline-subalkaline of Irvine and Baragar (1971) for volcanic rocks of N&V prospects is mainly fall in the basaltic andesite (Fig. 5.3).

For classification of nomenclature, proper discrimination diagrams were applied. Plots of Zr/TiO_2 versus Nb/Y for volcanic rocks of N&V prospects based on the diagram of Winchester and Floyd (1977) and the rock plots fall in the field of subalkalic-basalt (Fig. 5.4). The studied andesite samples belong to magmatic group which is subalkalic-basalt.

Table 5.1 Major-oxide and trace element contents of the Chatree igneous rocks determined using XRF and ICP-OES method.

Rock type	Granodiorite	Granodiorite	Granodiorite	Granodiorite	Granodiorite	Granodiorite	Granodiorite	Granodiorite	Granodiorite	
Sample no	DDN4	DDN7	DDN12	DDN15	DDN20	DDN22	DDN25			
Depth (m)	22.4-22.5	28.4-28.5	42.0-42.1	51.6-51.7	64.0-64.1	70.7-70.8	82.6-82.7			
Element	XRF	XRF	ICP-OES	XRF	XRF	XRF	ICP-OES	XRF	ICP-OES	XRF
Na ₂ O	4.48	3.93	-	4.72	3.99	4.24	-	3.98	-	4.13
P ₂ O ₅	0.16	0.22	-	0.22	0.17	0.17	-	0.17	-	0.21
MgO	4.04	3.49	-	3.62	3.27	3.06	-	2.92	-	3.74
Al ₂ O ₃	18.96	18.72	-	18.07	20.01	17.84	-	18.02	-	17.85
SiO ₂	65.81	66.44	-	66.23	66.55	68.17	-	67.57	-	65.79
SO ₃	0.96	1.52	-	1.78	0.92	0.94	-	0.51	-	0.85
K ₂ O	0.66	1.08	-	0.73	0.77	0.65	-	0.47	-	0.68
CaO	2.43	2.54	-	3.01	2.63	3.09	-	3.40	-	3.52
TiO ₂	0.51	0.48	-	0.46	0.45	0.39	-	0.48	-	0.48
MnO	0.02	0.02	-	0.02	0.01	0.02	-	0.04	-	0.03
Fe ₂ O ₃	2.96	2.76	-	2.69	2.40	2.64	-	3.27	-	3.75
V	67.79	68.38	55.71	133.63	210.91	93.52	40.64	74.13	52.84	88.24
Cr	217.71	159.32	6.76	170.34	112.80	168.65	5.70	170.46	7.31	152.90
Ni	8.03	5.84	-1.63	1.96	7.83	4.97	0.99	173.46	3.15	683.67
Cu	1246.22	938.24	930.55	3603.36	1791.64	1012.16	600.02	367.66	242.37	1460.85
Zn	44.38	35.34	20.56	43.12	34.99	34.59	17.67	41.81	92.74	34.59
Rb	-0.62	7.51	128.99	58.75	7.20	1.04	16.47	3.57	70.32	2.29
Sr	1070.41	957.58	550.67	1065.36	960.61	886.65	573.49	957.49	605.54	1082.84
Y	16.02	18.54	16.74	16.18	13.97	14.07	15.48	14.34	16.14	19.39
Zr	104.44	115.02	25.67	110.48	123.27	103.66	11.22	122.27	29.00	109.41
Nb	11.35	11.29	-	18.35	11.33	11.30	-	11.29	-	11.29
Ba	-	-	210.44	-	-	-	202.98	-	168.85	-
Li	-	-	86.18	-	-	-	89.41	-	27.37	-
Sc	-	-	9.21	-	-	-	77.44	-	8.77	-
Ce	-	-	30.85	-	-	-	31.42	-	24.14	-
Nd	-	-	-6.08	-	-	-	-8.41	-	-8.21	-

Table 5.1 (cont.)

Rock type	Granodiorite	Granodiorite	Granodiorite	Granodiorite	Granodiorite	Granodiorite	Granodiorite	Granodiorite	
Sample no	DDN27	DDN28	DDN31	DDN36	DDN38	DDN39	DDN45		
Depth (m)	89.0-89.1	92.4-92.5	102.4-102.5	113.4-113.5	117.6-117.7	124.9-125	139.4-139.5		
	XRF	XRF	XRF	ICP-OES	XRF	XRF	XRF	XRF	ICP-OES
Element									
Na ₂ O	4.27	3.67	4.47	-	4.94	2.95	5.00	3.15	
P ₂ O ₅	0.22	0.23	0.22	-	0.19	0.22	0.22	0.20	-
MgO	3.20	3.08	3.39	-	3.06	3.25	3.03	6.51	-
Al ₂ O ₃	17.72	18.37	17.79	-	17.19	19.27	17.63	19.22	-
SiO ₂	67.24	65.34	67.29	-	67.50	66.69	66.51	57.02	-
SO ₃	1.13	1.89	1.18	-	0.99	1.48	1.28	1.19	-
K ₂ O	0.59	1.46	0.86	-	0.40	1.67	0.39	1.55	-
CaO	3.58	2.84	3.15	-	3.72	2.47	3.82	4.33	-
TiO ₂	0.43	0.44	0.42	-	0.39	0.49	0.40	0.62	-
MnO	0.02	0.03	0.02	-	0.02	0.02	0.02	0.06	-
Fe ₂ O ₃	2.82	3.86	2.54	-	2.89	2.57	2.94	6.71	-
V	43.24	121.05	88.31	52.35	57.04	212.31	47.82	438.59	224.18
Cr	177.04	109.63	148.67	5.33	206.98	521.18	193.63	50.25	17.06
Ni	7.22	9.59	7.04	605.17	5.12	4.77	5.66	15.70	8.06
Cu	1010.12	703.78	952.06	2.50	1559.16	521.10	1378.55	567.46	741.32
Zn	34.59	34.59	34.59	12.73	34.59	34.59	34.59	68.73	93.03
Rb	5.22	14.02	3.56	86.75	-3.91	14.00	-0.97	30.04	67.46
Sr	1018.19	881.96	1081.37	648.96	1020.23	743.60	1091.37	587.49	374.22
Y	18.06	15.38	14.28	15.59	15.56	17.90	17.45	18.64	17.40
Zr	98.45	113.58	111.23	24.05	105.60	98.16	109.29	34.57	11.91
Nb	11.29	11.68	12.26	-	11.29	11.29	11.29	11.29	-
Ba	-	-	-	214.56	-	-	-	-	550.83
Li	-	-	-	87.25	-	-	-	-	35.01
Sc	-	-	-	10.60	-	-	-	-	28.01
Ce	-	-	-	31.16	-	-	-	-	18.24
Nd	-	-	-	-9.00	-	-	-	-	-15.45

Table 5.1 (cont.)

Rock type	Granodiorite		Granodiorite		Granodiorite		Andesite	Andesite	Andesite	Andesite	Andesite
Sample no	DDN49		DDN57		DDN60		DDV10	DDV 16	DDV 19	DDV 24	DDV 32
Depth (m)	148.6-148.7		165.4-165.5		168.4-168.5		30.1-30.2	47.1-47.2	59.5-59.6	68.1-68.2	89.5-89.6
Element	XRF	ICP-OES	XRF	XRF	ICP-OES	XRF	XRF	XRF	XRF	XRF	XRF
Na ₂ O	1.04	-	2.51	3.45	-	1.70	1.79	3.72	2.55	2.43	
P ₂ O ₅	0.27	-	0.27	0.25	-	0.18	0.29	0.20	0.21	0.21	
MgO	6.33	-	6.06	5.28	-	6.73	8.11	9.19	8.30	7.77	
Al ₂ O ₃	18.72	-	17.81	19.19	-	20.05	17.86	16.89	16.54	15.93	
SiO ₂	54.39	-	57.16	55.93	-	49.15	49.98	55.89	54.42	56.18	
SO ₃	1.87	-	2.18	1.56	-	0.36	2.39	1.53	1.28	1.35	
K ₂ O	1.02	-	1.24	0.74	-	5.59	1.01	1.16	0.79	1.34	
CaO	10.83	-	7.33	7.06	-	5.98	7.29	3.31	4.72	4.49	
TiO ₂	0.51	-	0.52	0.54	-	0.73	0.55	0.52	0.61	0.62	
MnO	0.12	-	0.12	0.10	-	0.13	0.16	0.24	0.16	0.20	
Fe ₂ O ₃	5.43	-	5.60	6.63	-	9.32	10.76	8.46	10.47	9.62	
V	472.04	282.28	400.22	395.07	254.07	447.34	293.34	307.83	298.75	340.31	
Cr	186.31	78.45	54.90	74.15	13.64	-8.06	124.40	104.91	94.97	154.18	
Ni	10.45	13.56	11.82	13.63	7.60	17.20	22.59	11.97	23.63	16.39	
Cu	1091.47	770.16	843.02	517.42	349.31	7.86	226.93	115.13	175.07	118.42	
Zn	51.75	27.99	98.38	42.83	24.89	87.51	63.20	119.14	75.15	80.95	
Rb	10.98	39.28	22.22	14.41	49.38	82.67	34.12	35.25	28.47	31.74	
Sr	472.59	310.44	547.65	620.78	416.84	483.63	434.24	567.80	379.87	287.85	
Y	17.60	20.63	19.52	18.54	21.05	19.71	20.54	24.27	17.02	18.89	
Zr	35.70	13.45	30.41	32.86	9.81	32.31	33.12	30.40	32.81	37.25	
Nb	11.29	-	11.29	11.29	-	11.29	-	11.29	11.29	11.29	
Ba	-	129.19	-	-	94.34	-	-	-	-	-	
Li	-	84.19	-	-	95.41	-	-	-	-	-	
Sc	-	30.02	-	-	31.39	-	-	-	-	-	
Ce	-	18.75	-	-	17.83	-	-	-	-	-	
Nd	-	-14.69	-	-	-13.01	-	-	-	-	-	

Table 5.2 Trace and REE concentrations of the Chatree granodiorite rock determining using ICP-MS method.

Rock type	Sample no.	Depth (m)	Sc	Mn	Co	Cu	Zn	Ga	Rb	Sr	Y	Zr	Nb	Cs
Granodiorite	DDN15	51.6-51.7	5.43	108.50	5.07	970.40	23.53	17.33	8.52	485.10	5.20	7.07	2.00	0.34
Granodiorite	DDN28	92.4-92.5	8.17	178.90	14.10	495.30	19.79	18.83	13.62	564.80	5.94	24.83	1.61	0.14
Granodiorite	DDN39	124.9-125	0.31	171.40	14.88	1170.00	27.39	17.71	5.74	843.40	5.46	16.05	2.00	0.12
Rock type	Sample no.	Depth (m)	Sm	Eu	Gd	Tb	Dy	Ho	Er	Tm	Yb	Lu	Hf	Ta
Granodiorite	DDN15	51.6-51.7	1.92	0.76	1.62	0.24	1.01	0.15	0.36	0.05	0.45	0.03	0.33	0.17
Granodiorite	DDN28	92.4-92.5	1.92	0.69	1.81	0.18	1.06	0.20	0.51	0.06	0.41	0.05	0.73	0.35
Granodiorite	DDN39	124.9-125	2.08	0.66	1.95	0.17	1.11	0.21	0.48	0.10	0.32	0.05	0.40	0.12
Rock type	Sample no.	Depth (m)	Ba	La	Ce	Pr	Nd	Pb	Bi	Th	U	Sb		
Granodiorite	DDN15	51.6-51.7	179.50	8.38	18.38	2.30	9.04	2.80	0.03	0.52	0.14	172.00		
Granodiorite	DDN28	92.4-92.5	280.60	8.74	19.49	2.48	9.98	1.71	0.00	0.57	0.13	947.50		
Granodiorite	DDN39	124.9-125	178.30	11.50	23.75	2.90	12.13	3.18	-0.02	0.57	0.20	797.80		

Table 5.3 Chemical analyses of major elements and their CIPW Norms.

Rock Name	Granodiorite	Granodiorite	Granodiorite	Granodiorite	Granodiorite	Granodiorite	Granodiorite
Sample no	N4	N7	N12	N15	N20	N22	N25
Depth (m)	22.40-22.50	28.40-28.50	42.00-42.10	51.60-51.70	64.00-64.10	70.70-70.80	82.60-82.70
Major elements							
SiO ₂	65.34	65.82	65.37	65.91	67.52	67.21	65.35
TiO ₂	0.50	0.47	0.45	0.45	0.38	0.48	0.47
Al ₂ O ₃	18.82	18.54	17.84	19.82	17.67	17.92	17.73
Fe ₂ O ₃	0.29	0.27	0.27	0.24	0.26	0.32	0.37
FeO	2.38	2.22	2.15	1.93	2.12	2.63	3.01
MnO	0.02	0.02	0.02	0.01	0.02	0.04	0.03
MgO	4.01	3.45	3.58	3.24	3.03	2.91	3.71
CaO	2.41	2.52	2.97	2.6	3.06	3.38	3.5
Na ₂ O	4.44	3.89	4.66	3.95	4.2	3.96	4.1
K ₂ O	0.65	1.07	0.72	0.77	0.64	0.47	0.67
P ₂ O ₅	0.16	0.22	0.22	0.17	0.17	0.17	0.21
SO ₃	0.96	1.5	1.75	0.91	0.93	0.51	0.85
Total	99.98	99.99	100	100	100	100	100
CIPW							
Quartz	31.06	36.77	32.75	35.08	34.57	33.62	30.03
Anorthite	11.17	11.32	13.52	12.04	14.23	15.88	16.30
Hypersthene	11.20	9.80	9.96	8.97	8.76	9.07	11.33
Albite	33.72	24.88	29.95	29.55	31.36	32.23	31.28
Orthoclase	4.24	6.97	4.66	5.01	4.12	3.04	4.35
Apatite	0.33	0.45	0.45	0.35	0.34	0.34	0.43
Thenardite	1.80	2.80	3.25	1.70	1.72	0.95	1.58
Ilmenite	0.56	0.53	0.50	0.51	0.42	0.54	0.53
Corundum	5.70	6.27	4.76	6.61	4.27	4.09	3.88
Magnetite	0.23	0.21	0.21	0.19	0.20	0.25	0.29
Total	100.00	100.00	100.00	100.00	100.00	100.00	100.00

สถาบันวิทยบริการ
จุฬาลงกรณ์มหาวิทยาลัย

Table 5.3 (cont.)

Rock Name	Granodiorite	Granodiorite	Granodiorite	Granodiorite	Granodiorite	Granodiorite
Sample no	N27	N28	N31	N36	N38	N39
Depth (m)	89.00-89.10	92.40-92.50	102.40-102.50	113.40-113.50	117.60-117.70	124.90-125
Major elements						
SiO ₂	66.6	64.79	66.56	66.82	66.13	65.87
TiO ₂	0.42	0.44	0.41	0.39	0.49	0.4
Al ₂ O ₃	17.55	18.21	17.59	17.01	19.11	17.46
Fe ₂ O ₃	0.28	0.38	0.25	0.29	0.25	0.29
FeO	2.26	3.1	2.04	2.32	2.07	2.36
MnO	0.02	0.03	0.02	0.02	0.02	0.02
MgO	3.17	3.05	3.36	3.03	3.22	3
CaO	3.54	2.82	3.11	3.68	2.45	3.78
Na ₂ O	4.23	3.64	4.42	4.89	2.92	4.95
K ₂ O	0.58	1.44	0.86	0.4	1.66	0.39
P ₂ O ₅	0.21	0.23	0.21	0.19	0.22	0.22
SO ₃	1.12	1.88	1.17	0.98	1.47	1.27
Total	99.98	100.01	100	100.02	100.01	100.01
Quartz	33.33	36.86	32.02	29.12	41.35	29.14
Anorthite	16.39	12.81	14.20	17.09	11.00	17.44
Hypersthene	9.20	10.10	9.34	8.93	9.11	8.93
Albite	30.34	19.98	31.65	36.99	16.30	35.62
Orthoclase	3.74	9.41	5.54	2.56	10.85	2.50
Apatite	0.42	0.47	0.42	0.38	0.45	0.44
Thenardite	2.07	3.52	2.16	1.80	2.76	2.34
Ilmenite	0.47	0.50	0.46	0.43	0.55	0.44
Corundum	3.83	6.04	4.01	2.47	7.44	2.91
Magnetite	0.22	0.30	0.19	0.22	0.20	0.22
Total	100.00	100.00	100.00	100.00	100.00	100.00

สถาบันวิทยบริการ
จุฬาลงกรณ์มหาวิทยาลัย

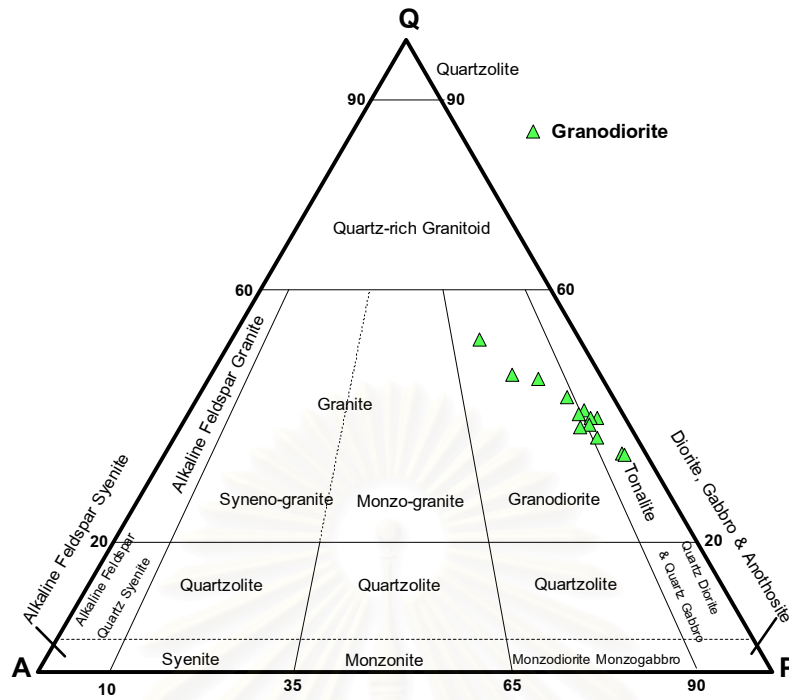


Fig. 5.1 Plot Q-A-P (Streckeisen, 1976) for the rocks from the N prospect. Chatree gold deposit is mainly set in tonalite and granodiorite field. Q=normative quartz, P=normative albite+anorthite and A=normative orthoclase.

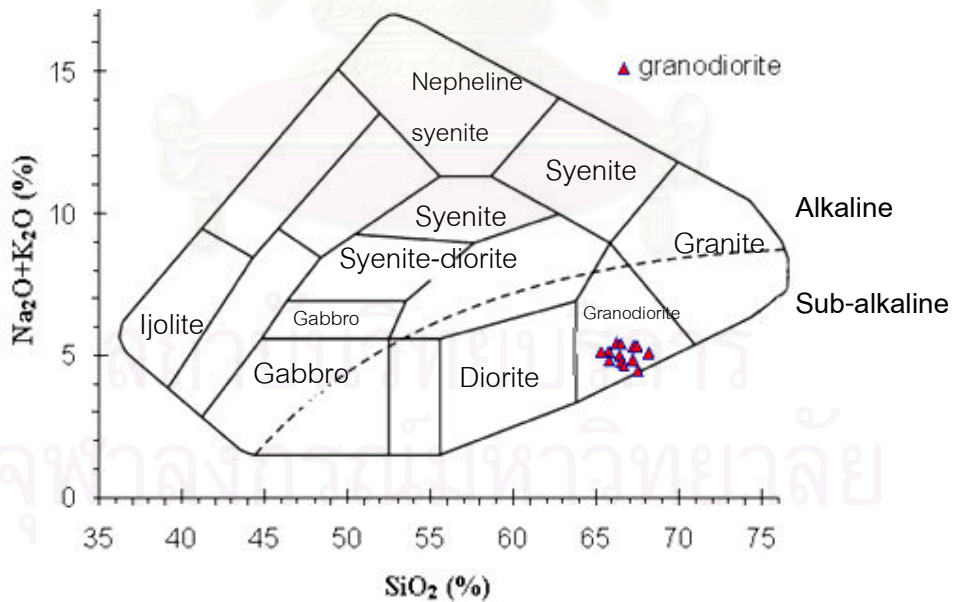


Fig. 5.2 Total alkali silica (TAS) diagram for intrusive rock of N prospects based on the diagram of Cox et al., (1979) alkaline-subalkaline (Irvine and Baragar, 1971) for volcanic rocks of N prospects is mainly fall in granodiorite.

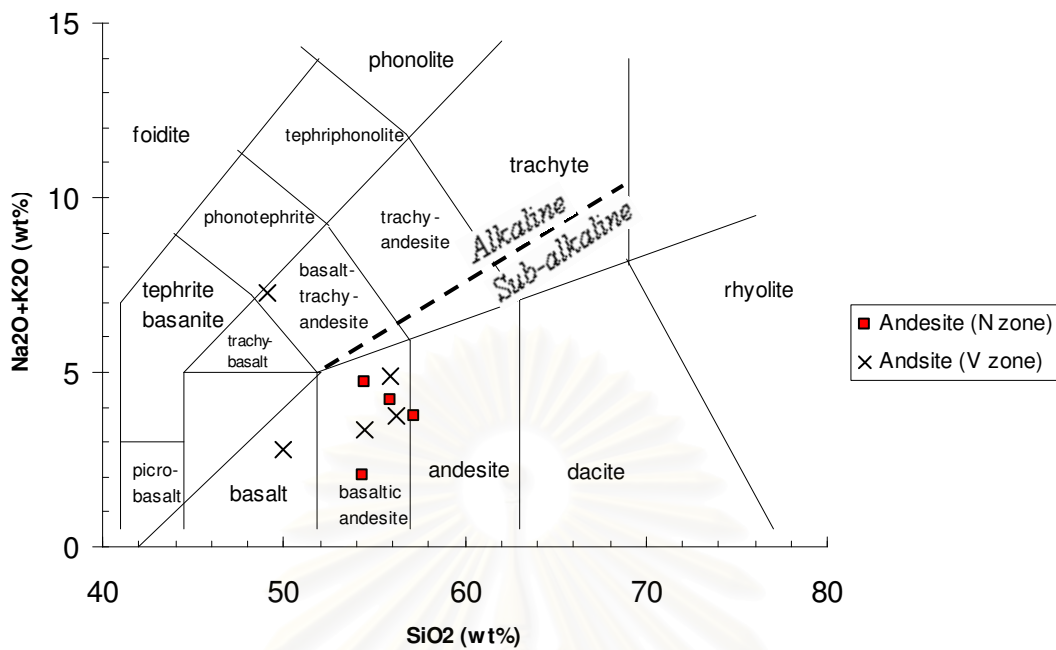


Fig. 5.3 Classification of alkaline and subalkaline basalts in terms of wt% Na₂O+K₂O versus % SiO₂ (Le Maitre, 2002) and alkaline-subalkaline (Irvine and Baragar, 1971) for volcanic rocks of N&V prospects is mainly fall in the basaltic andesite.

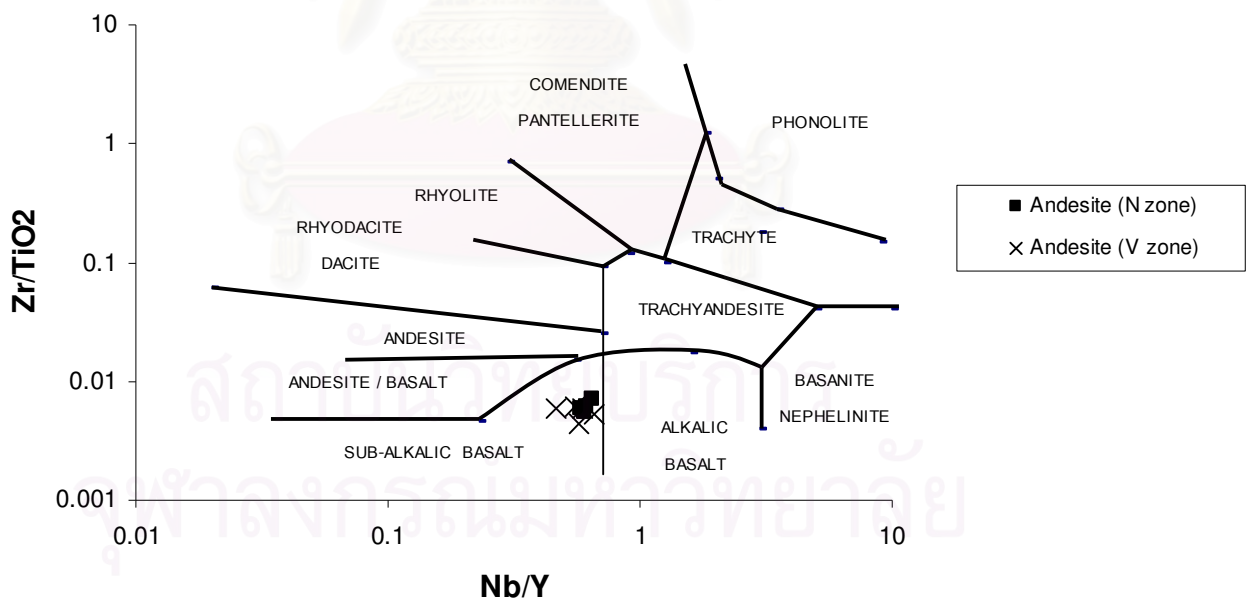


Fig. 5.4 Plots of Zr/TiO₂ versus Nb/Y for volcanic rocks of N&V prospects based on the diagram of Winchester and Floyd (1977). The rock plots fall in the field of subalkalic-basalt.

5.2 Chemical Affinity

Fine-grained granodiorite

The plot of Na_2O versus K_2O contents (Fig. 5.5) shows that intrusive rocks in the study area have the chemical characteristic of I-Type magma after the classification of Chappell and White (1974). Using the K_2O versus SiO_2 nomenclature of Peccerillo & Taylor (1976), the granitoid rocks are classified as calc-alkaline granitoid (Fig. 5.6).

Andesite

$\text{FeO}+\text{FeO}_3$ versus SiO_2 discrimination nomenclature of Miyashiro (1974) (Fig. 5.7) is similar to that of Peccerillo & Taylor (1976) (Fig. 5.8). The volcanic rocks at N and V prospect of Chatree gold deposit are classified as calc-alkaline volcanic rocks.

Alkali-iron-magnesium (AFM) plots showing the distribution of $\text{FeO}+\text{Fe}_2\text{O}_3$, MgO , and $\text{Na}_2\text{O} + \text{K}_2\text{O}$ in the andesite from N and V prospect at Chatree mine deposits (Fig. 5.9). According to Irvine and Barager (1974), AFM diagram is used to discriminate between tholeiitic versus calc-alkaline magma compositions by means of iron enrichment trends associated with fractional crystallization. Many of the andesite samples fall in the calc-alkaline field

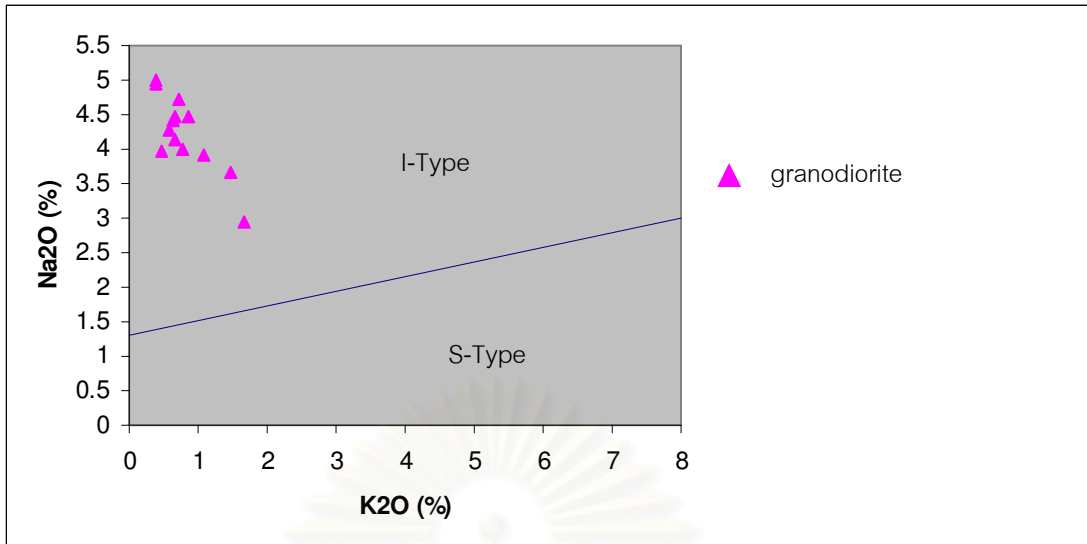


Fig. 5.5 Na₂O vs. K₂O diagram represents the affinity of granodiorite in study area (after Chappell and White, 1974).

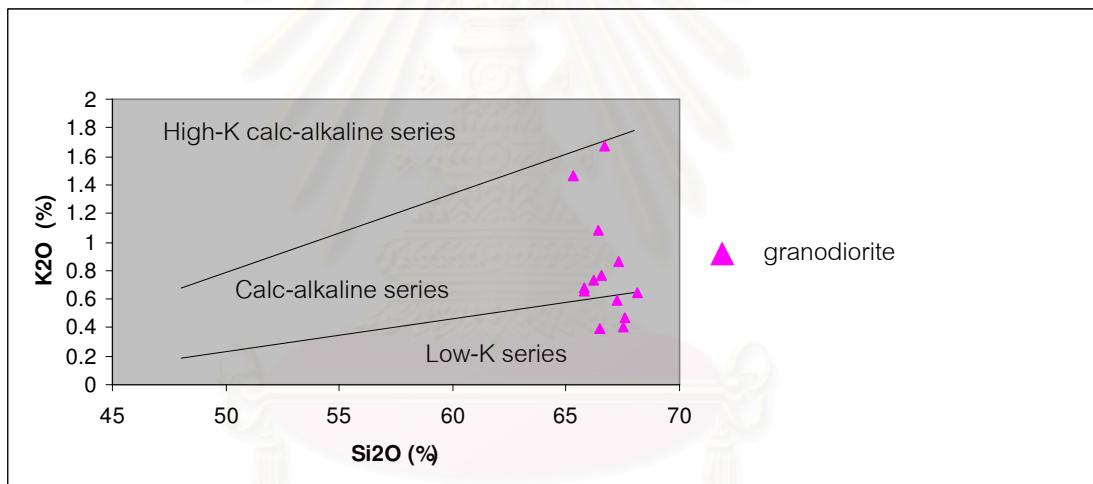


Fig. 5.6 Plots of Si₂O vs. K₂O, Low-K series, calc-alkaline and high-K calc-alkaline boundaries are from Peccerillo & Taylor (1976).

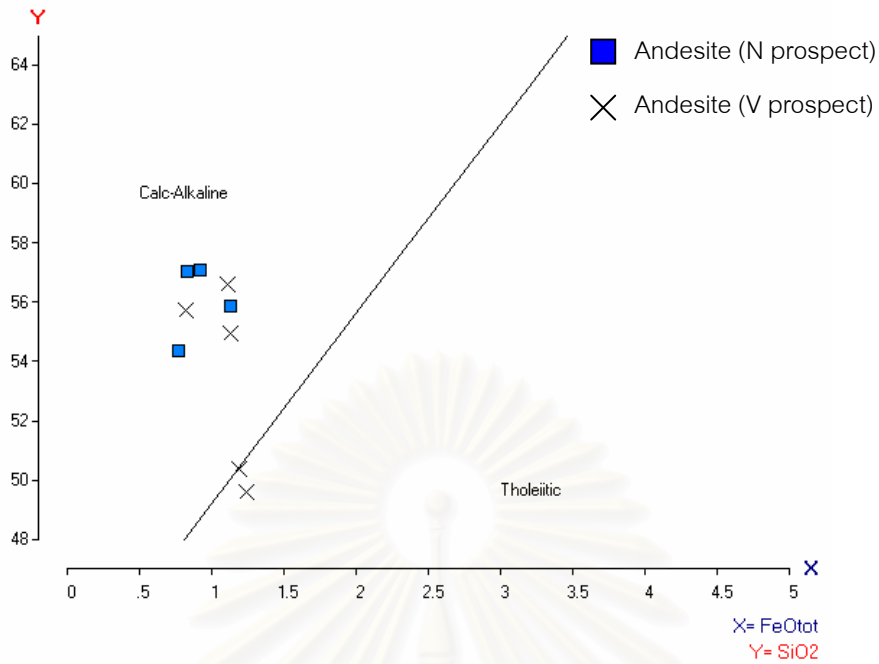


Fig. 5.7 $\text{FeO} + \text{FeO}_3$ versus SiO_2 nomenclature of Miyashiro (1974), the volcanic rocks at N and V prospect of Chatree gold deposits are classified as calc-alkaline rocks.

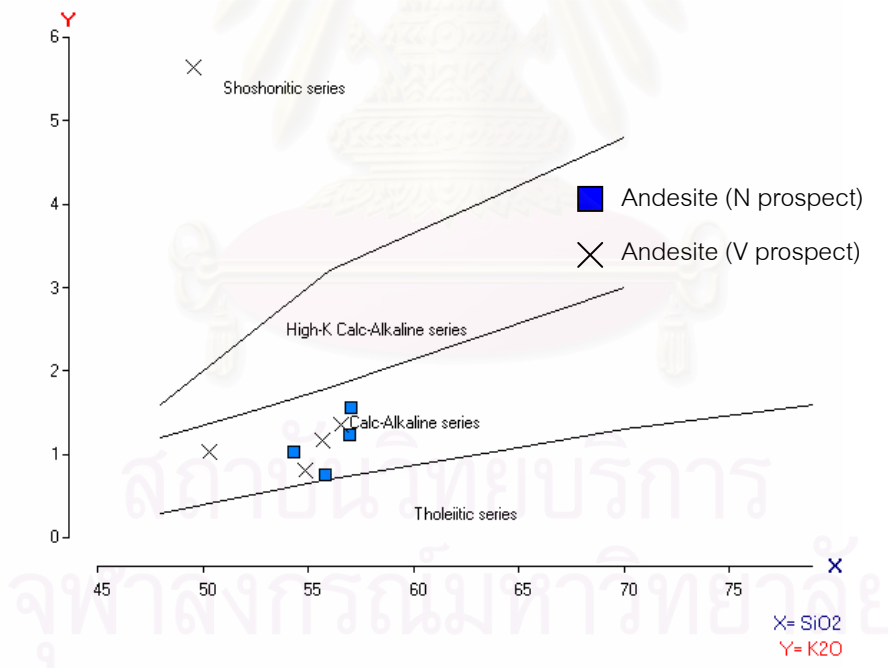


Fig. 5.8 K_2O versus SiO_2 nomenclature of Peccerillo & Taylor (1976), the volcanic rocks at N and V prospect of Chatree gold deposits are classified as calc-alkaline rocks.

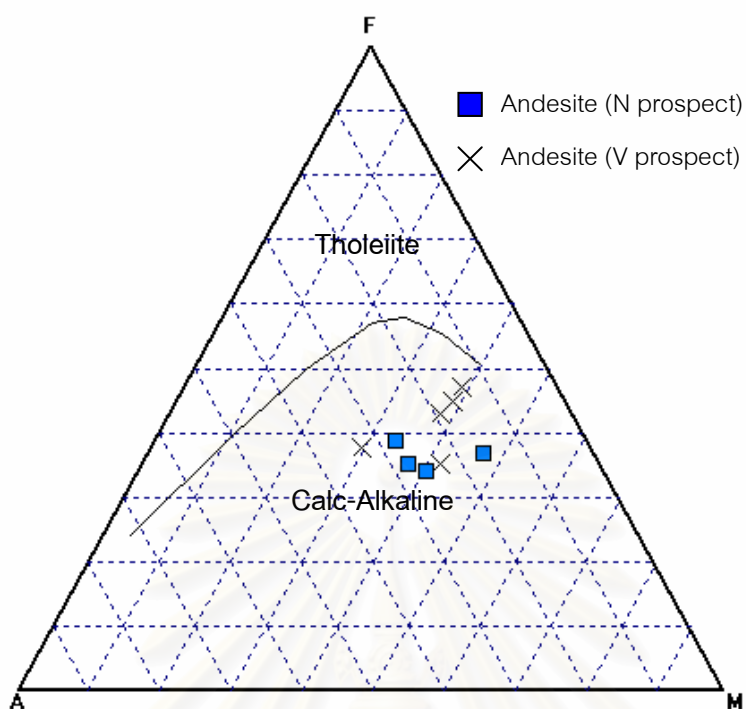


Fig. 5.9 AFM diagrams with the Irvine and Baragar (1974) dividing line for tholeiitic and calc-alkaline trends. The volcanic rock is mainly filled into the calc-alkaline field. Abbreviations, F= FeO+Fe₂O₃; M= MgO; A= K₂O + Na₂O.

5.3 Signatures of trace and rare earth elements

Discrimination diagram used Y versus Cr for volcanic rocks of N&V prospects based on diagram of modified after Pearce et al. (1984) (Fig. 5.10). The diagram illustrated that the volcanic samples fall in area of volcanic-arc basalt.

Discrimination diagram Zr/Y versus Zr plots and used for volcanic rocks samples based on the work of Norry (1979). The diagram demonstrates that of the volcanic samples fall in area of volcanic-arc basalt (Fig. 5.11).

Zr versus Ti for volcanic rocks of N&V Prospects was also plotted based on diagram of Pearce & Cann (1973). The discrimination diagram reveals that the samples referred to island-arc tholeiite (Fig. 5.12).

In Zr - Ti/100 - Sr/2 diagrams of Pearce and Cann (1973), the andesitic rock of Chatree plot within island arc tholeiites (IAT) fields (Fig. 5.13).

Tectonic discrimination diagrams Nb versus Y indicate that granodiorite in the study area are classified as volcanic-arc granitic rock (VAG) from Gill (1978) (Fig. 5.14).

Discrimination diagram of Pearce et al. (1984) (Fig. 5.15, 5.16 and 5.17) uses Yb, Y, Nb and Ta ratio to discriminate felsic rock types and is biased toward granitoid rocks. They define ocean ridge (ORG) as those recovered from deep oceanic dredging or from ophiolite complexes. Volcanic arc granite (VAG) encompasses a wide variety of compositions ranging from the tholeiitic through the calc-alkaline to shoshonitic. They may be associated with ocean island arcs or with active continental margins, but include only those involving the subduction of oceanic crust. Within plate granites (WPG) are intruded into the continental crust or oceanic crust. Collision granites (syn-COLG) are formed during continent-continent, continent-arc, or arc-arc collision. Granodiorite at N Prospect are of Chatree gold deposit plot Volcanic-arc Granite (VAG). These diagrams suggest that they are most likely related to subduction of Lampang-Chiangrai Plate under Nakhon Thai Plate in the Permo-Triassic age.

Spider diagram of trace and rare-earth elements reveal that calc-alkaline intermediate igneous rocks are consistent with those of the Tertiary intrusive rocks of Azerbaijan, Iran (Fig. 5.18) which occurred in the subduction zone related to the magmatic arc environment.

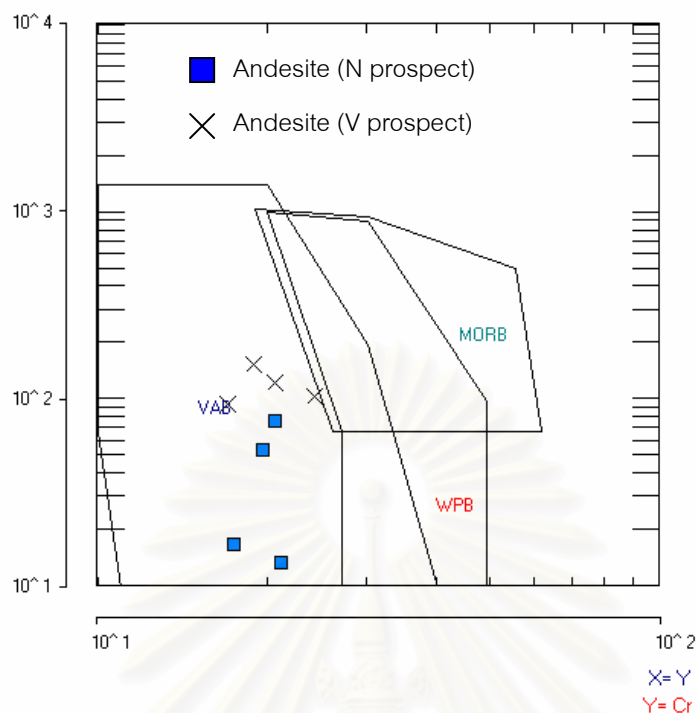


Fig. 5.10 Plots of Y versus Cr for volcanic rocks of N&V prospects based on diagram of modified after Pearce et al. (1984). Abbreviations: VAB, Volcanic-arc Basalt; MORB, Mid Oceanic Ridge Basalts; WPB, Within-plate Basalts.

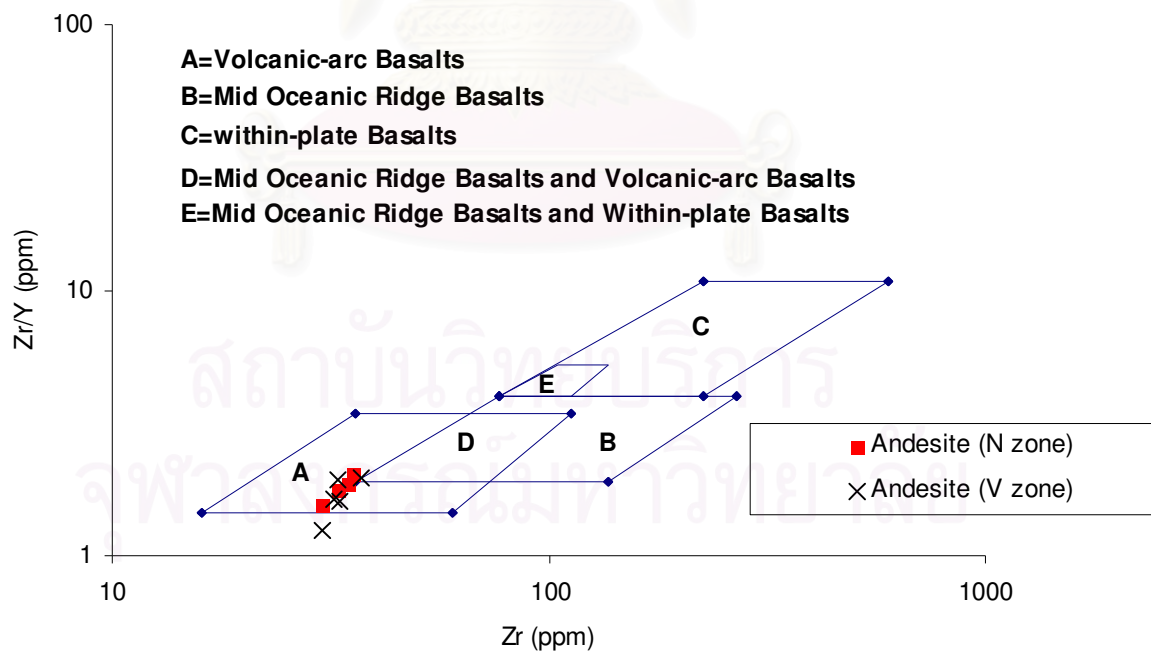


Fig. 5.11 Zr/Y vs. Zr plots for volcanic rocks of N&V prospects which fall within the field of volcanic arc basalts. Diagram from Pearce and Norry (1979).

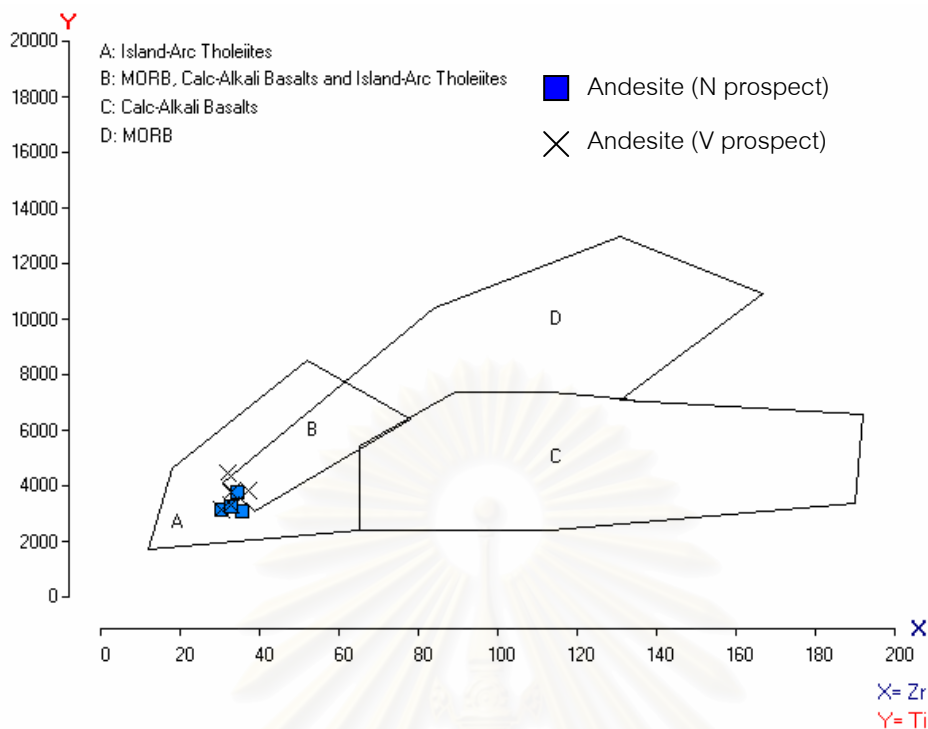


Fig. 5.12 Plots of Zr versus Ti for volcanic rocks of N&V prospects based on based on the diagram of Pearce & Cann (1973).

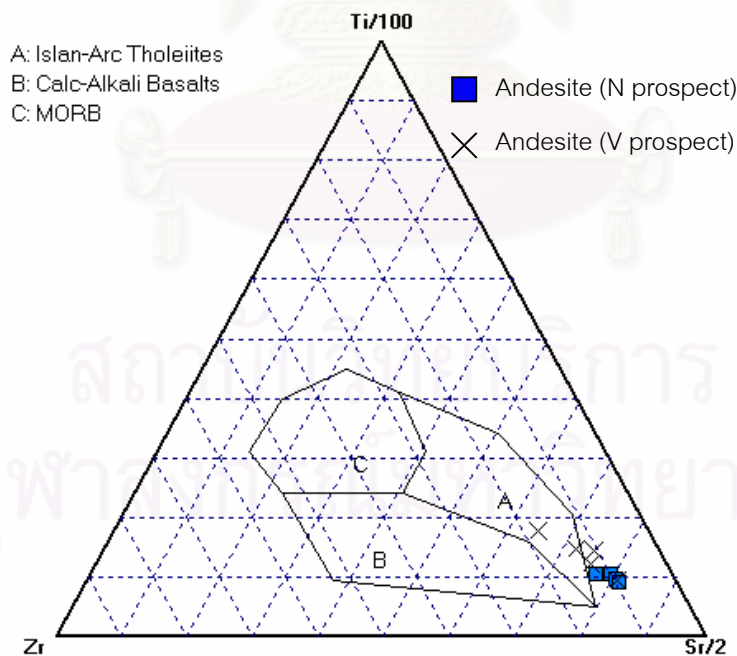


Fig. 5.13 Zr-Ti/100-Sr/2 diagram of Pearce and Cann (1973), wherein N and V prospect volcanic rock exhibits Island-Arc Tholeiites.

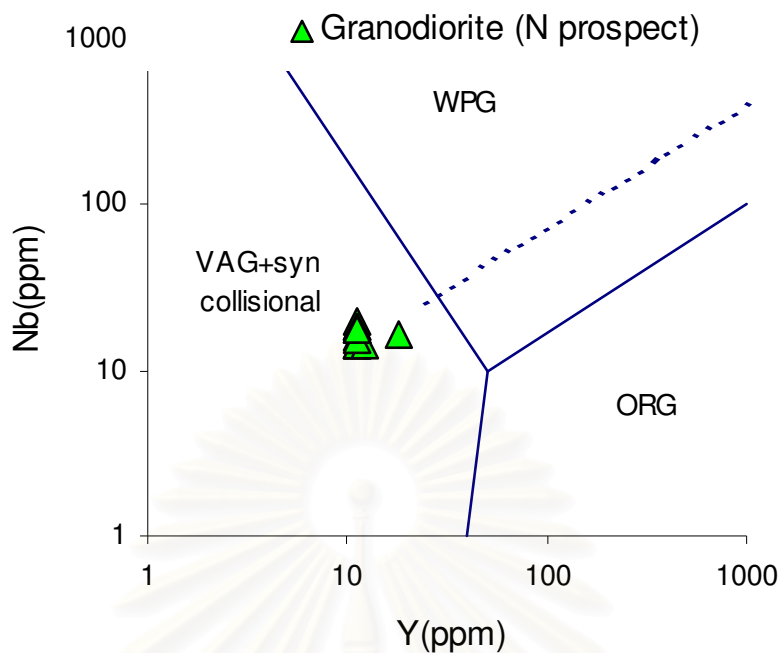


Fig. 5.14 Log Nb vs. log Y which show the rocks in the N zone fall in the volcanic arc felsic field. Abbreviations: WPG, within plate granite; ORG, ocean ridge granites; VAG, volcanic arc granites. Diagram from Gill (1978).

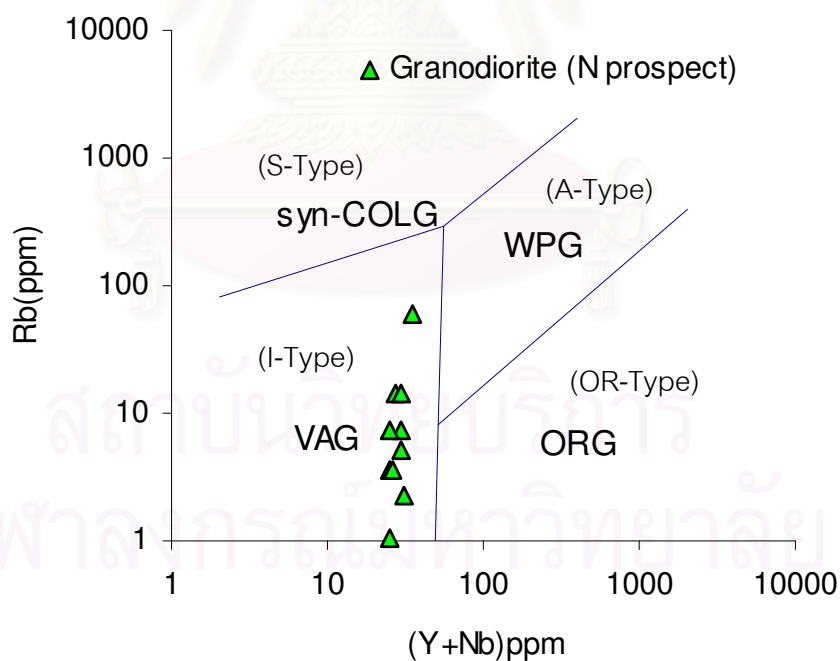


Fig. 5.15 Log Rb vs. (Nb+Y) discrimination plot of granitic rocks from the N-zone of Chatree gold mine. Abbreviations: WPG, within plate granite; ORG, ocean ridge granites; VAG, volcanic arc granites; syn-COLG, Syn Collisional Granite. Diagram from Pearce et al. (1984).

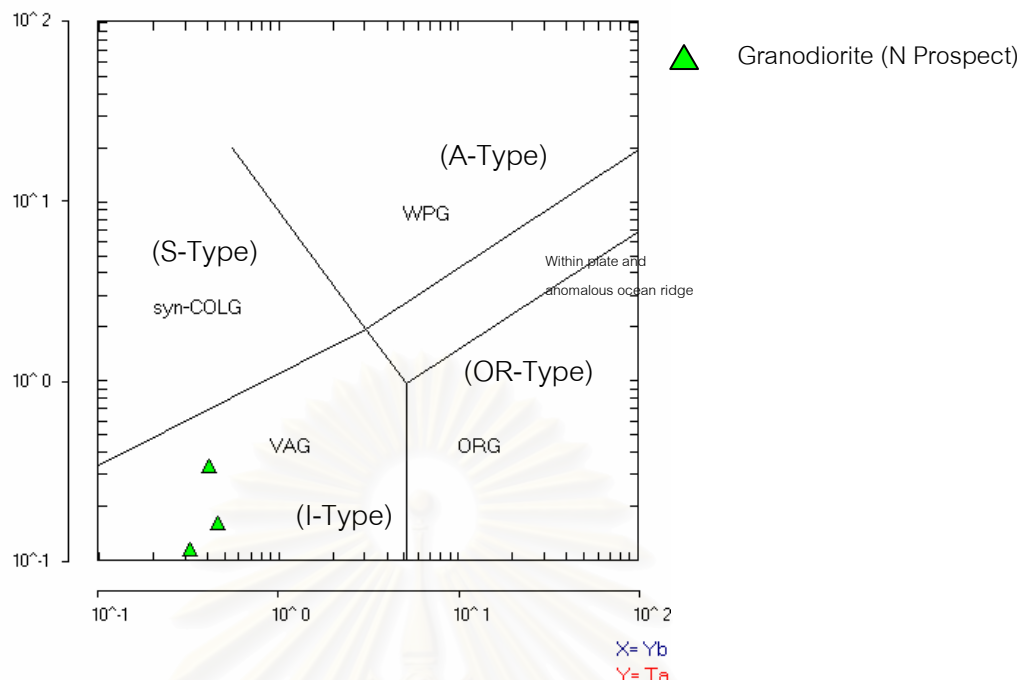


Fig. 5.16 Log Rb vs. (Nb-Y) discrimination plot of granitic rocks from the N prospect of Chatree gold mine is fall in Volcanic-arc Granite field (VAG). Abbreviations: WPG, within plate granite; ORG, ocean ridge granites; VAG, volcanic arc granites; syn-COLG, Syn Collisional Granite. Diagram from Pearce et al. (1984).

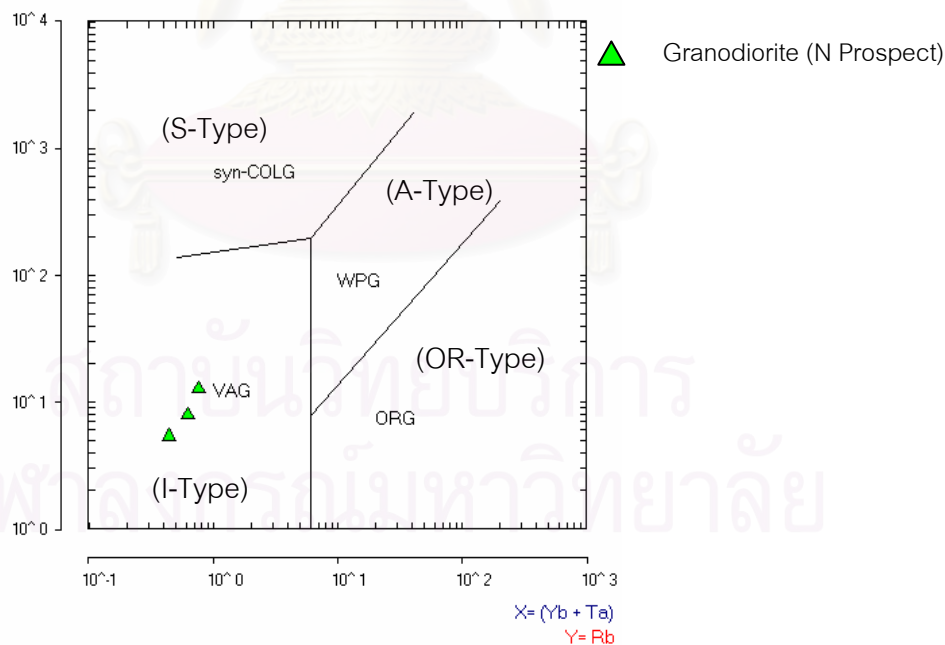


Fig. 5.17 Log Rb vs. (Y-Ta) discrimination plot of granitic rocks from the N prospect of Chatree gold mine is fall in Volcanic-arc Granite field. Abbreviations: WPG, within plate granite; ORG, ocean ridge granites; VAG, volcanic arc granites; syn-COLG, Syn Collisional Granite. Diagram from Pearce et al. (1984).

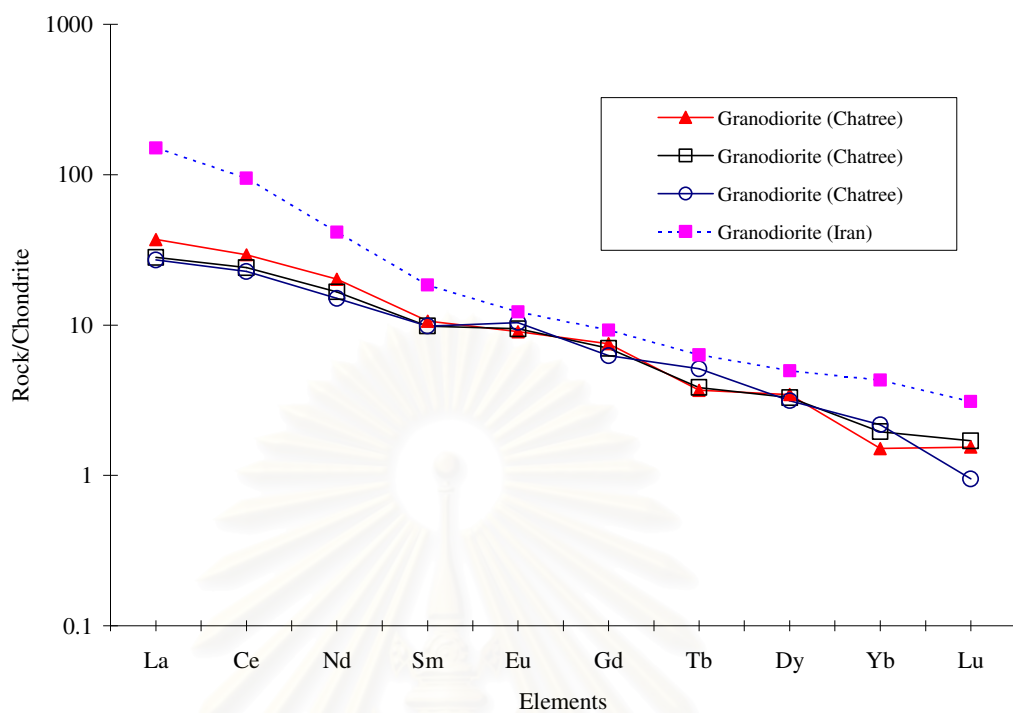


Fig. 5.18 Chondrite-normalized REE plots of selected samples from the same suit in the Chatree granodiorite. The rock displays lack a Eu anomaly. Also shown on the diagram is the pattern of Azerbaijan granodiorite, Iran (Hezarkhani, 2005).

สถาบันวิทยบริการ
จุฬาลงกรณ์มหาวิทยาลัย

CHAPTER VI

DISCUSSION

Based upon the results of the present study, discussion can be categorized into 4 topics including (1) petrochemical characteristics of the studied igneous rocks, (2) relationships of mineralization/alteration to the studied rock (3) Age constraint, and (4) tectonic setting.

6.1 Petrochemical characteristics of the studied igneous rocks

Petrographic investigation reveals that the plutonic rocks in N prospect of the Chatree gold mine is relatively fine-grained and characterized by porphyritic textures (Fig6.1b). Such diagnostic features are quite similar to those of the felsic to intermediate rocks in Philippines (Sillitoe, 2000), southwest USA (Lowell&Guilbert, 1970), southern Peru (Gustafson, 2001), Hong Kong (Wan, 1994) (Fig6.1a). These porphyritic rocks and their related alteration are always associated with copper-molybdenite mineralization or the so-called porphyry copper deposit (Guilbert & Lowell, 1974). In the model proposed by Lowell & Guilbert (1970), the host genetic rock is felsic plutonic rock of the clan through granodiorite.

At N prospect, the granodiorite is characterized by av. andesine (An_{35}) phenocryst, K-feldspar, vermicular/anhydral quartz, relic hornblende and biotite set in fine-grained quartz - enriched groundmass. Andesite is characterized by plagioclase, phenocryst set in glassy groundmass. The rock in the V zone is dominated by porphyritic andesite composed of altered plagioclase and relic hornblende phenocrysts set in glassy-microlite groundmass. The studied rock can be compared with those of the earlier works as shown below.

According to Myron (1982), the porphyritic fabric generally originates as magma that has been slowly cooling and forming large crystals and is then more quickly cooled, depending upon the grain size of the matrix.

Porphyry (Gustafson, 2001) is a term restricted to conspicuously porphyritic intrusive felsic rocks with a fine phaneritic even aphanitic matrix. Porphyry occurs in fairly small, relatively shallow intrusive magma bodies with growth of abundant large

phenocryst, followed by an episode of rapid crystallization, forming the fine phaneritic or aphanitic matrix. In the case of the N and V prospect the studied rocks are similar to what Gustafson (2001) mentioned as “porphyry” and possibly have similar genesis. Zoning of plagioclase which is common in porphyry has been interpreted by Myron (1982) as progressively recording changes in magmatic environments. Similar situation has been observed in the studied rocks of the Chatree gold mine. It is considered that the changes from volcanic system to a (shallow) intrusive system may have happened for the Chatree mining area.

Porphyry deposits, as proposed by Lowell and Gillbert (1970) are intimately associated with intermediate to felsic plutonic intrusives, characterized by intense and extensive hydrothermal alteration of the host rocks, as recognized by Lowell and Gillbert (1970). All these characteristics have also been found at the Chatree gold mine based upon petrographical and geochemical investigations.

Ore minerals are scattered throughout the host rock either as disseminated mineralization or restricted to quartz veinlets that form a ramifying complex called a stockwork. As shown in the previous chapter on petrography, the Chatree mineralization has similar disseminated ores and vein/veinlet styles. The host intrusion characteristic rock is acid plutonic rocks of the granite clan through granodiorite to tonalite, quartz monzodiorite and diorite with multiple intrusions common, and mineralization commonly late (Lowell and Gillbert, 1970).

Plagioclase crystals in magmatic rocks, especially in porphyry deposits (Gustafson, 2001) possess various textural types and zoning such as sieve texture, oscillatory, patchy and normal zoning. In the case of the Chatree studied rocks, petrographic investigation reveals that plagioclase is the abundant phenocryst and shows various texture styles of zonings (see Fig. 6.2). These textures provide information concerning conditions of magmatic evolution and histories of magmatic systems. Sieve textures in plagioclase indicate rapid decompression (Stomer, 1972) and magma mixing (Tsuchiyama 1985) in magma chambers, while oscillatory zoning infers repeated injections of mafic melts, fluctuations in total pressure or temperature, or diffusion-crystallization kinetics (Hattori & Sato 1996).

In addition, patchy zoning is interpreted to be caused by rapid increase in crystals,

decompression, supersaturation, and/or decrease in confining pressure on water-deficient magma during crustal ascent (Vance, 1965; Anderson 1984). Patchy zoning is also common in some specimen studies for the Chatree rocks. So mechanism for the occurrence of the patchy zoning may be the same for the Chatree magma. Zoning is especially typical of plagioclase in intermediate silica volcanic rocks and shallow intrusions, such as porphyries (Sibley et al., 1976). So in the case of the Chatree porphyry it is also interpreted to be shallow intrusion based upon the plagioclase signature.

Embayed or vermicular quartz phenocrysts are common in many volcanic rocks and shallow plutonic rocks. The intrusive rocks associated with some ore deposits, such as the granite porphyry of Empire Mine, Idaho, USA (Chang et al., 2004) contain quartz phenocrysts that are embayed to an extreme, which is here called vermicular similar (see Fig. 6.3e). Petrography analysis of the shallow intrusive rocks of the N prospect that quartz phenocrysts are quite abundant and vermicular quartz (Fig 6.3f) is also present in several specimens studies. The origin of embayed quartz has been interpreted to result from: (1) resorption of quartz by the melt due to ascending and decompression (e.g. Nekvasil, 1991; Eklund and Shebanov, 1999); (2) resorption of quartz due to magma mixing (e.g. Sakuyama, 1979, 1981; Burt et al., 1996; Kontak and Clark, 1997; Kuscü and Floyd, 2001); (3) resorption of quartz due to decreased F activity in the melt after some F partitions into the magmatic aqueous fluid (Webster, 1990); (4) rapid growth due to undercooling, which results in skeletal textures (e.g. Swanson and Fenn, 1986; Candela, 1997); and (5) cellular growth (McCutcheon and Robinson, 1988; McCutcheon, 1990). Model for the development of vermicular textures in quartz phenocrysts is shown in figure 6.3 a, 6.3 b, 6.3 c, and 6.3 d.

Comparing all above mentioned data, it is quite likely, for the Chatree gold mine of N Zone, that the studied rocks of the Chatree mine are intermediate (granodiorite) with plagioclase crystals often displaying a compositional twinning and zoning, vermicular quartz (Fig. 6.3f) phenocryst, porphyritic containing large phenocryst. The studied rocks have fine-grained matrix with disseminated and veinlet ores of Cu-Mo-Au-Zn-Fe. The fine-grained granodiorite in the N zone is interpreted to be "Cu-Mo±Au porphyries". Similar to those reported in this study for the shallow intrusive rocks of the Chatree gold

mine. Some of western North America porphyries are hydrothermally altered and mineralized with disseminated Mo or Cu sulfides, forming the so-called copper or molybdenum porphyries (Myron, 1982). Environment of molybdenite is high temperature hydrothermal veins. Therefore, in term of ore association, the prospects can be regarded as disseminated deposits of the porphyry type (Lowell and Gillbert, 1971).

As shown in Figs. 6.4 and 6.5, the studied rocks from the drilled core samples show an evidence of injection of younger shallow intrusive granodioritic rocks into the older andesitic host rock (Fig. 6.5a). Under microscope, inclusions (or xenoliths) were encountered in the older volcanic rock adjacent to the central zone between the younger intrusive and older andesite rocks (Fig. 6.5b). A model proposed by Huber (1973) can be used to determine sequence of intrusion or the evolution of igneous rock in the porphyry system.

The granodiorite porphyry at N prospect is younger than andesite rock form evidence based on Huber (1987) which is indicated by intrusion and xenoliths or inclusions. Figure 6.4 is a model of Huber (1987) similar to the studied granodiorite porphyry which intruded the andesite host as shown in figure 6.5.

Sillitoe (1973) suggested that porphyry copper deposits always occur in a subvolcanic environment associated with small high level stocks, and he emphasized their close association with subaerial calc-alkaline volcanism. Geochemically, the result reveals that the studied granodiorites in the prospect area are granodiorite to tonalite, with calc-alkaline, I-type and, volcanic arc granite system similar to those reported by previous work of the same Eastern plutonic belt by Charusiri et al. (1991), (1993), Nantasini et al. (2005). Volcanic rocks of N and V prospects are collectively classified as basaltic rock, calc-alkaline, island arc tholeiite, volcanic arc basalt similar to those of the previous data in the Loei-Petchabun-Nakhon Nayok volcanic belts by Intasopa, (1993), Vivatpinyo (2006), Janplook (2006), Nakchaiya et al. (2008), Tangwattananukul et al. (2008), Panjasawanwong et al. (2008), Khositantont et al. (2008). These studied rocks of both prospects therefore show close association with (subaerial) cal-alkaline volcanism.

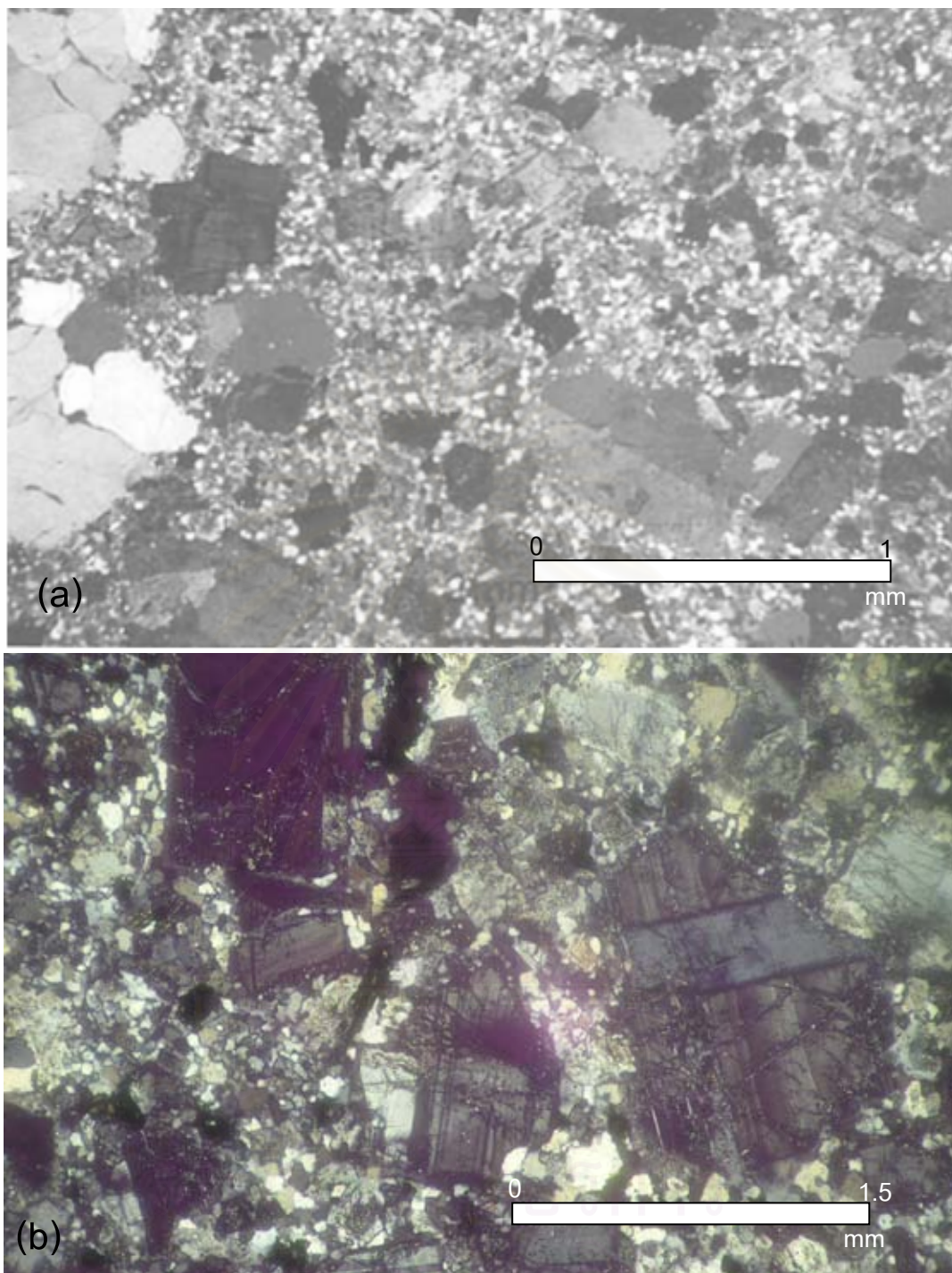


Fig. 6.1 Photomicrographs of characteristic of porphyritic granodiorite (a,b in plane-polarized light). (a) Porphyritic granodiorite from Borehole at Kam Chang Kok, Hong Kong, and photo by Wan (1994). (b) Porphyritic granodiorite from the study area, N Prospect, Chatree mine.

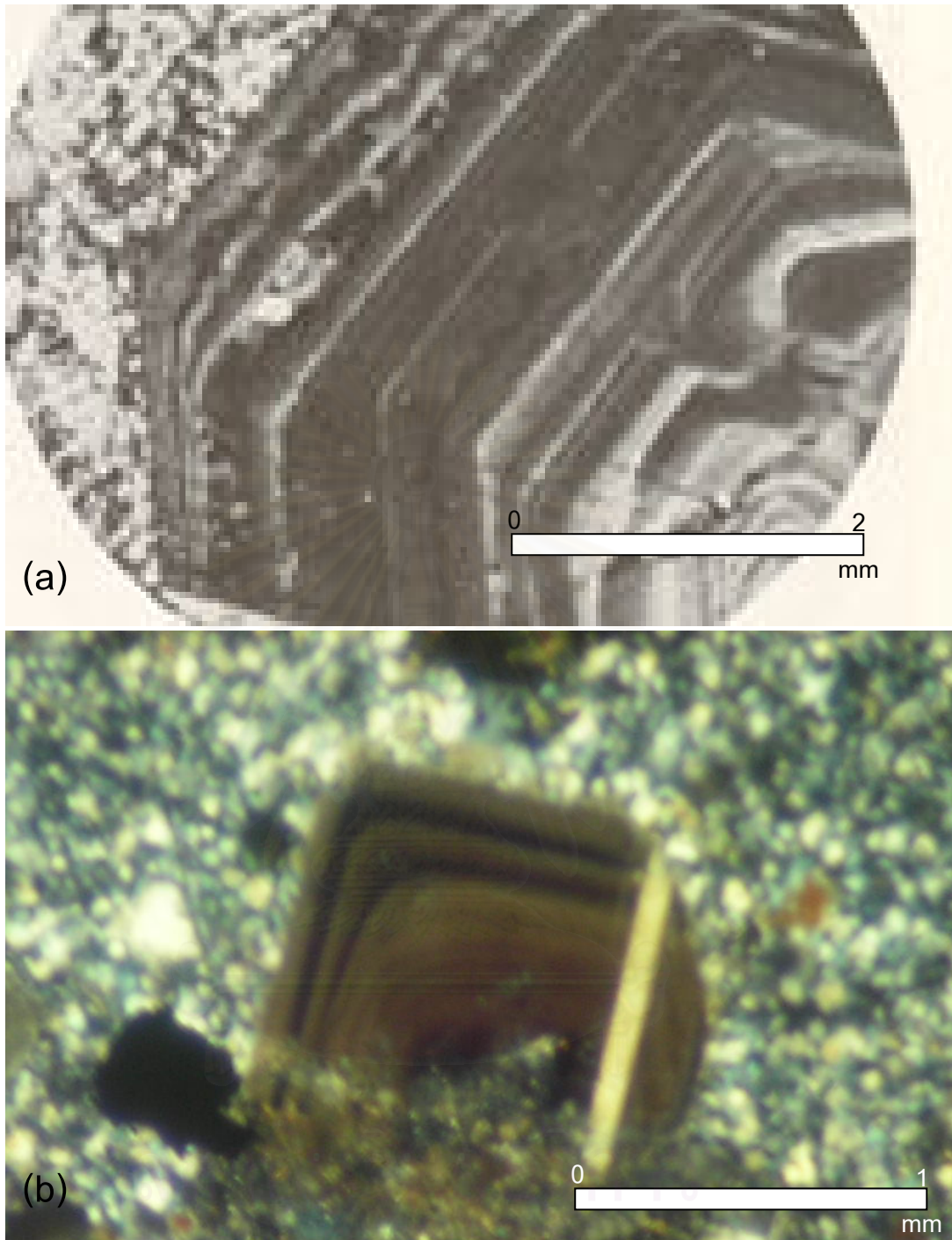


Fig. 6.2 Photomicrographs (a, b in plane-polarized light) of (a) very fine-grained groundmass and oscillatory zoning in a plagioclase phenocryst in a diorite porphyry, western North America (Sibley et al., 1976). (b) Zoned plagioclase set in fine grained groundmass of porphyritic granodiorite, Chatree gold mine.

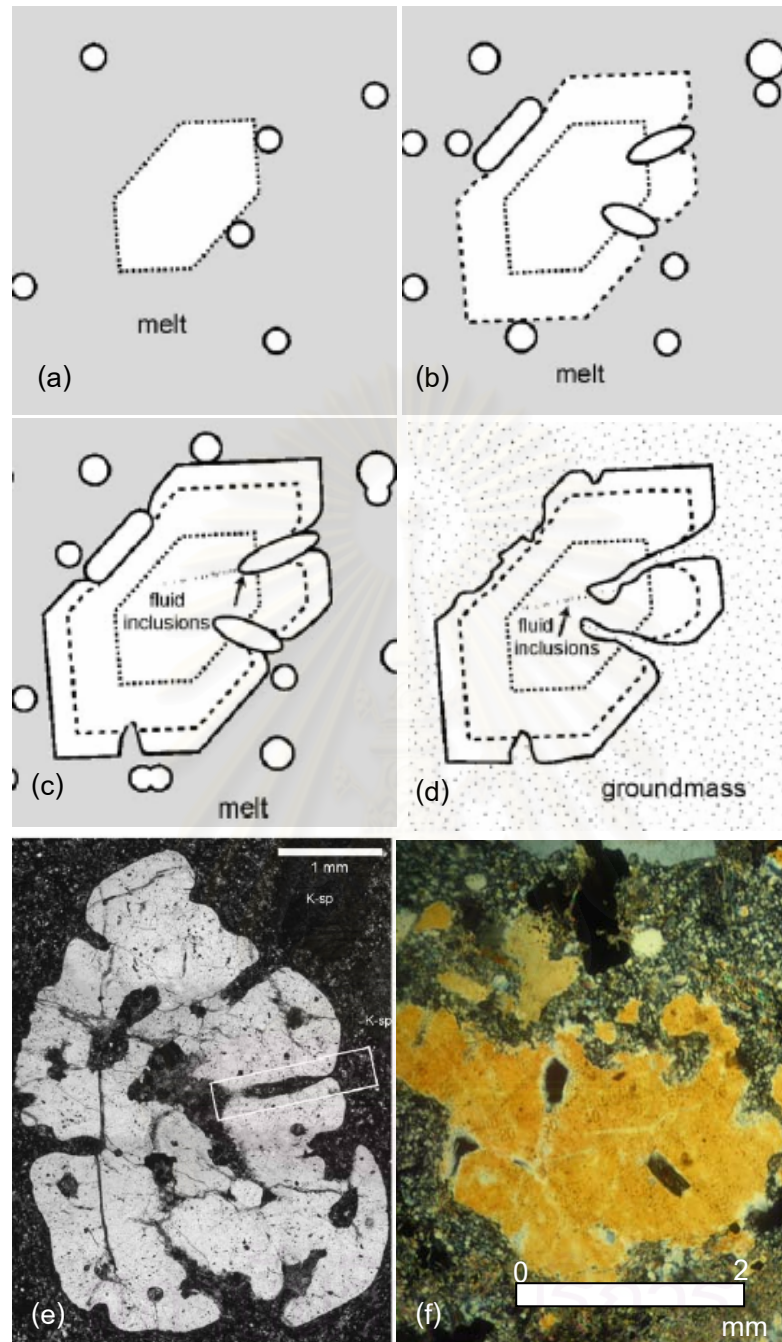


Fig. 6.3 Model for the development of vermicular textures in quartz phenocrysts (Fig a, b, c and d. Empire Mine, Idaho, USA) base on the work proposed by Chang et al. (2004) contain quartz phenocrysts that are embayed to an extreme case, which is here called vermicular quartz (Fig. e). Photomicrograph of embayed quartz phenocryst set in a groundmass of fine-grained silicate minerals, Chatree gole deposit (Fig. d).

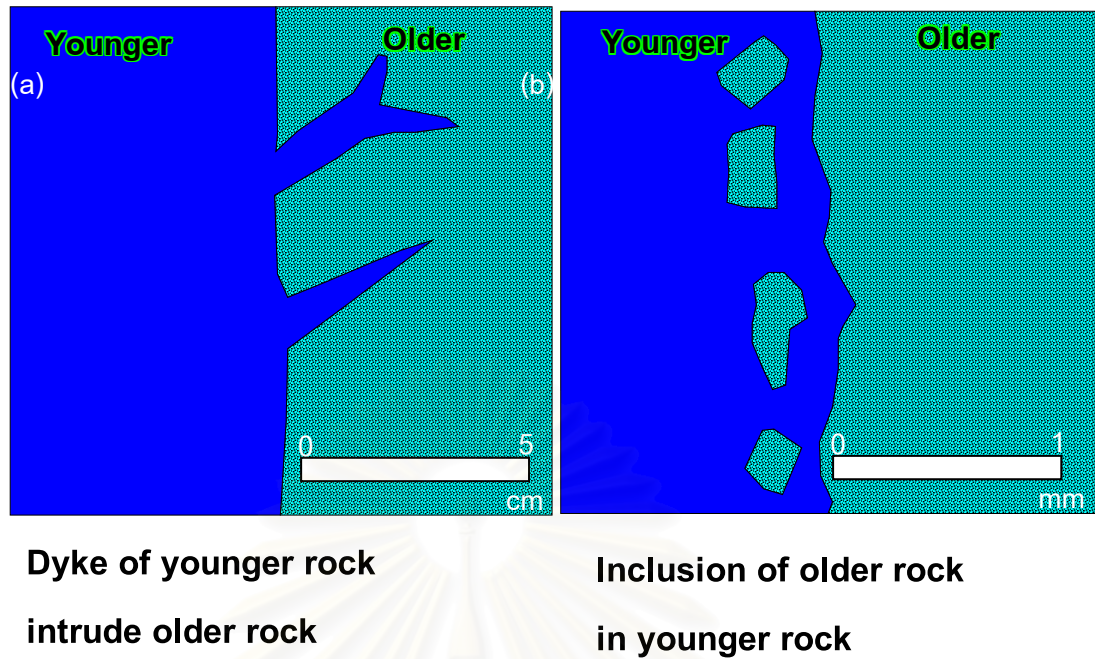


Fig 6.4 Features seen in outcrop (a) and photomicrograph under microscope (b) that help determine the relative ages of plutonic rocks (Huber, 1987).

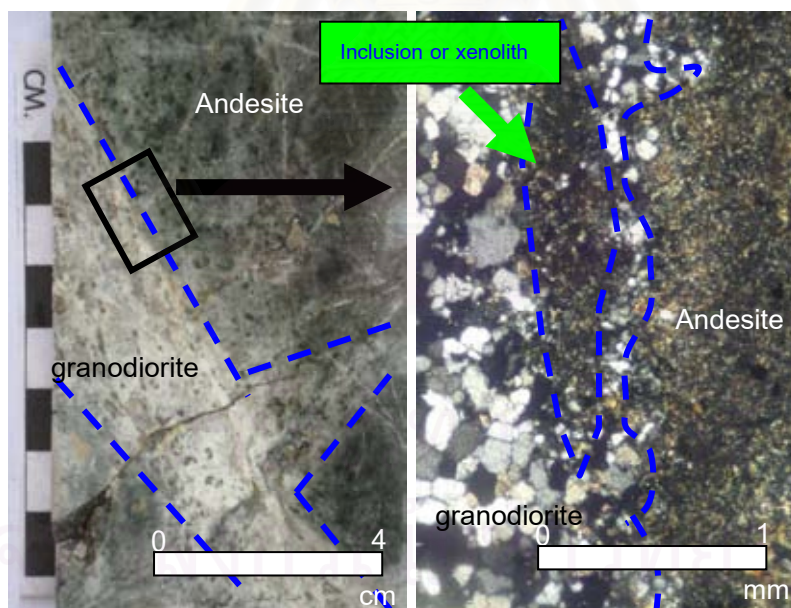


Fig 6.5 Features seen in hand specimen of the drill-core sample (a) and photomicrograph under microscope from the core (b) showing intrusion of granodiorite and andesite inclusion in granodiorite, N prospect, Chatree gold deposit.

6.2 Relationships of mineralization/alteration to the studied rock

The previous section (6.1) shows the high possibility for the studied intrusive rocks to be the “porphyry copper-type rock”. In this section, concentration is made for relationship between mineralization/alteration and these “porphyry copper-type rock”.

6.2.1 Classification of Mineralization

El-Shazly (2004) reported porphyry Cu deposits which are defined as large, medium-to low-grade Cu deposits, in which hypogene sulfides are primarily structurally controlled, and which are spatially related to felsic or intermediate porphyritic intrusions (I-type granitoids ± their volcanic equivalents). As noted earlier, not all porphyry type deposits are mined for Cu only, but in some cases are mined for Mo, Sn, and Au (hence the terms “porphyry Mo” and “porphyry Cu-Au” deposits). Based on El-Shazly (2004), the chemistry of rocks with which they are associated, porphyry Cu deposits are classified into:

A- Calcalkaline (subduction related) deposits: which are associated with intermediate porphyritic plutonic rocks. These deposits may be further classified into:

1. Cordilleran Porphyry Cu type: Which are associated with quartz monzonites and granodiorites (rocks with 55 - 70 weight % SiO_2). This type is characterized by large tonnages of ore (100 - 2000 million tonnes), and grades of 0.45 - 1.2 % Cu, 0.01 - 0.03 % Mo. Examples: El-Salvador and Chiquicamata in Chile, Bingham, Utah.

2. Island Arc Porphyry Cu: Associated with quartz diorites and granodiorites (55 - 65% SiO_2), with ore tonnages of 30 - 600 million tonnes, and grades of 0.35 - 0.7 % Cu, but < 0.001 % Mo. Generally, these deposits appear to have a higher Au/Cu and lower Mo/Cu ratios compared to the cordilleran types. Examples: Panguna, Papua New Guinea, and Mamut, Malaysia.

B- Alkaline Porphyry Cu deposits: which are associated with alkaline rocks (monzonite - syenodiorite; 47 - 55% SiO_2). These types appear to occur in areas of incipient rifting? or transform faulting?, and are characterized by relatively small tonnages (10 -65 million), and grades of 0.45 - 1% Cu, < 0.001% Mo, and an overall lower concentration of S (resulting in a higher modal abundance of magnetite). Significant amounts of Au may occur in these deposits as well. Example: Cu Mountain, British Columbia, Canada.

It is therefore important to note that the island arc and alkaline type deposits often contain significant amounts of Au and/or Ag.

Based upon El-Shazly (2004) for the porphyry copper deposit, it is quite likely that the studied porphyry deposit of the N and V prospects belong to class A-2 which is dominated by island-arc porphyry copper type similar to Panguna (Papue New Guinea) and Mamut (Malaysia) deposits with low-grade Cu.

6.2.2 Alteration styles

Alteration patterns are among the most characteristic features of porphyry copper deposit that the "idealized" or "model" spatial and temporal relationships between the various types of hydrothermal alteration are to a large extent well represented by most porphyry copper deposits (especially the Cordilleran type). Moreover, there is a very close spatial and temporal relationship between the alteration patterns and the zonation of ore minerals. This relationship strongly suggests that porphyry copper deposit mineralization and wall rock alteration are indeed genetically related.

In general, alteration patterns from core to rim, for porphyry copper deposit as suggested by El-Shazly (2004) follow the zonal sequence: Potassic → sericitic → propylitic → argillic, with the latter zone usually restricted to shallow depths. .

The zonal distribution of ore minerals follows closely the wall rock alteration zones:

1. The potassic zone: is characterized by the minerals - bornite, chalcopyrite and magnetite, with chalcopyrite > pyrite. Textures suggest that magnetite was replaced by chalcopyrite and bornite.
2. The sericitic zone: contains pyrite, chalcopyrite ± tennantite ± sphalerite, with pyrite > chalcopyrite. Textural relations suggest that pyrite formed at the expense of magnetite ± chalcopyrite (by sulfidation).
3. The argillic zone, representing the zone of supergene enrichment, contains the minerals chalcocite, pyrite, or covellite + pyrite, depending on the intensity of alteration.

In the case of the alteration in the N and V prospects, classification of hydrothermal alteration was made following that of Lowell and Gillbert (1970). Three types of alteration are recognized.

Potassic alteration (biotite, K-feldspar and adularia) is a relatively high temperature type of alteration which results from potassium enrichment (see Figs. 4.8

and 4.9). This style of alteration forms before complete crystallization of magma. As in the case of this study, it is evidenced by the typically sinuous and rather discontinuous vein patterns. Potassic alteration may occur in deeper plutonic environments, where orthoclase is formed. But in this study it forms in shallow, volcanic environments where adularia is formed.

Propylitic alteration (chlorite, epidote and actinolite) turns rocks green, because the new minerals formed are green (see Figs. 4.20 and 4.21). These minerals include chlorite, actinolite and epidote. They usually form from the decomposition of Fe-Mg-bearing minerals, such as hornblende in the case of this study, although some replace feldspar. Propylitic alteration occurs at relatively low temperatures. Propylitic alteration generally forms in a distal setting relative to other alteration types.

Sericitic alteration alters the rock to the mineral sericite, which is a very fine-grained white mica (sericite) (Figs. 4.4, 4.7, 4.8, and 4.22). It typically forms by the decomposition of feldspars, so it replaces feldspar. Sericitic alteration implies low pH (acidic) conditions. Alteration consisting of sericite + quartz or the so-called "phyllitic" alteration is always associated with porphyry copper deposits. It usually contains appreciable quantities of fine-grained, disseminated pyrite (see Figs 4.25, 4.27, 4.28, and 4.29).

Sillitoe (2000) reported exploration of base metal and precious metal deposits in the Cardia Ridgeway. The deposits lie immediately northwest of the equigranular intrusion and are centered on a restricted monzonite porphyry stock emplaced mainly into volcanoclastic rocks. Ore-related alteration is K-silicate, characterized by orthoclase, albite, magnetite and biotite, overprinted by a propylitic assemblage. The principal copper minerals are chalcopyrite and bornite along with native gold and abundant magnetite occurring mainly in veinlets and as disseminated grains (Holliday et al., 1999).

In the study area of N prospect, the major rock composed of plagioclase, quartz, K feldspar, hornblende and biotite. Alteration assemblage is mainly biotite-K-feldspar-chlorite±sericite. Sulfide ores are characterized by chalcopyrite-molybdenite-pyrite-sphalerite. In term of alteration mineralogy, the N prospect shows strong alteration of biotite- K-feldspar-chlorite±sericite assemblage and fits very well to potassic alteration

assemblages of Gillbert and Lewell (1970). The result of geochemical analysis data of the N zone shows average Au of 0.017 ppm and the range of 0.01-0.11 ppm. Cu and Zn which formed at the edge of granodiorite have the contents of 1538 ppm (0.15 % Cu) and 34 ppm, respectively. But in the core of granodiorite, contents of Cu and Zn are lower than of the edge which is 715 ppm (0.07 % Cu) and 26 ppm, respectively.

In the V prospect of Chatree gold deposit, the rock is mainly composed of altered plagioclase and hornblende. Sulfide ores are characterized by pyrite-chalcopyrite-sphalerite. Tremolite-actinolite-quartz-epidote-calcite vein formed as selective alteration locally. The V prospect is the quartz-sulfide veinlet which is less abundant than N prospect. Alteration assemblage is mainly epidote-chlorite and rare sericite. The alteration styles of this zone are similar to propylitic alteration which is formed distal from the porphyry based on Gillbert and Lewell (1970). The result of geochemical analysis data of the V prospect show the Au of 0.014 ppm and the range of 0.01-0.17 ppm, and the data of one drill-hole no. 3131 DD that is 107 ppm (0.01 % Cu) and 122 ppm Zn.

It is interpreted that both the N and V prospects have low significant Au because the economic gold extraction can be achieved from ore grades as little as 0.5 g/1000 kg (0.5 parts per million, ppm) on average in large easily mined deposits. Typical ore grades in open-pit mines are 1–5 g/1000 kg (1–5 ppm); ore grades in underground or hard rock mines are usually at least 3 g/1000 kg (3 ppm) (<http://en.citizendium.org/wiki/Gold>). In addition, the Cu of N and V prospects have also low grade of Cu based on the classification of El-Shazly (2004). Porphyry copper deposits are characterized by their very large sizes (several km² in outcrop) and tonnages, and are therefore often mined by the open pit method. Therefore, it is concluded that average Cu (< 1%) ore grade of the studied prospects is low in comparison with those of the other deposits with 0.6 - 0.9% Cu equivalent ranges (El-Shazly, 2004). However, a careful ore reserve calculation is required for the more detailed exploration.

Therefore based on the result of ore assays, ore petrography, mineralization types, and alteration mineralogy, it is concluded that the alteration of porphyry styles of N and V prospect fit to model of Gillbert (1983) as shown in Figure 6.8.

6.3 Age Constraints

As explained in the previous section, two major types of rocks are recognized in the study N and V prospects, namely granodiorite of shallow intrusive and andesitic calc-alkaline volcanic rocks. They are all located in the so-called Eastern Granite Belt of Charusiri et al. (1993) and Loei-Petchabun-Nakhon Nayok (LPN) volcanic belt (Intasopa, 1993). In general, the main plutonic rocks of the Eastern Granite Belt become older in the north (~240 Ma) and younger in the south (220-225 Ma). The study area is located not too far from Petchabun which is regarded as the central part. So the plutonic age should be placed between the reported ages. However, based on the study of Salam et al. (2008), it is found that the age of the granodiorite, based on Re-Os from molybdenite, was reported to 244 ± 1 Ma (Early Triassic). Alteration and porphyry Cu±Mo±Au mineralization may have occurred immediately after the felsic intrusion. It is evident from both field and petrographic investigations that the shallow-intrusive granodiorite stock emplaced into the andesitic volcanic host rocks. These subducted, calc-alkaline volcanic rocks of the LPN belt (see also Fig 6.6) were dated as 250 ± 6 Ma (Early Triassic) using LA ICP-MS U-Pb zircon dating. Pervasive and selective-style alteration associated with low-sulfidation epithermal Au-Ag mineralization formed after the main-stage calc-alkaline volcanism as evident by the Ar-Ar age of adularia in the Au-Ag vein at ca. 250 ± 0.8 Ma (Early Triassic). The cessation of volcanism associated with epithermal Au-Ag mineralization is characterized by the intermediate dike rock which was dated by LA ICP-MS U-Pb zircon as 238 ± 6 Ma (Middle Triassic). The schematic model of the porphyry Cu mineralization associated with volcanic-plutonic system is shown in Figure 6.7. Figure 6.8 displays the model for the alteration styles associated with ore mineralization.

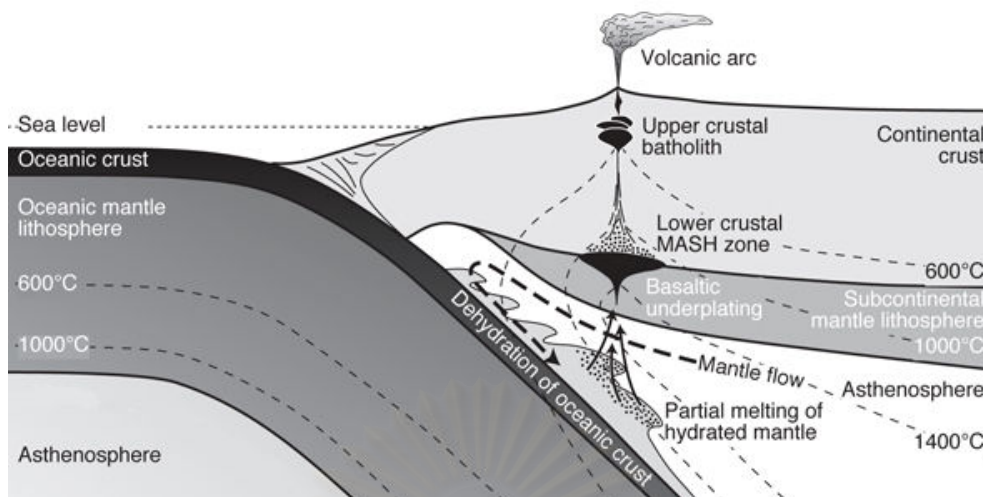


Fig 6.6. Cross section through a subduction zone and continental arc (modified from Winter, 2001 and Richards, 2003). Note that this scenario can be applied to the N-and V-Prospepects of the chatree Au mine for subduction related to alteration and mineralization.

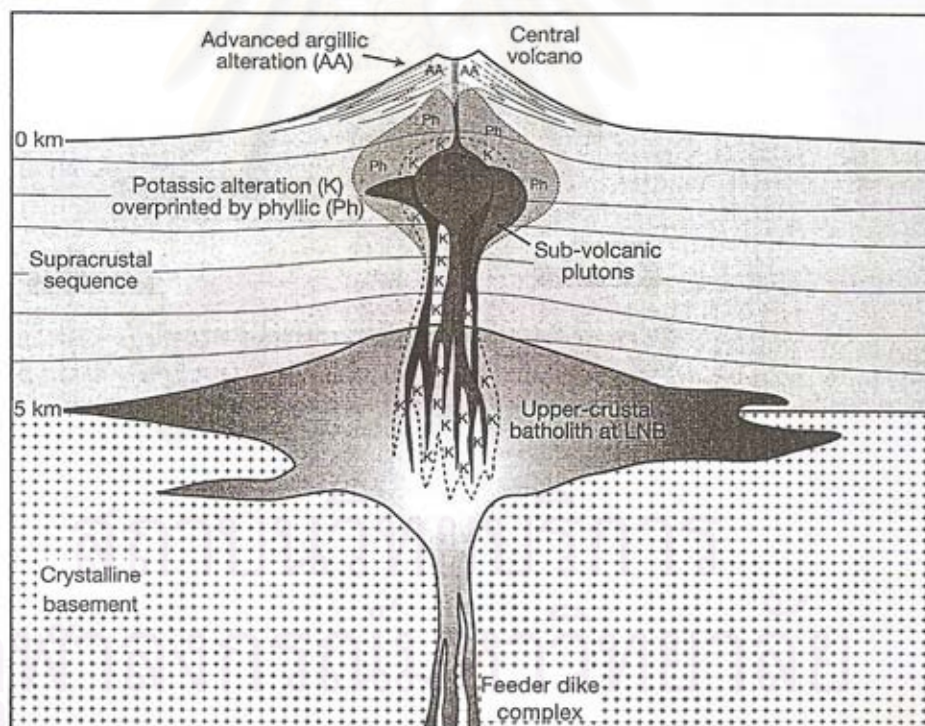


Fig 6.7. Schematic cross section through a porphyry Cu-forming volcanic-plutonic system (modified after Lowell and Guilbert, 1970, Silotoe, 1973, Irianto and Clark, 1995, Richards, 2003). Abbreviations: Pro, Propylitic alteration; AA, Argillic alteration; Ph, Phyllic alteration; K, Pottassic alteration. Note that the occurrence of volcanic and plutonic rocks of N and V Prospects may be formed by almost the same process.

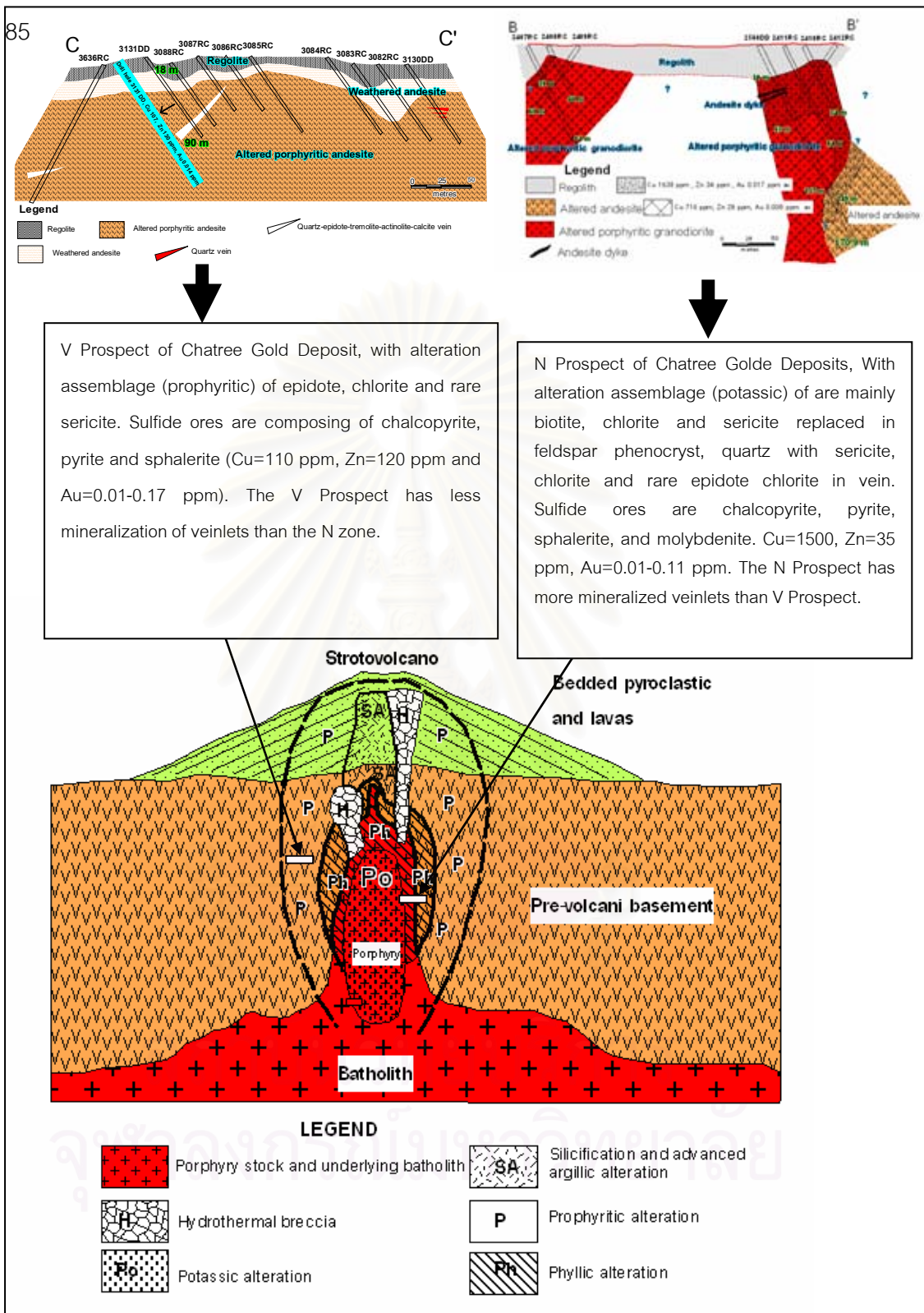


Fig. 6.8 Model for the alteration&porphyry show styles of the N and V Prospect, Chatree gold mine (modified after Lowell and Guilbert, 1970, Silotoe, 1973, Irianto and Clark, 1995, Richards, 2003). N Prospect shows characteristic of potassic alteration with minor phyllic alteration whereas the V Prospect is propylitic alteration style.

6.4 Tectonic setting

With all of the results mentioned above, the tectonic activity of the N and V prospect can be visualized. The igneous rocks of the N- and V- prospects are Permo-Triassic calc-alkaline magmatism commenced with volcanism and followed by plutonism of possibly similar composition. The volcanism was formed by the eastward subduction of the Lampang-Chiang Rai oceanic plate (or slab) beneath the Nakhon Thai oceanic plate during Permo-Triassic Period (Fig. 6.9). Partial melting of oceanic slab beneath the mantle wedge may have caused partial melting of the upper slab. Subsequently mafic magma ascending and differentiation of melts eventually gave rise to arc andesite of the N and V prospects. This arc andesite may have formed as part of a north-south-trending linear belt of the Loei-Phetchabun-Nakhon Nayok (LPN) volcanic arc. The arc magma pooled near the base of the crust, forming an underplated layer (Hildreth, 1981). Hydrothermal fluids were formed by interaction and mixtures of less amount magmatic fluids and large amount meteoric or sea water formed from the arc volcanism of ascending melts and differentiated. These fluids may have caused intensive alteration with temporally and spatially associated Au-Ag mineralization in the N and V prospects. This kind of mineralization was considered to be epithermal deposit of low-sulphidation type. Subduction of Lampang-Chiang Rai plate was progressively continued until early Triassic age and perhaps provided appropriate heat for partial melting of the mantle wedge. Ascending of melts was in the same style as the arc volcanism. But the differentiated and ascending magma was not raised to surface and then formed shallow-intensive granodiorite porphyry of the N and V prospects. Hydrothermal fluids were formed and accumulated by the influx mixture of hot magmatic water with (meteoric-)sea water into the shallow stock. Then hydrothermal alteration together with associated low-grade porphyry copper±Mo±Au mineralization was formed and overprinted the earlier mineralized arc andesite. The N and V prospects of the Chatree Au mine have similar tectonic setting to the other porphyry Cu-Mo±Au deposits reported by Quadts et al. (2005), Sotnikov et al. (2005), Berzina and Sotnikov (2007) and Sillitoe (2000) (see summary in Table 6.1), even though Cu and Au ores of the prospects are lower in grades and tonnage than those of above-mentioned deposits.

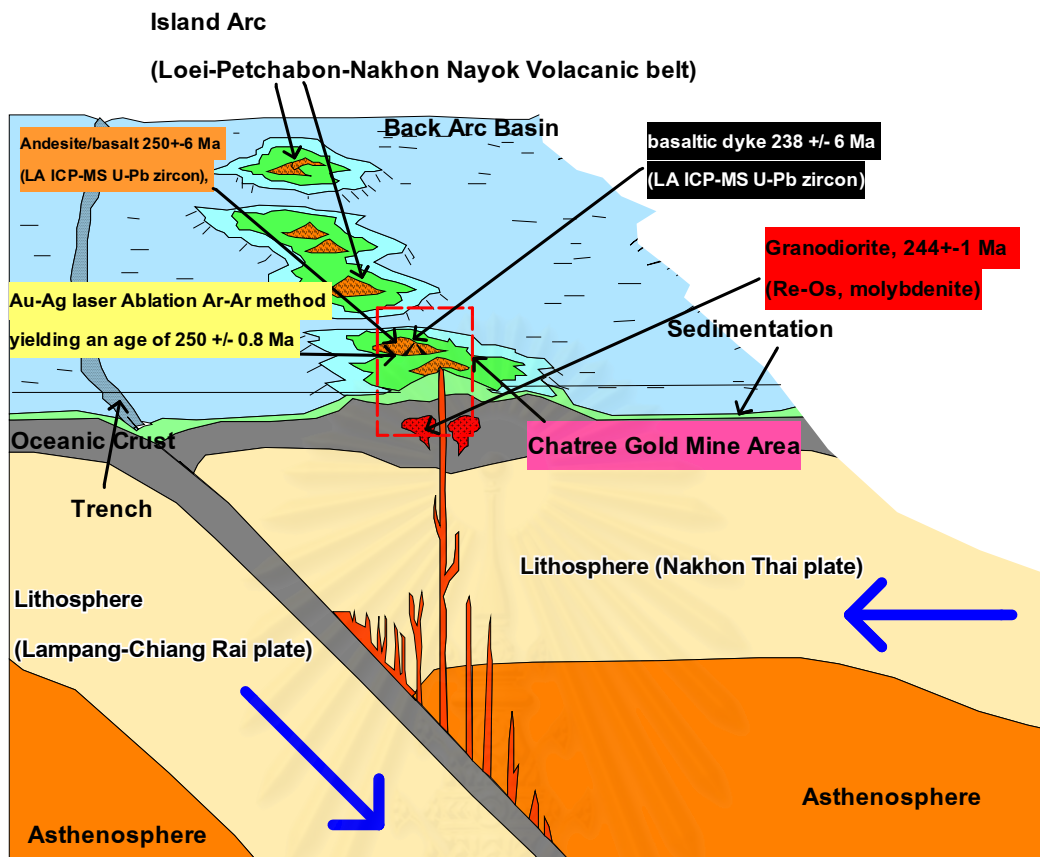


Fig. 6.9 Model of tectonic setting of Loei-Perchabun volcanic belt. (modified from , Charusiri et.al, 2002, Salam et al., 2008 and Gene , 2009)

Table 6.1 Previous data of porphyry type.

Location	Porphyry type	Host rock intrusive	Country rock	Mineralization	Alteration	Tectonic setting	Author's name
Panagyurishte , Bulgaria.	Cu-Au	calc-alkaline magmatism	Late Cretaceous phase of the Alpine-Himalayan orogeny.	Pyrite and chalcopyrite are the most common ore minerals; bornite and magnetite are subsidiary and variable in abundance, and molybdenite, gold and platinum-group minerals are occasional	K-silicate alteration, surrounded by propylitic alteration, is recognized in the early hydrothermal stages of most porphyry copper deposits, with local overprints by sericite alteration, and at some localities advanced argillic alteration	subduction	Quadt et al. (2005)
Borgulikan, Russia	Cu-Mo-(Au)	quartz monzodiorite	Taldan complex volcanics	Hypogene mineralization includes magnetite-bornite-chalcopyrite, pyrite-chalcopyrite-molybdenite, and pyrite-chalcopyrite-galena-fahlore-sphalerite assemblages. The average element contents in the best studied Ikan and Borgulikan ore zones are as follows: 0.16–0.31% Cu, 0.005% Mo, and 0.43–0.47 ppm Au	quartz-K-feldspar-biotite metasomatites, propylites (albite-epidote-actinolite assemblage), quartz-sericite-chlorite metasomatites (with pyrite, rutile, and, sometimes, tourmaline), and argillizites.	subduction	Sotnikov et al. (2005)
Azərbaycan province, Iran	Cu	associated with calc-alkaline intrusive rocks (I-type) (monzonite, quartz-monzonite and a later diorite/granodiorite phase)	Cretaceous limestone and Eocene tuff and agglomerate of andesitic to trachytic composition	The sulphide minerals are rare and consist of pyrite and traces of chalcopyrite, galena and sphalerite.	Anorthitic core which becomes unstable on cooling and is subsequently hydrothermally altered to sericite and calcite. Biotite phenocrysts have been altered to chlorite and sericite. Chlorite replaces biotite or occurs interstitially to quartz and feldspar in the groundmass.	subduction	Hezarkhani (2005)
Spence, Chile	Cu	stocks and dykes of quartz monzonite porphyry	andesitic volcanic and volcanoclastic rocks of Late Jurassic and Cretaceous age	pyrite and chalcopyrite, accompanied by subsidiary amounts of bornite and molybdenite	centrally located K –silicate and peripheral propylitic assemblages partially overprinted by a later sericitic event	subduction	Sillitoe (2000)
Antapaccy, Peru,	Cu-Au	quartz monzonite porphyry stock	cretaceous age	bornite, hypogene chalcocite and molybdenite	Early K-Silicate alteration is characterized by biotite and magnetite after mafic phenocrysts, and is flowed by introduction of K-feldspar accompanied by disseminated, fracture and veinlet sulphides	subduction	Sillitoe (2000)
Cardia Ridgeway, New South Wales, Australia	Cu-Au	monzonite porphyry stock	into volcanoclastic rocks	chalcopyrite and bornite which along with native gold and abundant magnetite	K-silicate, Characterized by orthoclase, albite, magnetite and biotite, which overprinted by a propylitic assemblage	subduction	Sillitoe (2000)
Erdene-Ovoo , northern Mongolia	Cu-Mo	Permo-Triassic plume	basalt-andesite-dacite-rhyolite series and rifting stage	-	-	subduction	Berzina and Sotnikov (2007)

Table 6.1 (cont.)

Gaby Sur, Chile.	Cu	mainly equigranular granodiorite and swarm of quartz diorite dykes of post- Paleozoic age	metamorphose andesitic and siltstone	chalcopyrite and subsidiary bornite centrally to pyrite alone on the periphery	K-silicate altered is transitional outwards to propylitic alteration	subduction	Sillitoe (2000)
N and V Prospect, Chatree, Pichit, Thailand	Cu-MozAu	Cal-alkaline intrusive rock, I-type (granodiorite to tonalite)	Basaltic andesite	Abundant Cu-Zn at potassic zone related with Au but low significant. Cu-Zn of propylitic zone is less than potassic zone.	Potassic, monor phyllic closed to porphyry and, propylitic at distal.	subduction	Marhotorn , 2008 (this thesis)



สถาบันวิทยบริการ
จุฬาลงกรณ์มหาวิทยาลัย

CHAPTER VII

CONCLUSION

Based on petrographic and geochemical investigations, the studied igneous rocks at Akara Mining area regarded as the calc-alkaline, intermediate extrusive and intrusive rocks and belong to the I-type affinity. The Akara studied rocks show some characteristics as shown below.

A. The intrusive rocks are mainly porphyritic granodiorite (to tonalite) with late stage andesitic dyke. The groundmass rock is mainly composed of andesine to oligoclase phenocryst (altered to sericite in fractures and cores), relic hornblende (altered to biotite-chlorite), quartz and K-feldspar. The rock intruded porphyritic andesite host rock. The rock shows characteristic of the porphyry-type deposit.

B. In term of the tectonic setting, these plutonic rocks possess assemblage of volcanic-arc granitic rocks,

C. Alteration assemblages are mainly biotite-chlorite and potash feldspar (of K-potassic alteration). Locally, sericite formed in fractures of plagioclase as veinlets (of phyllic alteration) with hosted low-grade Cu-Au ores.

D. The rare earth-chondrite normalized patterns and variation triangular diagrams suggest co-magmatic series which generate from the fractional partial melting process rather than from the batch partial melting process.

E. The extrusive host rock in the study area also belongs to calc-alkaline affinity which is mainly basaltic andesite with associated propylitic alteration.

F. The studied rocks occurred in the tectonic setting of island arc tholeiite with eastward subduction of Lampang-Chiang beneath Nakhon Thai Tectonic blocks. These extrusive rocks occurred during 250 Ma which were formed in the island-arc setting.

REFERENCES

- Andeson, A. L. JR. 1985. Probable relations between plagioclase zoning and magma dynamics, Fuego Volcano, Guatemala. American Mineralogist 69: 660-676.
- Arias, D. 2000. Special Issue on Gold Exploration in NW Iberian Peninsula. Journal of Geochemical Exploration 2, 71 (November): 87.
- Aswasareelert, W., and Durongkadech, P. 2001. Petrography and Major Element Geochemistry of Volcanic Rocks at Khao Khana, Amphoe Chon Daen, Changwat Petchabun. Dept. Geol. Sci. Chulalongkorn University: 25: 22-30
- Barker, D. S. 1983. Igneous Rocks. 2nd ed. Englewood Cliffs. Prentice Hall Incl.
- Barr, S., and Macdonald, A. S. 1981. Nam River suture zone, north Thailand. Geology 15: 907-910.
- Barr, S. M., Tantisukrit, C., Yaowanoyothin, W., and Macdonald, A. S. 1990. Petrology and tectonic implications of Upper Paleozoic volcanic rocks of the Chiang Mai Belt, northern Thailand. Jour. of Southeast Asian Earth Science 4: 37-47.
- Boss, C. B., Kenneth, J. C. 2004. Instrumentation and techniques in inductively coupled plasma optical emission spectrometry. Available from:
<http://www.atoomspectrometrie.nl/lcpcconceptsbook.pdf>. [2007, Jan 16]
- Beane, R. E., and Tittley, S. R. 1981. Porphyry copper deposits. Part II. Hydrothermal alteration and mineralization. Econ.Geol, 75th Anniv: 235-263.
- Beckinsale, R. D., Suensilpong, S., Nakapadungrat, S., and Walsh, J. N. 1979. Geochronology of granite magmatism in Thailand in relation to a plate tectonic model. Jour. of Geol. Soc. of London 136: 529-540.
- Belogub, E. V., Novoselov, K. A., Yakovleva, V. A., and Spiro, B. 2008. Supergene sulphides and related minerals in the supergene profiles of VHMS deposits from the South Urals. Ore Geology Reviews. 3-4, 33 (June): 239-254.
- Berzina, A. P., and Sotnikov, V. I. 2005. Character of formation of the Erdenet-Ovoo porphyry Cu-Mo magmatic center (northern Mongolia) in the zone of influence of a Permo-Triassic plume. Russian Geology and Geophysics 48: 141-156.
- Bignell, J. D. and Snelling, N. J. 1977. Geochronology of Malayan granites, Inst. Geol. Soc. London, Overseas Geol. Mineral Res. 47: 40-51.

- Botros, N.S. 2004. A new classification of the gold deposits of Egypt. Ore Geology Reviews 1-2 25 (August):1-37.
- Boyle, R. W. 1979. The geochemistry of gold and its deposits. Canada Geol. Survey Bull. 280: 584.
- Braun, E. V. and Hahn, L. 1976. Geological map of northern Thailand 1:250,000 Sheet 2 (Chiangrai) Federal Institute of Geosciences and Natural Resource. Thailand: Hanover.
- Braun, E. V., Besang, C., Eberle, W., Harre, W., Kreuzer, H., Lenz, H., Muller, P., and Wendt, I. 1976. Radiometric age determination of granites in northern Thailand. Geologisches Jahrbuch. 21: 171-204.
- Bunopas, S. 1981. Paleogeographic History of Westory of Western Thailand and Adjacent Parts of Southeast Asia: A Plate Tectonics Interpretation. Geol. Surv. Paper, Department Mineral Resources, Bangkok 5: 810.
- Bunopas, S. and Vella, P. 1983. Tectonic and geologic evolution of Thailand. Workshop Stratigraphic Correlation Thailand Malaysia. pp. 307-322. Had Yai, Thailand, 8-10. 1983. Thailand.
- Bunopas, S., and Vella, P. 1992. Geotectonics and geologic evolution of Thailand. National Conference on Geologic Resources of Thailand: Potential for Future Development, Bangkok, Thailand. 209-228.
- Burnham, C.W. 1967. Hydrothermal fluids at the magmatic stage. In Geochemistry of Hydrothermal Ore Deposits. 1st ed. New York: N.Y press.
- Burnham, C.W. 1979. Magmas and hydrothermal fluids. In Geochemistry of Hydrothermal Ore Deposits. 2nd ed. New York: N.Y press.
- Burnham, C.W. 1997. Magmas and hydrothermal fluids. In Geochemistry of Hydrothermal Ore Deposits. 3rd ed., New York: N.Y press.
- Burt, R. M., Cole, J. W., Vroon, P. Z., 1996. Volcanic geology and geochemistry of Motuhora (Whale Island), Bay of Plenty, New Zealand. New Zealand J. Geol. Geophys. 39: 565–580.
- Candela, P. A., Blevin, P. L. 1995. Do some miarolitic granites preserve evidence of magmatic volatile phase permeability? J. Econ. Geol. 90: 2310-2316.

- Chairangsee, C., Ginze, C., Macharoensap, S., Nakornsri, N., Silpalit, M., and Sinpool-Anunt, S. 1990. Geological map of Thailand 1:50,000 Exploration for sheet Amphoe Pak Chom 5345 I Ban Na Kho 5344 I, Ban Huai Khop 5445 III, King Amphoe Nam Som 5444 V. pp. 1-109. Thailand. Hanover.
- Chappell, B.W. and White, A.J.R. 1974. Two contrasting Granite types. Pacific Geology 8: 713-174.
- Chareonpravat, A., Sripongpan, P., Thammadusadee, V., and Wolfrat, R. 1987. Geology of Amphoe Sop Prap and Amphoe Wang Chin. pp. 1-52 Thailand. Hanover. (Unpublished Manuscript)
- Charusiri, P. 1989. Lithophile Metallogenetic Epochs of Thailand: a Geological and Geochronological investigation. Doctoral dissertation, Department of Geology Queen's University, Kingston, Canada.
- Charusiri, P., Pongsapich, P., Daorerk W. and Khantaprab, C. 1991. Granitoid belts in Thailand: New evidence from $^{40}\text{Ar}/^{39}\text{Ar}$ and K-Ar Geochronology and isotopic investigation. J. Sci. Res. Chulalongkorn University: 1-16
- Charusiri, P., Clark, A.H., Farrar, E., Archibald, D. and Charusiri, B. 1993. Granite belts in Thailand: evidence from the $^{40}\text{Ar}/^{39}\text{Ar}$ geochronological and geological synthesis. Journal of Southeast Asian Earth Science 1-4, 8:127-136.
- Charusiri, P., Daorerk, V., Archibald, D., Hisada, K., and Ampaiwan, T. 2002. Geotectonic Evolution of Thailand: A new Synthesis. Journal of the Geological Society of Thailand 1:1-20.
- Charusiri, P., Arunsrisangchai, W., Nunsamai, S., Deesawat, W., 2003. Knowledge on Gold: Epithermal Au Deposits and their Exploration. Journal of Scientific Research, Chulalongkorn University 1:2.
- Chongrakmani, C. and Sattayarak., N. 2004. Geological map of Changwat Phetchabun Thailand 1:250000, Department of Mineral Resources Bangkok, Thailand.
- Charusiri, P., Sutthirat, C., Plathong, C., and Pongsapich. W. 2004. Geology and Petrochemistry of Basaltic Rocks at Khao Kradong, Burirum, NE Thailand: Implications for Rock Wool Potentials and Tectonic Setting. J. Sci. Res. Chula. Univ. 2, 29 (May): 83-103.

- Chuaviroj, S., Chaturongkawanich, S., and Sukawattananan, P. 1980. Geology of geothermal resources of northern Thailand (Part I, San Kamphaeng. pp 20-31. Thailand. Department of Mineral Resources. (Unpublished Manuscript)
- Clark, M. C. G., and Neddoe-Stepheres, B. 1987. Geochemistry miner alogy and plate tectonic setting of a Late Cretaceous Sn-W granite from Sumatra, Indonesia. Mineralogy Mag.51: 371-387.
- Cline, J. S., and R. J. Bodnar. 1991. Can economic porphyry copper mineralization be generated by a typical calc-alkaline melt? Journal of Geophysical Research 96: 8113-8126.
- Cobbing, E. J., Mallicj, D. I. J., Pitfield. P. E. J., and Teoh, L. H. 1986. The granites of the SE Asian Tin Belt. J. Geol. Soc. London. 143: 537-550.
- Cobbing, E. J., Pitfield, P. E. J., Darbyshire, D. P. F., and Mallick, D. I. J. 1992. The granites of the South-East Asian tin belt. British Geol. Surv. 10: 250-261.
- Corbett, G. 2004. Comments on controls to gold mineralization at gold prospects in the vicinity of the charee gold mine, Thailand. pp. 2-23. Australia: Corbett Geological Services. (Unpublished Manuscript)
- Cox, K.G., Bell, J.D., and Pankhurst, R.J. 1979. Interpretation of Igneous Rocks. pp. 210-215. London: George Allen and Unwin Press.
- COX, D.P. 1986. Descriptive model for porphyry Cu. In D.P. Cox, & D.A. Singer (eds.) Mineral Deposit Models. p. 76. America: Geological Survey Bulletin.
- Crossing, J. 2004. Geology of the Chatree region Thailand. Compass Geological. Australia. p 3. Australia. 24 Walpole Street, St James, WA 6102. (Unpublished Manuscript)
- Cumming, G., Lunwongsa, W., and Nuanlaong, S. 2006. The Geology and Mineralization at Chatree, Central Thailand. A report prepared for Kingsgate Consolidated Limited. pp. 9-35. Thailand. (Unpublished Manuscript)
- Deer, W. A., Howie, R. A., and Zussman, J. 1966. An introduction to the Rock-Forming Mineral. pp. 121-125. USA: Hardcover.
- Department of Mineral Resources. 1999. Geology of Thailand, Department of Mineral Resources. Thailand. Thailand: Department of Mineral Resource. (Unpublished Manuscript)

- Department of Mineral Resources. 2002. Geology and Mineral Resources of Thailand Conference. Depart of Mineral Resource. Thailand. Thailand: Department of Mineral Resource. (Unpublished Manuscript)
- . (Unpublished Manuscript)
- Deesawat, W. 2002. Preliminary Investigation on Hydrothermal Alteration of the Chatree Gold Deposit, Wangpong Area, Petcgabun. Beachelor's Senior Project. Department of Geology. Faculty of Science. Chulalongkorn University.
- Diemar M.G., Diemar V.A., and Udompornwirat S. 2000. The Chatree Epithermal Gold-Silver Deposit, Phichit-Petchabun Provinces, Thailand. In Symposium on Mineral, Energy, and Water Resource of Thailand. pp. 423-427. Bangkok, Thailand, October 28-29, 2000. Thailand.
- Dilles, J.H. 1987. Petrology of the Yerington Batholith, Nevada; evidence for evolution of porphyry copper ore fluids. Economic Geology 7, 82 (November): 1750-1789.
- El-Shazly, A.K. 2004. Porphyry Cu Deposits. Available from:
<http://www.science.marshall.edu/elshazly/Econ/porph.doc>. [2008 June 11]
- Garwin, S.L. 1993. The Gold Potential of the Loei-Prachinburi Mineralized Belt, Northeastern Thailand. pp. 56-70. Thailand: Newmont (Thailand) Limited. (Unpublished Manuscript)
- Gene, J. P. 2009. Plate Tectonics, Plate Boundaries and picture by Tasa Graphic Arts. Avialable from: http://blue.utb.edu/paullgj/physci1417/Lectures/Plate_Tectonics.html [Jan, 20 2009]
- George, P.M. 1897. Regolith. Available from: <http://en.wikipedia.org/wiki/Regolith> [2009, Jan 14]
- German Geological Mission. 1972. Final report of the Geman Geological mission to Thailand 1965-1971. pp.1-94. Bundesanstalt fur Bodenforschung. Hanover. (Unpublished Manuscript)
- Gill, J.B. 1978. The role of trace element partition coefficients in models of andesite genesis. Geochimica et Cosmochimica Acta 42: 709-724.
- Grove, T.L., and Kinzler, R.J. 1986. Petrogenesis od andesites: Annual Review of Earth and Planetary Science. 14: 417-454.

- Guilbert, J. M., and Lowell, J.D. 1974. Variations in zoning patterns in porphyry ore deposits. Can. Inst. Mining Metall., Bull. 67: 99-109.
- Gustafson, L. B., Orquera, W., McWilliams, M., Castro, M., Olivares, O., Rojas, G., Maluenda, J., and Mendez, M. 2001. Multiple Centers of Mineralization in the Indio Muerto District, El Salvador, Chile. Economic Geology 96:325-350
- Hattory, K., and Sato, H. 1996. Magma evolution recorded in plagioclase zoning in 1991 Pinatubo eruption products. American Mineralogist. 81: 982-994.
- Hasawek, R. 1983. Petrochemical features of granites associated with tin-tungsten mineralization at Mae Chedi, Wing Pa Pao, Chingrai. Master's Thesis. Department of Geology. Faculty of Science. Chulalongkorn University.
- Hedenquist, J.W., and Lowenstern, J.B. 1994. The role of magmas in the formation of hydrothermal ore deposits. Nature. 370: 519-526.
- Hezarkhani, A. 2005. Petrology of the intrusive rocks within the Sungun Porphyry Copper Deposit, Azerbaijan, Iran. Journal of Asian Earth Sciences 3, 27(August):326–340
- Hibbard, M. J. 1995. Petrography to Petrogenesis. 2nd ed Newjersey. Prentice Hall Incl.
- Hildreth, W. 1981, gradients in silica magma chambers: Implications for lithospheric magmatism: Journal of Geophysical Research 86: 10,153 -10,192.
- Hildreth, W., and Moorbath, S. 1988. Crustal contributions to arc magmatism in the Andes of central Chile. Contributions to Mineralogy and Petrology 98: 455–489.
- Hisada, K., Chutakositkanon, V., Charusiri, P., and Arai, S., 2000. Tectonic significance deduced from detrital chromian spinel in the Permian Nam Duk Formation, Central Thailand. Geosciences Journal, special edition 4: 102-104.
- Holliday, J., Mcmillan, C., and Tedder, I. 1999. Discovery of the Cadia Ridgeway gold-copper porphyry deposit. Proceeding of New Generation Gold Mines '99': Case Histories of discovery, Perth. pp. 101-107. Glenside, South Australia, 1999. Australia.
- Huber, N.K. 1987. The Geologic Story of Yosemite National Park. Available from: http://www.yosemite.ca.us/library/geologic_story_of_yosemite/rocks.html [2008, Oct 15]

- Hughes, C.J. 1982. Igneous Petrology. 2nd ed. pp. 1-551. New York: Elsevier Scientific Publishing Co.
- Hutchison, C. S. 1975. Ophiolite in SE Asia Bull. Geol. Soc. Am. 86: 797-806.
- Hutchison, C. S. 1978. Southeast Asian Tin Granitoids of Contrasting tectonic setting. J. Phys. Earth Tokyo 26: 221-232.
- Hutchison, C. S. 1983. Multiple Mesozoic Sn-W-Sb granitoids of Southeast Asia. Circum-Pacific Plutonic Terranes. Geol. Soc. American. Memoir 159: 35-60.
- Irvine, T. N., and Baragar, W. R. A., 1971. A guide to the chemical classification of the common volcanic rocks. Canadian Journal of Earth Sciences 8: 523-548.
- Intasopa, S. B 1992. Petrology and geochronology of the volcanic rocks of the Central Thailand Volcanic Belt. Doctoral dissertation. Department of Geology, Faculty of Science, New Brunswick University.
- Ishihara, S. 1977. The magnetite-series and ilmenite-series granite rocks. Mining Geol. 27: 293-305
- Ishihara, S. 1981. The granitoid series and mineralization. Econ. Geol., 75th Anniversary Volume: 458-484.
- Irianto, B., and Clark, G.H., 1995, The Batu Hijau porphyry copper gold deposit, Sumbawa Island, Indonesia. In Pacific Rim Congress, 19-22 November 1995, Auckland, New Zealand, proceedings: Carlton South, The Australasian Institute of Mining and Metallurgy 95: 299-304.
- Jacobson, H.S., Pierson, C.T., Danusawad, T., Japakasetr, T., Inthaputi, B., Siriratanamongkol, C., Prapassornkul, S., and Pholphan, N. 1969. Mineral Investigations in Northeastern Thailand. Geological Survey Professional. p. 618. Washington: United States Government Printing Office.
- Jones, B., Fierro, J., and Lenzi, G. 2000. Antapaccy project-geology. In Seminario Internacional "Yacimientos Tipo Porfido de Cu-Au", Lima, 2000, Resumenes. 1p. Fracultad de Ingenieria Geologica, Mineray Metalurgica, Promocion de Geologigos 2000-2002. Peru.
- Jungyusuk, N., and Sinsakul, S. 1989. Geology of Ban Na Chaliang, Amphoe Nong Phai and Amphoe Wichianburi. Geological Survey Report 127: 51-60.

- Jungyusuk, N., and Khositant, S. 1992. Volcanic rocks and associated mineralization in Thailand, Bangkok. Conference on Geologic Resources of Thailand. pp.528-532. Department of Mineral Resource, Bangkok, Thailand, 1992. Thailand.
- Janplook, S. 2006. Petrochemistry of Volcanic rocks at Khao Champa Area in Chulalongkorn University Land Development Project, Amphoe Kaeng Khoi, Changwat Saraburi. Bachelor's Senior Project. Department of Geology. Faculty of Science. Chulalongkorn University.
- Khantaparb and colleagues. 1990. Geological assessment on the potential of rare-earth-bearing mineral resources in Thailand. pp. 1-71. Bangkok. Office of the National Research Council. (Unpublished Manuscript)
- Kontak, D. J., and Clark, A. H. 1997. The Minastira paraluminous granite, Puno, southeastern Peru: a quenched, hypabyssal intrusion recording magma commingling and mixing. Min. Mag 61: 743– 764.
- Khositant, S., Panjasawatwong, Y., Ounchanum, O., Thanasuthipitak, T., Zaw, K., and Meffre, S. (2008). Petrochemistry and Zircon Age Determination of Loei-Phetchabun Volcanic Rocks. Proceedings of the International Symposia on Geoscience Resources and Environments of Asian Terranes (GREAT 2008), 4th IGCP 516, and 5th APSEG. pp. 272-278. Bangkok, Thailand, November 24-26, 2008. Thailand.
- Kingsgate Company. 2006. Geology and mineralization at the Chatree Gold Mine: Part I and Geology and mineralization at the Chatree Gold Mine: Part II. Available from: <http://www.kingsgate.com.au> [2006, June 8]
- Kretz, R. 1983. Symbols for rock-forming minerals, American Mineralogist 68: 277-279.
- Kromkham, K., and Zaw, K. 2005. Geological Setting, Mineralogy and Alteration of the H Zone, the Chatree Deposit, central Thailand, In Proceeding of the International Conference on Geology, Geotechnology and Mineral Resource of Indochailand. pp. 319-323. Khon Kaen, Thailand, November 28-30, 2005. Thailand.
- Kuscu, G.G., and Floyd, P.A. 2001. Mineral compositional and textural evidence for magma mingling in the Saraykent volcanics. Lithos. 56: 207-230.
- LeMaitre R. W. 2002. Igneous Rocks, A Classification and Glossary of Terms. 2nd ed. London: Cambridge Univ. Press.

- Lofgren, G. E., and Donaldson, C. H. 1975. Curved branching crystals and differentiation in comb-layered rocks. Contributions to Mineralogy and Petrology 49: 309 -319.
- Lowell, J. D., and Guilbert, J. M. 1970. Lateral and vertical zonation in porphyry ore deposits. Econ. Geol. 65: 373-408.
- Macdonald, A. S., Barr, S. W., Dunning, D.R., and Yaowanoyothin, W. 1991. The Doi Inthanon metamorphic core complex in NW Thailand : age and tectonic significance. In 7th Regional Conf. Geology and Mineral Resources of Southeast Asia. pp. 1-24. Bangkok, Thailand, 5-8 November, 1991. Thailand.
- Mackenzie, W.S., Donaldson, C.H., and Guildford, C., 1982, Atlas of igneous rocks and their textures. 2nd ed. London: Longman Group Limited.
- Mahawat, C., 1982. The Petrology and Geochemistry of the Granitic Rocks of the Tak Batholith, Thailand. Doctoral dissertation. Department of Geology, University of London.
- Marhotorn, K. 2002. Preliminary Fluid Inclusion Study of the Chatree Gold deposit, Changwat Pichit. Bachelor's Senior Project. Department of Geology. Faculty of Science. Chulalongkorn University.
- Marhotorn, K., Mizuta, T., Ishiyama, D., Takashima, I., Won-in, K., Nuanlaong, S., and Charusiri, P. 2008. Petrochemistry of Igneous rocks in the Southern Parts of the Chatree Gold Mine, Pichit, and Central Thailand: Implication for Tectonic Setting. Proceedings of the International Symposia on Geoscience Resources and Environments of Asian Terranes (GREAT 2008), 4th IGCP 516, and 5th APSEG. pp. 289-298. Bangkok, Thailand, November 24-26, 2008. Thailand.
- McCutcheon, S. R., and Robinson, P. T. 1988. Embayed volcanic quartz; a product of bcellular growth rather than resorption. Marit. Sediments Atl. Geol. 24: 203.
- McCutcheon, S. R. 1990. The Late Devonian Mount Pleasant Caldera Complex: stratigraphy, mineralogy, geochemistry and geologic setting of a Sn-W deposit in southwestern New Brunswick. Doctoral dissertation. Department of Geology, Dalhousie University.
- Mitchell, A. H. G. 1977. Tectonic setting for emplacement of SE Asia tin granodiorite: Bull. Geol. Soc. Malaysia Bull. 9: 123-140.

- Michael, C. 2004. Epithermal Systems and Gold Mineralization in Western Thrace (North Greece). Bulletin of the Geological Society of Greece vol. XXXVI, 2004. Proceedings of the 10th International Congress, Thessaloniki, April 2004. XXXVI: 416-423
- Mishra, B., Pal, N., and Sarbadhikari, A.B. 2005. Fluid inclusion characteristics of the Uti gold deposit, Hutti-Maski greenstone belt, southern India. Ore Geology Reviews 1-2, 26 (March): 1-16
- Miyashiro, A., 1974. Volcanic rock series in island arcs and active continental margins. Am. J. Sci. 274: 321-355.
- Muenlek, S., Choochotiros, P., Muenlek, P., and Vudhichatiwanich, S., 1988. Phu Lon-Ban Na Ngiu Gold Prospect, Amphoe Sangkhom, Changwat Nong Khai. Economic Geology Report, Department of Mineral Resources, Thailand 14: 25-36
- Neacsu, A., Popescu, G. C., Constantinescu, B., Vasilescu, A., and Ceccato, D. 2009. The geochemical signature of native gold from Rosia Montana and Musariu ore deposits, Metaliferi Mts. (Romania); Preliminary Data"-Carpathian. Journal of Earth and Environmental Sciences. 1, 4: 49-59.
- Nantasin, P. 2005. Petrography and geochemistry of intrusive rocks at Ban Pho-Sawan area, Amphoe Bung Samphan, Changwat Phetchabun, In Proceeding of the International Conference on Geology, Geotechnology and Mineral Resource of Indochailand. pp. 374-385. Khon Kaen, Thailand, November 28-30, 2005. Thailand.
- Nakapadungrat, S. 1982. Geochronology and Geochemistry of the Thong-Lang Granite Complex, Central Thailand. Doctoral dissertation. Department of Geology, University of London.
- Nakapadungrat, S. Beckensale, R. D., and Suensilpong. S. 1984. Geochronology and geology of Thai granites. Proc. Conf. on Application of Geology and National Development. pp. 75-93. Chulalongkorn University, Bangkok, Thailand, November, 1984. Thailand.
- Nakchaiya, T., Mitzuta, T., Ishiyama, D., Takashima, I., Won-In, K., Lunwongsa, V., and Charusiri, P. 2008. Stratigraphy and Petrochemistry of Volcanic Rocks in the Chatree Gold Mine, Central Thailand: Implication for Tectonic Setting. Proceedings of the International Symposia on Geoscience Resources and Environments of Asian

- Terranes (GREAT 2008), 4th IGCP 516, and 5th APSEG. pp. 302-311. Bangkok, Thailand, November 24-26, 2008. Thailand.
- Nekvasil, H., 1991. Ascent of felsic magmas and formation of rapakivi. Am. Mineral. 76: 1279-1290.
- Panjasawatwong, Y. 1993. Petrology, geochemistry and tectonic implications of igneous rocks in the Nan Suture, Thailand and an H₂O on plagioclase-melt equilibria at 5-10 kb pressure. Doctoral dissertation. Department of Geology, University of Tasmania.
- Panjasawatwong, Y., Kanpeng, K., and Ruangvatanasirikul, K. 1995. Basalts in Li basin, northern Thailand. In Proceedings of the International Conference on Geology, Geotechnology and Mineral Resources of Indochina. pp. 225-234. Khon Kaen University, Khon Kaen, Thailand, 1995. Thailand.
- Pearce, J. A., and Cann, J. R. 1973. Tectonic setting of basic volcanic rocks determined using trace element analyses. Earth and Planetary Science Letters 19:290-300.
- Pearce, J. A., and Norry, M. J. 1979. Petrogenetic Implications of Ti, Zr, Y, and Nb Variations in Volcanic Rocks. Contributions to Mineralogy and Petrology 69:33-47.
- Pearce, J.A., Harris, N.B.W., and Tindle, A.G. 1984. Trace element discrimination diagrams for the tectonic interpretation of granitic rocks. Journal of Petrology 25: 956-983.
- Phajuy, B., Panjasawatwong, Y., and Osataporn, P. 2004 preliminary geochemical study of volcanic rocks in the Pang Mayao area, Phrao. Chiang Mai, northern Thailand: tectonic of formation. Journal of Asian Earth Science 24:767-776.
- Pichler, H., and Schmitt-Riegraf, C. 1997. Rock-forming Minerals in Thin Section,. Translated by L. Hoke, Weinheim, etc. (Chapman & Hall). London.
- Piyasin, S. 1972. Geology of Lampang sheet (NE 41-11), scale 1:250,000, Department of Mineral Resources, Bangkok, Thailand. Report of investigation 14: 1-98.
- Piyasin, S. 1975. Geology of Changwat Uttaradit (NE 47-11) Qyadrabgkem Scale 1:250,000, DMR. Report of Investigation 16:1-68.
- Pongsapich, W., Pisutha-Armond, V., and Charusiri, P. 1983. Reviews of felsic plutonic rocks of Thailand. Proc. Of the workshop on Stratigraphic Correlation of Thailand and Malasia. pp. 213-232. Hadyai, Thailand, September, 1983. Thailand.

- Philpotts, A. R. 1989. Petrography of Igneous and Metamorphic Rocks. 2nd ed. pp. 1-192. New Jersey: Prentice-Hall.
- Punyaprasiddhi, P. 1980. Investigation of the Geology and Mineralization of in and Tungsten at Samoeng Mine Area, North Thailand. Doctoral dissertation. Department of Geology, Univerasity of Sheffield.
- Putthapiban, P. 1984. Geochemistry, Geochronology and tin mineralization of Phuket granites, Phuket, Thailand. Doctoral dissertation, Department of Geology, La Trobe University Victoria.
- Quadt, A.V., Moritz, R., Peytcheva, I., and Heinrich, C.A. 2005. Geochronology and geodynamics of Late Cretaceous magmatism and Cu–Au mineralization in the Panagyurishte region of the Apuseni–Banat–Timok–Srednogie belt, Bulgaria, Ore Geology Reviews 27: 95–126
- Richards J. P., 2003. Tectono-Magmatic Precursors for Porphyry Cu-(Mo-Au) Deposit Formation, Economic Geology. 8, 98 (December): 1515-1533.
- Ringwood, A.E. 1977. Petrogenesis in island arc systems. In M. Talwani and W.C. Pitman (eds.), In Island Arcs, Deep Sea Trenches and Back-Arc Basins, pp. 311-324. Washington: Am. Geophys. Union.
- Satoh, H., Ishiyama, D., Mizuta, T., and Ishikawa, Y. 1999. Rare Earth Element Analysis of Rock Thermal Water Samples by Inductively Coupled Plasma Mass Spectrometry (ICP-MS). pp. 1-8. Japan: Akita University.
- Sibley, D. F., Vogel, T. A., Walker, B. M. and Byerly, G. (1976), the origin of oscillatory zoning in plagioclase: a diffusion and growth controlled model. American Journal of Science 276: 275-284.
- Singharajwarapan, S., and Berry, R. 2000. Tectonic implications of the Nan Suture Zone and its relationship to the Sukhothai Fold Belt, Northern Thailand. Journal of Asian Earth Sciences 6, 18 (December): 663-673.
- Sakuyama, M. 1981. Petrological study of the Myoko and Kurohime volcanoes, Japan; crystallization sequence and evidence for magma mixing. J. Petrol. 22: 553–583.
- Salam A., Zaw, K., Meffre, S., James, R., and Stein, H. 2007. Geological setting, alteration, mineralization and geochronology of Chatree epithermal gold silver

- deposit, Phetchabun Province, central Thailand. Available From: <http://agssymposium.org/media/AbsPdfs/Abstract105.pdf> [2008, Dec 17]
- Sangsiri, P., and Pisutha-Armond, V. 2008 Host Rock Alteration at the A Prospect of the Chatree Gold Deposits, Phichit Province, Central Thailand: A Preliminary Re-Evaluation. Proceedings of the International Symposia on Geoscience Resources and Environments of Asian Terranes (GREAT 2008), 4th IGCP 516, and 5th APSEG; pp. 258-261. Bangkok, Thailand, November 24-26, 2008. Thailand.
- Siivola, J., and Schmid, R. 2007. List of Mineral Abbreviations. Recommendations by the IUGS Subcommittee on the Systematics of Metamorphic Rocks. Available from: <http://www.docstoc.com/docs/2195938/List-of-Mineral-abbreviations>. [13, Feb 2007]
- Sillitoe, R. H. 1973. Environment of formation of volcanic massive sulfide deposits Econ. Geol. 98: 1321-1325.
- Sillitoe, R. H. 2000. Exploration and Discovery of Base-and Precious-metal Deposits in the Circum-Pacific Region-A late 1990s Update, Resource Geology Special Issue. Society of Resource Geology 21: 6-16.
- Sitthithaworn, E., and Tiypairach, S. 1982. Report of magnetic anomaly investigation, Tambon Ban Na, Amphoe Ban Na, Changwat Nakhon Nayok. Ferro-alloy mineral exploration project. Bangkok. Thailand: Department of Mineral Resource. (Unpublished Manuscript)
- Sitthithaworn, E., 1989. Gold mineralization at Phu Lan Cu- Fe skarn prospect in northern Thailand. Master's Thesis. Department of Geology, University of Western Ontario.
- Sitthithaworn, E., 1992. Metallogenic map of Thailand: National conference on Geologic Resource of Thailand, Potential for future Development. pp 1-14. Department of Mineral Resources, Bangkok, Thailand, 17-24 November, 1992. Thailand.
- Sotnikov V.I., Sorokin A.A., Ponomarchuk, V.A, Gimon, V.O., Sorokin, A.P., 2007 Porphyry Cu-Mo-(Au) mineralization: the age and relationship with igneous rock complexes of the Borgulikan ore field (upper-Amur region). Russian Geology and Geophysics 48: 177-184.

- Spiering, E. D., Pevida, L. R., Maldonado, C., González, S., Garcia, J., Varela, A., Arias D., and Martín-Izard, A. 2000. The gold belts of western Asturias and Galicia (NW Spain). Journal of Geochemical Exploration 2, 71 (November): 89-101.
- Stomer, J.C. 1972. Mineralogy and Petrology of the Raton-Clayton volcanic field, northeastern New Mexico. Geological Society of America Bulletin 83: 3299-3322.
- Streckeisen, A. L. 1976. To each plutonic rock its proper name. Earth Sci. Rev. 12: 1-32.
- Sutthirat, C., Saminpanya, S., Droop, G. T. R., Henderson, C. M. B., and Manning, D. A. C. 2001 Clinopyroxene-corundum assemblages from alkali basalt and alluvium, eastern Thailand: constraints on the origin of Thai rubies. Mineralogical Society of Great Britain and Ireland. Mineralogical Magazine 2 65 (April): 277-295.
- Swanson, S.E., Fenn, P.M. 1986. Quartz crystallization in igneous rocks. Am. Mineral. 71: 331-342.
- Tangwattananukul, L., Lunwongsa, W., Mitsuta, T., Ishiyama, H., Takashima I., Won-In, K., and Charusiri, P. 2008. Geology and Petrochemistry of Dike Rocks in the Chatree Gold Mine, Central Thailand: Implication for Tectonic Setting, Proceedings of the International Symposia on Geoscience Resources and Environments of Asian Terranes (GREAT 2008), 4th IGCP 516, and 5th APSEG; November 24-26, 2008, Bangkok, Thailand: 299-301.
- Takashima, I., Sucipta, I. E., and Soc., Myint, S. 2005. Accuracy of Chemical Analysis of Rocks Samples by Portable Energy Dispersive X-ray fluorescence Spectrometer. Scientific and Technical Reports of Faculty of Engineering and Resource Science, Akita University 26: 29-34
- Teggin, D. E. 1975. The Granites of Northern Thailand. Doctoral dissertation. Department of Geology, University of Manchester.
- Tsuchiyama, A. 1985. Dissolution kinetics of plagioclase in melt of the system diopside-albite-anorthite and the origin of dusty plagioclase in andesites. Contributions to Mineralogy and Petrology 89: 1-16.
- Vance, J.A. 1965. Zoning in igneous plagioclase: patchy zoning. Journal of Geology 73: 637-651.
- Vivatpinyo, J. 2006. Petrochemistry of volcanic rocks at Khao Tham Sua area in

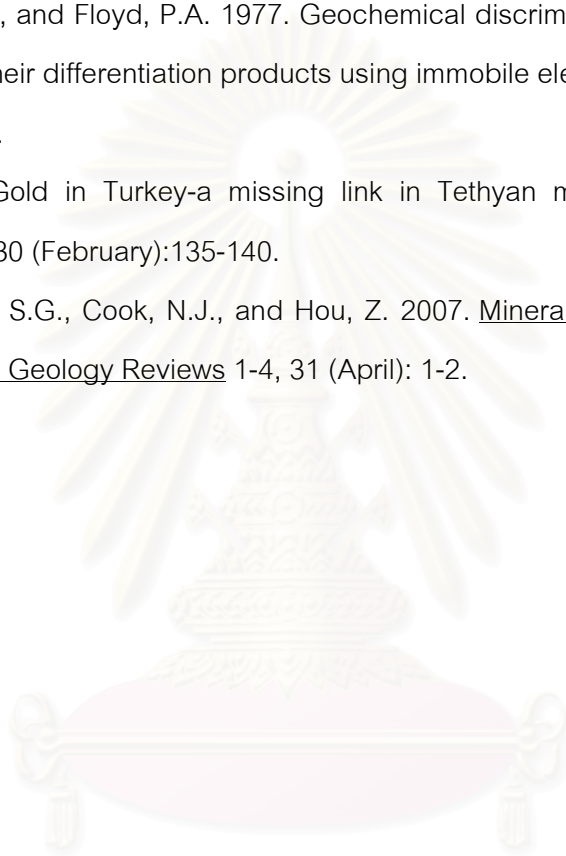
Chulalongkorn University land development project, Amphoe Kaeng Khoi, Changwat Saraburi. Bachelor's Senior Project. Department of Geology. Faculty of Science. Chulalongkorn University.

Webster, J.D., Holloway, J.R., and Hervig, R.L., 1987. Phase equilibria of a Be, U and F-enriched vitrophyre from Spor Mountain, Utah. Geochim. Cosmochim. Acta. 51:389-402.

Winchester, J.A., and Floyd, P.A. 1977. Geochemical discrimination of different magma series and their differentiation products using immobile elements. Chemical Geology 20: 325-343.

Yigit, O.2007. Gold in Turkey-a missing link in Tethyan metallogeny. Ore Geology Reviews. 2, 30 (February):135-140.

Zaw, K., Peters, S.G., Cook, N.J., and Hou, Z. 2007. Mineral deposits of South China: Preface. Ore Geology Reviews 1-4, 31 (April): 1-2.



สถาบันวิทยบริการ
จุฬาลงกรณ์มหาวิทยาลัย



APPENDICES

สถาบันวิทยบริการ
จุฬาลงกรณ์มหาวิทยาลัย

APPENDIX A

Petrographic description of igneous rocks of N and V prospect

Running No.	Sample No.	Depth (m)	Micro-Texture	Mineral composition	Main Alteration styles	Rock name
1	DDN 7	28.4-28.5	Fine-grained groundmass, phenocryst, altered, veinlets,	Quartz, plagioclase, k-feldspar, biotite, chlorite and opaque mineral	Potassic alteration	Altered porphyritic granodiorite
2	DDN 11	39.4-39.5	Dyke, phenocryst, very fine-grained groundmass, microlite, flowed, relic hornblende, altered	Quartz, plagioclase, k-feldspar, hornblende(relic), epidote (rare) and altered biotite	Potassic alteration	Andesite dyke
3	DDN 13	43.5-43.6	Dyke, Phenocryst, very fine-grained groundmass, microlite, flowed, corroded, fractured, altered	Quartz, plagioclase, k-feldspar, biotite, epidote(rare) and chlorite(rare)	Potassic alteration	Andesite dyke
4	DDN 15	51.6-51.7	Ffine-grained groundmass, phenocryst, altered, zoned, replaced, fractured	Quartz, plagioclase, k-feldspar, biotite-chlorite, sericite, rare muscovite, apatite and opaque mineral	Potassic alteration	Altered porphyritic granodiorite
5	DDN 17	57.9-57.0	Ffine-grained groundmass, phenocryst, altered, fractured, rimmed, replaced, corroded, veinlet	Quartz, plagioclase, k-feldspar, biotite-chlorite, sericite , apatite and opaque mineral	Potassic alteration	Altered porphyritic granodiorite
6	DDN 22	70.7-70.8	Ffine-grained groundmass, phenocryst, altered, cored, oscillatory zoned, fractured, veinlet	Quartz, plagioclase, k-feldspar, sericite, biotite-chlorite, apatite, opaque and clay mineral?	Potassic alteration	Altered porphyritic granodiorite
7	DDN 23	74.6-74.7	Ffine-grained groundmass, phenocryst, altered, cored, veinlet	Quartz, plagioclase, k-feldspar, biotite-chlorite, sericite, apatite, sphene, opaque mineral and	Potassic alteration	Altered porphyritic granodiorite
6	DDN 25	82.6-82.7	Ffine-grained groundmass, phenocryst, altered, fractured, oscillatory zoned , replaced, veinlet,	Quartz, plagioclase, k-feldspar, sericite, biotite-chlorite, apatite, sphene and opaque mineral	Potassic alteration	Altered porphyritic granodiorite
9	DDN 27	89.0-89.1	Fine-grained groundmass, phenocryst, altered, fractured, oscillatory zoned , replaced, rimmed, relic biotite, veinlet	Quartz, plagioclase, k-feldspar, sericite, chlorite, apatite, biotite(relic) and opaque mineral	Potassic alteration	Altered porphyritic granodiorite
10	DDN 28	92.4-92.5	Fine -grained groundmass, phenocryst, altered, fractured, relic biotite, veinlet	Quartz, plagioclase, k-feldspar, sericite, chlorite, biotite (relic), Sphene? and opaque mineral	Potassic alteration	Altered porphyritic granodiorite
11	DDN 30	99.4-99.5	Fine -grained groundmass, phenocryst, altered, fractured, replaced, rimmed	Quartz, plagioclase, k-feldspar, sericite, chlorite-biotite, and opaque mineral	Potassic alteration	Altered porphyritic granodiorite
12	DDN 31	42.0-42.10	very fine-grained and porphyritic, altered, relic biotite altered, veinlet, relic cubic opaque and replaced,	Quartz, plagioclase, k-feldspar, quartz, relic biotite, sericite, chlorite-biotite. Opaque mineral	Potassic alteration	Altered porphyritic granodiorite
13	DDN 33	102.4-102.5	Fine -grained groundmass, phenocrysts, altered, fractured, oscillatory zoned , inclusion, engulf,	Quartz, plagioclase, k-feldspar, chlorite-biotite and sericite, opaque mineral	Potassic alteration	Altered porphyritic granodiorite
14	DDN 34	109.5-109.6	Fine -grained groundmass, phenocrysts, altered, fractured, corroded, engulf, veinlet	Quartz, plagioclase, k-feldspar, sericite, chlorite and opaque mineral	Potassic alteration	Altered porphyritic granodiorite
15	DDN 36	113.4-113.5	Fine -grained groundmass, phenocrysts, altered, fractured, inclusion, oscillatory zoned , veinlet	Quartz, plagioclase, k-feldspar, sericite, chlorite, biotite and opaque mineral	Potassic alteration	Altered porphyritic granodiorite
16	DDN 39	121.0-121.1	Fine -grained groundmass, phenocrysts, altered, fractured, oscillatory zoned , replaced, rimmed,	Quartz, plagioclase, k-feldspar, chlorite-biotite, sericite, and opaque mineral	Potassic alteration	Altered porphyritic granodiorite
17	DDN 40	124.9-125.0	Fine -grained groundmass, phenocrysts, altered, fractured, oscillatory zoned , replaced, veinlet	Quartz, plagioclase, k-feldspar, sericite, chlorite, apatite and opaque mineral	Potassic alteration	Altered porphyritic granodiorite

APPENDIX A (cont.)

Running No.	Sample No.	Depth (m)	Micro-Texture	Mineral composition	Main alteration styles	Rock name
18	DDN 43	135.9 - 136.0	Fine -grained groundmass, phenocrysts, altered, fractured, replaced, branched(biotite).	Quartz, plagioclase, k-feldspar, biotite-chlorite, sericite, hornblende(relic), opaque	Potassic alteration	Altered porphyritic granodiorite
19	DDN 46	140.6 - 140.7	Fine -grained groundmass, phenocrysts, high altered, fractured, replaced, veinlet	Quartz, plagioclase, biotite, chlorite, calcite, biotite and rare epidote and opaque	Potassic alteration	Altered porphyritic andesite
20	DDN 49	148.6 - 148.7	Fine -grained groundmass, phenocrysts, altered, veinlet	Quartz, plagioclase, biotite, chlorite, calcite and opaque mineral	Potassic alteration	Altered porphyritic andesite
21	DDN 51	152.2 - 152.3	Fine -grained groundmass, phenocrysts, altered	Quartz, plagioclase, biotite, chlorite, rare epidote and opaque mineral	Potassic alteration	Altered porphyritic andesite
22	DDN 53	155.4 - 155.5	Fine -grained groundmass, phenocrysts, altered, veinlet	Quartz, plagioclase, biotite, chlorite, calcite rare epidote and opaque mineral	Potassic alteration	Altered porphyritic andesite
23	DDN 54	157.4 - 157.5	Fine-grained groundmass, phenocrysts, altered, replaced, veinlet	Quartz, plagioclase, biotite, chlorite, rare epidote and opaque mineral	Potassic alteration	Altered porphyritic andesite
24	DDN 55	159.5 - 159.6	Fine-grained groundmass, phenocrysts, altered, veinlet	Quartz, plagioclase, biotite, chlorite, rare epidote and opaque mineral	Potassic alteration	Altered porphyritic andesite
25	DDN 58	167.4 - 167.5	Fine-grained groundmass, phenocrysts, altered	Quartz, plagioclase, sericite, chlorite, epidote(veinlet) and opaque mineral	Potassic alteration	Altered porphyritic andesite
26	DDN 60	168.4 - 168.5	Fine-grained groundmass, prophyritic, anhedral to subhedral, altered, and veinlet.	k-feldspar?, calcite, chlorite, opaque, rare epidote	Potassic alteration	Altered porphyritic andesite
27	DDV 7	20.1- 20.2	Fine -grained groundmass, phenocryst, altered, relic (hornblende), lath shaped(plagioclase), veinlets	Quartz, plagioclase, chlorite, hornblende(relic), epidote, rare apatite, sericite, and opaque	Propylitic alteration	weathered andesite
28	DDV 11	25.5- 25.6	Fine-grained groundmass, phenocryst, flow, altered, relic (hornblende), veinlets	plagioclase, chlorite, hornblende(relic) epidote, apatite and sericite, and opaque	Propylitic alteration	weathered andesite
29	DDV 10	30.1- 30.2	Fine-grained groundmass, phenocryst, altered, inclusion, relic (hornblende), veinlets	plagioclase, rare epidote, chlorite, rare sericite and opaque mineral	Propylitic alteration	Altered porphyritic andesite
30	DDV 14	38.2- 38.3	Fine-grained groundmass, phenocryst, altered, glassy, corrode, relic(hornblende)	plagioclase, hornblende(relic), epidote, chlorite, apatite and opaque mineral	Propylitic alteration	Altered porphyritic andesite
31	DDV 15	42.1- 42.2	Fine-grained groundmass, phenocryst, altered, glassy, relic(hornblende), veinlets	plagioclase, hornblende(relic), epidote, chlorite, apatite and opaque mineral	Propylitic alteration	Altered porphyritic andesite
32	DDV 16	47.1- 47.2	Fine-grained groundmass, phenocryst, altered, relic(hornblende), corroded, vesicular, veinlets	plagioclase, hornblende(relic), epidote, chlorite, biotite, rare sericite, rare opaque mineral	Propylitic alteration	Altered porphyritic andesite
33	DDV 19	59.5- 59.6	Fine-grained groundmass, phenocryst, altered, flow, glassy, relic(hornblende), replaced, fractured	plagioclase, hornblende(relic), epidote, varies mica, chlorite and opaque mineral	Propylitic alteration	Altered porphyritic andesite
34	DDV 23	67.4- 67.6	Fine -grained groundmass, phenocryst, altered, flow, glassy, relic(hornblende), replaced	plagioclase, hornblende(relic), epidote, chlorite and opaque mineral	Propylitic alteration	Altered porphyritic andesite

APPENDIX A (cont.)

Running No.	Sample No.	Depth (m)	Micro-Texture	Mineral composition	Main alteration styles	Rock name
36	DDV 33	84.7-84.8	vein, recrystalline, phenocryst, altered, cubic to rectangular(opaque), veinlets	Quartz, tremolite-actinolite, epidote and opaque mineral	Propylitic alteration	Quartz-epidote-tremolite-
37	DDV 31	86.7-86.8	Fine-grained groundmass, phenocryst, microlite, diamond shaped (amphibole), cubic to rectangular(opaque), glassy ,	plagioclase, amphibole?,hornblende(relic), chlorite,	Propylitic alteration	Altered porphyritic andesite



สถาบันวิทยบริการ
จุฬาลงกรณ์มหาวิทยาลัย

APPENDIX B

Geochemical data of Igneous rocks of N&V Prospects

Rock type		Granodiorite			Granodiorite			Granodiorite	
Sample no		DDN4			DDN7			DDN12	
Depth (m)		22.4-22.5			28.4-28.5			42.0-42.1	
	XRF	ICP-OES	ICP-Ms	XRF	ICP-OES	ICP-Ms	XRF	ICP-OES	ICP-Ms
Element									
Na2O	4.48	-	-	3.93	-	-	4.72	-	-
P2O5	0.16	-	-	0.22	-	-	0.22	-	-
MgO	4.04	-	-	3.49	-	-	3.62	-	-
Al2O3	18.96	-	-	18.72	-	-	18.07	-	-
SiO2	65.81	-	-	66.44	-	-	66.23	-	-
SO3	0.96	-	-	1.52	-	-	1.78	-	-
K2O	0.66	-	-	1.08	-	-	0.73	-	-
CaO	2.43	-	-	2.54	-	-	3.01	-	-
TiO2	0.51	-	-	0.48	-	-	0.46	-	-
MnO	0.02	-	-	0.02	-	-	0.02	-	-
Fe2O3	2.96	-	-	2.76	-	-	2.69	-	-
V	67.79	-	-	68.38	55.71	-	133.63	-	-
Cr	217.71	-	-	159.32	6.76	-	170.34	-	-
Ni	8.03	-	-	5.84	-1.63	-	1.96	-	-
Cu	1246.22	-	-	938.24	930.55	-	3603.36	-	-
Zn	44.38	-	-	35.34	20.56	-	43.12	-	-
Rb	-0.62	-	-	7.51	128.99	-	58.75	-	-
Sr	1070.41	-	-	957.58	550.67	-	1065.36	-	-
Y	16.02	-	-	18.54	16.74	-	16.18	-	-
Zr	104.44	-	-	115.02	25.67	-	110.48	-	-
Nb	11.35	-	-	11.29	-	-	18.35	-	-
Ba	-	-	-	-	210.44	-	-	-	-
Li	-	-	-	-	86.18	-	-	-	-
Sc	-	-	-	-	9.21	-	-	-	-
Ce	-	-	-	-	30.85	-	-	-	-
Nd	-	-	-	-	-6.08	-	-	-	-
Rock type		Granodiorite			Granodiorite			Granodiorite	
Sample no		DDN15			DDN20			DDN22	
Depth (m)		51.6-51.7			64.0-64.1			DDN22	
	XRF	ICP-OES	ICP-Ms	XRF	ICP-OES	ICP-Ms	XRF	ICP-OES	ICP-Ms
Element									
Na2O	3.99	-	-	4.24	-	-	3.98	-	-
P2O5	0.17	-	-	0.17	-	-	0.17	-	-
MgO	3.27	-	-	3.06	-	-	2.92	-	-
Al2O3	20.01	-	-	17.84	-	-	18.02	-	-
SiO2	66.55	-	-	68.17	-	-	67.57	-	-
SO3	0.92	-	-	0.94	-	-	0.51	-	-
K2O	0.77	-	-	0.65	-	-	0.47	-	-
CaO	2.63	-	-	3.09	-	-	3.40	-	-
TiO2	0.45	-	-	0.39	-	-	0.48	-	-
MnO	0.01	-	-	0.02	-	-	0.04	-	-
Fe2O3	2.40	-	-	2.64	-	-	3.27	-	-
V	210.91	-	-	93.52	40.64	-	74.13	52.84	-
Cr	112.80	-	-	168.65	5.70	-	170.46	7.31	-
Ni	7.83	-	-	4.97	0.99	-	173.46	3.15	-
Cu	1791.64	-	970.40	1012.16	600.02	-	367.66	242.37	-
Zn	34.99	-	23.53	34.59	17.67	-	41.81	92.74	-
Rb	7.20	-	8.52	1.04	16.47	-	3.57	70.32	-
Sr	960.61	-	485.10	886.65	573.49	-	957.49	605.54	-
Y	13.97	-	5.20	14.07	15.48	-	14.34	16.14	-

APPENDIX B (cont.)

Zr	123.27	-	7.07	103.66	11.22	-	122.27	29.00	-
Nb	11.33	-	2.00	11.30	-	-	11.29	-	-
Ba	-	-	179.50	-	202.98	-	-	168.85	-
Li	-	-	-	-	89.41	-	-	27.37	-
Sc	-	-	-	-	77.44	-	-	8.77	-
La	-	-	8.38	-	-	-	-	-	-
Ce	-	-	18.38	-	31.42	-	-	24.14	-
Pr	-	-	2.30	-	-	-	-	-	-
Nd	-	-	9.04	-	-8.41	-	-	-8.21	-
Sm	-	-	1.92	-	-	-	-	-	-
Eu	-	-	0.76	-	-	-	-	-	-
Gd	-	-	1.62	-	-	-	-	-	-
Tb	-	-	0.24	-	-	-	-	-	-
Dy	-	-	1.01	-	-	-	-	-	-
Er	-	-	0.36	-	-	-	-	-	-
Tm	-	-	0.05	-	-	-	-	-	-
Yb	-	-	0.45	-	-	-	-	-	-
Hf	-	-	0.33	-	-	-	-	-	-
Lu	-	-	0.03	-	-	-	-	-	-
Th	-	-	0.52	-	-	-	-	-	-
U	-	-	0.14	-	-	-	-	-	-
Li	-	-	-68.11	-	-	-	-	-	-
Be	-	-	-5.39	-	-	-	-	-	-
Sc	-	-	5.43	-	-	-	-	-	-
Mn	-	-	108.50	-	-	-	-	-	-
Co	-	-	5.07	-	-	-	-	-	-
Ga	-	-	17.33	-	-	-	-	-	-
Sn	-	-	2176.00	-	-	-	-	-	-
Sb	-	-	172.00	-	-	-	-	-	-
Cs	-	-	0.34	-	-	-	-	-	-
Ho	-	-	0.15	-	-	-	-	-	-
Ta	-	-	0.17	-	-	-	-	-	-
W	-	-	4214.00	-	-	-	-	-	-
Pb	-	-	2.80	-	-	-	-	-	-
Bi	-	-	0.03	-	-	-	-	-	-
Rock type		Granodiorite			Granodiorite			Granodiorite	
Sample no		DDN25			DDN27			DDN28	
Depth (m)		82.6-82.7			89.0-89.1			92.4-92.5	
	XRF	ICP-OES	ICP-MS	XRF	ICP-OES	ICP-MS	XRF	ICP-OES	ICP-MS
Element									
Na2O	4.13	-	-	4.27	-	-	3.67	-	-
P2O5	0.21	-	-	0.22	-	-	0.23	-	-
MgO	3.74	-	-	3.20	-	-	3.08	-	-
Al2O3	17.85	-	-	17.72	-	-	18.37	-	-
:SiO2	65.79	-	-	67.24	-	-	65.34	-	-
SO3	0.85	-	-	1.13	-	-	1.89	-	-
K2O	0.68	-	-	0.59	-	-	1.46	-	-
CaO	3.52	-	-	3.58	-	-	2.84	-	-
TiO2	0.48	-	-	0.43	-	-	0.44	-	-
MnO	0.03	-	-	0.02	-	-	0.03	-	-
Fe2O3	3.75	-	-	2.82	-	-	3.86	-	-
V	88.24	-	-	43.24	-	-	121.05	-	-
Cr	152.90	-	-	177.04	-	-	109.63	-	-
Ni	683.67	-	-	7.22	-	-	9.59	-	-
Cu	1460.85	-	-	1010.12	-	-	703.78	-	495.30
Zn	34.59	-	-	34.59	-	-	34.59	-	19.79
Rb	2.29	-	-	5.22	-	-	14.02	-	13.62

APPENDIX B (cont.)

Sr	1082.84	-	-	1018.19	-	-	881.96	-	564.80	
Y	19.39	-	-	18.06	-	-	15.38	-	5.94	
Zr	109.41	-	-	98.45	-	-	113.58	-	24.83	
Nb	11.29	-	-	11.29	-	-	11.68	-	1.61	
Ba	-	-	-	-	-	-	-	-	280.60	
La	-	-	-	-	-	-	-	-	8.74	
Ce	-	-	-	-	-	-	-	-	19.49	
Pr	-	-	-	-	-	-	-	-	2.48	
Nd	-	-	-	-	-	-	-	-	9.98	
Sm	-	-	-	-	-	-	-	-	1.92	
Eu	-	-	-	-	-	-	-	-	0.69	
Gd	-	-	-	-	-	-	-	-	1.81	
Tb	-	-	-	-	-	-	-	-	0.18	
Dy	-	-	-	-	-	-	-	-	1.06	
Er	-	-	-	-	-	-	-	-	0.51	
Tm	-	-	-	-	-	-	-	-	0.06	
Yb	-	-	-	-	-	-	-	-	0.41	
Hf	-	-	-	-	-	-	-	-	0.73	
Lu	-	-	-	-	-	-	-	-	0.05	
Th	-	-	-	-	-	-	-	-	0.57	
U	-	-	-	-	-	-	-	-	0.13	
Li	-	-	-	-	-	-	-	-	-30.94	
Be	-	-	-	-	-	-	-	-	-6.64	
Sc	-	-	-	-	-	-	-	-	8.17	
Mn	-	-	-	-	-	-	-	-	178.90	
Co	-	-	-	-	-	-	-	-	14.10	
Ga	-	-	-	-	-	-	-	-	18.83	
Sn	-	-	-	-	-	-	-	-	-32.10	
Sb	-	-	-	-	-	-	-	-	947.50	
Cs	-	-	-	-	-	-	-	-	-0.14	
Ho	-	-	-	-	-	-	-	-	0.20	
Ta	-	-	-	-	-	-	-	-	0.35	
W	-	-	-	-	-	-	-	-	5556.00	
Pb	-	-	-	-	-	-	-	-	1.71	
Bi	-	-	-	-	-	-	-	-	0.00	
Rock type		Granodiorite				Granodiorite				Granodiorite
Sample no		DDN31				DDN36				DDN38
Depth (m)		102.4-102.5				113.4-113.5				117.6-117.7
	XRF	ICP-OES	ICP-Ms	XRF	ICP-OES	ICP-Ms	XRF	ICP-OES	ICP-Ms	
Element										
Na2O	4.47	-	-	4.94	-	-	2.95	-	-	
P2O5	0.22	-	-	0.19	-	-	0.22	-	-	
MgO	3.39	-	-	3.06	-	-	3.25	-	-	
Al2O3	17.79	-	-	17.19	-	-	19.27	-	-	
:SiO2	67.29	-	-	67.50	-	-	66.69	-	-	
SO3	1.18	-	-	0.99	-	-	1.48	-	-	
K2O	0.86	-	-	0.40	-	-	1.67	-	-	
CaO	3.15	-	-	3.72	-	-	2.47	-	-	
TiO2	0.42	-	-	0.39	-	-	0.49	-	-	
MnO	0.02	-	-	0.02	-	-	0.02	-	-	
Fe2O3	2.54	-	-	2.89	-	-	2.57	-	-	
V	88.31	52.35	-	57.04	-	-	212.31	-	-	
Cr	148.67	5.33	-	206.98	-	-	521.18	-	-	
Ni	7.04	605.17	-	5.12	-	-	4.77	-	-	
Cu	952.06	2.50	-	1559.16	-	-	521.10	-	-	
Zn	34.59	12.73	-	34.59	-	-	34.59	-	-	
Rb	3.56	86.75	-	-3.91	-	-	14.00	-	-	

APPENDIX B (cont.)

Sr	1081.37	648.96	-	1020.23	-	-	743.60	-	-
Y	14.28	15.59	-	15.56	-	-	17.90	-	-
Zr	111.23	24.05	-	105.60	-	-	98.16	-	-
Nb	12.26	-	-	11.29	-	-	11.29	-	-
Ba	-	214.56	-	-	-	-	-	-	-
Li	-	87.25	-	-	-	-	-	-	-
Sc	-	10.60	-	-	-	-	-	-	-
Ce	-	31.16	-	-	-	-	-	-	-
Nd	-	-9.00	-	-	-	-	-	-	-
Rock type		Granodiorite			Andesite			Andesite	
Sample no		DDN39			DDN45			DDN49	
Depth (m)		124.9-125			139.4-139.5			148.6-148.7	
	XRF	ICP-OES	ICP-MS	XRF	ICP-OES	ICP-MS	XRF	ICP-OES	ICP-MS
Element									
	XRF	ICP-OES	ICP-MS	XRF	ICP-OES	ICP-MS	XRF	ICP-OES	ICP-MS
Na2O	5.00	-	-	3.15	-	-	1.04	-	-
P2O5	0.22	-	-	0.20	-	-	0.27	-	-
MgO	3.03	-	-	6.51	-	-	6.33	-	-
Al2O3	17.63	-	-	19.22	-	-	18.72	-	-
:SiO2	66.51	-	-	57.02	-	-	54.39	-	-
SO3	1.28	-	-	1.19	-	-	1.87	-	-
K2O	0.39	-	-	1.55	-	-	1.02	-	-
CaO	3.82	-	-	4.33	-	-	10.83	-	-
TiO2	0.40	-	-	0.62	-	-	0.51	-	-
MnO	0.02	-	-	0.06	-	-	0.12	-	-
Fe2O3	2.94	-	-	6.71	-	-	5.43	-	-
V	47.82	-	-	438.59	224.18	-	472.04	282.28	-
Cr	193.63	-	-	50.25	17.06	-	186.31	78.45	-
Ni	5.66	-	-	15.70	8.06	-	10.45	13.56	-
Cu	1378.55	-	1170.00	567.46	741.32	-	1091.47	770.16	-
Zn	34.59	-	27.39	68.73	93.03	-	51.75	27.99	-
Rb	-0.97	-	5.74	30.04	67.46	-	10.98	39.28	-
Sr	1091.37	-	843.40	587.49	374.22	-	472.59	310.44	-
Y	17.45	-	5.46	18.64	17.40	-	17.60	20.63	-
Zr	109.29	-	16.05	34.57	11.91	-	35.70	13.45	-
Nb	11.29	-	2.00	11.29	-	-	11.29	-	-
Ba	-	-	178.30	-	550.83	-	-	129.19	-
Li	-	-	-	-	35.01	-	-	84.19	-
Co	-	-	-	-	-	-	-	-	-
Ga	-	-	-	-	-	-	-	-	-
Sc	-	-	-	-	28.01	-	-	30.02	-
La	-	-	11.50	-	-	-	-	-	-
Ce	-	-	23.75	-	18.24	-	-	18.75	-
Pr	-	-	2.90	-	-	-	-	-	-
Nd	-	-	12.13	-	-15.45	-	-	-14.69	-
Sm	-	-	2.08	-	-	-	-	-	-
Eu	-	-	0.66	-	-	-	-	-	-
Gd	-	-	1.95	-	-	-	-	-	-
Tb	-	-	0.17	-	-	-	-	-	-
Dy	-	-	1.11	-	-	-	-	-	-
Er	-	-	0.48	-	-	-	-	-	-
Tm	-	-	0.10	-	-	-	-	-	-
Yb	-	-	0.32	-	-	-	-	-	-
Hf	-	-	0.40	-	-	-	-	-	-

APPENDIX B (cont.)

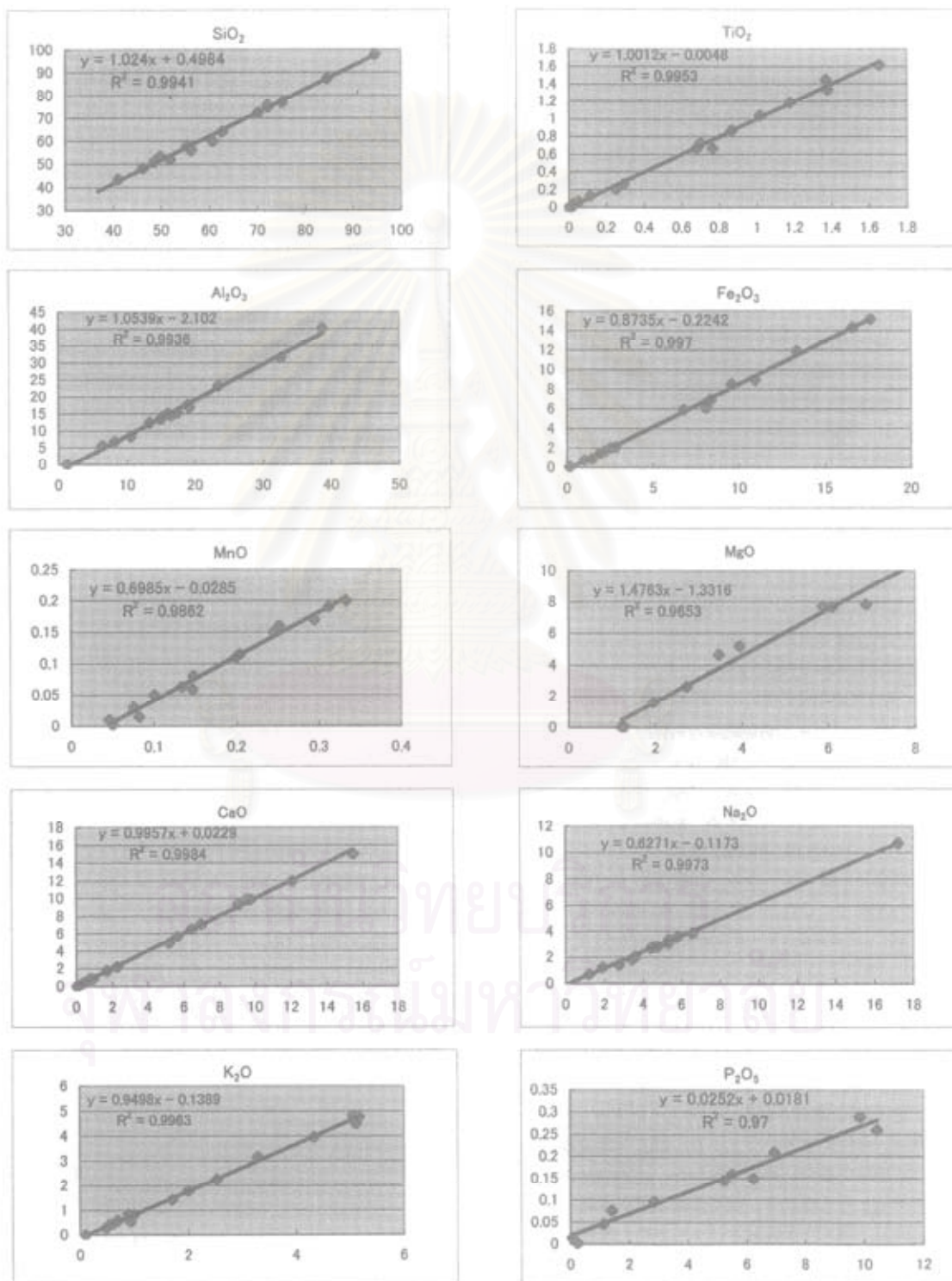
Lu	-	-	0.05	-	-	-	-	-	-
Th	-	-	0.57	-	-	-	-	-	-
U	-	-	0.20	-	-	-	-	-	-
Li	-	-	-73.02	-	-	-	-	-	-
Be	-	-	-9.31	-	-	-	-	-	-
Sc	-	-	0.31	-	-	-	-	-	-
Mn	-	-	171.40	-	-	-	-	-	-
Co	-	-	14.88	-	-	-	-	-	-
Ga	-	-	17.71	-	-	-	-	-	-
Sn	-	-	5430.00	-	-	-	-	-	-
Sb	-	-	797.80	-	-	-	-	-	-
Cs	-	-	0.12	-	-	-	-	-	-
Ho	-	-	0.21	-	-	-	-	-	-
Ta	-	-	0.12	-	-	-	-	-	-
W	-	-	4383.00	-	-	-	-	-	-
Pb	-	-	3.18	-	-	-	-	-	-
Bi	-	-	-0.02	-	-	-	-	-	-
Rock type		Andesite			Andesite			Andesite	
Sample no		DDN57			DDN60			DDV10	
Depth (m)		165.4-165.5			168.4-168.5			30.1-30.2	
	XRF	ICP-OES	ICP-Ms	XRF	ICP-OES	ICP-Ms	XRF	ICP-OES	ICP-Ms
Element									
	XRF	ICP-OES	ICP-Ms	XRF	ICP-OES	ICP-Ms	XRF	ICP-OES	ICP-Ms
Na2O	2.51	-	-	3.45	-	-	1.70	-	-
P2O5	0.27	-	-	0.25	-	-	0.18	-	-
MgO	6.06	-	-	5.28	-	-	6.73	-	-
Al2O3	17.81	-	-	19.19	-	-	20.05	-	-
:SiO2	57.16	-	-	55.93	-	-	49.15	-	-
SO3	2.18	-	-	1.56	-	-	0.36	-	-
K2O	1.24	-	-	0.74	-	-	5.59	-	-
CaO	7.33	-	-	7.06	-	-	5.98	-	-
TiO2	0.52	-	-	0.54	-	-	0.73	-	-
MnO	0.12	-	-	0.10	-	-	0.13	-	-
Fe2O3	5.60	-	-	6.63	-	-	9.32	-	-
V	400.22	-	-	395.07	254.07	-	447.34	-	-
Cr	54.90	-	-	74.15	13.64	-	-8.06	-	-
Ni	11.82	-	-	13.63	7.60	-	17.20	-	-
Cu	843.02	-	-	517.42	349.31	-	7.86	-	-
Zn	98.38	-	-	42.83	24.89	-	87.51	-	-
Rb	22.22	-	-	14.41	49.38	-	82.67	-	-
Sr	547.65	-	-	620.78	416.84	-	483.63	-	-
Y	19.52	-	-	18.54	21.05	-	19.71	-	-
Zr	30.41	-	-	32.86	9.81	-	32.31	-	-
Nb	11.29	-	-	11.29	-	-	11.29	-	-
Ba	-	-	-	-	94.34	-	-	-	-
Li	-	-	-	-	95.41	-	-	-	-
Sc	-	-	-	-	31.39	-	-	-	-
Ce	-	-	-	-	17.83	-	-	-	-
Nd	-	-	-	-	-13.01	-	-	-	-

APPENDIX B (cont.)

Rock type		Andesite			Andesite			Andesite	
Sample no		V16			V19			V24	
Depth (m)		47.1-47.2			59.5-59.6			68.1-68.2	
	XRF	ICP-OES	ICP-Ms	XRF	ICP-OES	ICP-Ms	XRF	ICP-OES	ICP-Ms
Element									
Na2O	1.79	-	-	3.72	-	-	2.55	-	-
P2O5	0.29	-	-	0.20	-	-	0.21	-	-
MgO	8.11	-	-	9.19	-	-	8.30	-	-
Al2O3	17.86	-	-	16.89	-	-	16.54	-	-
:SiO2	49.98	-	-	55.89	-	-	54.42	-	-
SO3	2.39	-	-	1.53	-	-	1.28	-	-
K2O	1.01	-	-	1.16	-	-	0.79	-	-
CaO	7.29	-	-	3.31	-	-	4.72	-	-
TiO2	0.55	-	-	0.52	-	-	0.61	-	-
MnO	0.16	-	-	0.24	-	-	0.16	-	-
Fe2O3	10.76	-	-	8.46	-	-	10.47	-	-
V	293.34	-	-	307.83	-	-	296.75	-	-
Cr	124.40	-	-	104.91	-	-	94.97	-	-
Ni	22.59	-	-	11.97	-	-	23.63	-	-
Cu	226.93	-	-	115.13	-	-	175.07	-	-
Zn	63.20	-	-	119.14	-	-	75.15	-	-
Rb	34.12	-	-	35.25	-	-	28.47	-	-
Sr	434.24	-	-	567.80	-	-	379.87	-	-
Y	20.54	-	-	24.27	-	-	17.02	-	-
Zr	33.12	-	-	30.40	-	-	32.81	-	-
Nb	-	-	-	11.29	-	-	11.29	-	-
Rock type		Andesite							
Sample no		V32							
Depth (m)		89.5-89.6							
	XRF	ICP-OES	ICP-Ms						
Element									
Na2O	2.43	-	-						
P2O5	0.21	-	-						
MgO	7.77	-	-						
Al2O3	15.93	-	-						
:SiO2	56.18	-	-						
SO3	1.35	-	-						
K2O	1.34	-	-						
CaO	4.49	-	-						
TiO2	0.62	-	-						
MnO	0.20	-	-						
Fe2O3	9.62	-	-						
V	340.31	-	-						
Cr	154.18	-	-						
Ni	16.39	-	-						
Cu	118.42	-	-						
Zn	80.95	-	-						
Rb	31.74	-	-						
Sr	287.85	-	-						
Y	18.89	-	-						
Zr	37.25	-	-						
Nb	11.29	-	-						

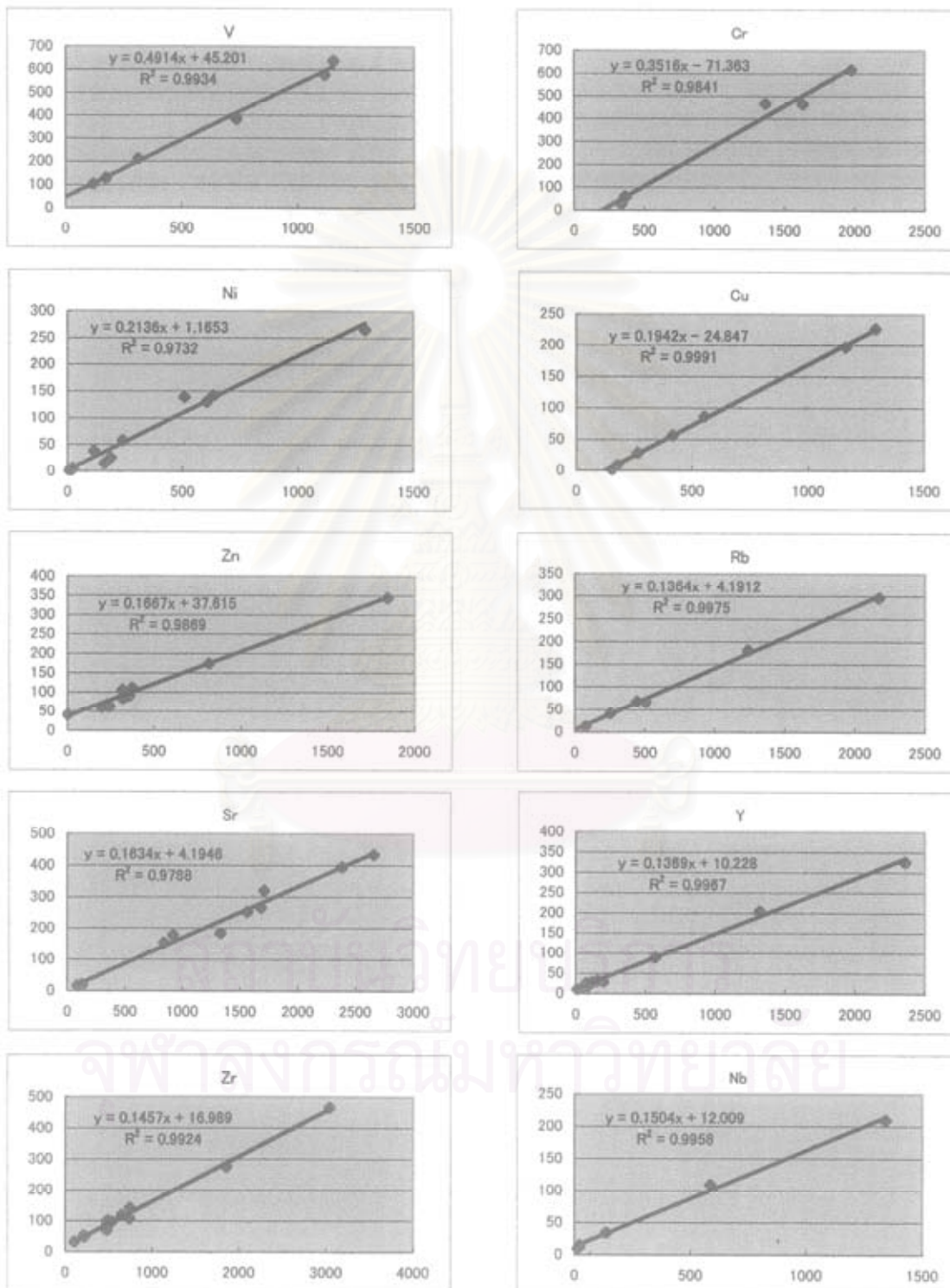
APPENDIX C-1

Calibration curves for 10 major elements. Horizontal axes are collected contents (%) and vertical axes are contents of standard samples (%). Horizontal axes for MgO, Na₂O and P₂O are collected counts (cps).



APPENDIX C-2.

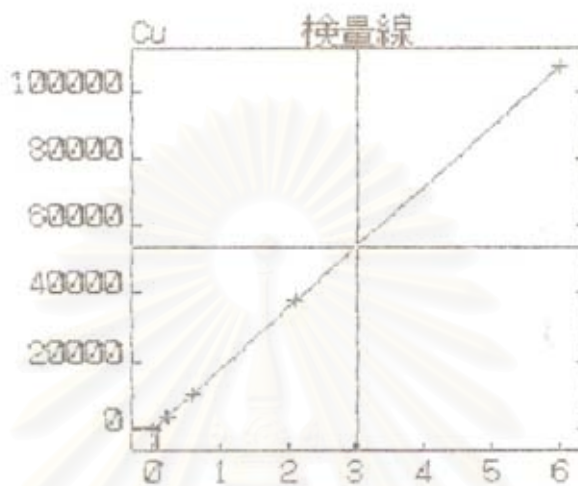
Calibration curves for 10 trace elements. Horizontal axes are collected contents (ppm) and vertical are contents of standard samples (ppm).



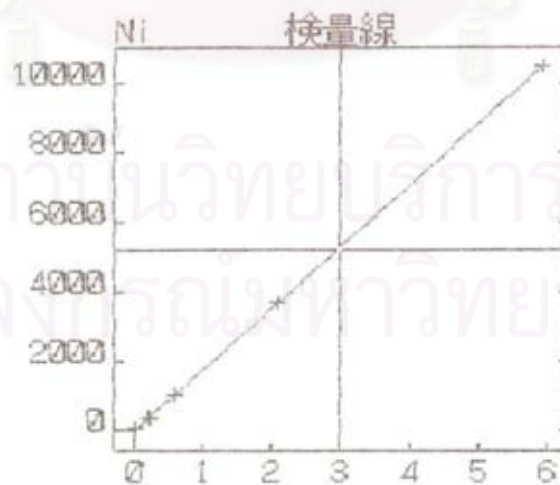
APPENDIX D

Calibration curves of trace element by ICP-OES

相関係数 0.999995
回帰誤差 0.00708

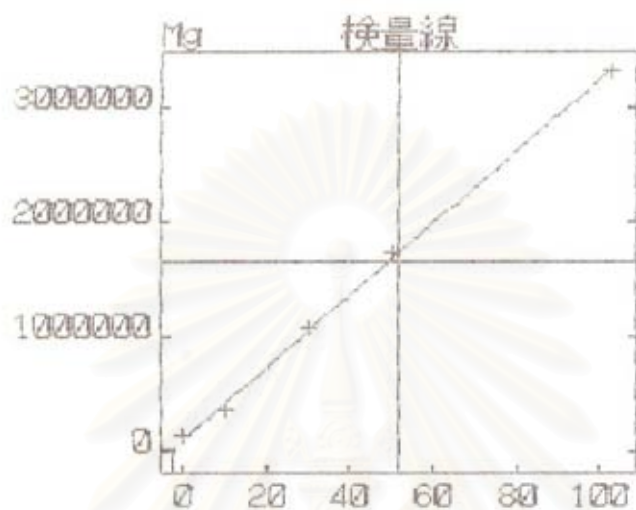


相関係数 0.999947
回帰誤差 0.02264

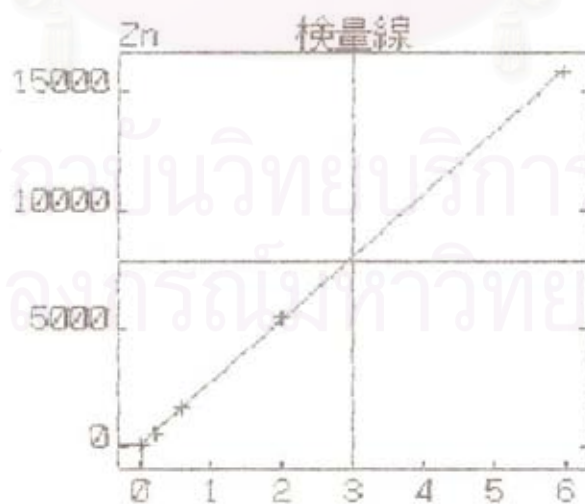


APPENDIX D (cont.)

相関係数 0.999433
回帰誤差 1.223

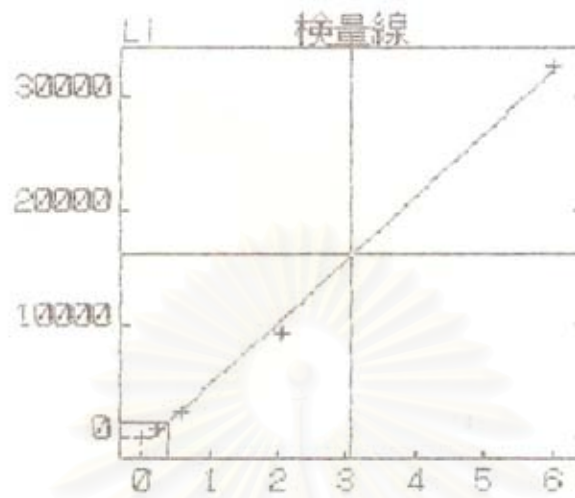


相関係数 0.999929
回帰誤差 0.02649

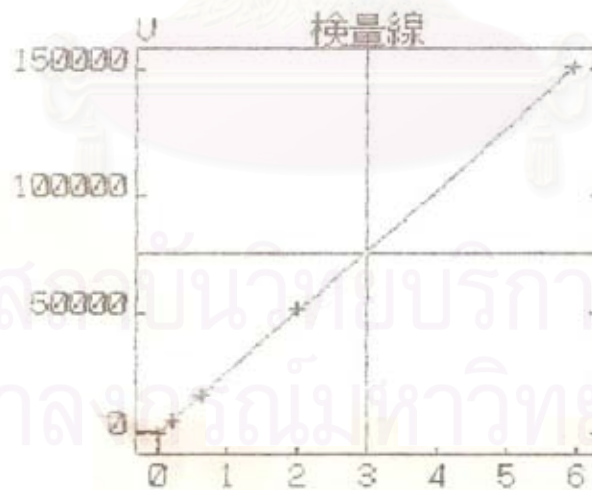


相関係数
回帰誤差

APPENDIX D (cont.)



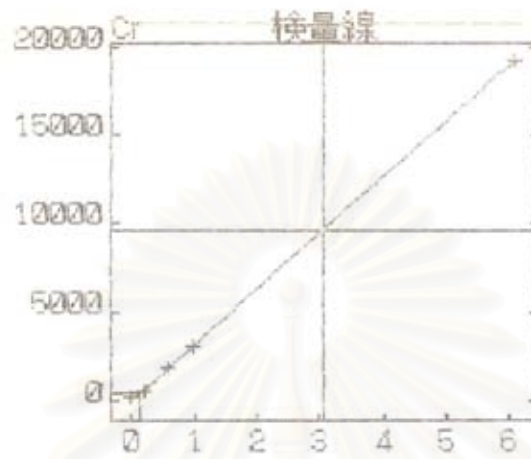
相関係数 0.999986
回帰誤差 0.01163



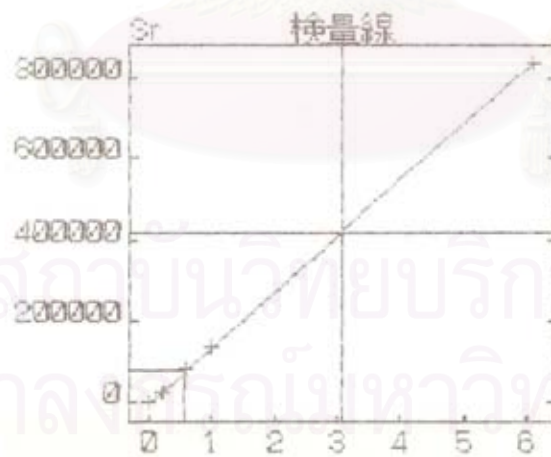
สถาบันวิทยบริการ
จุฬาลงกรณ์มหาวิทยาลัย

APPENDIX D (cont.)

相関係数 0.99993
回帰誤差 0.02637

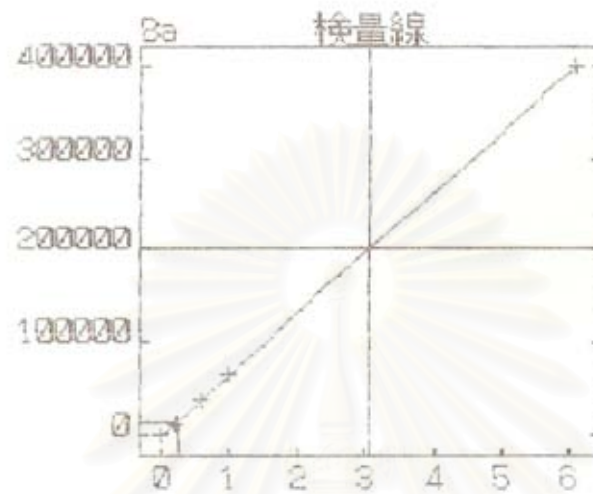


相関係数 0.999988
回帰誤差 0.01124

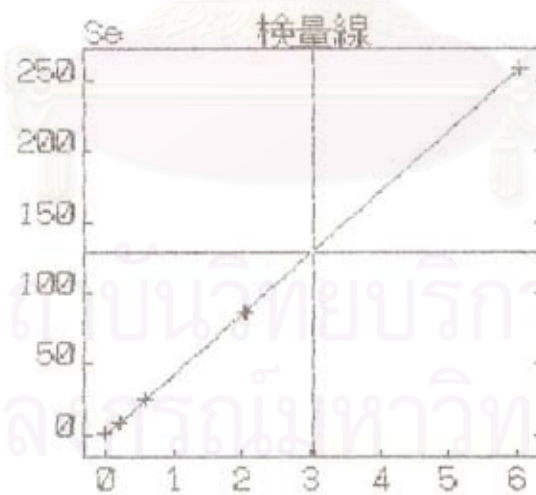


APPENDIX D (cont.)

相関係数 0.999986
 回帰誤差 0.01202

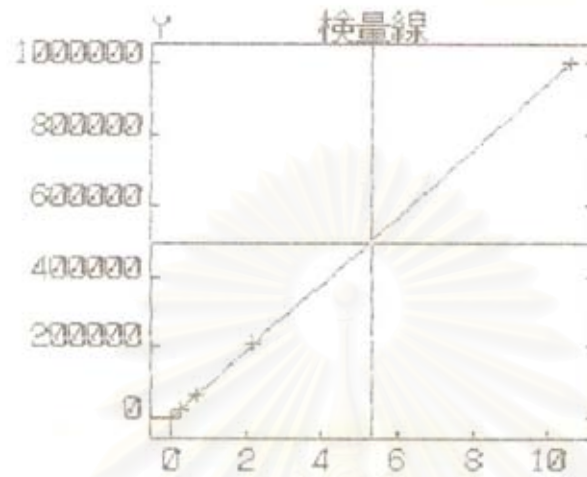


相関係数 0.999989
 回帰誤差 0.01072

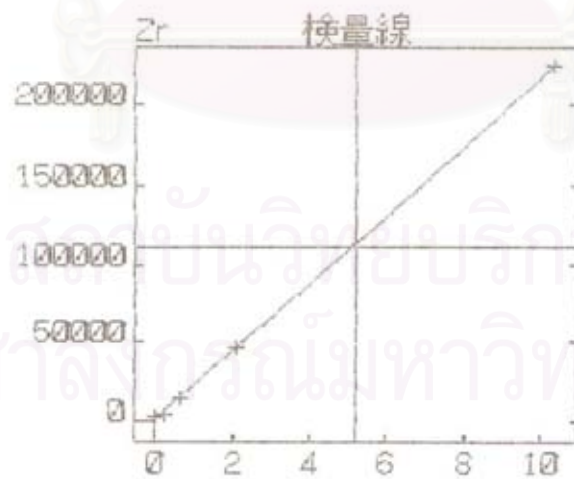


APPENDIX D (cont.)

相関係数 0.999992
 回帰誤差 0.01595

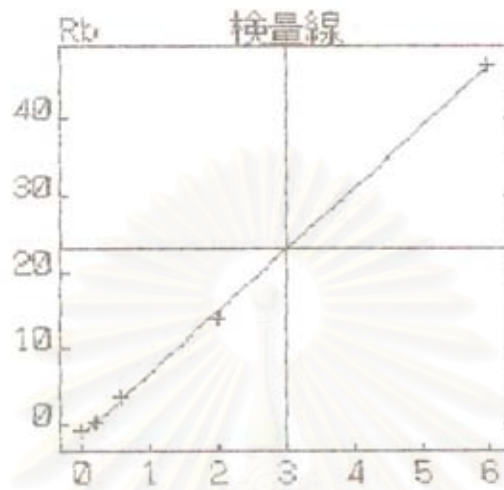


相関係数 0.999954
 回帰誤差 0.0374

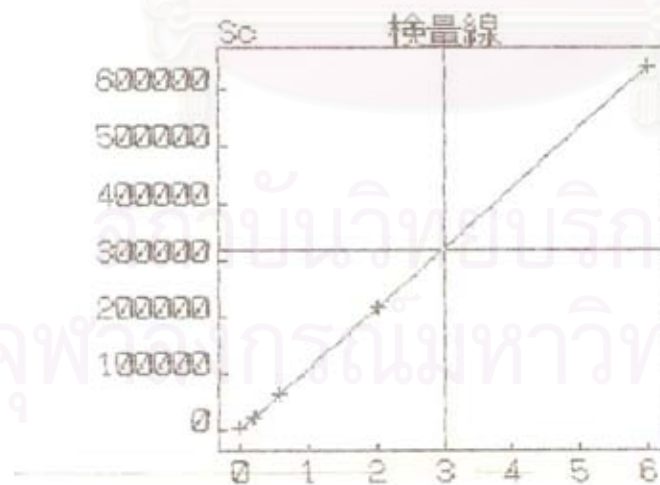


APPENDIX D (cont.)

相関係数 0.999627
 回帰誤差 0.06043

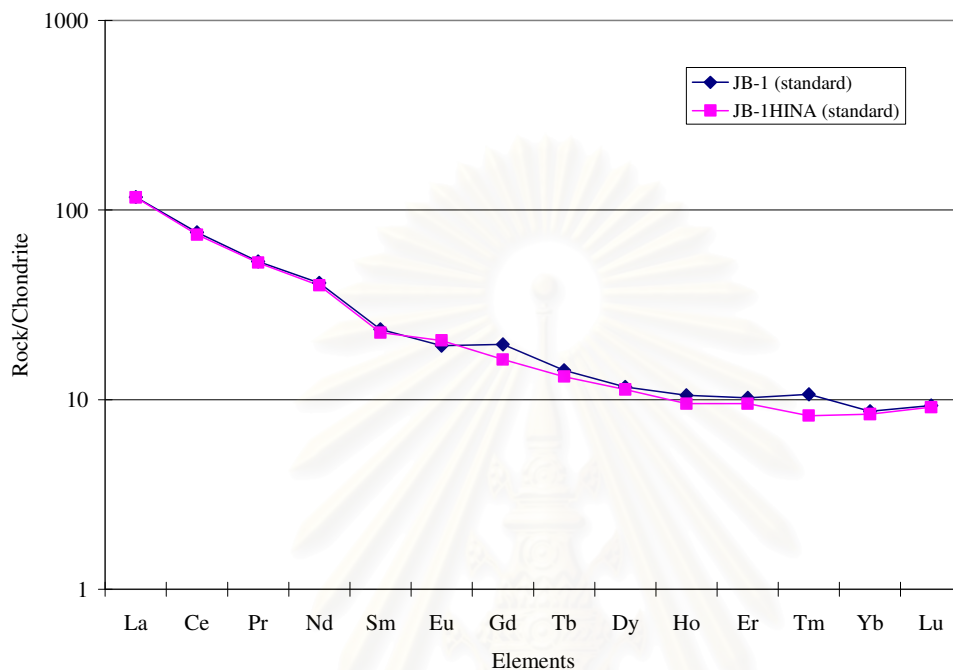


相関係数 0.999955
 回帰誤差 0.02106

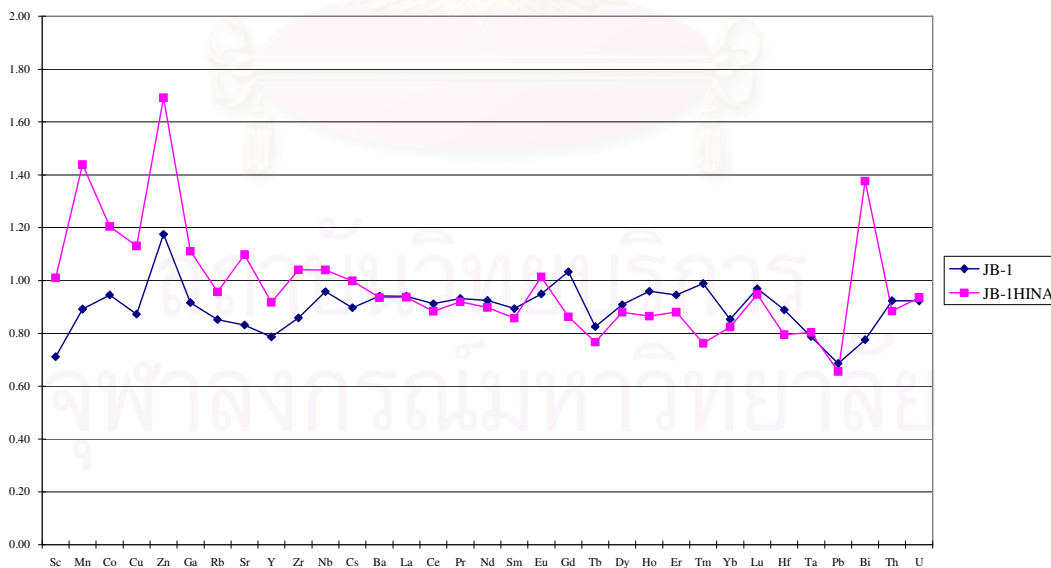


APPDENDIX E

Condrite normalized patterns for 2 rock standard supplied from Geological Survey of Japan analysed by ICP-MS



%Error



BIOGRAPHY

Mr. Kuakul Marhotorn was born in Nakhon Nayok province, central Thailand on 5 January 1981. He graduated with a B. Sc. degree in Geology from Chulalongkorn University, Bangkok, in 2003. After his graduation, he worked in ATOP Technology Company and started his two-year career as exploration geologist working in areas of Chiang Mai, Phare, Payao, Chiang Rai province of northern Thailand. Then, he continued his study as the M. Sc. geology student at Chulalongkorn University, Bangkok, in 2006. The research work has been focussed on igneous rocks and prospect geology. During his thesis work, he got a scholarship to geochemical do a research rock at Institute of Material and Resources, Akita University for 2 months. He also got some experiences on base metal exploration, gold exploration, damsite investigation and sand-gravel reserves in central Lao, PPR, limestone reserve in Cambodia and Indonesia for Siam Cement Group (SCG) and TEAM Consulting companies, as a part-time geologist. In addition, he helps Department of Geology, Chulalongkorn University, for both ore and rock petrographic investigation.



สถาบันวิทยบริการ
จุฬาลงกรณ์มหาวิทยาลัย